Self Assembly of Hybrid Nanostructures Encompassing Inorganic, Organic and Biological Applications

Nicola McMillan
MSci

Submitted in fulfilment of the requirements for the Degree of Master of Science

University of Glasgow
Department of Chemistry

September 2011

Abstract

The work presented in this thesis will highlight the modification of inorganic and biological materials with organic tethers; the subsequent characterisation of these compounds and the surface studies used to investigate them further. On moving from materials science to cell biology, a variety of techniques are used to demonstrate the chemical modifications and the role the surface has to play in not only visualising the effect of the modification but the surface itself mediating reactions.

Described within is the further investigation of Mn Anderson based polyoxometalate clusters .This report documents the grafting of C-16, C-18 alkyl chains and pyrene to hydrophilic Mn Anderson clusters. Solid state studies using scanning electron microscopy and transmission electron microscopy demonstrates the effect of cation exchange from tetrabutyl ammonium (TBA) to dimethyldioctadecyl ammonium (DMDOA) resulting in new POM assemblies. For the C-18 and to some extent the C-16 grafted clusters, uniform, highly ordered assemblies are reported in contrast to the “sea urchin” like structures observed on cation and solvent exchange. The generation of surfactant encapsulated clusters in conjunction with surface grafted clusters has been achieved.

For the first time these organically tethered POM’s have been patterned successfully onto self assembled monolayers (SAMs) using microcontact printing. In addition to this, studies involving human fibroblast cells (hTERT-BJI) are reported. Cells have been found to attach and spread on monolayers terminated in pyrene terminated POM. It has been observed that POMs play a crucial role in the adhesion of cells to surfaces.

Solid state techniques scanning electron microscopy (SEM) and atomic force microscopy (AFM) are used in the investigation of not only inorganic compounds but the post translational modification of proteins. Highlighting the importance of these techniques in the further understanding or reactions and the effects the reactions have on the molecules

Further the investigation of polyoxometalates herein the development of molybdenum (VI) oxide polyoxometalate cluster, β-$[Mo_{18}O_{54}(SO_3)_2]^{4-}$, that can

undergo a reversible conversion between two electronic states, upon thermal activation is described. Experiments have uncovered the fact that the two embedded redox agents can be thermally activated and ejected from the sulfite anions and delocalised over the metal oxide cluster. The role of the surface in such a reaction is described detailing its importance in the reaction from a fully oxidised state to a two electron reduced state. This work demonstrates the use of a POM as a potential starting point to create a single molecule device at the nanoscale.

Publications

Micropatterned Surfaces with Covelantly Grafted Unsymmetrical Polyoxometalate Hybrid Clusters Lead to Selective Cell Adhesion

Yu-Fei Song, Nicola McMillan, De-Liang Long, Struan Kane, Jakob Malm, Mathis O Riehle, Chullikkattil P. Pradeep, Nikolaj Gadegaard and Leroy Cronin, *J. Am. Chem. Soc.*, **2009**, *131* (4), pp 1340–1341

Reversible electron-transfer reactions within a nanoscale metal oxide cage mediated by metallic substrates

C. Fleming, D.-L. Long, N. McMillan, J. Johnson, N. Bovet, V. Dhanak, N. Gadegaard, P. Kögerler, L. Cronin, M. Kadodwala, *Nature Nano.,* **2008**, *3*, 229-333

Design of Hydrophobic Polyoxometalate Hybrid Assemblies Beyond Surfactant Encapsulation

Y.-F. Song, N. McMillan, D.-L. Long, J. Thiel, Y. Ding, H. Chen, N. Gadegaard, L. Cronin, *Chem. Eur. J.* **2008**, *14*, 2349-2354

From polyoxometalate building blocks to polymers and materials: The silver connection

Y.-F. Song, H. Abbas, C. Ritchie, N. McMillian, D.-L. Long, N. Gadegaard, and L. Cronin, *J. Mater Chem.*, **2007**, *17*, 1903-1908

Supramolecular Assembly Facilitating Adsorbate-Induced Chiral Electronic States in a Metal Surface

Nicolas Bovet, Nicola McMillan, Nikolaj Gadegaard, and Malcolm Kadodwala. *J. Phys. Chem. B*, **2007**, *111* (33), pp 10005–10011

Incorporation of N-heterocyclic cations into proteins with a highly directed chemical modification

N. McMillan, L. V. Smith, J. M. de la Fuente, A. D. C. Parenty, N. Gadegaard, A. R. Pitt, K. Thomson, C. MacKenzie, S. M. Kelly, and L. Cronin, *Chem. Commun.*, **2007**, 2581-2583

Table of Contents

List of Figures

List of Tables

Acknowledgment

Firstly I would like to thank my supervisor's Lee and Nikolaj. Thank you for the opportunity to express myself through my science for the greater good, we have had a turbulent time but have got there in the end. Your support and words of wisdom as well as giving me a free run to discover has been invaluable and allowed me to grow in ways I never thought possible. It hasn't been the easiest – but at least it hasn't been boring!

My group – you guys rocked – true professionals in every sense of the word. A few people in particular to thank. Jim McIver – you are my science Guru, if ever a man could fix things I messed up it was you, and Chris Ritchie – you endured 3 years of sharing an office with me – you are a star! Moving on to YuFei Song, for pure unadulterated science chat – you understood. Louise Smith and Hamera Abbas, the girls that got me through the group meetings and introduced me to internet shopping – what have you done? Geoff Cooper and Alexis Parenty, just thank you for making me laugh!

To Wendy Hanson, thank you for the help, support and the opportunities.

I couldn't submit this thesis without the support of my parents – you are my guardians – without whom I would not shine – this is for you and I hope it makes you proud. Dad I always said if I could be like someone I would be like you, I hope this gets me there. To Liam, what you have added to this experience will never be forgotten – you hold my hand in the metaphorical way and at times you are the big brother, something I will repay when it comes to your thesis time and any time you need me. We'll do it together like we always have done. To my wee gran who taught me all there is to know about life, that hard work always pays off, you made me who and what I am. And finally to mum, my best friend, you taught me not to be frightened and to do whatever I truly believed in – well I've got there in the end. This is as much for you all as it is for me.

To the best friends a girl could dream of. For the chats, the support and the wine. Christine, Catriona and Fiona, although you didn't understand the science – you still listened to my ramblings. For that I will be eternally grateful. This brings me onto the ones who do understand the science. Katrina, I don't know what I would

have done without you, you were my rock and remain so, Gemma, because you knew what it felt like and held my hand and my organic chemists Jenny and Kate – organic chemistry ain't fun but you two certainly made up for that. For my boys, Davie, Graham and Fergie, we did it together from day 1 and lunchtime will never ever be the same. In fact let's hear it for lunchtime – when is that ever going to happen again? That department will miss us!

To my David, I've not been easy to live with through this – no excuses I guess! Thanks for picking up after me, for wiping my tears and for being there when I moaned. You told me I was good enough and believed in me wholeheartedly. You will never know what that means to me. It didn't matter when or where – you were there. I hope this makes you proud.

And finally to the science – it's my belief that science is for the greater good, and one day the dreams of many will be uncovered – my grandfather instilled this belief in me – and I hope one day his and indeed our faith will be rewarded.

Declaration

The work contained in this thesis, submitted for the degree of MSc, is my own original work, except where due reference is made to other authors. No material within has been previously submitted for a degree at this or any other university.

Nicola McMillan

Aims

At the outset of this project the primary aim was to design surfaces with potentially new and interesting applications, as well as using surfaces to visualise the fuctionalisation of other molecules in the hope this will elucidate some information as to the mechanism of their formation.

This work can be viewed as a continuation of several other projects that are as diverse as:

- Creating new and interesting inorganic materials and the extension of POM chemistry
- Designing new organic compounds that have been created for their anti cancer activity and to further investigate their properties in a novel way and use interesting techniques to do so.
- Surface mediated reactions – what role, if any, does the surface play on intramolecular reactions?

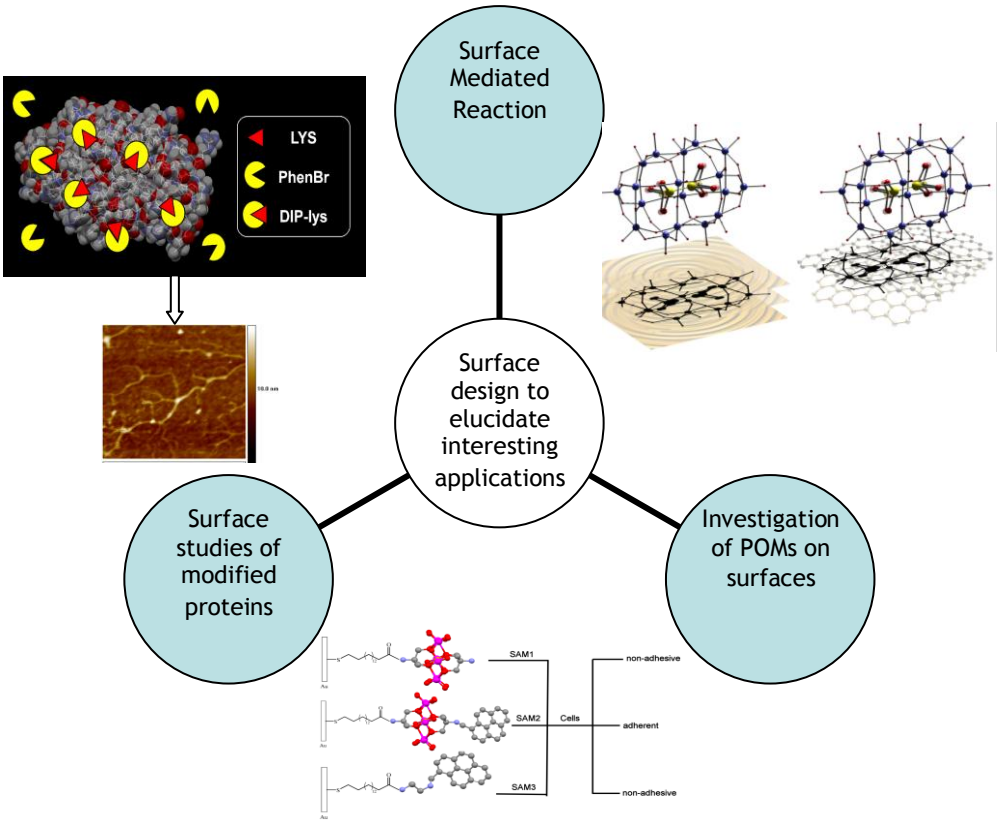

Figure 1 Overview of the aims of the project; to determine the possibility of a surface mediated reaction, to investigate the patterning of POMs on a surface and to investigate the effect modification has on a protein through its behaviour on a surface.

As described in Figure 1 using different approaches to both visualise, and in some cases use the surface as a medium to extend a reaction, forms the basis of this investigation which can essentially be divided into 3 sub categories as follows:

1. Surface patterning of Polyoxometalate's; both the self organisation mediated by external factors such as cation and solvent exchange, to patterning of POMs in a specific orientation.
2. Protein modification with Dihydro-Imidazo Phenanthridinium bromide and surface analysis of the effect of this modification.
3. Transition Metal Oxide clusters and the effect a gold surface has on an intramolecular redox reaction.

1 Introduction

1.1 Self assembly and nanoscience

For generations the increased demand for science to scale down to the nano scale has inspired many to pioneer the development of the latest nano scale device, whether it is for biological purposes, materials science, or the development of nano scale engineering components.

Looking at the human body has always inspired scientists to try and emulate Nature's materials and conquer the nano scale issues. If Nature can do it, why can't we? Chemistry has, in the last two decades, provided us with new routes to these dimensions. Different and more sophisticated methodologies have opened the way to allow devices to be constructed down to the nano scale. Not quite reaching atomic scale, nano materials that exist today generally have at least one of their dimensions typically within the 1-100nm size. Whether it is the height of a self assembled monolayer or the formation of nano rods or tubes, the nano world has finally become achievable in a normal laboratory environment.

One area of science that is, at present, pushing the boundaries of the nano – dimension is that of Self Assembled Monolayers (SAMs) and surfaces designed with nano scale features. The development of SAMs and the pioneering work of George M. Whitesides[1] have opened many avenues not only in engineering but also in biological, chemical and materials science.

1.2 Self Assembled Monolayers (SAMs)

One of the main driving forces for a metal or a metal oxide to absorb a material is the fact that, once absorbed, a lower free energy exists between the surface and the external environment.[2] In addition the absorbed molecules have a great influence on the stability of the material.[2] The absorbate decreases the reactivity of the surface atoms and in doing so alters the surface properties of the metal/metal oxide. The production of SAMs is one area where the effect of the absorbate has been intensively studied.

The main focus on the preparation of SAMs began in the decade spanning 1983 – 1993 with studies primarily focussing on the adsorption of organosulfur compounds onto gold or silver substrates.[3] SAMs can be defined as organic assemblies that form either from solution or the gas phase, where the molecular constituent is adsorbed onto a surface in a regular repeated arrangement. This organisation on the surface is spontaneous forming a crystalline layer. The molecules or ligands within the crystalline layer will have a specific chemical functionality, also known as the headgroup that has an affinity for the substrate. In the main these molecules are alkanethiols on a gold substrate where the sulfur atom has an affinity for the gold substrate. This however is not exclusive to thiols on gold instead there are a number of functionalities available which will bind to specific materials.

The formation of SAMs is essentially the spontaneous chemisorption of molecules onto the surface. Self assembly occurs when there is a high affinity for the molecule to the surface – this will result in the self organisation of that molecule in a manner which will maximise the packing density of the molecules. Many types of absorption occur, each with different strengths of attraction. Chemisorptions in the case of an alkanethiol and a gold surface has a very strong interaction with its surface – in the region of an enthalpy of 10 kcal/mol, compared with physisorption – or Van der Waals interactions -, which have a substantially smaller enthalpy of interaction.

Initial studies led to the elucidation of the basic principles that govern the formation of SAMs, including the orientation of the molecules on the surface and their organisation, as well as identifying easily reproducible protocols for the preparation of SAMS which are still used and continue to be adapted today.

With these basic principles in mind the investigation into different SAM characteristics, their fabrication and of course their applications ensued. Today the continued development of the methodology is used to create surfaces with a wide variety of applications.

1.2.1 SAMs for use in Nanotechnology

SAMs are nanostructures with a thickness of around 1-3 nm. What makes them interesting to nanoscience[4] is the ability to control the atomic composition of the

SAM perpendicular to the surface with pre determined molecular materials ,coupled with positional control that is in the region of 0.1 nm.

The fact that SAMs can also be fabricated with a designed pattern using micro contact printing is also an advantage meaning the structures are true nanomaterials with dimensions that range from 10 – 100 nm in the plane of the surface. Micro contact printing is not the only method of patterning; the use of scanning probes, as well as beams of photons, atoms and electrons are also used. [4]

The main advantages of using SAMs within the area of nanoscience and technology are outlined as follows[4]:

- Easy preparation using cheap materials with little need for specialised equipment.
- The dimensions of the monolayer are ultimately controllable.
- The stabilising ability the SAMs have on the metal or the metal oxide is key in the formation and use of thin films and other nanaostructures.
- They can add function to these nanostructures with relative ease.
- The number of techniques available to characterise/ visualise a SAM is vast and outlined in Table 1.
- They can be used to understand features such as wettability, adhesion and friction.

Technique	Abbreviation	Associated Reference
Reflectance Absorption infrared spectroscopy	RAIRS	[5]
Raman Spectroscopy		[3i]
X-ray photoelectron spectroscopy	XPS	[6,7]
High resolution electron energy loss spectroscopy	HREELS	[7]
Near edge X-ray absorption fine structure spectroscopy	NEXAFS	[8]
Helium atom scattering		[3h]
X-ray diffraction		[9]
Contact angle geometry		[10]
Scanning probe microscopy	SPM	[11]
Electron microscopy		[12]
Edge X-ray absorption fine structure spectroscopy	EXAFS	[13]
X-ray absorption near edge spectroscopy	XANES	[13]
Infrared Spectroscopy	IR	[14]
UV –vis spectroscopy		[15]
Differential scanning calorimetry	DSC	[14a,16]
High Pressure liquid Chromatography	HPLC	[17]
NMR Spectroscopy		[14a]

Table 1 Techniques used to characterise and visualise a SAM

These techniques can give a wide variety of detail about a surface and its contents and can be used singularly, or in conjunction with a number of other techniques, depending on the application and the desired outcome. For the purpose of this project the techniques used are SPM and contact angle measurements which are used complimentary to each other and not only confirm the surfaces have been prepared correctly, but the effect of the modification.

1.2.2 Surface design carrier

The substrate is the physical object that supports the self assembled monolayer and can be a variety of materials including glass, metal, colloids and nanorods to name a few. In general the use of planar substrates is preferred due to the ease in

which the surface can be characterised and visualised using a variety of well established techniques as outlined in Table 1

The choice of substrate is generally associated with the application of the particular SAM *e.g*. planar substrates of polycrystalline films on metal substrates are generally used for biological studies because of the ease of preparation and characterisation.

Typically a silicon wafer is used as the carrier for the evaporation of the desired metal as the first step in preparing the surface for SAM formation, and is normally done, by physical vapour deposition (PVD)[18]. To the silicon wafer an “adhesive” layer of generally 1-5 nm of titanium, chromium or nickel is applied to the silicon to allow the gold or other metal to bind.

Gold is the mostly widely used surface on which to create a SAM – and as such is the most studied and understood this makes this surface a good starting point. The ease with which gold can be obtained through simple metal deposition onto a support of metals e.g. silicon, glass or polystyrene or the colloid form, makes it an ideal candidate for extensive studies.

This ease coupled with the fact that gold is a relatively inert metal and does not react readily with the external environment, allows the clean transfer of molecules onto the surface without much contamination, or the need to work under Ultra High Vacuum (UHV) conditions. This property is essential for techniques such as microfabrication; the substrate can be handled outwith a clean room environment meaning reactions can be carried out with little inconvenience.[4] Despite its expense gold is also an exceptionally easy surface to pattern, which makes it an ideal surface.

The surface topography of the deposited gold is a polycrystalline film with a (111) texture that appears as a hexagonal pattern of atoms.[19]

The main attraction of gold is the high affinity it has for alkanethiols.[3a] This affinity means that the sulfur containing head groups can displace other molecules on the surface with relative ease. In addition to this, gold is relatively easy to pattern, using a variety of lithographic techniques. Its affinity for the thiol groups means a high degree of accuracy is achieved in combining these two parameters.

This is coupled with the compatibility of gold in analysis of biological molecules. Cells adhere to gold with little effect on their morphology as it is non toxic, which is a key criterion when examining cell behaviour on a patterned substrate.

1.2.3 Preparation of SAMs

The preparation of a SAM on a substrate such as gold or silver is a relatively simple procedure. Assuming a clean substrate, all that is necessary for the SAM to be formed is a dilute solution of the thiolate, usually 1-10 mM in ethanol, and the immersion of the substrate within it. Factors such as time submersed into the solution and the concentration of the solution are key and are described in the following sections.

1.2.3.1Adsorption of thiols

SAMs of alkanethiols on gold surfaces are the most widely used and are formed by the spontaneous chemisorption of the alkanethiol onto the gold surface with the loss of hydrogen. Other molecules which can form SAMs include silanes and phosphonic acids. The alkane chain of the molecule assembles in a trans conformation to maximise the packing density of the hydrocarbon tails as shown in Figure 2. Coverage of the surface happens quickly from dilute solutions in a timescale of milliseconds to minutes and the longer the substrate stays in solution, the more time there is to maximise the coverage of the molecules on the surface allowing reduction of defects.

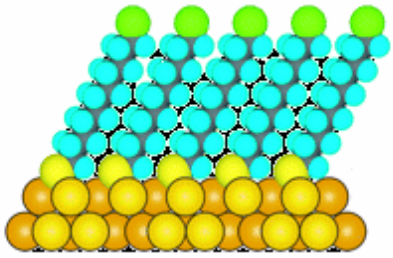

Figure 2 Schematic representation of the alkanethiol on a SAM showing the terminal region free and the tilt angle of the molecule.[4]

The head groups of the chains are important in the formation stage as they determine the specific tilt angle that the chain will fall into. The important part of

the molecule is the functional group situated at the end of the alkane chain; it is at this point that there is the potential to add various molecules, like gold nanoparticles, and offer a variety of potential uses in materials science. How the organic molecules organise themselves onto a surface is dependent on a variety of criteria. The density of the molecules on the surface is determined by the molecule's ability to pack closely together to minimise the free energy corresponding to that layer. In addition to this, the molecules wish to pack together in a conformation that will allow the adjacent molecules to have a high degree of Van der Waals interactions[20] and in some cases even hydrogen bonding.[21] For alkanethiols on gold, the chains exist in a *trans* conformation with a 30° tilt angle.[19b]

1.2.3.2 The role of the solvent

The solvent of choice for the preparation of SAMs is ethanol. The fact that it is cheap, readily available and has low toxicity add to its popularity. Other solvents include tetrahydrofuran, dimethylformaldehyde and acetonitrile and any differences in the resulting SAM is insignificant. [22] However where ethanol really stands alone is in its ability to solvate a number of alkanethiol molecules.

Where the role of the solvent is important is ensuring that it does not hinder the process of SAM formation. Studies have shown that SAMs formed by dissolving alkanethiols in non polar organic solvents show more defects and less well organised structures.[22-23]

The effect the solvent has on the formation of the SAM is however poorly understood. What is known however is that in order for successful formation of SAMs, the solvent must not hinder the interaction between the substrate – absorbate interactions and so the solvent must be displaced from the surface in order for the SAM to be formed.

1.2.3.3 The role of temperature, concentration and immersion time on SAM preparation

There is some evidence that temperature does have an affect on the formation of SAMs. Work carried out by Uosaka *et al* has concluded that the temperature effect is at its most significant at the initial stages of the formation of the SAM.[24] It is believed that temperatures in excess of 25 °C would aid the formation of the SAM without defects as it would improve the kinetics of formation.[24-25]

The concentration of the solvent and immersion time are key parameters that dictate the formation of a well organised SAM. In order to prepare a SAM that has a surface density of 4.5 x 10^{14} molecules/cm^2 [19a] a concentration of at least 1 µM thiol is needed. As mentioned previously the typical concentration used is between 1-10 µM. Low concentrations of thiol need longer contact with the surface than higher concentration solutions to create a well structured SAM.[22,26] SAMs that are formed in solutions of a lower concentration do not have the same physical properties as those formed using a higher concentration[22] and instead are found to have uneven surface coverage. Therefore, it can be concluded that concentration and immersion time are directly related and many experimental techniques have been developed taking these parameters into consideration in order to achieve the desired SAM.

1.2.4 Purity of the thiol and substrate cleanliness

As the formation of a SAM is essentially a displacement reaction, the purity of the solvent and the subsequent alkanethiol, as well as the cleanliness of the substrate all play an important role in the formation of the SAM. When the gold surface is in contact with materials that are not easily displaced, this presents a problem for the formation of a good standard of SAM – this can be overcome by immersion of the surface in piranha solution (sulfuric acid and hydrogen peroxide mixture) to essentially strip the surface of any contaminants.

With respect to the purity of the thiol – and the fact that the reaction is a displacement reaction – the assumption is that because the alkanethiols have a high affinity for the gold, they would essentially compete with other impurities in

the solution. A common impurity in thiol solutions is the presence of disulphides; however studies have shown that they have little effect on the structure of the SAM.[22,27]

1.2.5 SAM modification

Direct modification of a surface *eg* alkanthiolates on gold is an excellent starting point for further reactions to be carried out. Where the modification of a standard alkanethiol is used for studies including determining the wettablity [28] and adhesion of a surface [29], the further modification of the surface to include more complex material is essential for the development of fields such as biochemistry and materials science.

The method of derivitising a surface further after the initial formation of a SAM has developed is due to the difficulty in synthesising the desired molecule directly before the adhesion to the surface. The synthesis of an alkanethiol linked to various other moieties has proven difficult; and so step wise adhesion and synthesis seems to have overcome the many issues associated with synthesis and subsequent addition approach.

The advantages and disadvantages of forming SAMs are outlined in Table 2.

Advantages	Disadvantages
• Simple functionalisation procedure using well documented techniques can be carried out before further derivitisation • Allows terminal functionality to be added that may not be compatible with the reactive thiol group • Very little material is needed to carry out a successful reaction – essential when using material which may be in limited supply • The structure of the SAM remains intact	• The reaction may not go to completion at every reactive site. • This may result in a variety of functional groups at the terminal region resulting in an uneven surface coverage. • Limited structural control on the formation of the SAM

Table 2 Advantages and disadvantages of chemical functionalisation after initial SAM formation

In terms of simplicity, SAM formation is a relatively easy process and, given a clean substrate and pure reactive materials, should result in a well formed SAM. It is on further functionalisation that problems can arise, and in some cases a poorly developed SAM may result.

1.2.6 Activation of terminal Functionality

The most common approach used to change the functionality of a SAM Is through the activation of the terminal region. A common approach when using alkanethiols on gold is to exploit the terminal carboxylic acid group to form an amide bond via an anhydride intermediate. This results in the terminal –COOH group reacting with an amine to form a peptide bond.

The amide bond is generally formed by the activation of the free –COOH with N-hydroxysucinimide (NHS) yielding an amide bond.[30] This is not the only method available, in fact there are many examples within the literature.[31]

This method is particularly useful when derivitising surfaces after microcontact printing to allow the immobilisation of other molecules in a particular orientation.

1.2.7 Soft Lithography

Soft lithography can be described as a technique used to transfer a pattern in the plane of the surface with features as small as 10 nm. This technique can be used to fabricate surfaces with a predetermined pattern with predetermined lateral features.

The main technique used to pattern SAMs is called Microcontact printing and can be used to create a pattern on a surface with many pre designed features. The technique can be likened to printing ink onto paper using a stamp. The pattern of the stamp is transferred to the paper with a single press. The stamp used in this procedure is commonly prepared from polydimethylsiloxane (PDMS)[32], the use of this has many advantages. Not only is it cheap and commercially available, it is resistant to contamination from external material, such as dust, which is essential in producing well organised, complete patterns. In addition to these advantages, using PDMS as a stamping material also allows the procedure to be carried out with relative ease due to its low surface energy $\gamma = 21.6$ dyn/cm^2 [33] allowing the stamp to be easily removed from the surface with little resistance.

The procedure for creating a stamp begins, in the main ,with the fabrication of a master by photolithography[34]; however there are a variety of techniques that can be used. The PDMS is then cast onto the mould and allowed to cure and take the

shape of the master. When the PDMS has solidified, normally at temperatures around 80 °C the PDMS is removed from the mould of the master, which can then be reused.

The mould or stamp is then wetted with the thiol and allowed to settle to allow the absorption of the thiol into the PDMS[35]. The solvent evaporates from the surface over time and any remaining solvent is dried under a stream of nitrogen. The non – polar thiols including n – alkanethiols will generally diffuse into the stamp when in contact – the same cannot be said for polar molecules[36]; they generally require a further step to aid wettability of the stamp and ensure a good general coverage.

Once dry the stamp is brought into contact with the gold surface and the process of diffusion begins between the thiols and the surface and the formation of the SAM is complete as shown in Figure 3.[37]

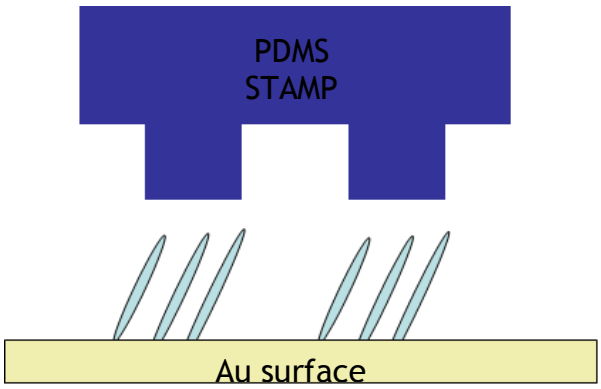

Figure 3 Schematic representation of stamp transferring thiol to gold surface in a predetermined pattern.

This technique forms the basis of many applications for microcontact printing.

1.2.8 Patterning proteins and other biomolecules

Another purpose for microcontact printing is the addition of biomolecules such as cells and proteins in a patterned array for use as biosensors and in molecular electronics[38]. This, coupled with its use in cell biology[39], proves that microcontact printing and the subsequent addition of biomolecules to a surface is an important technique.

The patterning of cells on a surface offers the ability to control cell adhesion and growth to particular molecules to which it has an affinity and hence it is possible to study cell behaviour. It is cell shape which governs if a cell will die[40], and so patterned surfaces offer an environment where this can be studied.

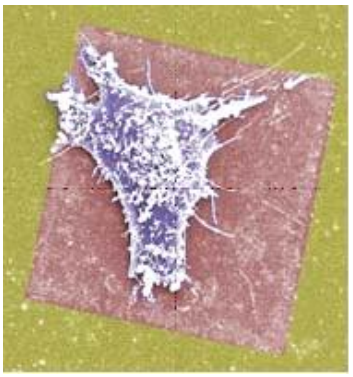

Figure 4 SEM image of a cell on a patterned gold surface. The cell is comfortable to exist on the patterned surface [41]

In order for cells to proliferate they must be adhered to a surface and once the proliferation yields enough cells for them all to exist comfortably without overcrowding, the process will stop[42]. It is the extracellular matrix proteins which allow the adhesion of the cells to a surface, these include fibronectin, vitronectin and laminin[43]. As described by Chen *et al*[40], surfaces of sizes ranging from 5µm to 40µm squares were coated with fibronectin and the adhesion of human capillary endothelial cells were studied.

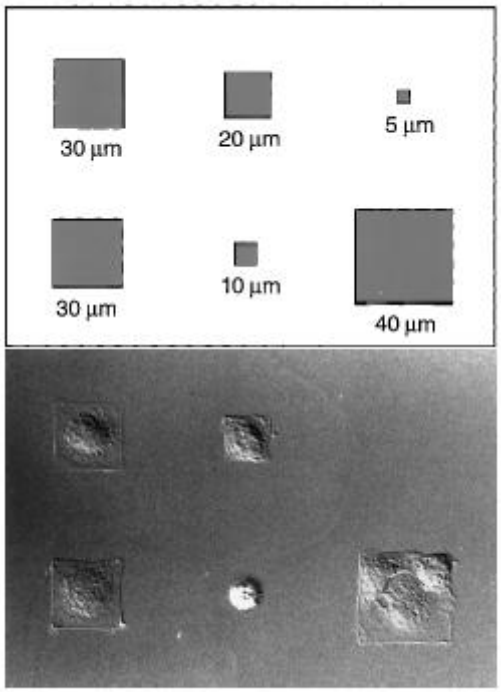

Figure 5 Top -Schematic diagram showing the dimensions of the patterns used to attach the cells to the surface. Bottom- A view of the manner of which the bovine adrenal capillary endothelial cells adhere to the surface, as studied by Chen et al [40].

Cells undergo suicide or “apoptosis” when exposed to surfaces which do not allow their adhesion. Putting the cells into a variety of different environments allows their behaviour to be studied and controlling cell growth offers great potential for understanding cell life and death.[44]

It has been found that the addition of proteins to a patterned surface is a difficult procedure due to the fact that the chemicals used in the technique often denature the protein and render them useless.[45] Using microcontact printing to pattern proteins on a surface has the obvious advantages of being a cheap and relatively simple method to carry out[43]. As mentioned previously the ability to functionalise the terminal region of a self assembled monolayer is an important tool and the alteration of the functional group can be carried out with relative ease. The hydrophobicity and charge of the surface can be altered in such a way that will allow specific proteins to interact with the terminal functionality and physically bind to the surface, retaining much of their activity[46]. The opposite is also true. There are certain functionalities, *e.g.* oligo (ethylene glycol) groups which when bound to a surface resist the binding of proteins and as such surfaces can be produced which will selectively bind proteins in certain areas resulting in a patterned array of biomolecules[42].

The physical addition of proteins is a reversible process which takes advantage of the electrostatic and hydrophobic interactions which exist between the protein and the surface. This is in contrast to the chemical addition of proteins, which can lead to some of the protein activity being lost due to the nature of the process. Chemical addition means there is a covalent bond formed between the protein and the surface, resulting in a strong irreversible bond being formed[46]. Both methods have their advantages and disadvantages.

The physical adsorption of proteins onto a surface is carried out by the preparation of self assembled monolayers with terminal regions containing hydrophobic and charged areas in order for the proteins to interact with these sections. The chemical attachment of the protein to a surface involves the formation of an amide bond. A SAM is formed with a carboxylic acid terminal region. To this, *N*-

hydroxysuccinimide and EDC are added to the terminal region resulting in a self assembled monolayer terminated with an NHS ester. The addition of the protein to this occurs through the reaction between this ester functionality and the lysine residues of the protein.

The analysis of the surface is often carried out by microscopic techniques such as Atomic Force Microscopy (AFM) which can give insight into the spatial distribution of molecules on the surface and measure forces of interaction between biomolecules[47].

The addition of DNA to a surface is a well documented process, which has been carried out by various techniques and for a variety of reasons.[48] As mentioned previously the addition of biomolecules to a solid surface is important in many areas of science and the addition of DNA is at the forefront of this ever growing region, primarily as it allows a deeper understanding of this important molecule and again is increasingly important in areas such as nanotechnology and in particular biosensing.[48] In a similar manner to the way proteins can be patterned directly onto a surface, it has been demonstrated that DNA can also be added through direct microcontact printing of the DNA molecule.[49]

1.3 **Inorganic materials**

1.3.1 Polyoxometalates

Polyoxometalates (POMs)[50] are a class of compounds currently enjoying widespread interest.

Inorganic metal oxides clusters, POMs are made from individual MO_x units where M can be a transition metal such as V, Mo and W. POMs share the same general structure where a variety of clusters can be produced with low to high level nuclearites, containing metal atoms in the region of 6 – 368 in a single cluster. The study of POMs has expanded in the last decade due to advances in X-ray diffraction and it is this, coupled with their semi conducting, magnetic, thermal, photochemical properties and their versatility that have launched these materials to the forefront of materials science[51].

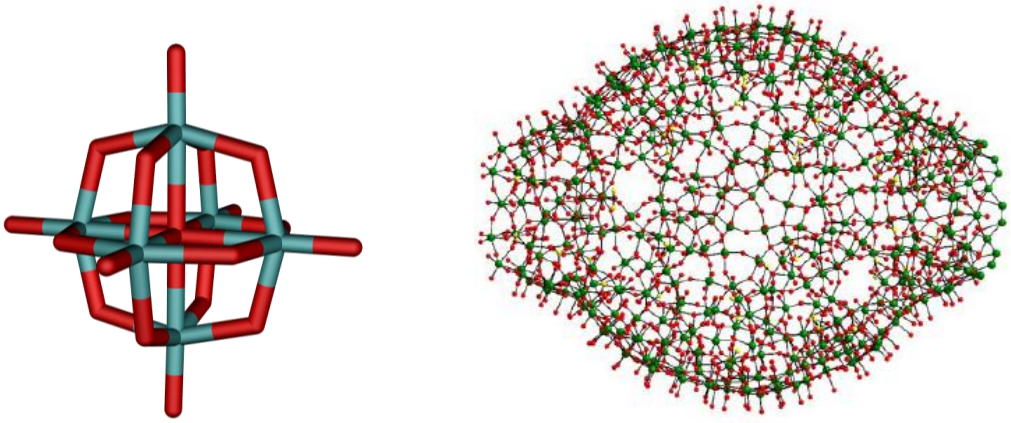

Figure 6 Representation of a POM building block and large POM cluster, LHS M=6 and RHS M = 368

The diverse structural characteristics and the vast range of potential applications are drawing widespread interest. The clusters have a high level of stability and rich redox chemistry and it is these properties that have led to them being established as an important class of molecules. The development of POMs in areas as diverse as catalysis[52], surface science[53], molecular materials[54] and as sensors[54c,d] as well as moving in to areas such as nanotechnology[55], biology[53,56], anti cancer and anti-viral applications [57] has only highlighted their diversity and earned them the right to be thought of as a division of inorganic chemistry in their own right.

1.3.2 Synthesis of POMs and general structure

The general synthesis of POMs is represented by the following equation outlining the acid condensation of $[MO_x]$ units with the loss of water, again using the transition metals Mo, V and W in the main.

$$36[MoO_4] + 72H^+ \rightleftharpoons [Mo_{36}O_{112}]^{8-} + 36H_20$$

Scheme 1 scheme demonstrating the general synthesis of POMs

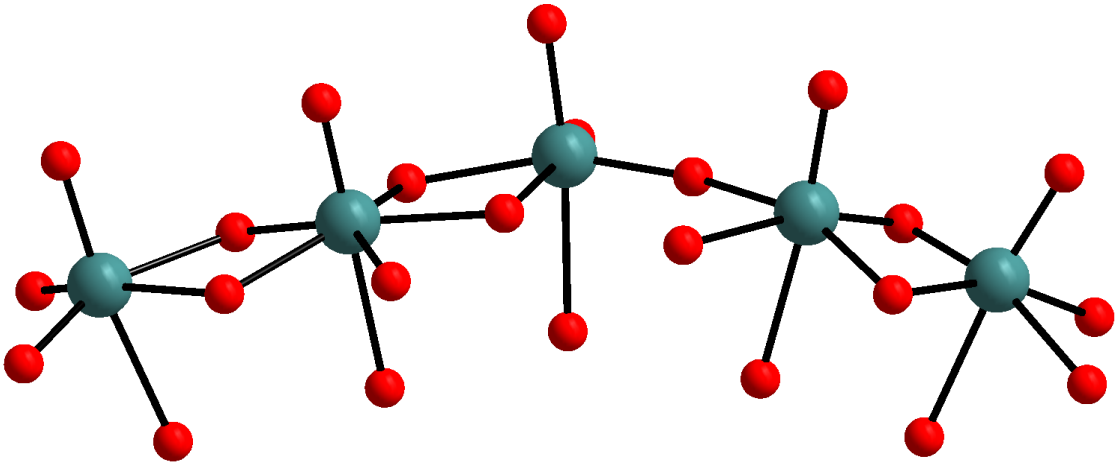

Figure 7 Schematic representation of POM structure and bonding.

A number of parameters dictate the structure including pH, temperature and the solvent used to carry out the reaction; the sheer number of parameters that exist give rise to molecules with an incredible variety of structures some of which are detailed below:

1. pH and type of acid
2. concentration
3. type of metal oxide anion
4. type and concentration of electrolyte
5. heteroatom concentration
6. additional ligands
7. temperature
8. solvent
9. reducing agent

The clusters are linked through metal oxide units which are further linked through edge, corner or face sharing principles. The early transition metals described previously form POM clusters more readily than other transition metal due to the

presence of the empty d-orbitals for the metal –oxygen π bonding, their ionic radii and the charge on the molecule.

There is a hierarchy that exists to broadly classify POM clusters which can be broken down as follows:

1. Isopolyanions – MO clusters that contain a single metal type with no internal heteroatom often making these molecules relatively unstable. However this instability is insignificant when compared to the vast number of interesting properties these clusters exhibit. Their high charges coupled with the strongly basic oxygen surfaces make these clusters an excellent starting point for the development of novel materials.

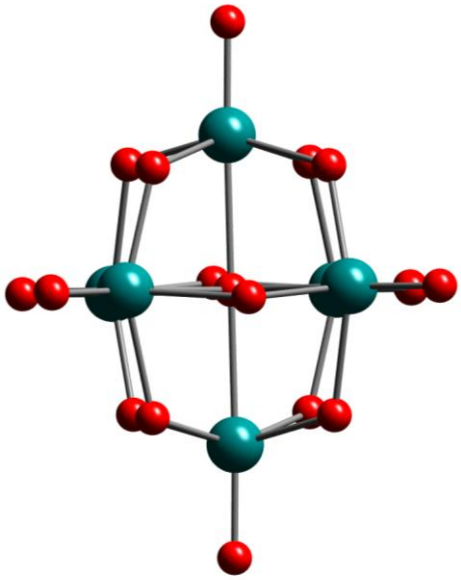

Figure 8 Representation of the $[Mo_6O_{19}]^{2-}$ isopolyanion. $Mo^{VI}O_6$ = Teal, O = Red spheres.

2. Molybdenum blues and browns – in relation to a discovery by Scheel in 1783[58] these clusters were pioneered by Muller et al from 1995 where the synthesis and characterisation of a $\{Mo_{154}\}$ cluster was reported. The relatively simple methodologies used to create molybdenum blue species is what makes this sub section of clusters so interesting. These molecules can achieve nuclearities of up to 368 molybdenum centres and yet these giant molecules are constructed through self assembly into clusters that can achieve sizes similar to that of proteins as demonstrated in Figure 9

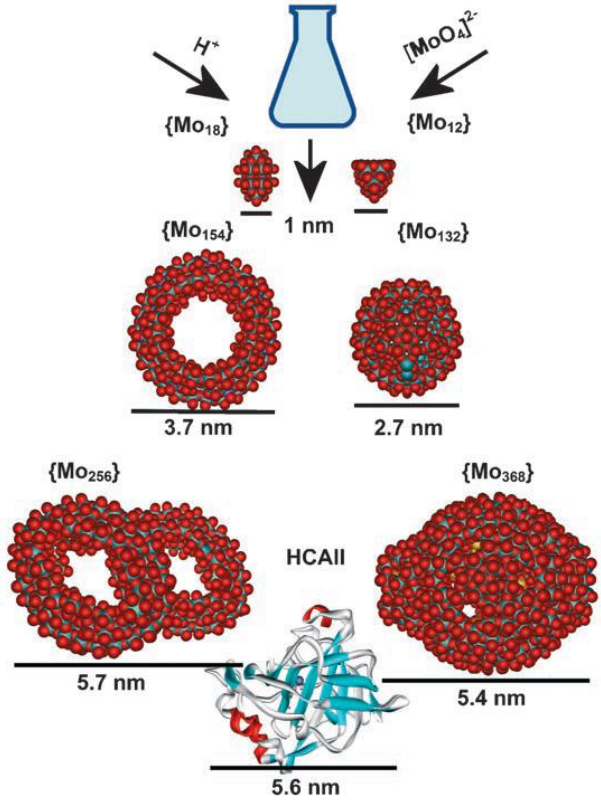

Figure 9 Schematic demonstrating the "one pot" formation of POMs that can be in some cases be comparable size to proteins.[55]

The work by Muller et al has uncovered some of the largest POM clusters known.[59] These giant wheel clusters are remarkable in that their assembly comes from a "one pot" methodology. Each of the building blocks must be thought of individually. The simplest being the $\{Mo_1\}$ unit that can exist either as an octahedral species or instead the unit can edge share with 5 other $\{Mo_1\}$ units to create an $\{MoO_7\}$ species with a pentagonal bi-pyramidal structure. This unit can then act as a template for $\{Mo(Mo)_5\}$ units that form the basis for many of the giant wheel type architectures. It is this component that gives the clusters their ring shaped arrangement and adds curvature to the surface of the clusters.

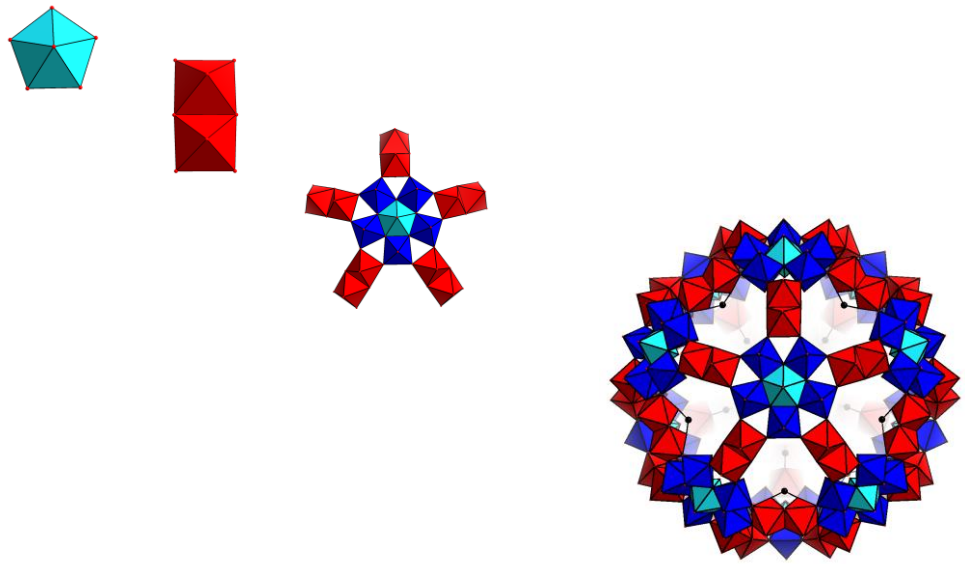

Figure 10 Graphical representation of the basic growth principle involved in the construction of the $[Mo_{132}O_{372}(CH_3COO)_{30}(H_2O)_{72}]^{42-}$ molybdenum blue cluster by sequential aggregation. $\{MoO_7\}$ = Light blue polyhedra, $\{Mo_2O_{10}\}$ = Red polyhedra, $\{MoO_6\}$ = Dark blue polyhedra.

The most famous of these clusters is the 368 molybdate centre cluster which utilises the $\{(Mo)Mo_5\}$ units as well as {Mo1} and {Mo2} components, and is often thought of as a lemon shaped cluster.

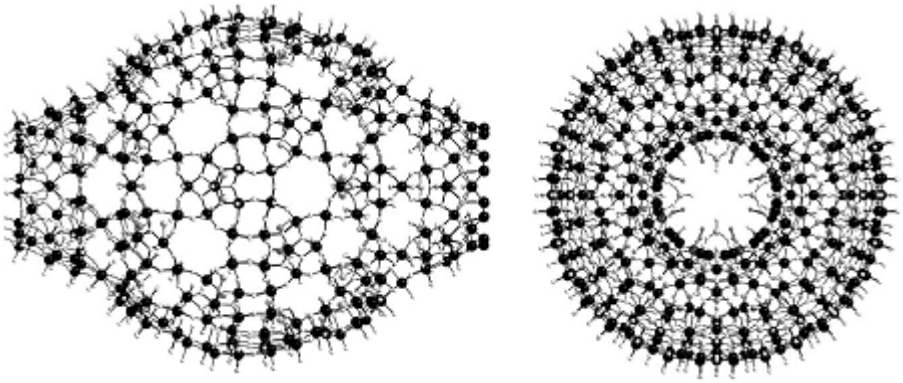

Figure 11 Representation of front and side on view on the Mo 368 cluster.

The discovery of the $\{H_xMo_{368}O_{1032}(H_2O)(SO_4)_{48}\}^{48-}$ has led the way in designing architectures of similar size and also the continued study of the self assembly process that governs this class of molecule.

3. Heteropolyanions represent the widely studied area of these clusters. They are a class of metal oxide clusters with the addition of heteroanioins such as SO_4^{2-} and PO_4^{3-}. An example of such a molecule is the Keggin anion, with the general formula $[XM_{12}O_{40}\}^{n-}$ where X can be any main group element. The Keggin cluster can undergo hydrolytic removal of tungstates

to yield a lacunary species under basic conditions. Other cluster types in this section include the Dawson structures. [60]

Dawson type clusters have the general formula $[X_2M_{18}O_{62}]^{n-}$ and at present only Mo and W are the primary transition metals in the polyanion. As such these molecules do not exhibit the diverse range of chemistries that the Keggin clusters do due the spatial constraints within the cavity of the cluster. An interesting example of such a cluster is the Dawson type mixed valent POM $[Mo_{18}O_{54}(SO_3)_2]^{2-}$ which shows some interesting electronic properties. [60] The general structure shows two pyramidal sulphite anions encapsulated within the metal framework. Within this cavity the two S atoms form an interaction between the two lone pairs of electrons of the two anions. The interesting feature of this molecule lies in the study that resulted in a fully reversible colour change on heating the cluster from 77 K to 500 K. This is due to the partial electron loss from the sulfur atoms to the cluster shell, the colour change and cluster are shown in Figure 12

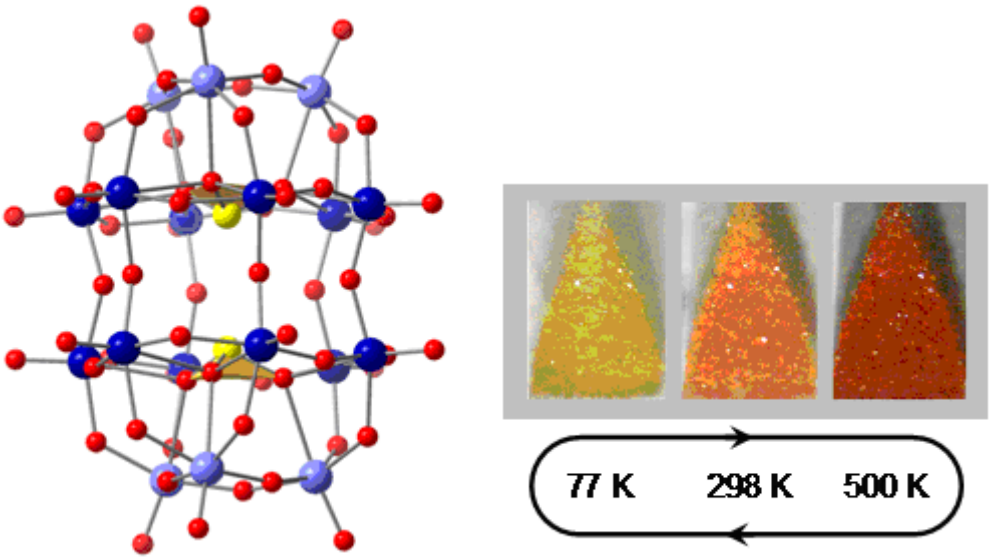

Figure 12 Schematic representation of the Dawson cluster with the 2 central S atoms highlighted in yellow. RHS shows the cyclic colour change on heating the cluster from 77 K (yellow crystals) to 500 K (red crystals) [60]

This molecule will be examined in more detail in later sections.

1.3.3 Applications of POMS

What makes POM clusters such an interesting subsection of inorganic clusters is the sheer variety of applications and it is extending these applications that forms

the basis for this project. The ability to produce clusters that have a function is essentially the purpose of their formation – and in understanding how the clusters are formed imparts knowledge that can be utilised to selectively design new and interesting materials with a useful function. As such POM clusters have already achieved status within the following fields:

1.3.3.1 Catalysis

Catalysis is probably the application which most dominates both the POM literature as well as continued study of these molecules. Indeed catalysis is potentially the most lucrative application in the development of POMS.

Currently used in several industrial processes, POMs exhibit activity in a number of reactions including redox reactions and a variety of acid base catalysed processes. The sheer scope of research is led by groups such as Hill[61], Finke[62], Neuman[63], Kozhevnikov[64], Misono[65] and Mizuno[66].

Research by Hill *et al* from 1989 showed the use of POMs, in particular $H_3[PN_{12}O_{40}]$, $H_3[PMo_{12}O_{40}]$ and $TBA_4[W_{10}O_{32}]$ clusters to catalyse reactions such as the dehydrogenation of saturated hydrocarbons.[67]

The discovery by Kozhevnikov *et al* details the use of heteropolyacids, in particular a Keggin HPA [68], to create an environmentally friendly alternative to acetylation reactions that require the use of acyl chlorides/anhydrides as either Lewis acids ($AlCl_3$) or mineral acids (HF). The use of the Keggin HPA reduces the volume of waste products and is recovered fully functional at the end of the reaction.

1.3.3.2 Nanothechnology

Nanotechnology is a new area for POM development and a recent study indicated that a POM cluster could be used as a functional nanomaterial.[69] The Keggin core of $[PMo_{12}O_{40}(VO_2)]^{9-}$ is the key to the mechanism of action. This core harbours electrons that can be transferred from the molybdenum centres which can then couple the vanadyl groups magnetically – leading to a cluster that can have its spin state controlled electronically.

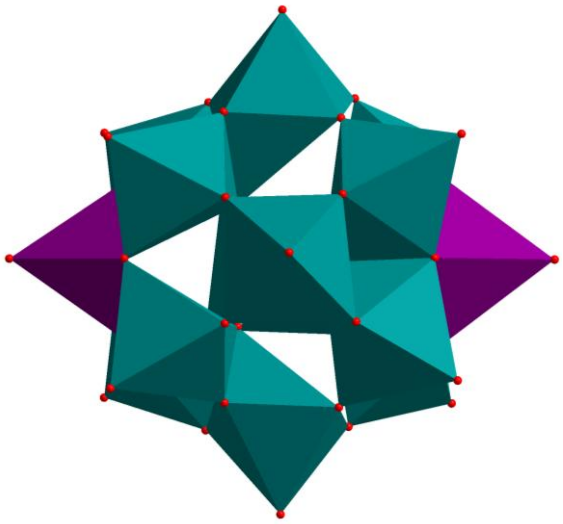

Figure 13 Polyhedral representation of the $[PMo_{12}O_{40}(VO)_2]^{q-}$ polyanion[70]. $Mo^{VI}O_6$ = Blue polyhedra/spheres, VO_5 = Purple polyhedra, O = red spheres

1.3.3.3 Anti – Viral activity

What makes POM clusters interesting molecules to be targeted as potential drug candidates is perhaps the large number of clusters available that have not yet been tested for any potential activity. The vast library of compounds available means there is a complete range of molecules that have the potential to be exploited within the pharmaceutical market. This is highlighted by the fact that at present there are a number of POM clusters that show some anti viral activity and are currently been used in tissue cultures as anti viral agents.[71]

One of the most interesting revelations in POM science has been the discovery that the monosubstituted Dawson clusters have been shown to be effective at inhibiting the HIV-1 virus with EC values, the half maxima concentration, also known as the potency, in the region of 0.1-0.83 µM. What is important about this discovery is that the molecules have low toxicity with IC50 values, that are between 50 µM and 100 µM[71], representing the maximal inhibitory concentration which gives information about how effective a chemical is at inhibiting a biological application.

In recent years, computational studies have postulated that the method of interaction is through the POMs binding with the cationic site of the virus. This is located close to the active site and so is thought to work by inhibiting the action of the HIV–1P enzyme.

Whereas these results show a promising route to the potential use of POMs in medicine, the drawback remains that these molecules are incredibly difficult to excrete from the body and will eventually reach toxic levels. Finely tuning the structures could perhaps lead to molecules where these issues are overcome.

1.3.4 Organic inorganic hybrid molecules

A major area of interest at present is the formation of inorganic – organic hybrid clusters[72]. Such molecules not only have interesting structures but their development could lead to new and interesting applications.[73]

In the past, the classification of such molecules are split according to the bonding between the organic and inorganic components. In general Class 1 would consist of molecules whose structures are based on weak interactions between the organic and inorganic component *e.g.* Van der Waals, ionic radii and hydrogen bonding. For Class 2, this consists of molecules where strong chemical bonds between the organic and inorganic material exist.

Recently, however, the classifications have changed in order to understand the interaction and the development of these clusters in more detail. Looking at the molecules in terms of host-guest relationship within the structure, the clusters can be divided into organic–inorganic materials (OI), where the organic molecule plays host to the inorganic portion, and inorganic–organic (IO) materials where the converse is true.

Interesting work by Hasenknoph *et al* shows the derivitisation of the Anderson type POM $[MMo_6O_{18}\{(OCH_2)_3CNH_2\}_2]^{3-}$ where M = Mn^{III} or Fe^{III} which shows the grafting of the organic moieties onto the metal frameworks[74]. Initial studies showed the Anderson structure can be capped with 2 tris(hydroxymethyl) methane segments on both sides of the structure, chosen because one side of the moiety could attach to the cluster and the other side has the potential to develop a coordination site. Initial studies concentrated on incorporating this moiety with the Anderson[74a], Dawson[75] and some other POMs. This work and the work of others has led to the development of this sub section of POM chemistry and uncovered interesting physical and structural characteristics that will be discussed in later sections.

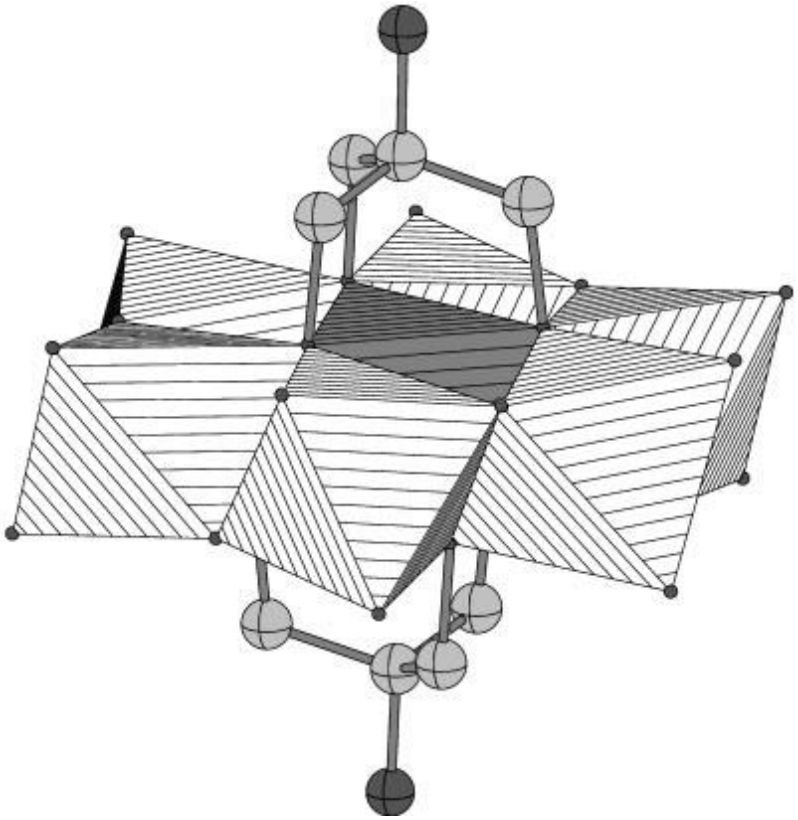

Figure 14 Schematic representation of the Mn Anderson cluster with the tris derivative in place [74b]

The use of aromatic compounds to derivitise is a popular choice in the rational design of organic-inorganic clusters, and in particular organo-imido compounds are generally favoured.[76] This is due to the added stability gained through the presence of the imido-metal link coupled with the organic π electrons that are delocalised within the POM cluster.[77] An example of such modification is the derivitisation of the molybdates $[Mo_6O_{19}]^{2-}$ to a phenanthroline ligand subsequently altering the electronic properties of the cluster through charge transfer.[78]

For this project the development of organic-inorganic hybrid clusters is critical. These molecules however are sought after for a reason – the difficulty in producing such molecules that have the potential for other functions has long since been the limiting factor. Not only does tethering organic molecules onto POM clusters offer new structural diversity and of course properties, their development may lead to a greater understanding of how POMs are formed.

1.4 **Organic materials**

Interesting discoveries in organic chemistry have led to the development of a one-pot, three step reaction yielding dihydro-imidazo-phenanthridinium bromide (DIP)

molecules from 2-bromo ethyl phenanthridinium bromide and a primary amine as seen in Scheme 2.[79]

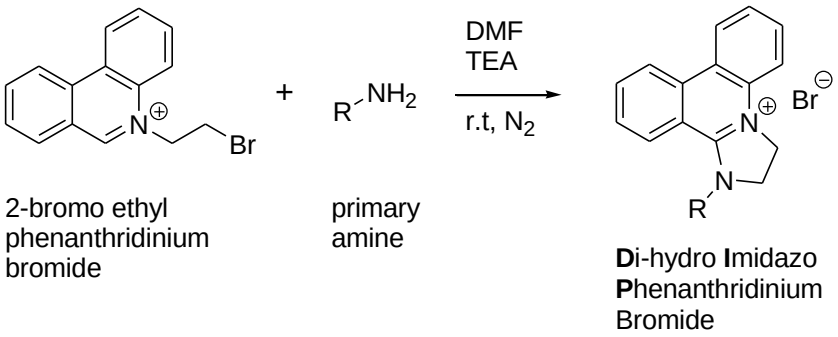

Scheme 2 Reaction of 2-bromo ethyl phenanthridinium and a primary amine to form DIP

The synthesis of extensive libraries of DIP cations has been a major focus of work by Cronin *et al*. These molecules contain various interesting structural characteristics[79-80] that have been explored. In particular extensive DNA binding experiments have been carried out on a number of these compounds giving positive results. An example of this is viscosity measurements that have demonstrated that once bound to the DNA there is significant lengthening of the DNA strand indicative of DNA intercalation. [81]

With this in mind, molecular modelling studies have also been carried out demonstrating the method of DNA-DIP interactions and significantly some results showed positive indications that the R- group connected to the primary amine may in actual fact facilitate binding by interacting with the DNA's minor groove a representation of which is shown in Figure 15.

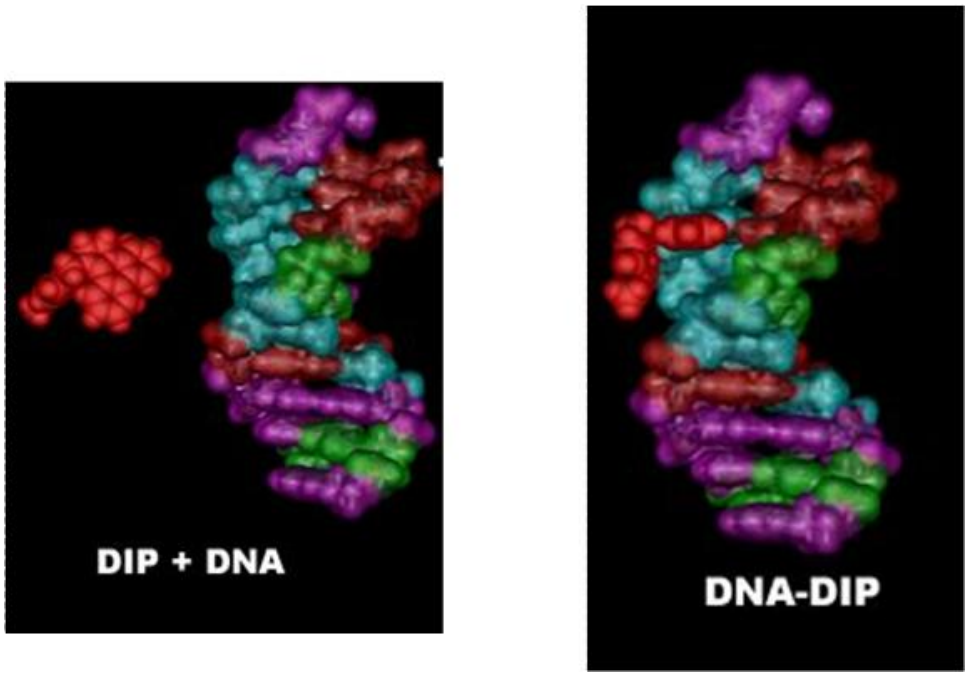

Figure 15 Representation of the proposed method of intercalation – the DIP can be seen to bind to the minor groove of the DNA

The initial studies began by tailoring the R- group in order to maximise DNA interaction. What was it about the R- group that made that particular heterocyclic compound a "good" intercalator? This question led to studies being carried out to understand the possible connection between structure affinity for DNA and cytotoxicity and so a library of compounds was developed.

It is here that another target for the DIP reaction was considered. As primary amines are the requirement for the reaction to go to completion – could amino acids be the target and therefore proteins? This could be of particular interest to lysine, a residue that contains a primary amine exposed on its side chain.

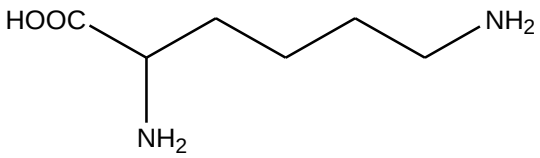

Figure 16 Schematic representation of lysine residue which could be a potential target for the DIP formation on the free primary amine of this amino acid.

The development of such a reaction could hold the key to producing biologically active molecules being decorated with a DNA intercalator which has the potential for many interesting applications.

The DIP moiety is an interesting addition to a protein due to its affinity for DNA and cytotoxity towards ovarian cancer cell lines. DIP binds to DNA through the intercalation between base pairs and the planar poly-aromatic section of the DIP molecule. Previous research has concentrated on the synthesis of monomeric and dimeric DIP molecules.[82] It seems likely that the more DIP molecules on the molecule, the more sites for DNA intercalation, thus polyvalent systems are an interesting set of molecules. Initial synthetic routes led to production of polyvalent systems that were extremely insoluble in aqueous media, a property essential for possible drug candidates. In order to overcome this problem it was thought that proteins would make an ideal starting material for the production of polyvalent intercalators. Not only would this be a breakthrough in the solubility problem but would also create an interesting starting point for these modified proteins to act as

carriers to direct the DIP moiety into specific cells, utilizing a protein's ability to move in and out of the cell.

2 Analytical Techniques

The following section describes the analytical tools common to some or all chapters within this thesis. Reactions specific to different sections will be described within the relevant chapter.

2.1 Atomic Force Microscopy (AFM)

AFM has revolutionised the manner by which scientists can visualise a surface.[83] Following on from IBM's Scanning Tunnelling Microscope (STM) which allowed, for the first time, the ability to visualise single atoms on a surface,[84] the AFM was developed to allow surfaces carrying biological material to be studied. Whereas the STM required a conducting surface the AFM did not therefore allowing for the first time biological surfaces to be mapped.

The AFM works on the principle that a cantilever maps the surface of the material as it is being moved by small piezoelectric crystals. As can be seen from Figure 17 the laser beam is focussed on the back of the cantilever where it is reflected towards a position sensitive photo detector. As the cantilever/tip scans the surface it will encounter different surface topographies and the deflection of the cantilever in relation to this will, in turn, deflect the laser beam to a different position which will then be converted by the photo detector to an electrical signal.

Contact mode AFM is the original mode of use. As the name suggests the cantilever is in continuous contact with the surface and the surface below is moved to allow the surface topography to be mapped. This method has several disadvantages; one in particular, the potential for damage to be caused to the surface by the cantilever as it comes into contact with it, the tip could in fact remove the material from the surface and in turn damage the tip with great expense and inconvenience.

Tapping mode AFM is the most commonly used technique to map the topography of a surface.[85] It does so by lightly oscillating at its resonance frequency, "tapping" the surface as it moves across it, therefore reducing any issues observed with contact mode since it is essentially not running across the surface. What is also an

advantage of tapping mode AFM is the fact that it overcomes limitations that can occur when samples are being analysed in air. With contact mode there is an issue with the fact that the samples often form a thin layer of liquid on top causing the cantilever to get stuck. With tapping mode, however, this is not the case as the amplitude of the cantilever oscillation is in the region of ~ 10 nm. The tip will then be able to clear the surface without getting stuck; this overcomes the issue with performing contact AFM at slower speeds.

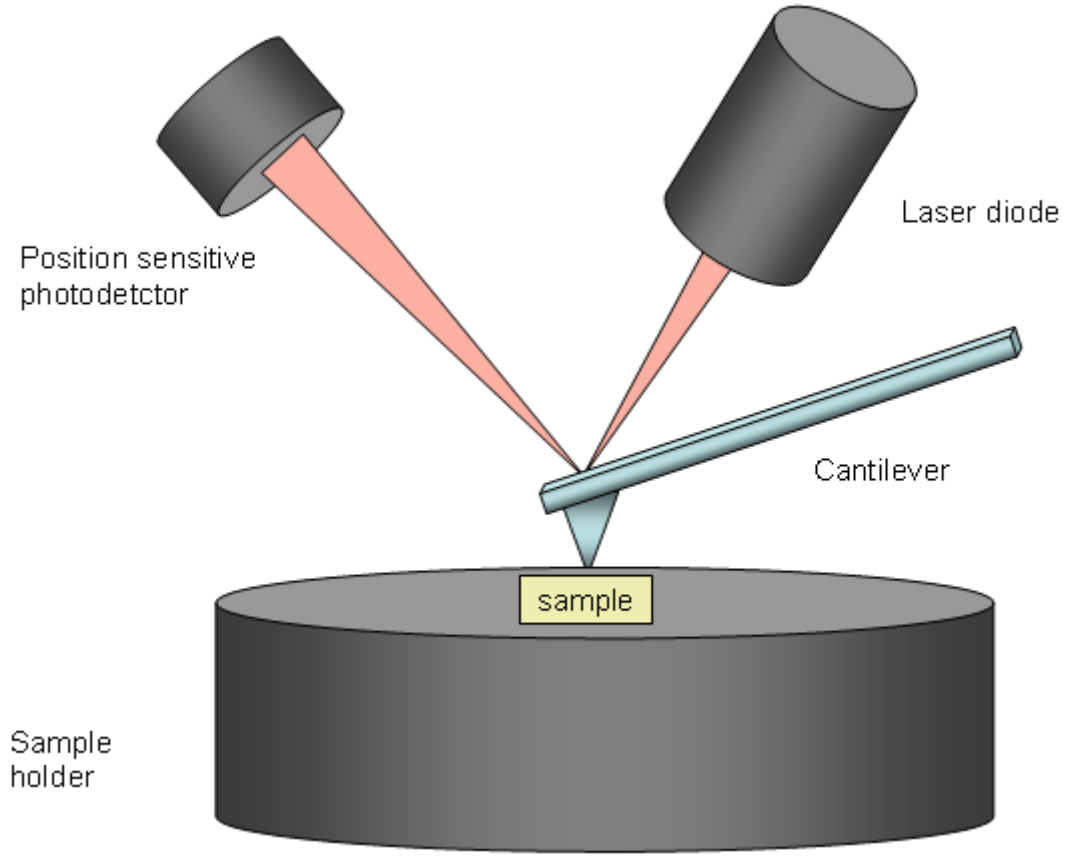

Figure 17 Basic structure of an AFM equipment depicting the laser beam hitting the back of the cantilever which detects any variation on surface topography which can then be recorded as an image.

In general, Tapping Mode is much more effective than non-contact AFM for imaging larger scan sizes that may include large variations in sample topography.

2.2 **Scanning electron Microscopy**

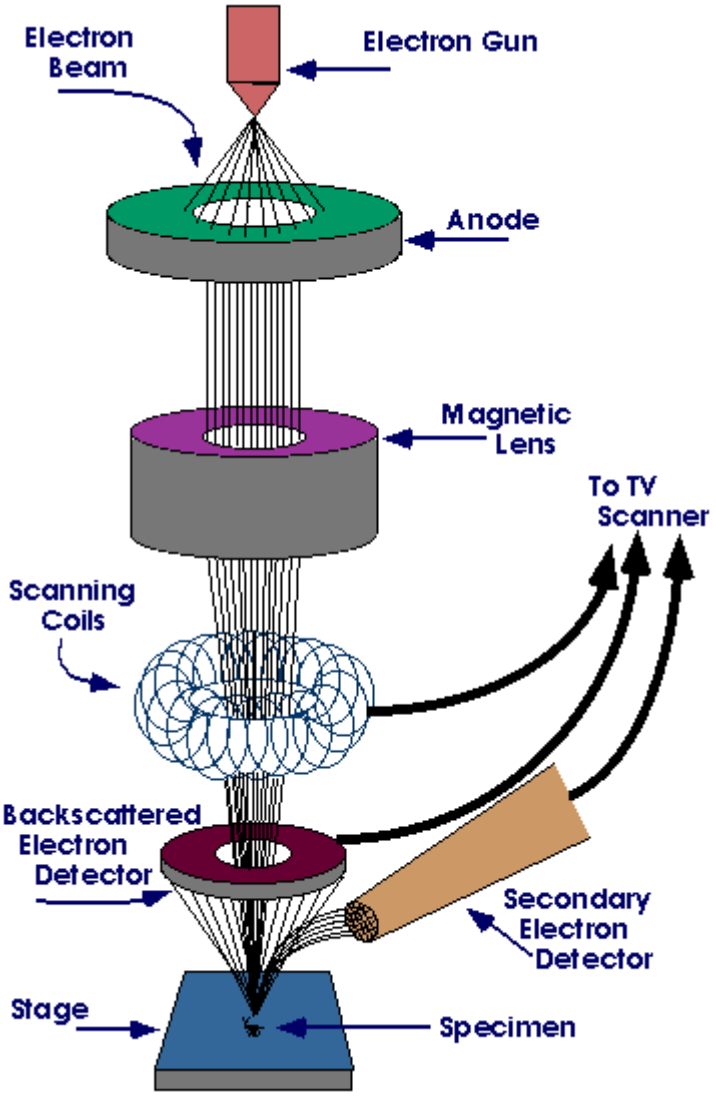

Figure 18 Schematic representation of the mechanism of action of SEM.[86]

The development of Scanning Electron Microscopy (SEM) in 1935 by Max Knoll [87] and the continuation of this work through to 1938[88], with the eventual production of the first instrument in 1965 has had a major impact on the applications of microscopy due to the variety of surfaces that can be observed using relatively simple methodology. [89]

The microscope works on the basis that an electron beam, typically 40 keV, is projected onto a sample as shown in Figure 18 in a raster fashion as the beam is focussed on both the x and y axis of the sample. When the electron beam reaches

the surface, the interaction of the electrons with the atoms on the surface causes secondary electrons to be released via inelastic scattering, this process forms the basis for the image formation.

The secondary electron beams are amplified and detected by a cathode ray tube with different intensities displayed as variations in brightness giving an image of the topography. [86]

For this project all SEM was carried out using the Hitachi – S800 model.

2.3 **Time of Flight Secondary Ion Mass Spectrometry**

Time of Flight Secondary Ion Mass Spectrometry (ToF SIMS) is a technique that is used to map the full chemical composition of a surface. It utilises primary ions (namely Bi_3^+, Au_n^+, C_{60}^+, Ga^+) to bombard the surface with an energy in the keV region. The extensive energy from these ions transfers to the molecules on the surface giving them well in excess the energy required to overcome the surface binding energy. Of the particles released, it is the negatively and positively charged ions that are of interest and the mass (m) to charge (z) ratio is analysed to give a detailed identification of the chemical composition of the upper 1-3 monolayers of the surface.[90]

Time of flight analysis is based on the principle that molecules of varying mass travel at different velocities. The secondary ions released from the surface during bombardment from the primary ions are accelerated by the electric field to a common kinetic energy in the extractor, Figure 19.

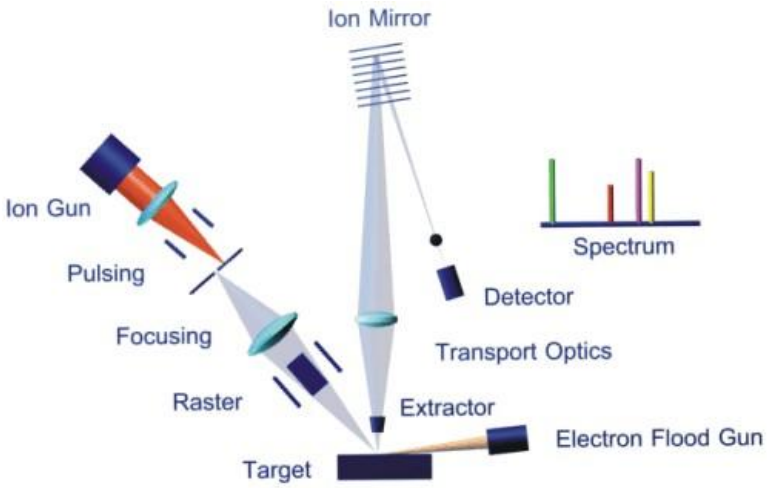

Figure 19 Schematic of a ToF-SIMs showing the orientation of the ion gun bombarding the surface with primary ions and the detector that analyses the secondary ions emitted using time of flight mass spectrometry.[91]

Fragments of smaller mass will travel at a higher velocity through the system than those of a higher mass and as a result the differing velocities can be measure. As the kinetic energy is constant, the determination of mass using $E_K=1/2\ mv^2$ can be used to determine the resulting mass of the fragment leading to the entire surface being mapped.[90] Each feature on the resulting image is accompanied by its own mass spectrometry analysis and this analysis builds up a detailed picture of the surface and its components as shown in Figure 20.

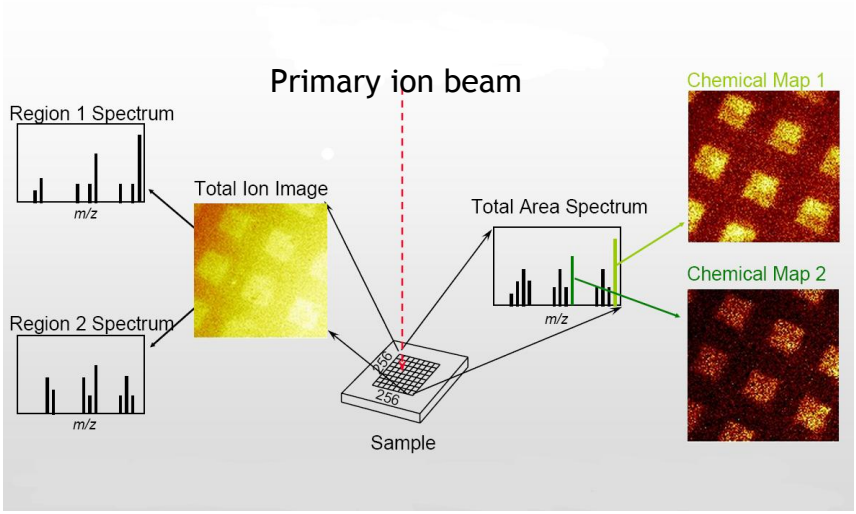

Figure 20 schematic representation of the ToF-SiMs operation showing the resulting mass spec profile and the chemical map image of the surface.[92]

2.4 **Transmission Electron Microscopy (TEM)**

TEM is a technique that images solid materials at atomic resolution. Similar to an optical microscope the TEM can gain information about the material structure and elemental and chemical analysis. Whereas an optical microscope utilises photons and optical lenses to create an image, TEM uses a source of high energy electrons (>100 kV) and electromagnetic lenses to create the image as is demonstrated by the schematic in Figure 21.

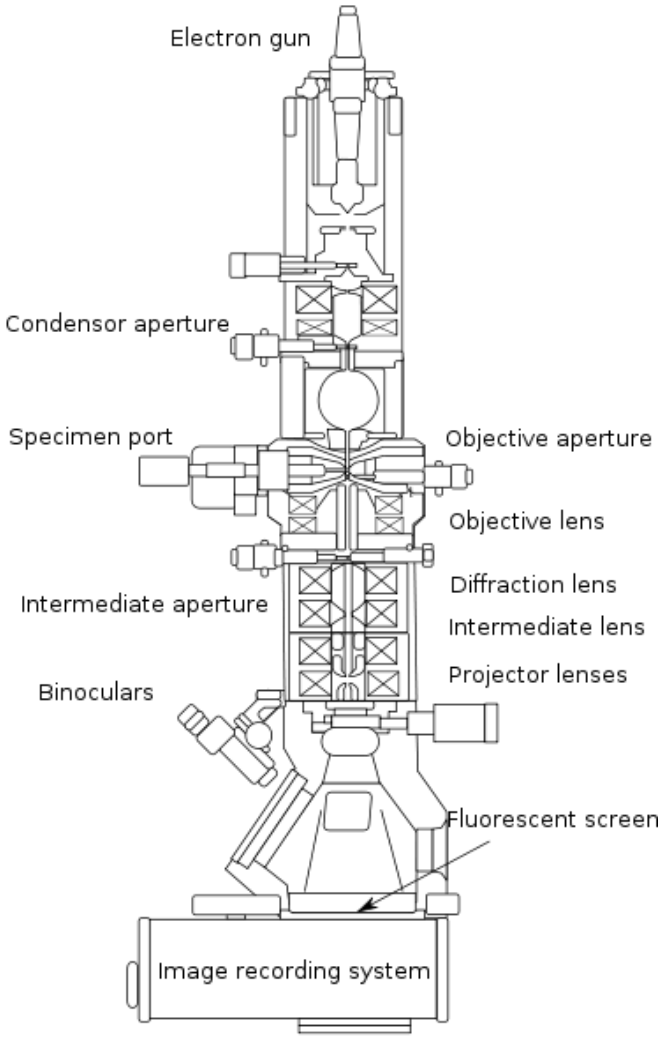

Figure 21 Image depicting a Transmission Electron Microscope.[93]

The electron beam is passed through the sample and an image is formed. With the aid of the lenses and using much smaller wavelength electrons means that an image at resolution 0.2 nm can be achieved through TEM. When imaging a surface the interaction with the sample is important. Darker images are created by heavier elements due to the scattering of electrons. Additionally diffraction contrast can be obtained from scattering from crystal planes allowing the ability to

distinguish between different materials. Since electron beams are invisible to the naked eye, the image is transferred to a fluorescent screen and is photographed.

2.5 **Protein purification via dialysis**

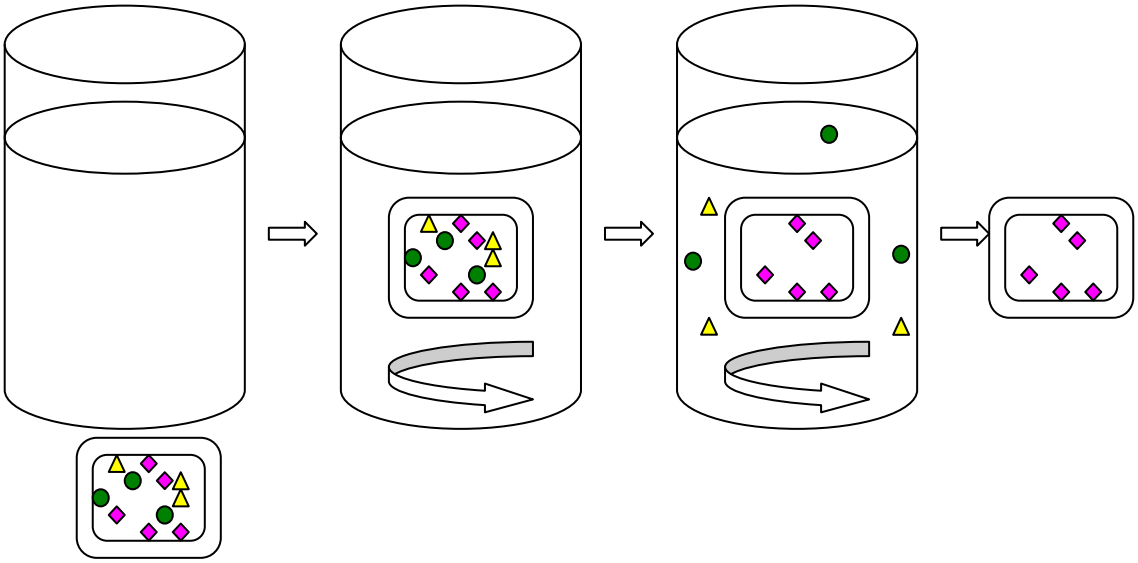

Figure 22 Schematic representation of dialysis of the modified protein showing removal of impurities through the dialysis membrane into bulk solution.

The basic principle of protein dialysis is to purify the protein mixture and remove any impurities, unreacted material and salt. This is achieved by placing the solution of protein within a dialysis bag that contains pores of a particular size which allow impurities to pass through whilst keeping the protein within the dialysis bag. The pore size is characterised according to the molecular weight of the protein and so it is crucial to choose a dialysis bag with pore size smaller than the molecular weight of the protein to ensure that the protein is not leaked to the bulk solution. With several changes in the low salt buffer this ensures the continual movement of salt and impurities from the dialysis bag and into the bulk solution outside as can be seen from Figure 22.

2.6 **Electron Spray Ionisation Mass Spectrometry**

Electron spray ionisation mass spectrometry is a relatively new technique used to give information on large biomolecules that were previously difficult to characterise. The process produces ions that are then able to be characterised by mass spectrometry.

The method of action for this technique relies on the analyte being introduced into a system through a syringe in liquid form. From here the solution is passed through an electrospray needle that has a high potential difference applied to it. Once in the vacuum chamber the charged droplets emitted from the syringe are attracted towards the sample electrode and are repelled by the needle head; in this process the volatile solvents used to carry the molecule of interest begins to evaporate. During this evaporation phase the droplets reach the “Rayleigh limit”, the point where the surface tension succumbs to the charge and the droplet essentially explodes. This produces a cascade effect of smaller droplets as well as the free charged analyte molecules. The analytes can at this stage hold single or multiple charges. Mass spectrometry subsequently allows the analysis of the molecules in relation to the mass to charge ratio.

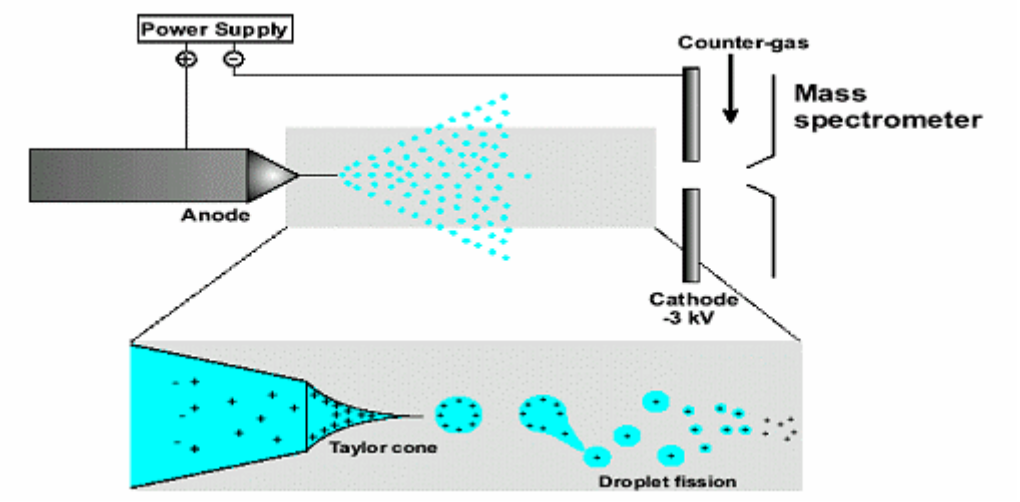

Figure 23 Demonstration of the process of ESI MS outlining the injection of the solvent containing biomolecules into the chamber and subsequent detection.[94]

2.7 **Circular Dichroism Spectroscopy**

Circular Dichroism (CD) spectroscopy is a technique used to determine the structural features of proteins.[95] The general principle of this technique uses the left and right components of circularly polarised light which are absorbed by chiral chromophores.[96] [97]The chromophores chirality can be either intrinsic, occur through bonds forming a chiral centre, or placed in an asymmetric environment. [95] The CD spectrum is measured over a range of wavelengths giving rise to a spectrum that is indicative of the structural features that exist within a protein and it is imperative that in aqueous phase CD that the sample is free of any dust particles which may cause light scattering and result in a shifted spectrum. The unit associated with CD is the mean residue ellipticity [θ] which is observed at a given wavelength and the associated units are deg.cm^2.dmol^{-1}.[98] Figure 24 demonstrates the polarization of light and the general structural features of a CD spectrum that highlights the secondary structure elements of the protein.

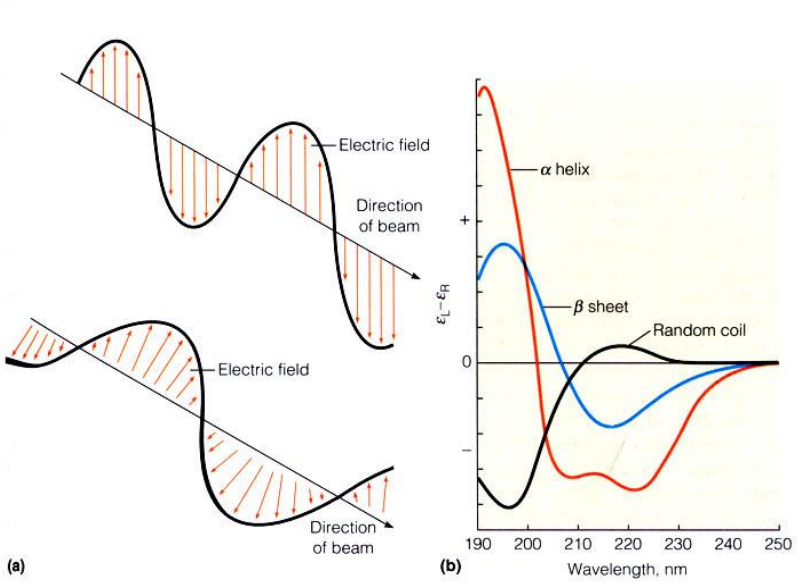

Figure 24 Circular Dichroism. (a) Polarization of light. Top, plane polarized light; bottom, circularly polarized light. (b) Circular dichroism spectra for polypeptides in various conformations.[99]

Within a protein there are 2 main classes of chromophore; the peptide backbone and the amino acid side chains. The peptide backbone can be analysed in the far UV region (240-180 nm) to determine the helical or sheet content of the protein whereas the CD of the aromatic amino acid side chains which can be observed in the near UV region (320-260 nm). This gives information about the side chains

and their environment in addition to the tertiary structure of the protein, i.e. the association between adjacent amino acid chains. [95,98]

CD can therefore be considered a useful tool when analysing the folding of a protein and determining the effects modifications have on the secondary and tertiary structure.

3 Polyoxometalates – self organisation and patterning of inorganic clusters

3.1.1 Chapter Aims

This chapter will describe some additional work with polyoxometalates that will go beyond single crystal measurements and look at the behaviour of the bulk material and the design of surfaces to include inorganic materials. The main focus of the investigation is outlined in Figure 25, and can be divided into 2 main areas of study. Firstly an investigation into the tethering of two very different organic components to the cluster and the effect this has on the surface organisation of the molecule. In addition; the cation, solvent mixture and concentration of the solutions will be investigated again in an attempt to identify any relationship between cluster's environment and the manner in which it organises or "self – patterns".

Secondly the use of microcontact printing as a tool to functionalise and order inorganic material will be described. The tethering of an inorganic cluster in this case Mn Andersons through peptide chemistry offers a unique method of locally functionalising a surface in a predetermined pattern and the preparation of 3 self assembled monolayers will be described:

- Mn-Anderson surfaces $[TBA]_3[MnMo_6O_{18}\{(OCH_2)_3C\text{-}NH_2\}_2]$ cluster **(SAM 1)**
- Mn Anderson-pyrene surfaces $[n\text{-}(C_4H_9)_4N]_3[MnMo_6O_{18}\{(OCH_2)_3C\text{-}NO_2\}\{(OCH_2)_3C\text{-}N{=}CH\text{-}(C_{16}H_9)\}]$:2-hydroxymethyl-2-[(pyren-4-methyl)-propane-1,3-diol] **(SAM 2)**
- Pyrene terminated control surfaces **(SAM 3)**

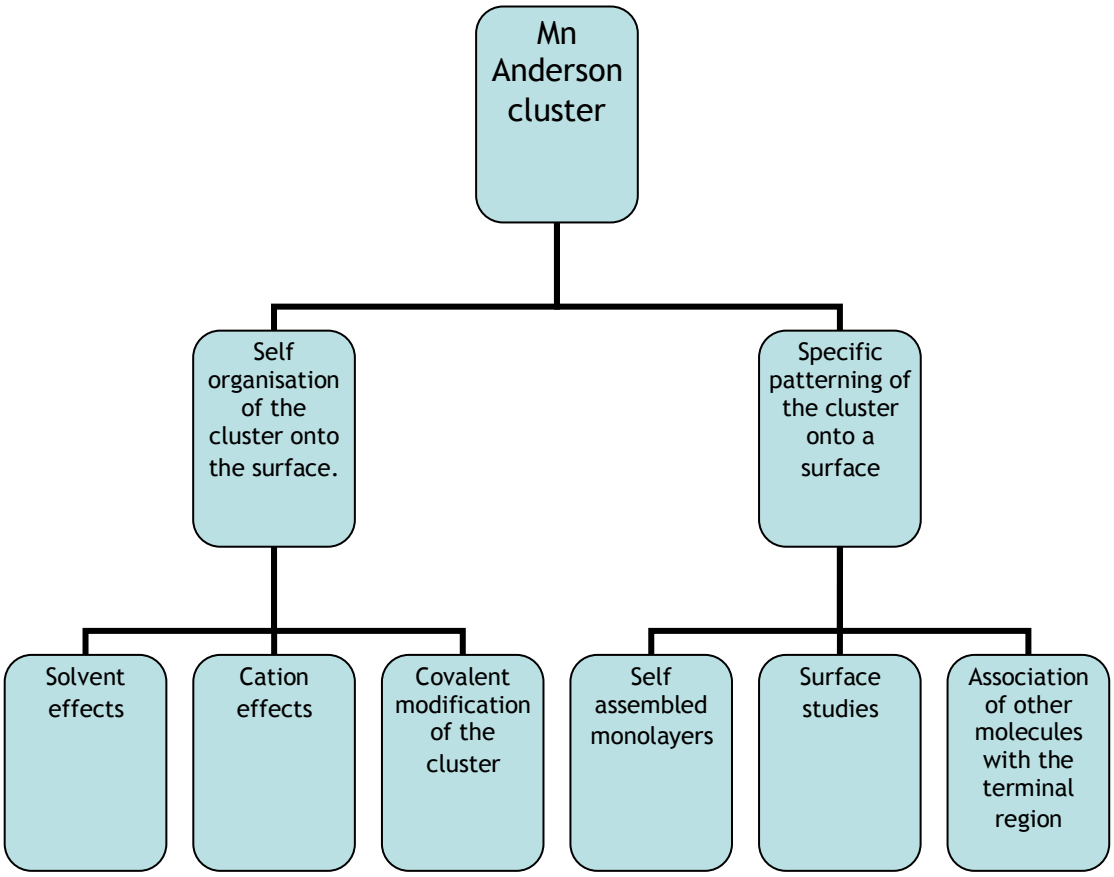

Figure 25 Scheme of proposed investigation

This chapter will also introduce not only the aforementioned self assembled monolayer preparation, but the successful interaction of the organic-inorganic hybrid molecule at the terminal region of the SAM with human fibroblast cells. This will demonstrate that a pyrene platform tethered to a Mn-Anderson shows selective cell adhesion behaviour bridging the gap between Polyoxometalate chemistry and cell biology.

All of the above outline a method to self pattern a surface using controllable factors within an experimental set up and pre design a surface on which to attach a cluster and localise the clusters in a pre determined manner.

3.2 **Chapter Introduction**

3.2.1 New polyoxometalate clusters for surface studies

As described previously Polyoxometalate (POM) cluster chemistry is an extremely active field of research due to the cluster's unmatched range of structural subsets,

physical properties[50b] and the fact POM clusters can be utilised in applications as wide ranging as catalysis to medicine.[100] It is the unique ability to control the assembly of POM clusters within a diverse range of sizes, in addition to recent developments, that have seen POM's being functionalised with organic tethers, that make this area of study so unique and interesting.

However despite their apparent importance, the development of POM containing multifunctional materials has proven difficult and slow to expand. This is partly due to POM formation being sensitive to reaction conditions and parameters in the reaction procedure such as pH, ionic strength and temperature that together make the synthesis difficult.

The recent interest in inorganic/organic hybrid molecules has uncovered new pathways to develop functional materials. This type of synthesis and the resulting molecule offers a new method to bring together two distinct areas of chemistry diversifying the clusters and uncovering a wide range of advantages. At present, the most common pathway to assemble functional material lies in the formation of POM hybrids that are linked through non covalent interactions e.g. Van der Waals, Hydrogen bonding and/or ionic interactions which lack the ability to control the stability of the cluster development.

Recent developments have also applied cationic surfactants to POM clusters resulting in Surface Encapsulated Clusters (SECs) that are compatible with organic functional groups. [4,101] This has resulted in the development of polymeric and liquid crystalline materials. This work has demonstrated that the physical and chemical properties of the core POM cluster can be maintained in conjunction with the existence of mainly electrostatic interactions between the organic and inorganic component of the assembly.

Examples in the literature where POMs have been developed in this manner is rare, despite the generation of amphiphilic molecules being incorporated with functional units that have resulted in unique physical properties. Examples include thiophene, fullerene and metal ions that have all been utilised to develop functional materials and yet POMs lag in their development in this field. What has been accomplished is the development of POM containing hydrophobic materials obtained through surface encapsulation with the main attractive force, as mentioned previously, being electrostatic interactions.

In contrast to this, POM hybrids that are formed via covalent interactions offer many advantages as these will not only improve the stability of the resulting POM hybrids, but also enhance the interactions between physical properties of the POM assemblies. Examples in the literature that demonstrate covalent functionalisation include the development of a class of compounds called heteropolymolybdates.

This class of compounds, which have the general formula $[H_X(MO_6)Mo_6O_{18}]^{n-}$ where x = 0-6 and n = 2-6, occur with metallic or non metallic heteroatoms and are common in the POM literature.[102] Two isomers of the compound are known: α and β. The α or the Anderson as it is more commonly known has two types: the non protonated A type and 2 - the hexaprotonated B type that has its heteroatoms in a low oxidation state. The six protons that exist on the B type Anderson structure have been replaced in several instances using different molecules. The first reported molecule to replace them was $(As_3O_3)^{3+}$ and secondly work by Hasenknopf et al by incorporating tris(hydroxymethly)[74b] methane derivatives RC-(CH_2OH) – replacing the three hydroxo groups on each side of the Anderson structure with three alkoxo groups, was done initially to enhance the stability of the complex and later to incorporate different functionalities onto the terminus of the Anderson cluster.

This work has lead to the development of functionalised Anderson type POMs $[XMo_6O_{18}\{(CH_2)_3OCNH_2\}_2]^{3-}$,where X is Mn^{III} or Fe^{III}, that contain organic groups with terminal functionality; i.e. grafting molecules onto the cluster that can then themselves be further functionalised through various reactions. As mentioned the work of Hasenknopf et al has inspired the development of inorganic – organic hybrid clusters containing such functional molecules. The chemically grafted molecules not only change the structure that can be obtained from these inorganic metal oxides but also offer the potential for interesting applications as a result.

Further developments are possible with the Mn Anderson cluster which are relatively unique in POM chemistry.[74a] The clusters have the ability to be functionalised with organic components due to the presence of a terminal amine on either end of the cluster through the tris (tris(hydroxymethyl)amino methane group, as shown in Figure 26. Direct modification of clusters is rare[103] and only recently in the literature have examples appeared where the incorporation of functional units onto clusters has been reported. The development of such molecules not only extends the wide range of clusters that are able to be

synthesised giving new structures and frameworks, but also implies that the cluster's behaviour will change thus the development of such chemistry is important in the wider understanding of POM materials that have incorporated reactive functionalities onto their frameworks. The ability to alter the cation in the cluster offers a wide range of diversity and a scope to investigate the behaviour of these clusters further. With this new found diversity comes difficulty. The synthesis is not straightforward and the ability to add organic motifs onto the inorganic cluster has proven to be a limitation in the past. The majority of cluster frameworks have no reactive area on which to functionalise further with organic material. This means the reported examples of such inorganic – organic hybrids is rare and so it is a positive and interesting result when these materials can be produced.

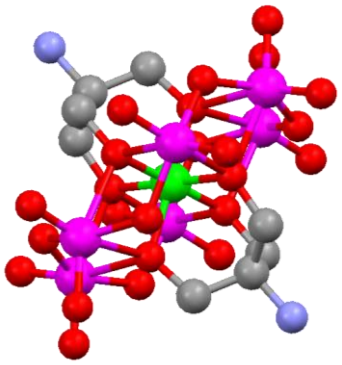

Figure 26 Mn Anderson cluster $[MnMo_6O_{18}\{(OCH_2)3CNH_2\}_2]^{3-}$, showing the terminal amine (in blue) at either end of the cluster allowing a range of different chemistries to be carried out on the cluster. Mn –green; Mo –pink; O –red; C –grey

This development offers a new method of bringing two areas of chemistry together that has in turn bestowed numerous advantages, one being the new found diversity these molecules have. The combination of an organic molecule with an inorganic material is important in materials science – not only does each component have individual importance, but the combination of the two chemistries brings into focus an area of study from one that had been perceived to have been exhausted. Now new materials are coming to the forefront that combine the areas of organic and inorganic chemistry.

3.2.2 Microcontact printing as a tool to pattern inorganic clusters

In the past decade the literature devoted to the production of highly ordered surfaces with a high degree of structural organisation has confirmed that self assembled monolayers have paved the way to allow the fabrication of features as small as 10nm with relative ease. [104]

The ability to pattern molecules down to the nano scale in a specific desired pattern is a simple procedure with a high level of reproducibility, making this technique favoured by those who wish to pattern a surface.[105] In addition, derivitisation of surfaces with various terminal functionalities allows the addition of other molecules to the surface using simple chemical reactions. Further advantages include the ability to wash away any impurities that existed in solution, as only the molecules with the reactive tether will be present on the surface. Here the surface acts like a chromatography medium by holding the reactive and pure molecules on the surface whilst being able to selectively wash away impurities.

The direct covalent addition of POM clusters to surfaces is rare[106]. The fact remains that POMs are incredibly difficult to functionalise with any kind of reactive group and so this has been the major drawback with this chemistry. However the advantage of linking POMs to surfaces is endless. Could POMs lead the way to having localised catalysis on surfaces, or electron transfer devices scaled down to the nano scale and in pre-designed patterned areas?[107] Until now almost all of the surface studies carried out on metal oxide clusters where the metal is either Mo, V or W, have used relatively simple clusters where the number of metal oxide centres has been less than 4. The patterning of POMs is an entirely new area of study, and the behaviour of POMs on a surface is not only an interesting addition to the wealth of available literature, but could perhaps open up a new pathway for the development of functional materials.

Now with the evolution of the derivitised Mn Anderson cluster and the ability to have reactive groups on these molecules, it is possible to directly link the inorganic cluster to an organised patterned surface.[108] It is not only exciting to imagine the possibilities of patterning a POM onto a surface but in doing so it is interesting to explore the behaviour of such materials and perhaps the endless possibilities they hold.

3.2.2.1 Self assembled monolayer applications in cell biology

The extensive literature on self assembled monolayers provides evidence that SAMs can exhibit a high degree of structural order after assembly and it is no coincidence that SAMs of alkanethiols on gold have become an important class of model substrate for mechanistic investigation of interactions of proteins and cells with surfaces.

In recent years the studies of cell biologists have looked towards surface design and the use of microcontact printing as a method to understand the complex topic of cell and tissue engineering.[42,109] Understanding the interaction proteins and cells have with a specific surface is a useful tool in understanding cell adhesion and SAMs offer a reproducible platform to explore this topic with relative simplicity.

To ensure the attachment of cells to areas compatible with cell growth an extracellular matrix protein must be used in order to prepare the surface for the cell adsorption. [110]There have been many studies into protein adsorption to different types of surfaces and yet the mechanism for such adsorption is not fully understood. However general rules are always followed. [111]The rate at which the protein adsorbs to a particular surface is fast and the process is irreversible, this is coupled with the fact the protein will be denatured on attachment to the surface. It is also difficult to know how much protein is actually on the surface and so this imposes limitations on the study of how protein adsorption aids cell attachment to the surface. Similar surfaces may seem to have a comparable density of protein and yet cell studies show very different results.

It is well documented in studies by Prime and Whitesides [112] that monolayers of oligo (ethylene glycol) groups are effective in resisting the absorption of extracellular matrix proteins,[112-113] making this surface a good model for the resistance of cells to certain functionalities. Even on preparing a mixed monolayer of ethylene glycol with an alkanethiol terminated in a methyl group – a functionality that should be compatible with cell adhesion - the proteins and therefore cells resist attachment to the surface even with 50% incorporation of the terminal methyl group.

The use of microconatct printing to pattern different functionalities onto certain pre-determined areas is an interesting addition to the catalogue of techniques used to study cell biology. The mixture of forming self assembled monolayers and subsequently being able to pattern a surface allows a quick demonstration of which terminal functional groups and indeed pattern shapes cells preferentially attach to. Cell adhesion is an important factor in the control of cell shape and consequently its function – and so determining if a cell adheres to a surface comfortably – has further implications in studying cell behaviour and activity.

Studies by Mrksich *et al* [114] show surfaces have been patterned with hydrophobic lines of dimensions ranging from 10–120 μm. These areas terminated in methyl groups are in contrast to the hydrophillic back filler oligo (ethylene glycol) groups, used to cover the rest of the surface. These hydrophilic regions have been found to be protein resistant and so serve to directly contrast with the patterned area. Results showed that when fibronectin was added in solution, the oligo ethylene groups resisted adhesion resulting in the formation of a layer of protein on the patterned areas. Cells were then added and attachment and spreading was seen exclusively on the patterned areas, demonstrating the ability to tailor a surface for orientating cells in a predetermined pattern is demonstrated in Figure 27.

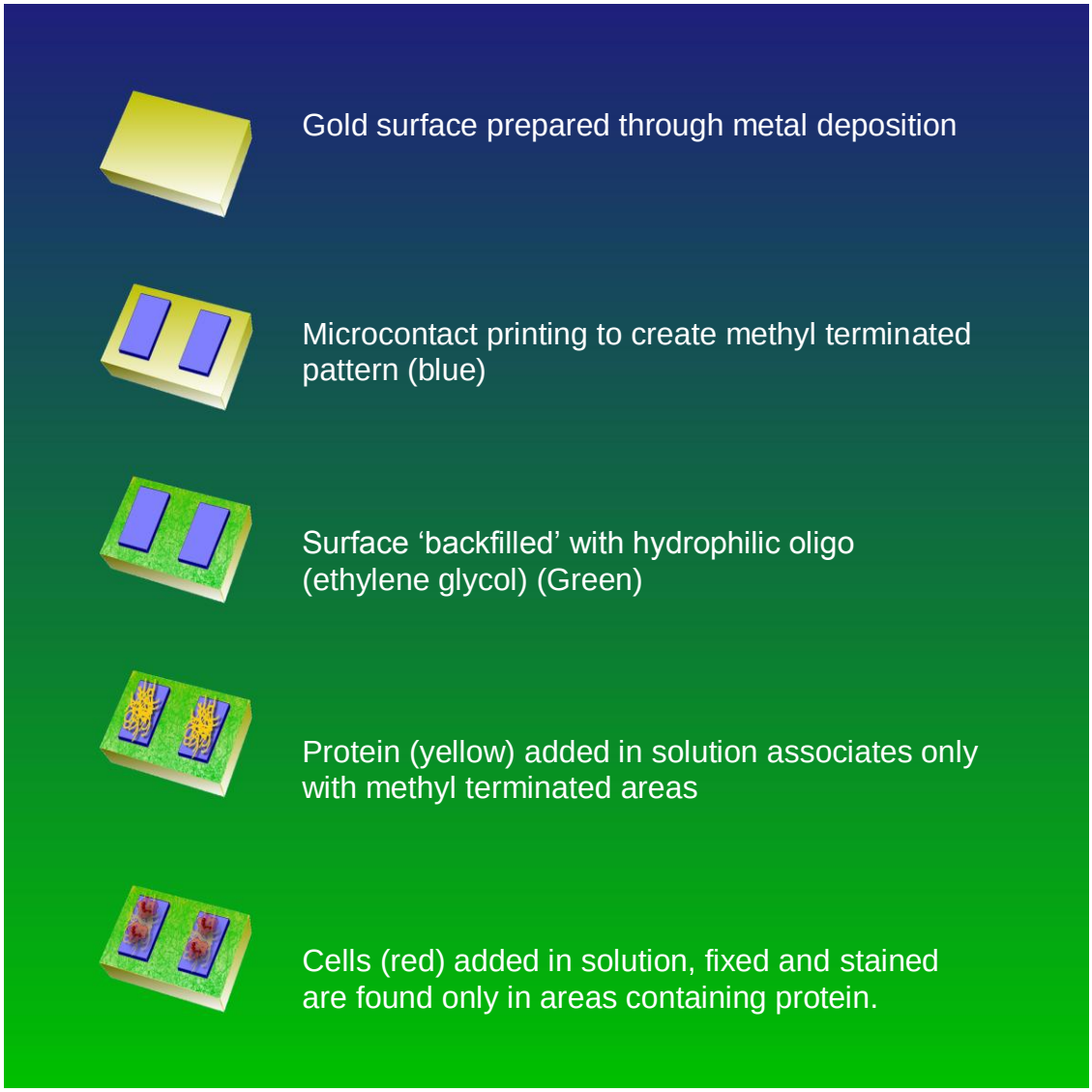

Figure 27 Schematic diagram of the procedure for microcontact printing and subsequent patterning of proteins and cells onto a gold surface.

There are certain advantages to using microcontact printing as a tool to pattern cells, not only is it a simple technique to carry out, but inexpensive compared to photolithography techniques.[1b,42,115] A wide variety of patterns can be reproduced onto surfaces in a short space of time, allowing conclusive studies to be carried out quickly.

Many other functional groups have been tested for their compatibility or otherwise with cell adhesion. Knowing that oligo(ethylene glycol) units are inert and prevent the attachment of most proteins and therefore cells[1b,42,115] they have been used as a control group to test if other terminal functionalities will allow the spreading of cells on a surface.

A recent development in understanding cell adhesion to a surface was the attachment of cells to areas with large aromatic platforms. Studies showed that in surfaces patterned with a large aromatic group and backfilled with alkanethiol, cells had an unexpected affinity for the aromatic areas[41] without the need for an adhesive protein in preference to the terminal alkanes surrounding them - an unexpected and important result. This offered many points of discussion – cell adhesion was not related to the charge of the aromatic group as both fluoroscein and rhodamine were used in the study – as fluoroscein has no charge and presented the same result. It has been postulated that the proteins in the extracellular matrix of the cell are attracted to the aromatic moiety through π-π interactions.[41]

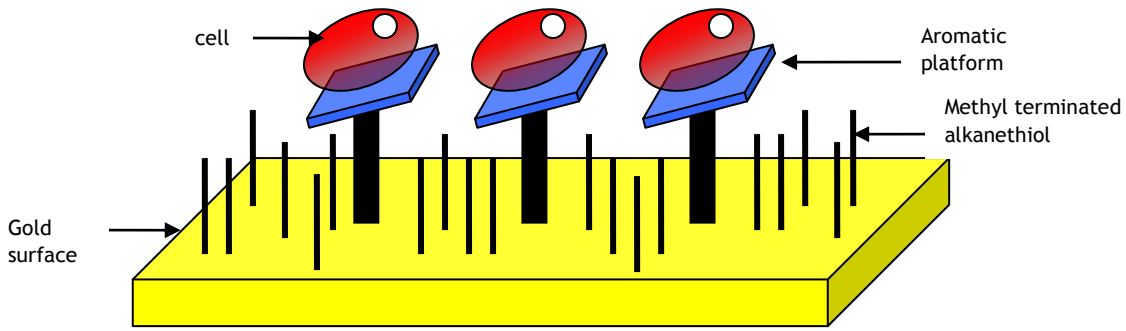

Figure 28 Schematic diagram representing the platform the aromatic region creates for the cell.

The association of cells for areas containing aromatic areas leads to the study of surfaces exclusively terminated in aromatic groups. Fluoroscein and rhodamine both contain atoms other than carbon and hydrogen that could enhance cell spreading in this area.

As such an investigation into how patterned POM clusters interact with biological material may lead to new and interesting applications for these inorganic materials that already exhibit a variety of applications.

3.3 **Experimental**

From the flow diagram outline in Figure 25 the investigation can be divided into two distinct areas; self organisation of clusters on a surface and specific patterning of clusters on to a surface. The experimental information related to this is described in the following sections.

3.3.1 Synthesis of hybrid assemblies for surface patterning

The following compounds 1-6 were synthesised to determine the effect of the concentration, solvent, counter ion and the organic tether have on the surface studies of the POM clusters.

3.3.1.1 $[(n\text{-}C_4H_9)_4N]_3\ [MnMo_6O_{18}\{(OCH_2)_3CNH_2\}_2]$ (Compound 1)

The basis for all experiments in this section is the preparation of $[(n\text{-}C_4H_9)_4N]_3\ [MnMo_6O_{18}\{(OCH_2)_3CNH_2\}_2]$ (compound 1). This was synthesid by Yu-Fei Song as described in the literature and fully characterized and illustrated by the schematic shown in Figure 29.[116]

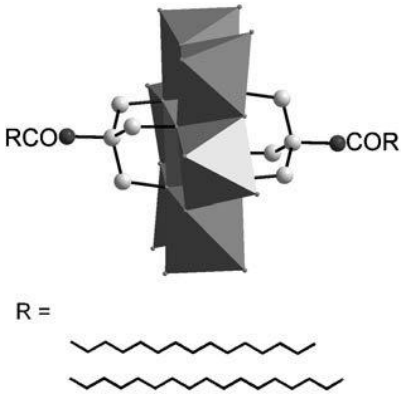

Figure 29 Schematic diagram of the Mn Anderson cluster that forms the basis for the following experiments highlighting the area where further functionalisation can occur and this moiety enables further functionalisation of the cluster, R groups can be C-16-18 giving compound 2 and 3. [116]

3.3.1.2 $[(nC_4H_9)4N]_3\ [MnMo_6O_{18}\{(OCH_2)_3CNH\text{-}CO\text{-}(CH_2)_{14}CH_3\}_2]$ ·7H2O·2DMF (Compound 2, C-16)

Compound 1 (0.50 g; 0.27 mmol) and Et_3N (150 mL; 0.11 g; 1.08 mmol) were dissolved in 30 mL of acetonitrile. Palmitoyl chloride (0.15 g; 0.53 mmol) was

added slowly and the solution was kept refluxing for 10 h. A white precipitate was filtered off and the solvent was evaporated. The orange residue was dissolved in a minimum amount of DMF (10 mL). Orange crystals with long, needle shape were obtained by ether diffusion into DMF solution after one week. Yield: 0.13 g (0.056 mmol, 21%). ^{1}H NMR (400 MHz, [D6]DMSO): d=0.86 (t, 6H; -CH_3), 0.94 (t, 36H; TBA), 1.24 (s, 56H; -CH_2-), 1.32 (m, 24H; TBA), 1.57 (m, 24H; TBA), 3.17 ppm (m, 24H; TBA); IR (KBr, cm^{-1}): υ =3432 (w), 2927 (s), 2873 (m), 1670 (m), 1549 (w), 1479 (m), 1383 (w), 1032 (m), 941 (s), 922 (s), 667 cm^{-1} (vs); ESI-MS (negative mode, MeCN): 937 $gmol^{-1}$ ([M-2DMF-7H_2O-2TAB]$^{2-}$); elemental analysis calculated (%) for $C_{88}H_{184}MnMo_6N_5O_{26}\cdot 7H_2O\cdot 2DMF$ (2631.3 $gmol^{-1}$): C 42.91, H 8.12, N 3.73; found: C 42.62, H 7.73, N 3.89.

3.3.1.3 $[(nC_4H_9)4N]3\ [MnMo_6O_{18}\{(OCH_2)_3CNH\text{-}CO\text{-}(CH_2)_{16}CH_3\}_2]\cdot 2DMF$ (Compound 3, C-18)

Compound 1 (0.50 g; 0.27 mmol) and Et_3N (150 mL; 0.109 g; 1.08 mmol) were dissolved in 30 mL of acetonitrile. Stearoyl chloride (0.16 g; 0.53 mmol) was added and the solution was set to reflux for 18 h. A white precipitate was filtered off and the solvent was evaporated. The solid orange residue was dissolved in a minimum amount of dry DMF and further white precipitate was filtered off. After three days of slow evaporation at room temperature, small orange crystals could be obtained. Yield: 0.17 g (0.067 mmol, 25%). ^{1}H NMR (400 MHz, [D6]DMSO, 25 8C): d=0.86 (t, 6H; -CH_3), 0.94 (t, 36H; TBA), 1.24 (s, 64H; -CH_2-), 1.34 (m, 24H; TBA), 1.57 (m, 24H; TBA), 3.171 ppm (m, 24H; TBA); IR (KBr, cm^{-1}): υ =3462 (w), 2925 (s), 2854 (m), 1670 (m), 1550 (w), 1483 (m), 1382 (w), 1027 (m), 941 (s), 921 (s), 666 ppm (vs); ESI-MS (negative mode, MeCN): 965 $gmol^{-1}$, ([M-2DMF- 3H_2O-2TAB]$^{2-}$); elemental analysis calculated (%) for $C_{92}H_{192}MnMo_6N_5O_{26}\cdot 2DMF\cdot 3H_2O$ (2615.3 $gmol^{-1}$): C 45.01, H 8.17, N 3.75; found: C 45.20, H 8.07, N 3.81.

3.3.1.4 $[DMDOA]_3\ [MnMo_6O_{18}\{(OCH_2)_3CNH\text{-}CO\text{-}(CH_2)_{14}CH_3\}_2]\text{-}2DMF\cdot 4H_2O$ (Compound 4)

The crystalline powder of compound 2 (150 mg, 0.057 mmol) was dissolved in 15 mL of MeCN and the solution was kept stirring for 30 min, then it was added dropwise to the clear solution of excess amount (1.80 g, 2.85 mmol) of

dimethyldioctadecylammonium bromide (DMDOABr) in a mixture of $CHCl_3$ and MeCN (1:3, 50 mL). Yellow-orange precipitates were formed immediately and filtered, dried under vacuum overnight. Yield: 0.17 g (0.048 mmol, 85%). ESI-MS (negative mode, MeCN) 2801 $gmol^{-1}$ ($[M-2DMF-4H_2O-\ 2TBA^+H^+]^-$); elemental analysis calculated (%) for $C_{154}H_{316}MnMo_6N_5O_{26}\cdot 2DMF\cdot 4H_2O$ (3503 $gmol^{-1}$): C 54.86, H 9.73, N 2.80; found C 54.55, H 9.30. N 2.74.

3.3.1.5 $[DMDOA]_3\ [MnMo6O_{18}\{(OCH_2)_3CNH\text{-}CO\text{-}(CH_2)_{16}CH_3\}_2]\cdot 2DMF\cdot 4H2O$ (compound 5)

The crystalline powder of compound 3 (150 mg, 0.057 mmol) was dissolved in 15 ml of MeCN and the solution was kept stirring for 30 min, then it was added dropwise to the clear solution of excess amount (1.80 g, 2.85 mmol) of dimethyldioctadecylammonium bromide (DMDOABr) in a mixture of $CHCl_3$ and MeCN (1:3, 50 mL). Yellow-orange precipitates were formed immediately and filtered, dried under vacuum overnight. Yield: 70%. ESI-MS (negative mode, MeCN) 2829 $gmol^{-1}$ ($[M-2DMF-4H_2O-2TBA^+H^+]^-$); elemental analysis calculated (%) for $C_{156}H_{320}MnMo_6N_5O_{26}\cdot 2DMF\cdot 4H_2O$ (3531 $gmol^{-1}$): C 55.10, H 9.76, N 2.78; found C 54.58, H 9.66. N 2.68.

3.3.1.6 Preparation of Compound 6 $[N(C_4H_9)_4]^{3-}[MnMo_6O_{18}\{(OCH_2)_3CNH\text{-}CH_2\text{-}C_{16}H_9\}_2]\cdot 2DMF\cdot 3H_2O$

Material was synthesized by reaction of $(HOCH_2)_3CNH_2$ (2.0 g, 16.5 mmol) with 1-pyrenecarbaldehyde (3.8 g, 16.5 mmol) in MeOH (100 mL) and the resulting Schiff base was reduced by $NaBH_4$ (0.91 g, 24.8 mmol). The reaction mixture was evaporated to dryness under vacuum and dissolved in water (100 mL). After the addition of HCl (4m, 30 mL), the water solution was extracted with CH_2Cl_2 (300 mL). NaOH solution (4m, 100 mL) was added to the aqueous phase, and the resulting solution was evaporated to dryness. Dry ethanol (50 mL) was added and the reaction mixture was then stirred for 10 min at 8°C. A light-yellowish solid was isolated by filtration and dried under vacuum. Yield: 67% (3.7 g). Elemental analysis (%) calculated for $C_{21}H_{21}O_3N$ (335 $gmol^{-1}$): C 75.2, H 6.3, N 4.2; found C 75.5, H 6.8, N 4.0. ESI-MS ($[MH]^+$): 336 $gmol^{-1}$. IR (KBr): υ =2926 (m), 2878 (m), 2853 (m), 1670 (m), 1458 (s), 1354 (m), 1244 (w), 1188 (m), 1117 (s), 1042 (s), 937 (s), 843 (s), 717 (m), 549 (m), 497 cm^{-1} (m). ^1H NMR(400 MHz; [D4]MeOD):

d=3.73 (s, 2H, -CH_2-), 3.88 (br, 6H, -CH_2-), 8.01 (t, J=8 Hz, 1H, -CH-), 8.10 (s, 2H, -CH-), 8.22 (m, 5H, -CH-), and 8.57 ppm (d, J= 10 Hz, 1H, -CH-).

The cluster was synthesised through a mixture of $[N(C_4H_9)_4]_4[a\text{-}Mo_8O_{26}]$ (8.0 g, 3.7 mmol), $MnOAc_3 \cdot 2H_2O$ (1.5 g, 5.6 mmol) and compound 1 (4.29 g, 12.8 mmol) were kept refluxing in MeCN for 24 hours, and the resulting brown precipitate was removed by filtration. The filtrate was evaporated to dryness under vacuum and the resulting solid was dissolved in a small amount of DMF. Yield: 19% (2.3 g, based on Mo). Melting point: 239–240°C. Elemental analysis (%) calculated for $C_{96}H_{164}MnMo_6N_7O_{29}$ (2510.9 $gmol^{-1}$): C 45.9, H 6.6, N 3.9; found C 45.7, H 6.8, N 4.0. ESIMS (negative mode): 2067 $gmol^{-1}$ ([M-2DMF-3H_2O-TBA]). IR (KBr): υ =2957 (m), 2933 (m), 2868 (m), 1668 (s), 1479 (s), 1383 (m), 1249 (w), 1071 (m), 1032 (m), 938 (s), 918 (s), 851 (w), 664 cm^{-1} (s). ^{1}H NMR (400 MHz; [D6]DMSO): 0.94 (t, J=8.0 Hz, 36H, 4-HTBA), 1.25 (m, 24H, 3-HTBA), 1.57 (m, 24H, 2-HTBA), 2.73 (s, 6H, -CH_3 (2DMF)), 2.90 (s, 6H, -CH_3 (2DMF)), 3.15 (m, 24H, 1-HTBA), 4.0 (broad, 4H, -CH_2-), 7.92 (s, 2H, -CH-), 8.08 (t, J=8.0 Hz, 2H, -CH-), 8.17 (m, 4H, -CH-), 8.28 (d, J=8.0 Hz, 8H, -CH-), 8.35 (broad, 2H, - CH-), 62.5 ppm (broad, 12H, CH_2O).

3.3.1.7 Preparation of surfaces to determine the effects of organic tether

Solutions of all clusters were prepared to 1mg/ml in chosen solvent and added drop wise to silicon substrates of 1cm^2 in size and dried overnight, for SEM studies into the effects these alterations have on the clusters structure on a surface. Silicon wafers of 3 inch diameter were purchased from Pi-Kem. And cut using a diamond tip pen to 1cm^2 size.

3.3.1.8 Transmission Electron Microscopy Preparation

The TEM (transmission electron microscopy) measurements were carried out by using TEC NAI T20 with GIF 2000: Gatan Imaging Filter. The samples for TEM measurement were prepared as follows: The solutions of compound 2-6 were dissolved in a mixture of MeCN/ $CHCl_3$ (1:4) to 1 $mgmL^{-1}$ and 5 mL of the solutions were deposited onto the Cu/C substrates and dried.

3.3.1.9 Scanning Electron Microscopy Preparation

The SEM (scanning electron microscopy) images were obtained by using a field emission scanning electron microscope (JEOL, JSM-6400) operated at an acceleration voltage of 10 kV. The silicon substrates and samples for SEM measurements were prepared as follows: the silicon substrates were cleaned by sonication in ethanol for 20 minutes and dried under a stream of nitrogen. The solutions of compounds 2–6 were dissolved in MeCN, $CHCl_3$ or mixture of MeCN/$CHCl_3$ to 1 mgmL^{-}1 according to different experimental conditions and 10 mL of each of the solutions was deposited onto the substrate and dried.

3.3.2 Self Assembled Monolayer Preparation

The second distinct area of this investigation is the specific patterning of clusters onto a surface.

3.3.2.1 Synthesis of compound 7 and compound 8 for investigation

The symmetric Mn-Anderson cluster of compound 1 was the starting material for the following investigation and synthesis is described previously.

3.3.2.2 Synthesis of $[n\text{-}(C_4H_9)_4N]_3[MnMo_6O_{18}\{(OCH_2)_3C\text{-}NO_2\}\{(OCH_2)_3C\text{-}N{=}CH\text{-}(C_{16}H_9)\}]$ (Compound 7)

2-hydroxymethyl-2-[(pyren-4-methyl)-propane-1,3-diol] (compound known as Pyrene-Tris moving forward) was prepared according to published procedure.[108] Tris(hydroxymethyl)aminomethane is commercially available from Aldrich.

A mixture of $[n\text{-}N(C_4H_9)_4]_4[\alpha\text{-}Mo_8O_{26}]$ (8.00 g, 3.7 mmol), $Mn(CH_3COO)_3{\bullet}2H_2O$ (1.49 g, 5.6 mmol), $(HOCH_2)_3C\text{-}NH_2$ (0.77 g, 6.4 mmol) and Pyrene-Tris (2.15 g, 6.4 mmol) in 150 ml of MeCN was refluxed for 16 hrs. The orange solution was cooled to room temperature and filtered to remove a very fine brown solid. The filtrate was exposed in air to evaporate slowly and it was filtered every 6 hours. The crystallized powder is collected. Around 11 batches of samples were collected and checked with ESI-MS spectroscopic measurement. Yield: 16% (1.65 g).

Calculated for $C_{73}H_{134}MnMo_6N_5O_{24}$ (2107.3 g/mol): C 41.57, H 6.36, N 3.32; Found C 41.80, H 6.24, N 3.35. ESI-MS (negative mode): 1853 g/mol ($[M\text{-}TBA]^-$); 1612 g/mol ($[M\text{-}2TBA^+H]^-$).

3.3.2.3 Synthesis of compound 8: amine terminated pyrene

N-Boc-ethylenediamine is commercially available from Aldrich. Reaction of 1-pyrenecarboxaldehyde with N-Boc-ethylenediamine in MeOH at 65 ^oC resulted in the formation of the corresponding Schiff-base, which is further reduced by adding excess amount of $NaBH_4$. The protecting Boc group was removed by adding excess amount of trifluoroacetic acid. Compound 8 was obtained as yellow powder form with the molecular formula of $C_{19}H_{20}N_2$. Yield: 52%. ESI-MS (MeCN): 277 g/mol ($[MH]^+$); Calculated for $C_{19}H_{20}N_2$ (276.4 g/mol): C 82.57; H 7.29, N 10.14; Found C 82.88, H 7.53, N 10.36. ^1H NMR (ppm, CD_3OD): 3.41 (2H, t); 3.52 (2H, t); 5.11 (2H, s); 8.15 (3H, t); 8.21 (3H, m), 8.33 (2H, t), 8.48 (1H, d).

3.3.2.4 Microcontact printing of POMs

In order to prepare surfaces using microcontact printing to create predetermined areas of inert and active functionality the following procedures were used.

In accordance with well documented procedures, moulds for the Polydimethylsiloxane (PDMS) stamps were prepared by photolithography. Glass slides were coated with AZ4562 resist to a thickness of 6.2µm. Patterns were designed previously with the circles of the size range 50 – 60 µm, with varying centre to centre dimensions and squares of 100µm in length. The patterns were defined in the resist using a chromium mask and developed.

PDMS (sylgard 184) was prepared using a ratio of 10:1 base material and curing agent. Stamp holders were prepared using plastic pipette tips of 1cm in diameter, placed over the pattern and the PDMS mixture poured on top. This was allowed to cure at 80ºC for 24 hours creating cylindrical stamps for ease of printing.

Silicon wafers were used as substrates for the experiment. The wafer was prepared using e-beam evaporation of 10nm titanium to aid gold adhesion to the silicon followed by 25nm of gold.

In accordance with the literature it was decided that SAMs that were composed of 16-mercaptohexadecanoic acid (MHA) with carboxylic acid group being the terminal functionality and 2-dodecyl mercaptane with a methyl group being the terminal functionality would be useful to allow further reaction to take place on the MHA chain due to the reactivity of the –COOH. The procedure used to prepare the SAMs is as follows:

Stamps were inked with THF:AcOH:H_2O solutions (1 mM) of 16-mercaptohexadecanoic acid (MHA) purchased from Sigma-Aldrich. The stamp was dried with a stream of nitrogen for 30 s and placed gently on a metallized surface with sufficient pressure to allow conformal contact between the stamp and the substrate. The substrate was immersed immediately in a solution of 2-dodecyl mercaptane (Sigma-Aldrich) in methanol (1 mM) for 5 min. The substrate was removed, rinsed with methanol and dried in a stream of nitrogen creating the surface shown in Figure 30.

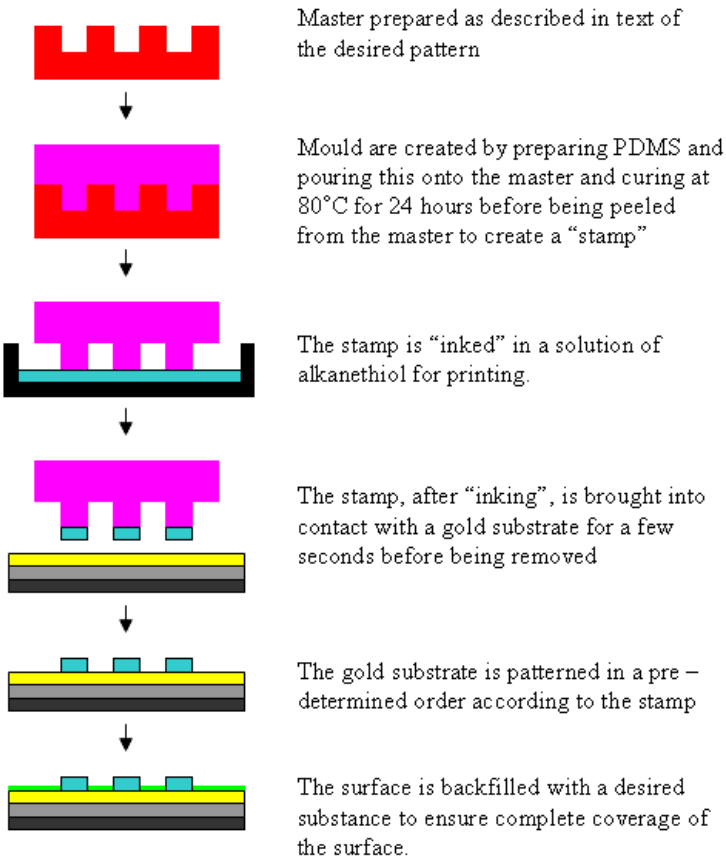

Figure 30 Schematic representation of the creation of self assembled monolayers using microcontact printing.

Due to the inert behaviour of the filler molecule with the terminal methyl region the basic surface has now been created onto which further chemical addition can be explored. Additionally, the reactivity of the –COOH region can be exploited. N-hydroxysuccinimide (NHS) and N-ethylcarbodimide hydrochloride (EDC) coupling can be used to chemically link the free carboxylic acid with a free amine group to form a peptide linkage at the terminal region further extending the self assembled monolayer. The NHS/EDC coupling is essential to ensure complete reaction at the reactive carboxylic acid site. The reaction proceeds as follows:

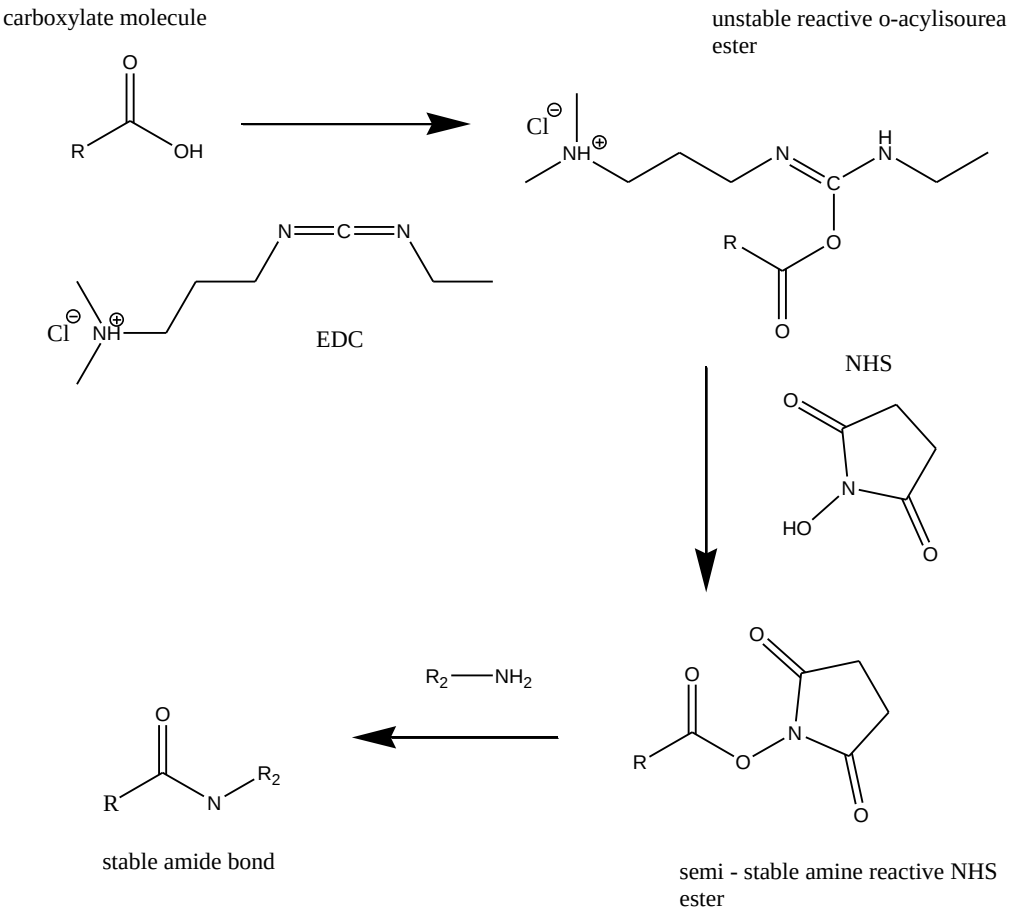

Scheme 3The EDC/NHS coupling of the amine to the stationary carboxylic acid is aided by the EDC/NHS coupling reaction

3.3.2.5 Preparation of SAM 1

SAMs terminating in the Mn-Anderson $[TBA]_3[MnMo_6O_{18}\{(OCH_2)_3C\text{-}NH_2\}_2]$ cluster , compound 1 were prepared by activating the terminal carboxyl region of a patterned surface to an ester to allow easy addition of a primary amine and therefore amide bond formation. The substrates were immersed in a catalytic reaction mixture containing excess of compound 1 and 5 mM of N-

hydroxysuccinimide NHS and 2 mM of N-ethylcarbodimide hydrochloride EDC in a 50 mM of 2-(N-morpholino) ethanesulfonic acid (MES, pH = 6.5) solution. [30]The mixture was kept stirring for 24 hours, allowing the coupling reaction to complete. The sample was then washed in acetonitrile and water to remove any unreacted material and dried in a stream of nitrogen.

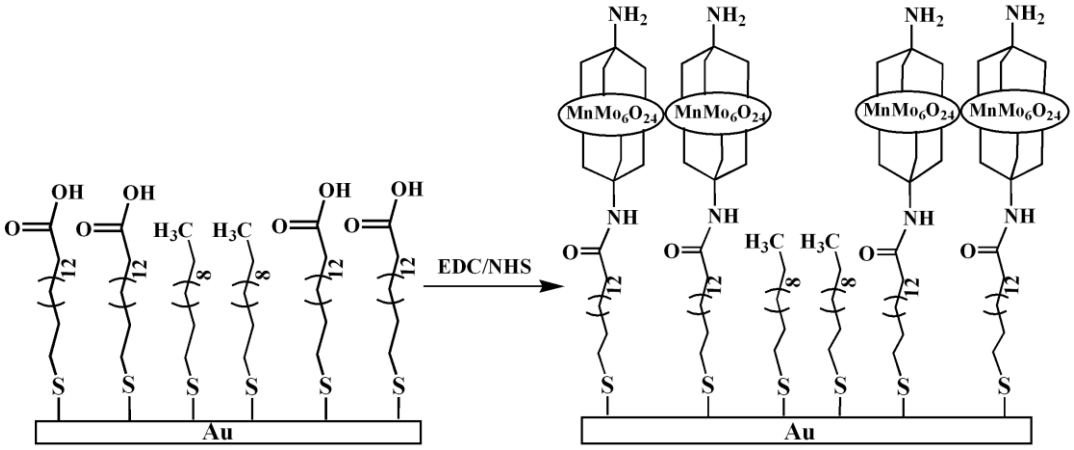

Figure 31 Schematic representation of patterned Au surface shows the surface covalent modification of areas terminated in carboxylic acid groups by attaching symmetric Mn-Anderson cluster $[TBA]_3[MnMo_6O_{18}\{(OCH_2)_3C\text{-}NH_2\}_2]$ onto SAMs via amide bond formation. (EDC 2 mM, NHS 5 mM, MES 50 mM, pH 6.5, solvent MeCN: H_2O = 1:4).

As shown in Figure 31, the modular approach to surface patterning is a stepwise addition of molecules that are reactive either to the surface or the terminal functionality of the groups that exist on the surface and so makes this an easy approach to adding the amine terminated cluster on to a carboxy terminated surface.

3.3.2.6Preparation of SAM 2

The mechanism for preparing the pyrene Mn Anderson pyrene surfaces [*n*-$(C_4H_9)_4N]_3[MnMo_6O_{18}\{(OCH_2)_3C\text{-}NO_2\}\{(OCH_2)_3C\text{-}N{=}CH\text{-}(C_{16}H_9)\}]$, compound 7, was to activate the terminal carboxyl region of a patterned surface to an ester to allow easy addition of a primary amine and therefore amide bond formation as shown in Figure 32. The substrates were immersed in a catalytic reaction mixture containing excess of compound 7 and 5 mM of NHS (N-hydroxysuccinimide) and 2 mM of EDC (N-ethylcarbodimide hydrochloride) in a 50 mM of 2-(N-morpholino) ethanesulfonic acid (MES, pH = 6.5) solution. The mixture was kept stirring for 24 hours, allowing the coupling reaction to complete. The sample was then washed in

acetonitrile and water to remove any unreacted material and dried with a stream of nitrogen.

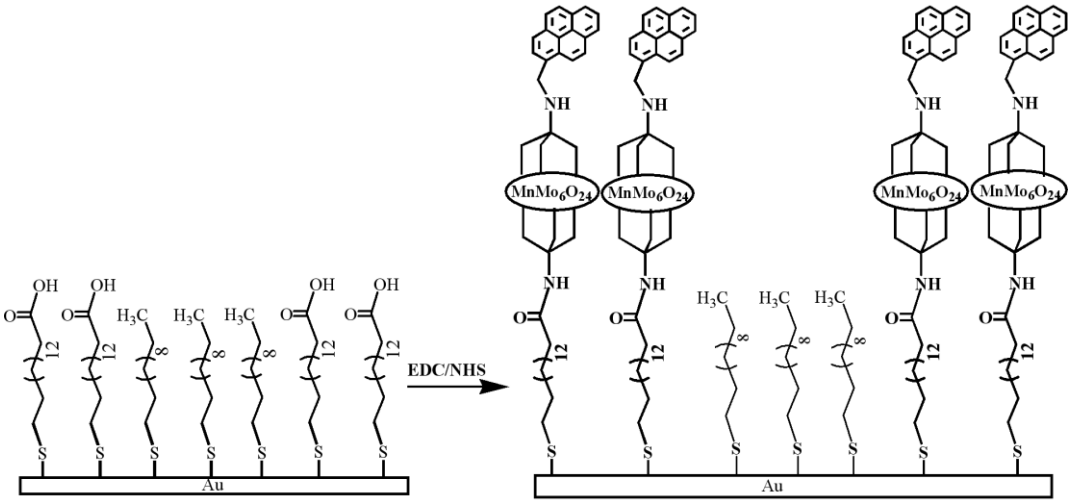

Figure 32 Schematic representation of the modular approach used to tether the pyrene Anderson onto the surface. Firstly patterning MHA with carboxylic acid functionality and then the esterification reaction with the primary amine of the Anderson (Compound 8).

The molecule therefore has one free amine in order to be coupled to the terminal carboxylic acid group through the NHS/EDC coupling explained previously. This leaves the terminal pyrene as the end region of the self assembled monolayer and imparts interesting chemical functionality as shown in Figure 32.

3.3.2.7Preparation of SAM 3

As a control experiment to the SAMs containing the functionalised and non functionalised Anderson clusters, a SAM containing terminal pyrene was prepared. The SAM was prepared as follows:

Compound 8 was added to the surface using the same procedure as described previously where Compound 8 was added to the surface resulting pyrene terminus (Figure 33)

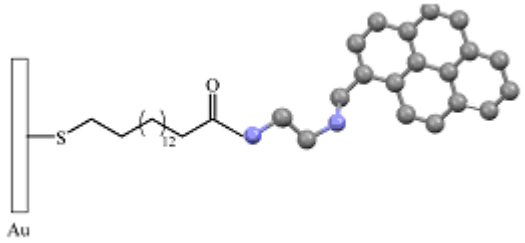

Figure 33 Schematic representation of pyrene terminated surface with the omission of the POM area.

3.3.2.8 ToF-SIMS Studies of Prepared Surfaces

To confirm the pattern formation, the samples were checked by imaging time-of-flight secondary ion mass spectrometry (ToF-SIMS). The analysis was performed on a ToF-SIMS IV instrument (ION-ToF GmbH, Germany), with settings optimized for high mass resolution (m/Δm = 3000-6000), using 25 keV Bi^{3+} primary ions (in total 1.5×10^{10} primary ions / cm^2).

3.3.2.9 AFM studies

AFM was used to determine the surface coverage of the SAMs. Data was acquired using a Nanoscope Dimension 3100 in tapping mode.

3.3.2.10 Contact angle measurements of prepared surface

Contact angle measurements were performed using a Kruss EasyDrop system to determine the effect the modification of the surface has on the wettability of the surface.

3.3.2.11 Cell studies

In order to test the cell behaviour on the patterned surface, cell adhesion experiments were performed using the Infinity™ Telomerase Immortalised primary human fibroblasts (hTERT-BJ1), Clonetech Laboratories, Inc., USA). The cells were seeded onto patterned glass slides at a density of 3×10^6 cells per sample in 5 mL of complete medium. The medium used was 71% Dubelccos Modified Eagles Medium (DMEM) (Sigma, UK), 17,5% Medium 199 (Sigma, UK), 9% foetal calf serum (FCS) (Life Technologies, UK), 1,6% 200 mM 1- glutamine (Life

Technologies, UK) and 0.9% 100 mM sodium Piruvate (Life Technologies, UK). The cells were incubated at 37ºC with a 5% CO_2 atmosphere for 24hrs.

SEM studies in conjunction with immunostaining and fluorescence microscopy were used to determine if the cells were adherent to the surfaces or not. Procedures for both are as follows:

For SEM studies the cells were fixed with 1.5% glutaraldehyde (Sigma, UK) buffered in 0.1 M sodium cacodylate (Agar, UK; 4 ^{o}C for 1 hour) after a 24 hr incubation on substrates. Cells were then post-fixed in 1% osmium tetroxide for 1 hr (Agar, UK) and 1% tannic acid (Agar, UK) was used as a mordant. Samples were dehydrated through a series of alcohol concentrations (20, 30, 40, 50, 60 70 %), stained in 0.5% uranyl acetate and followed by further dehydration (90%, and 100% alcohol). The final dehydration was in hexamethyl-disilazane (HMDA) and followed by air-drying. Once dry, the samples were sputter coated with gold before examination with a Joel field emission SEM at an accelerating voltage 10 & 20 kV.

3.4 **Results and discussion**

3.4.1 Cation exchange

For this study two new Mn-Anderson anions have been synthesised as TBA and later as DMDOA salts by reaction of the core Mn-Anderson $[TBA]^{3-}$ $[MnMo_6o_{18}\{(OCH_2)_3CNH_2\}_2]$ with a two different acetyl chloride chains (C-16 and C-18). The results were as follows and a schematic representation is found in Figure 34:

1. $[MnMo_6O_{18}\{(OCH_2)_3CNH\text{-}CO\text{-}(CH_2)_{14}\text{-}CH_3\}_2]^{3-}$ (Compound 2)
2. $[MnMo_6O_{18}\{(OCH_2)_3CNH\text{-}CO\text{-}(CH_2)_{16}\text{-}CH_3\}_2]^{3-}$ (Compound 3)

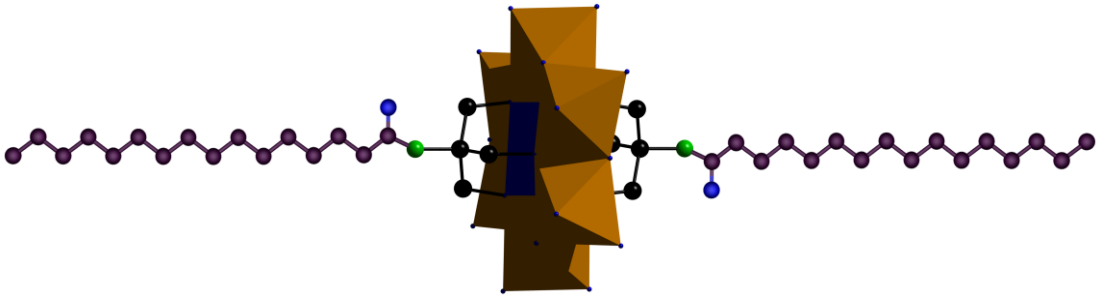

Figure 34. Representation of C-16 modified Mn Anderson showing the alkane tethers on either side adding large hydrophobic areas to the molecule.

Both the TBA and DMDOA prepared clusters were fully characterised by NMR, IR, elemental analysis and cryospray mass spectrometry[116]. These techniques have clarified that the amide bond formation between the Mn Anderson tether and the acetyl chloride chains have been successful. The mass spectrometry analysis has confirmed that there is little difference in the unit cell parameters between both the C-16 and the C-18 derivitised cluster and as expected there is a large degree of disorder associated with the alkyl chains; this is due to the many possible confirmations that the alkyl chains may align themselves to. The first 5-6 carbon atoms can be identified from this and used in conjunction with structural analysis and mass spectrometry results can confirm that the formation of the amide bonds has occurred and thus covalent attachment has been achieved resulting in a robust POM containing hybrid assembly.

The secondary investigation centred on determining the effects the cation has on the surface organisations of the clusters. Cation exchange from TBA to preparing the Mn Anderson clusters as dimethyldioctadecyl ammonium (DMDOA) salts (compounds 4 and 5) allows the exploration to what extent this surfactant like molecule affects the cluster in general. As a contrast to the TBA cations, the DMDOA is a surfactant molecule and has the potential to impart interesting surface activity onto the cluster, as the hydrophobic cations will interact differently to the previously used TBA cation.

The DMDOA cation as shown in Figure 35 has two long alkyl chains protruding from the quaternary nitrogen in comparison with the TBA cation that has 4 chains of equal length associated with it and this may have an effect on the organisation of the cluster on the surface.

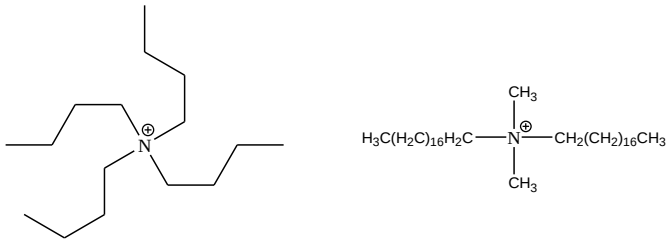

TBA Cation DMDOA

Figure 35 Schematic representation of the TBA and DMDOA cation showing the difference in each of the counter ions, the DMDOA has two long alkyl chains on either side of the quaternary nitrogen whereas the TBA has four shorter alkyl chains.

Samples of compound 2 and 3 were prepared as described and as the SEM images in Figure 36 show, crystalline material can be observed over the entire surface and closer examination of the material shows rod like features with dimensions in the range of 100-500 µm in length and a width of 10-15 µm when the C-18 cluster is dried on a surface. Example (a) demonstrates the uniform coverage of the rod like material across the surface and on closer inspection in b, c and d the specific features of the rods can be observed. The uniform nature of the rods implies the long chain alkanes are packed in such a way as to lie offset to each other in a “lamellar” fashion. On closer examination the clusters appear to generate a scattered needle like effect that is composed of highly ordered segmented rods fragmenting to a length of 10-25 µm and 5-10 µm in width.

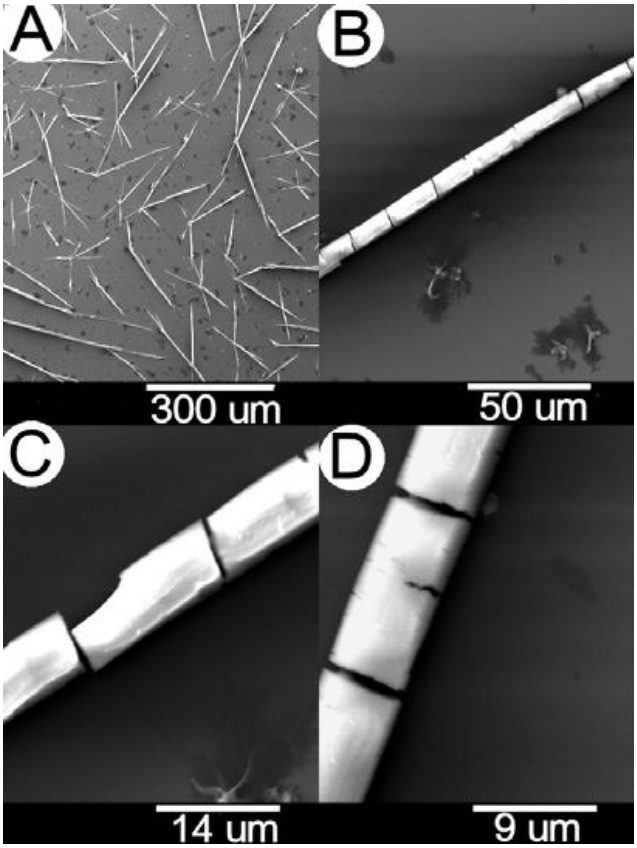

Figure 36. SEM images of C-18 functionalised Mn Anderson on a silicon surface showing the rod like features.

This was confirmed by Transmission Electron Microscopy (TEM) shown in Figure 37. Typical TEM samples were prepared from solvent cast films of the compounds. The lamellar structure of the clusters can be seen and the highly ordered rod like organisation and segmentation is consistent with the findings from the SEM. The anisotropic clusters form anisotropic features on the surface. This coupled with crystallographic data can conclude the Mn Anderson clusters prepared as TBA salts can be arranged with a high level of organisation.

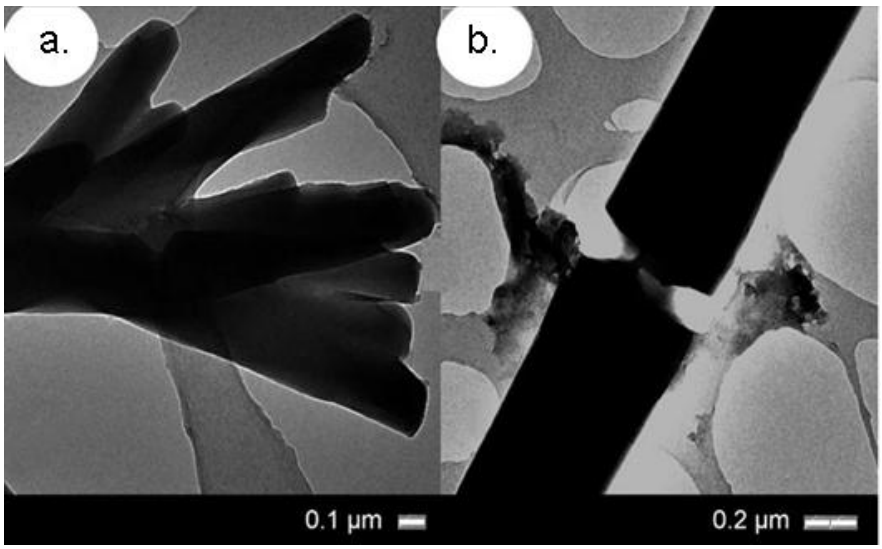

Figure 37 TEM images of the C-18 grafted Anderson showing similar results to the SEM.

These findings are in contrast to the C-16 modified cluster (Compound 2) which shows less organisation as shown in Figure 38. There is some evidence that rods have formed (a and b), however the majority of features on the surface show a less uniform crystalline pattern. This could be explained by the packing together of the molecules – the C-16 may not pack as uniformly as its C-18 counterpart when formed as a TBA salt.

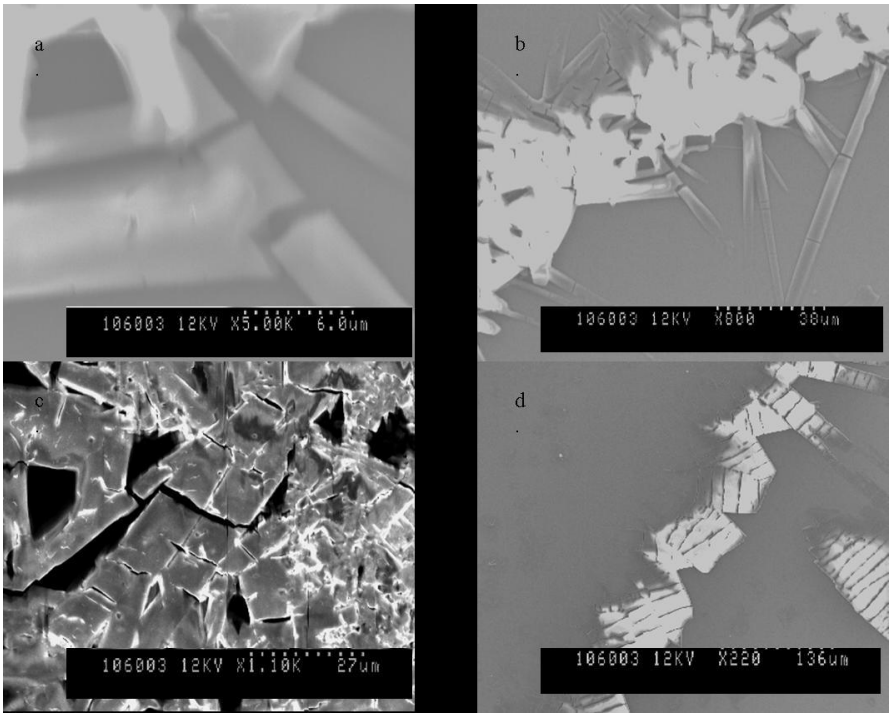

Figure 38 SEM showing the less well formed "rods" of the Mn Anderson tethered with C-16 chains. This is in contrast to the well formed structures of the C-18 chains; instead they form an almost crystalline material on the surface with little or no uniformity.

The examples here, and in particular image c and d demonstrate that although there is some rod like formation there is little uniformity or definition in contrast to the elongated and uniform needle like structures observed when C-18 (Compound 3) was added to the surface. Instead the image depicts a fragmented crystalline material that lacks in uniformity.

The crystal structure of the C-16 Anderson cluster can be depicted as shown in Figure 39. Only the 5th and 6th carbon atoms of the 16 carbon atoms in the chain can be found crystallographically. This is because there are many possible conformations for the chain and as such the structure can not be fully resolved however techniques such as NMR have concluded that the grafting of the organic chains has occurred successfully.

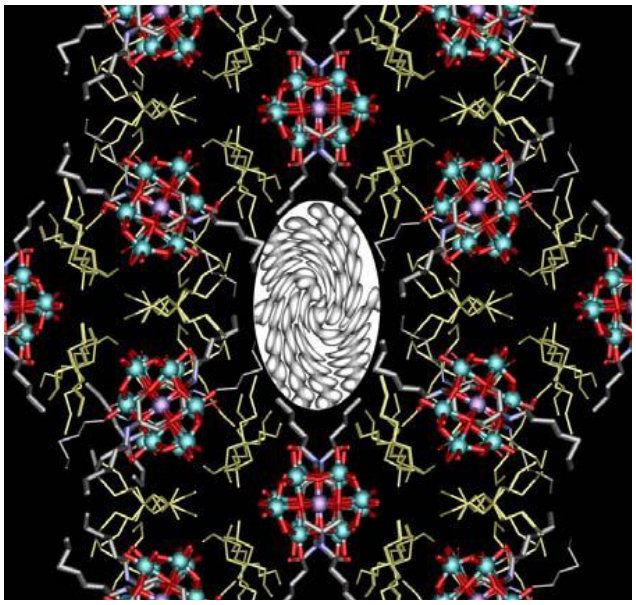

Figure 39 Structure of, $[MnMo_6O_{18}\{(OCH_2)_3CNH\text{-}CO\text{-}(CH_2)_{14}\text{-}CH_3\}_2](TBA)_3$. The white elipse depicts the void in the structure in which the alkyl chains are extremely disordered. The TBA cations are shown in yellow, the C-6 chain in grey and the cluster core in green, purple (Mo, Mn) and red (O).

This disorder may explain why there is little uniformity, the effect of the longer alkane chain may cause the structure to order and align as is seen, however with the shorter chains they alkane chains may pack together in a different orientation which lacks uniformity.

3.4.2 Cationic effects

An interesting observation is that the incorporation of this surfactant cation, containing long alkyl chains, makes the POM extremely soluble in chloroform and generates core-shell hydrophilic–hydrophobic surfactant encapsulated clusters

(SEC) in addition to surface grafted clusters (SGC). The three $DMDOA^+$ cations encapsulate the Mn Anderson and have two hydrophobic C-18 chains on their quaternary nitrogen atom in addition to the two hydrophobic C-16/C-18 chains grafted to the Mn Anderson (compounds 4 and 5 respectively).

The DMDOA salts were prepared as described in section 3.3.1.5-6 and substrates of $1cm^2$ silicon were prepared and investigated as described in section 3.3.1.7.

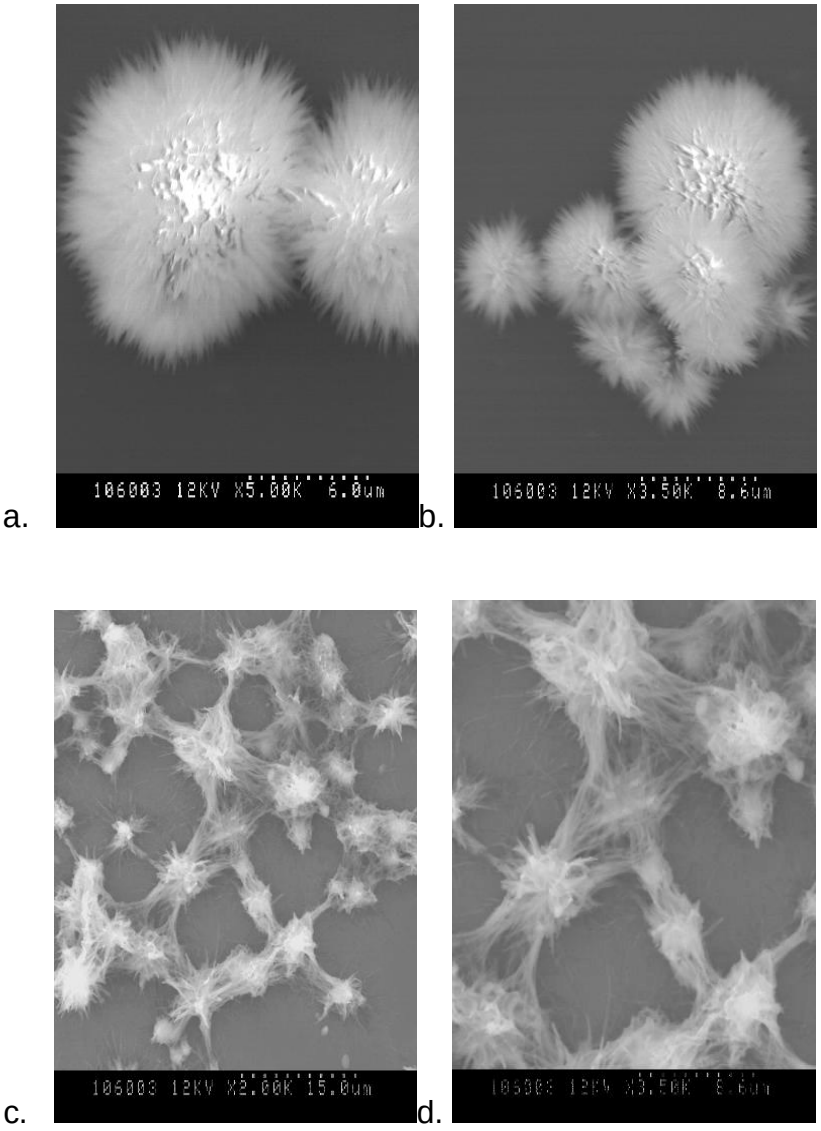

Figure 40. a-b SEM images of C-16 with ion exchanged cation (DMDOA) in a 4:1 mixture $CHCl_3$: MeCN. c-d C-18 chain with ion exchanged cation (DMDOA) in a 4:1 mixture $CHCl_3$: MeCN.

The striking difference between the TBA salt and the ion exchanged $DMDOA^+$ cluster is evident from Figure 40. The uniformity of the rods observed with the TBA cation has gone and large spherical molecules in the case of the C-16 molecule and disordered features for the C-18 molecule are observed. The cation exchange effect is obviously significant.

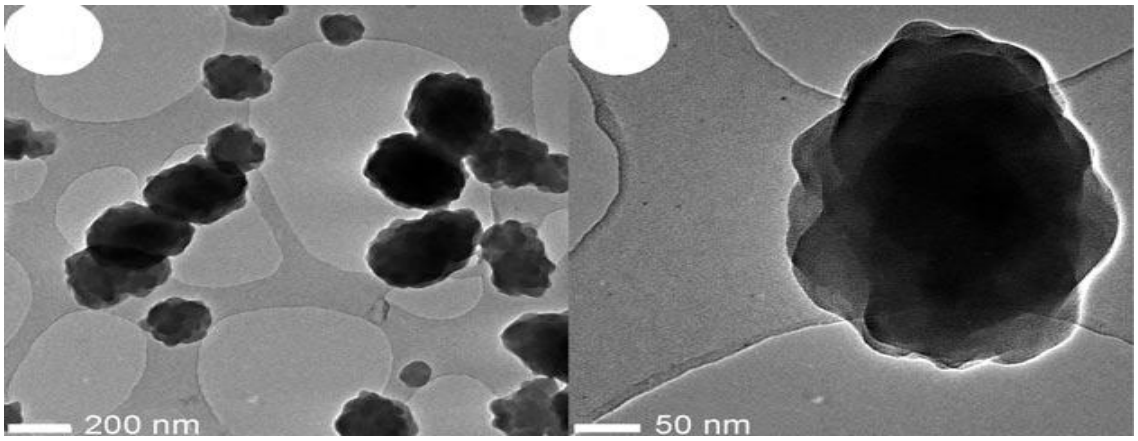

Figure 41 TEM images of the C16 cluster after cation exchange.

This is confirmed by TEM of the C-16 cluster that shows the full uniform formation of the composite on the surface in Figure 41. For every cluster there are three associated $DMDOA^+$ molecules, resulting in eight long chain alkyls per cluster. These long chain alkyls are effectively enveloping the inner region of the cluster with hydrophobic areas forming a surfactant-encapsulated cluster (SEC) a rare find in cluster chemistry. Not only is the tethering of the alkane chains affecting the ability to self organise, but the cations that are associated with the clusters have a definitive effect on the method of organisation.

3.4.3 Solvent effects on the cluster organisation

Not only does the grafting of the long chain alkyl groups on the cluster change the morphology on the surface, but the addition of the hydrophobic chains allows the clusters to be soluble in chloroform, allowing the formation of hydrophilic-hydrophobic surfactant encapsulated clusters (SECs). An interesting feature is that the DMDOA salts are soluble in chloroform compared with the TBA salts. The images show that 3-D spherical shaped features were observed on the surface in the size range from 1-20 µm.

This in turn resulted in the solvent being investigated by adding acetonitrile to the solvent mixture in a 4:1 ration with chloroform. This appeared to alter the morphology of the structures demonstrated in Figure 42 b and c which show more ordered structures in comparison to a. The structures exhibit an ordered sea-urchin like structure with needle like extensions protruding from the core in all directions. This is in contrast to the “honeycomb” morphology of other SECs that have been reported in the literature. [103]

The length of the tethered alkane also appears significant at this stage. Using the same 4:1 mixture of $CHCl_3$/MeCN, it can be seen from Figure 42 B and D that the formations on the surface differ in their level of order. The C-16 appears to form more needle like protrusions that are similar in length from the spherical feature whereas the C-18 structure appears to have needle like protrusions that vary in length. This could be due to a larger degree of disorder in terms of chain length of the alkane tethers in conjunction with the C-18 chains of the $DMDOA^+$ surfactant molecule.

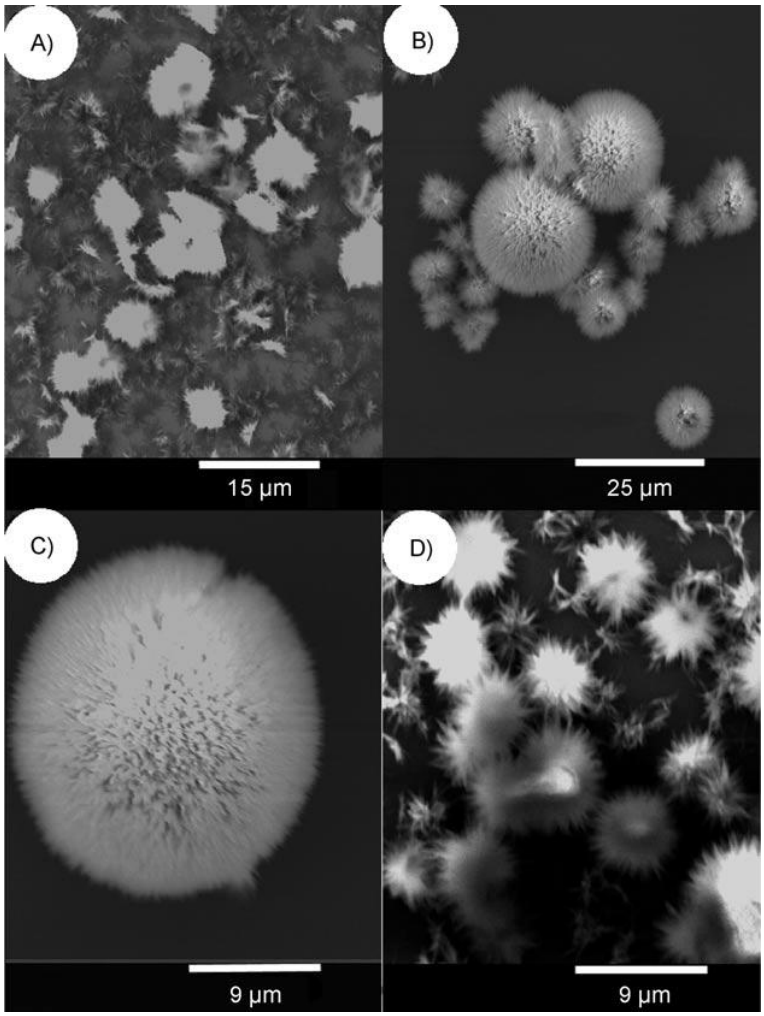

Figure 42 SEM image of a. C-16 cluster prepared from $CHCl_3$ solution and b. prepared from $CHCl_3$/MeCN =4:1. C. C-16 solution prepared from $CHCl_3$/MeCN =4:1. d. C-18 cluster prepared from $CHCl_3$/MeCN = 4:1.

Further to this when the TBA salts and DMDOA salts are compared, the direction of growth for the DMDOA salts lie out with the layers of the anion/cation, but the growth can be seen in the direction perpendicular to this. This difference can be attributed to the nature of the cation $DMDOA^+$ in contrast to TBA. The $DMDOA^+$ cation encapsulates the Mn-Anderson cluster and the long alkyl chains interact with the Mn-Anderson through electrostatic interactions.

3.4.4 Pyrene Functionalisation of the Mn Anderson cluster

Now the functionalisation of POM clusters has been achieved, the opportunity to explore this further is available. The ability to functionalise the Mn Anderson cluster has already been demonstrated with long alkane chains. However the covalent functionalisation of an electrically active POM with a highly conjugated electrically active material seems an interesting idea. This couples properties such as conductivity, electrochroism and redox activities of POMs with materials that are used in a number of applications such as light emitting diodes, field effect transistors and solid state lasers. The interesting feature of this chemistry is the potential to generate a complex that can potentially harbour an interaction between the d electrons of the cluster with the π electrons that are delocalised on the pyrene. This chemistry is still very much in its infancy due to the difficulties in grafting organic molecules directly onto a cluster and few reported structures of this type make the functionalisation of the Mn Anderson with a pyrene ring an interesting discovery.

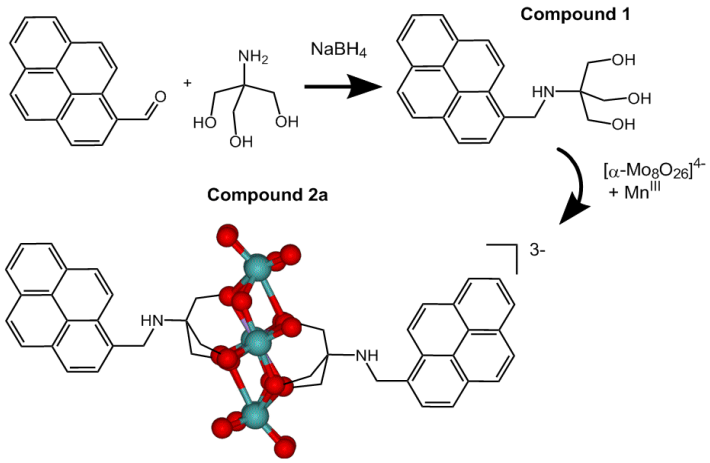

Figure 43 representation of the mechanism used to functionalise the cluster with pyrene rings tethered to the reactive amine of the tris group.[108]

The tethering of pyrene molecules to the terminal region of Mn Anderson as shown in Figure 43 changes the physical properties of the cluster as a result of the highly conjugated system it is now attached to. In direct comparison to the addition of the C-16 and C-18 chains to the Mn Anderson, the addition of the pyrene to either side of the cluster offers several interesting features. The hydrophobic interactions that were important on the alkane-modified cluster are now replaced with two large, highly conjugated molecules that have delocalised electrons that could interact with the d electrons of the cluster they are attached to. This study

compliments the investigation into inorganic – organic hybrid cluster molecules. Now not only the effect of the counter ion, solvent and concentration can be investigated and related to their effect on cluster organisation on a surface; but the organic material grafted onto the cluster can also be examined to determine the effect, if any, on the ability of the clusters to self organise.

The behaviour of the symmetric pyrene - Anderson was observed using SEM. A series of concentrations and solvent mixtures were made to observe the effect, if any, this has on the self organising ability of the clusters on the silicon substrate.

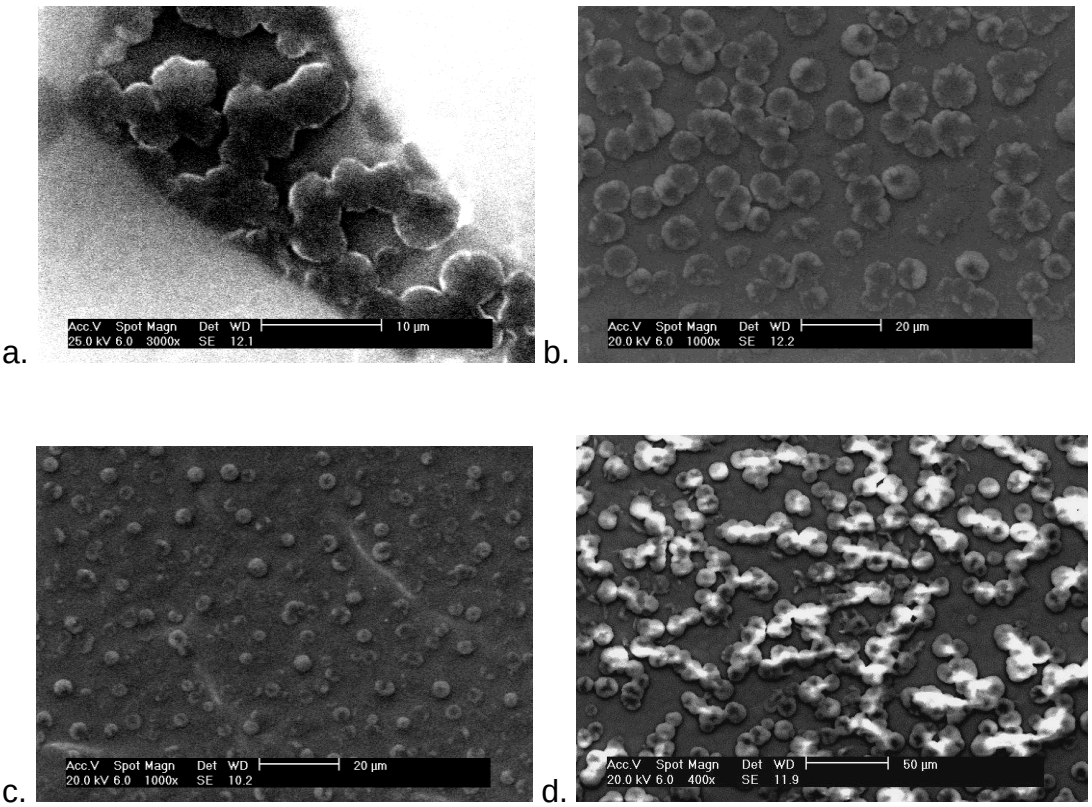

Figure 44 SEM images of symmetric pyrene Anderson under various conditions on silicon surfaces a.10mg in 5 ml chloroform b. 40mg in 5 ml chloroform c. 10mg in 1 ml acetonitrile + 5ml chloroform d. 40mg in 5ml chloroform + 1ml acetonitrile

Figure 44 a and b. Increasing the concentration four times gives a more definitive and uniform pattern across the surface showing a ‘micelle’ like morphology. Again this morphology can be seen with the addition of acetonitrile to the mixture, although less well formed and uniform across the surface. The increase in concentration of this mixture increases the number of “micelle” like structures as explained previously. These micelle like features are potentially due to the stacking of adjacent molecules and their pyrene rings interacting in a circular

arrangement π-π stacking with the clusters at the centre of the "micelle". In comparing b and d, the images represent the same concentration but the introduction of acetonitrile into the solvent mixture has been caused minimal effects in this instance. The concentration effects of this solvent mixture can be seen in comparing c and d. The increase in concentration shows a larger number of well formed "micelle" like features that in the lower concentration image.

A recent crystallographic study on the symmetric pyrene Anderson by the Cronin croup may also help understand this micelle like formation. [108] Crystallographic data shows the following formation and crystallographic organisation:

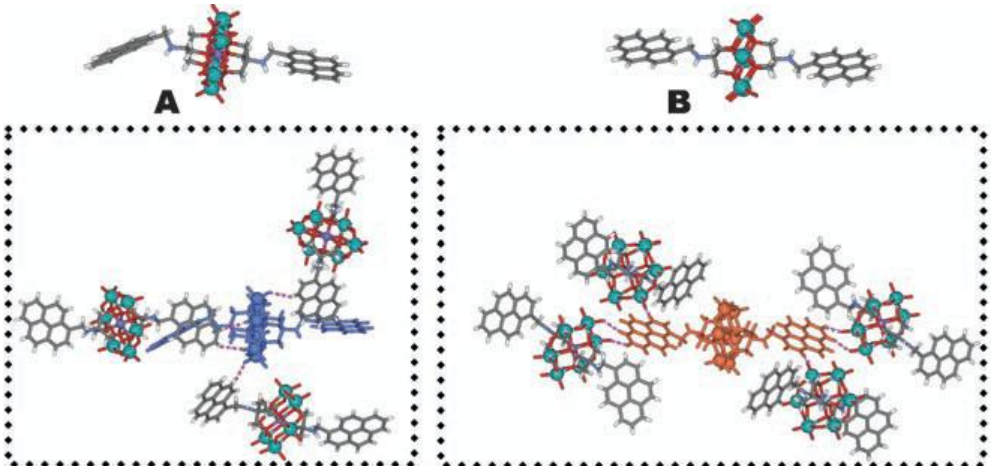

Figure 45. The two types of [Mn-Anderson (Tris–pyrene)$_2$]$^{3-}$ building blocks, A and B (top), and sections of the structure (bottom) containing the building blocks A (blue) and B (orange). The weak C-H···O= Mo interactions are shown by the purple dotted lines: the type A building blocks act as acceptors, and type B building blocks as donors. Mo green, Mn purple, C black, H white, N blue, O red. [108]

We may gain further insight into the formation of the micelle like structures seen on the silicon substrates by looking at the crystal structure of the cluster. The framework of the cluster is dictated by two types of building blocks that, through their confirmation, interact and connect the structure in different ways. Studies have identified that the type A and type B building blocks as shown in Figure 45 exist in different confirmations and act as complimentary donor and acceptor units that arrange into a one dimensional channel as shown in Figure 46. The units are arranged as A-B-A-A-B-A forming the hexangonal shaped channel in the centre as the rings appear to stack on top of each other.

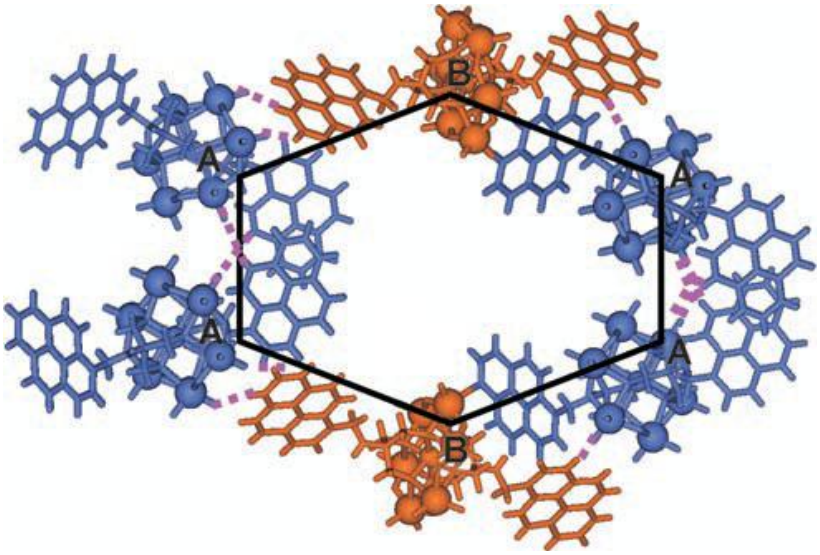

Figure 46 The walls of the pores are formed by [Mn-Anderson(Tris– pyrene)$_2$]$^{3-}$ building blocks (A blue, B orange) so that they are held together in a (-A-B-A-A-B-A-) fashion by weak C-H···O=Mo interactions (purple dotted lines) in the crystallographic ac plane. Stacks of these building blocks form the channel, which runs down the crystallographic b axis.

3.4.5 Surface studies of Patterned SAMs

In order to determine if the patterning via microcontact printing had been successful, the surface can be imaged using various surface analysis techniques. Scanning electron microscopy is a technique that can easily be used to determine if the patterning has been carried out successfully, but cannot determine the composition of the patterned areas.

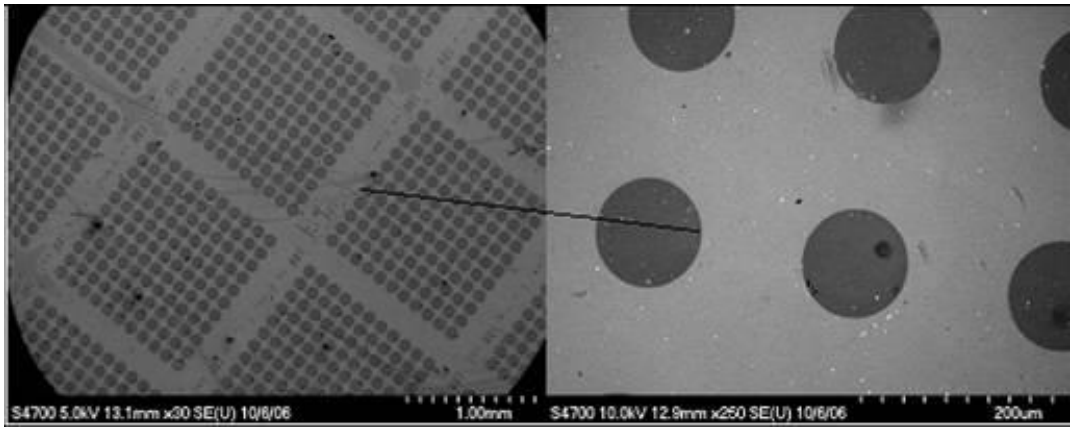

Figure 47 Scanning electron microscopy images showing patterned areas of 50µm circles.

Successful patterning can be confirmed as shown in Figure 47; where circular features of 50µm in diameter have been transferred from the PDMS stamp inked with mercaptohexadecanethiol (MHA) onto the gold surface through sulfur to gold bond. The terminal region of the pattern is a carboxy group which is then used to couple the primary amine of the *tris* group from the cluster to chemically attach the

molecule to the surface, leaving a further amine at terminal region of the self assembled monolayers. The surrounding light grey area which has been backfilled with an unreactive alkanethiol can be identified. The sulfur again links to the gold and the terminal region this time is an unreactive methyl group blocking the rest of the surface to further chemical reactions and allowing localised addition of the cluster on the predetermined patterned areas.

SEM only provides a route to determining if a pattern exists on the surface; time of flight secondary ion mass spectrometry (TOF-SIMS) was used to determine the elemental composition of the surface which can be identified with high sensitivity (~1ppm) to give a true reflection of the molecular composition.

The positive and negative ions present and their position on the surface, whether they be in the patterned regions or the surrounding area, can be identified from Figure 48. It is clear that from the surface images obtained that the Mn Anderson cluster is patterned on the surface with a high selectivity. From the negative ion spectra, the Mo ions can be seen in clearly defined patterned areas. In the positive ion spectra and related image the Mn ions can be seen occupying the same patterned area.

The presence of the amide bond is also important in determining the location of the cluster, as previous to the addition of the cluster no nitrogen was present on the surface. Identifying where this exists provides further evidence of the addition of the cluster and CN^- ions can be clearly identified in the negative ion image and spectrum. Further to this O^- ions can also be seen within the patterned area. As oxygen only exists on the MHA and Mn Anderson, it can be concluded that the cluster has indeed been patterned. Full Mass Spectrometry data can be found within the Appendix.

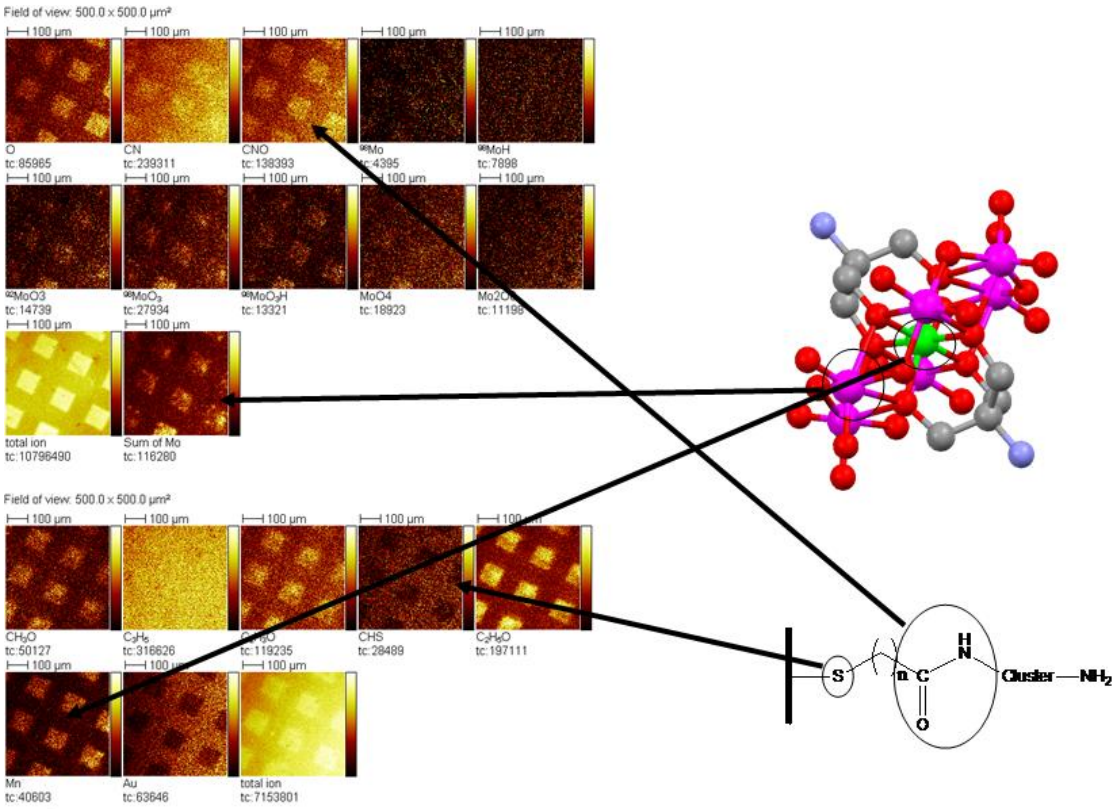

Figure 48 TOF-SIMs of the surface showing the patterned regions and the presence of the clusters in the patterned areas with corresponding mass spectrometry data indicating the mass of the secondary ions. [117]

The importance of this result is significant. For the first time it has been demonstrated that it is possible to pattern a POM cluster with a covalent bond linking the cluster to the surface in a pre-arranged design. The implications of this are significant and open up new and interesting ideas to develop POM surface chemistry.

3.4.6 Addition of pyrene-Anderson to patterned surfaces

In addition to the successful surface patterning of the POM cluster on a surface, creating surfaces with some functional potential is the next step in the process. Surfaces that have a terminal region and functionality that can be exploited are in high demand not only in an academic setting but are also important for industrial use within areas such as molecular and biological devices. Through the use of self assembled monolayers the route to these surfaces has become easier – and a new addition to this group is not only the addition of the polyoxometalate to the terminal region - but also the continued functionalisation of this molecule, to give new and interesting functionality. As described in previous sections, the Mn

Anderson cluster functionalised with the tris group has the potential to be significantly altered through the reaction of this with a pyrene ring and from this both a symmetric and unsymmetrical pyrene Anderson cluster is produced. The potential in this case is to link the free amine group of the tris section to the already patterned surface leaving the pyrene ring exposed at the terminus.

An interesting point of this synthesis lies in the fact the material is not purely asymmetric pyrene-Anderson but a mixture of both symmetric and asymmetric. The ability to add only the asymmetric Anderson through the terminal amine is a positive advance in the purification step – the symmetric Anderson has no functionality to add to the terminal carboxylic acid on the patterned surface. This method can then be used to purify the solution as a solid state chromatography method.

The addition of the pyrene-Anderson gives interesting electronic properties. As mentioned previously this is a highly conjugated system with the potential for interaction between the d electrons of the cluster and the π electrons of the pyrene. If tethered to a surface, this offers the potential to harbour electron storage devices that can be organised and patterned down to the nano scale. There is also the potential to stack pyrene and other planar molecules on top of the tethered cluster.

In order to compare this surface in further studies, a similar surface was prepared which omitted the Mn Anderson portion of the SAM. This would then act as a control experiment in future studies and in particular, to cell studies which are described.

3.4.7 ToF SIMS of Prepared SAMs

As was the case with the Mn Anderson SAM, ToF – SIMS was carried out on the 3 surfaces shown in Figure 48 in addition to a control SAM containing only the carboxylic acid functionality.

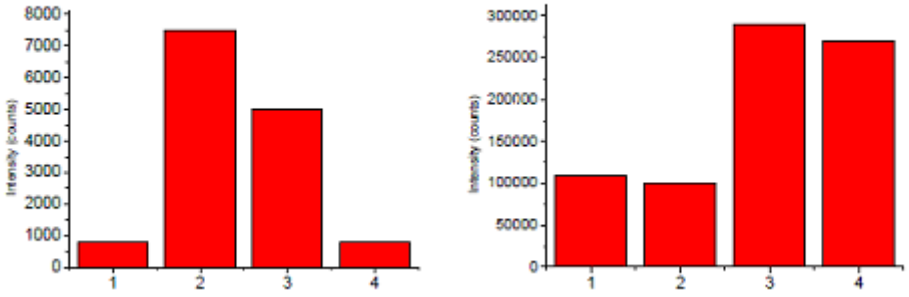

Figure 49 TOF-SIMS results for Mn (left) and pyrene $C_{16}H^{10+}$ (right) intensities for the control (1), SAM 1 (2), SAM 2 (3) and SAM 3 (4). [117]

The results show that SAM 1 and SAM 2 in the left hand graph, exhibit a strong presence of Mn, indicating the tethering of the Mn Anderson cluster and limited signal for Mn on the SAMS which do not contain the cluster. From the RHS graph, the presence of the pyrene is confirmed in SAM 3 and SAM 4, as expected. From these results it can be concluded that the surfaces have all been modified successfully.

3.4.8 Contact Angle measurements

The contact angle of each of the three SAMs as well as a control SAM of (16-mercaptohexadecanoic acid stamped onto gold surface through Au-S bonds) were carried out in order to determine if there were any differences in the surfaces hydrophobicity as a result of the changes in the terminal functional groups. The results are shown in Figure 50.

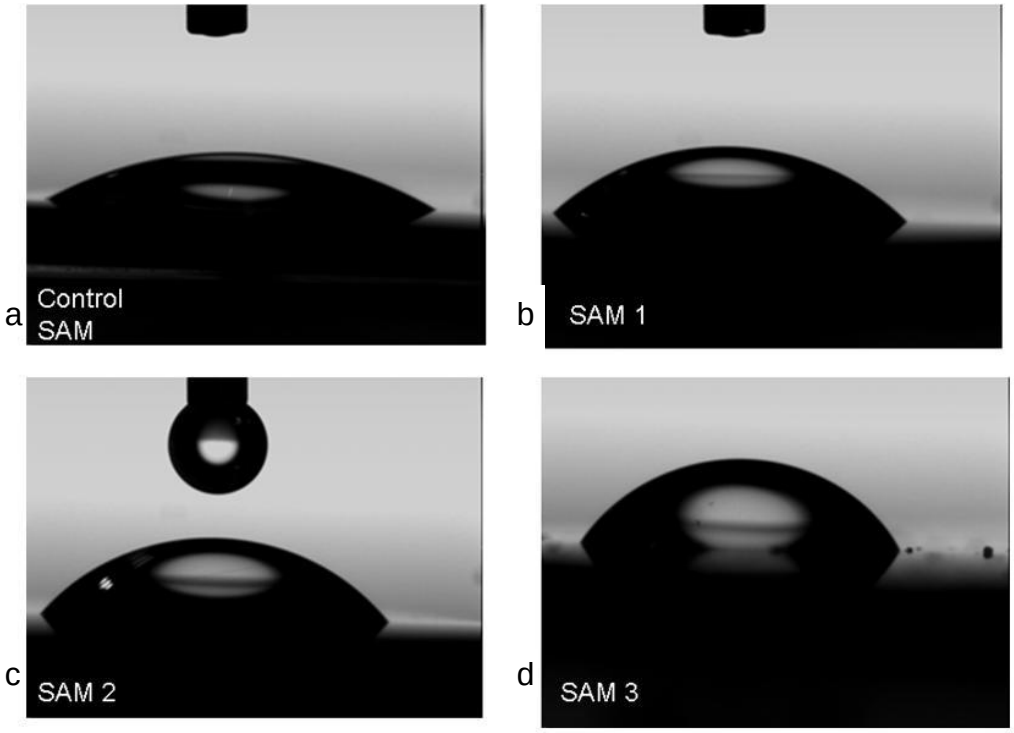

Figure 50 Contact Angle Images. Samples were measured using a Kruss EasyDrop system. Image a. control-SAM, Image b. SAM 1, Image c.SAM 2, Image d. SAM 3 [117]

The results depict that the control SAM with the underivitised carboxylic acid functionality exhibits the most hydrophylic characteristics with the hydrophobicity increasing from SAM 1 through to SAM 3. This is to be expected since the carboxylic acid terminated region of the control is more hydrophylic by nature than the terminal pyrene of SAM 3. Between SAM 1 and SAM 2, the introduction of a Pyrene terminal substitution on Anderson POM in SAM 2 makes it more hydrophobic than the NH_2 terminated Anderson in SAM 1. [117]

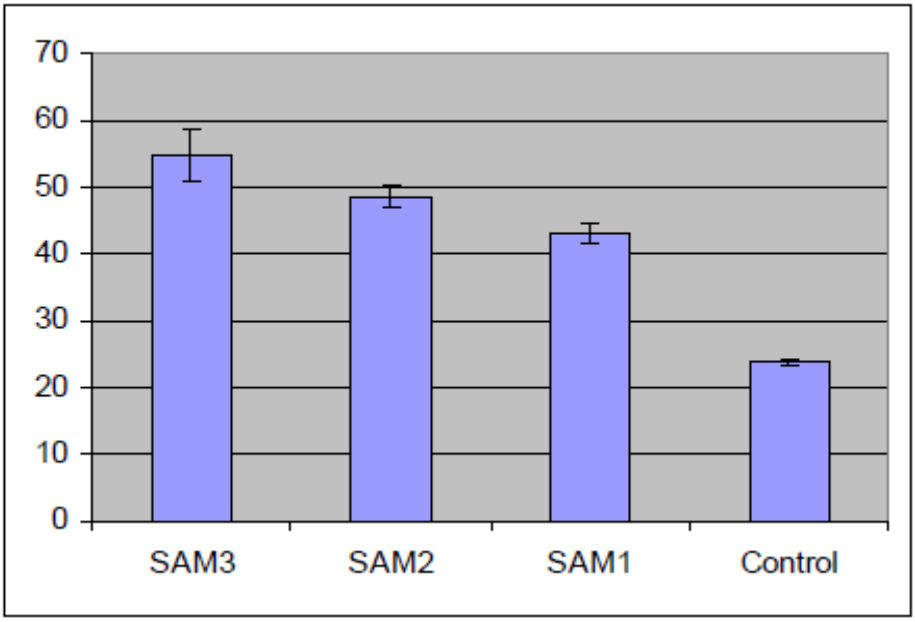

Figure 51 Chart showing the decrease in contact angles from SAM 3 to control-SAM [117]

These contact angle measurements shown in Figure 51 clearly suggest that the above 4 surfaces are patterned with different terminal functionalities. In addition these measurements indicate that the physical properties of surface grafted POMs can be tuned by grafting different functional groups onto it (*e.g*. the NH_2 terminated Anderson cluster on SAM 1 has different hydrophobicity than the pyrene terminated Anderson cluster on SAM 2).

3.4.9 AFM studies of modified surfaces

The surface coverage of the monolayers of each of the prepared SAMS was analysed by Nikolaj Gadegaard using AFM using a Nanoscope Dimension 3100 in tapping mode. The results are shown in Figure 52.

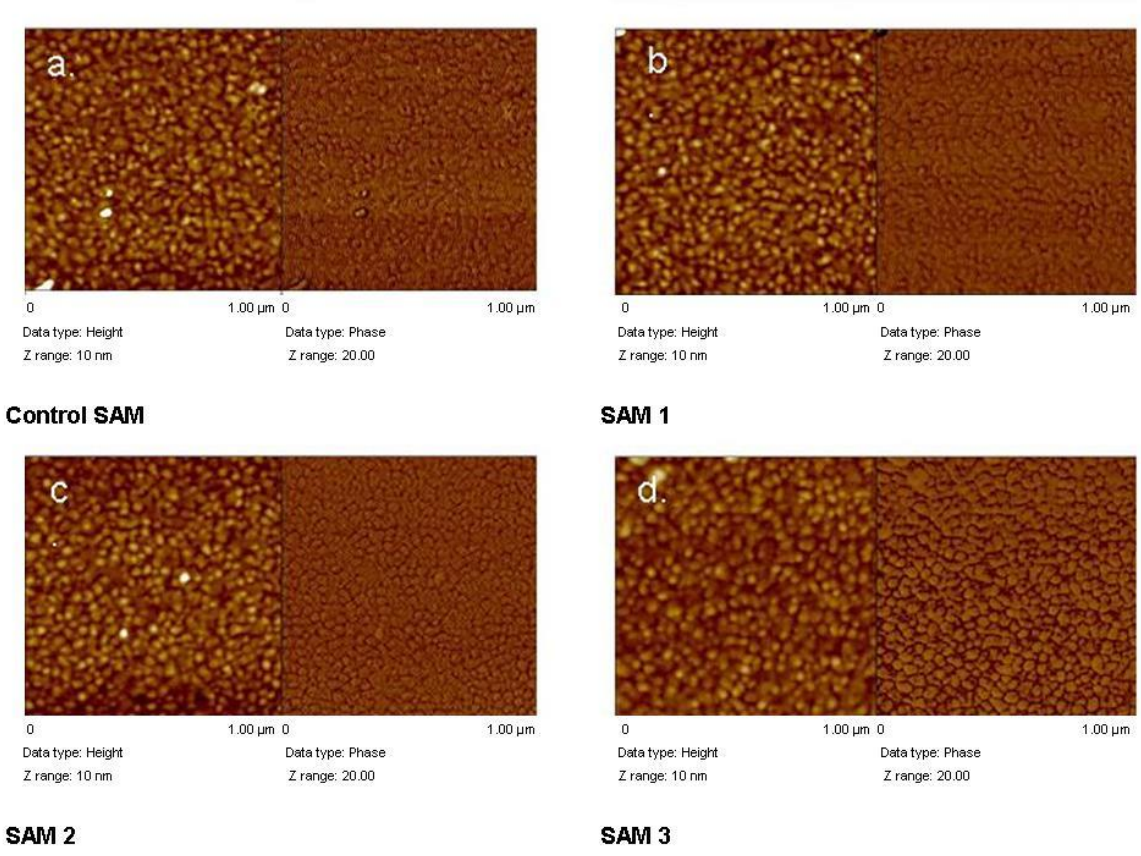

Figure 52 AFM images of the surface topography of the control SAM to SAM 3.

The AFM images confirm that there is a uniform coverage of material on the surface of each sample. The roughness is 1.0 nm +/- 0.1 for the different samples.

3.4.9.1Cell Study Results

As discussed, the recent study of of cell adhesion with areas patterned with fluroscein and rhodmaine have illustrated cell response to particular functionalities and in particular with aromatic regions. This has led to the design of a self assembled monolayer containing a covalently grafted pyrene moiety to see what effect, if any, this has on the specific orienteering of cells to this region. This not only has interesting applications in materials science, but the introduction of a pyrene ring to the POM offers potential interesting applications in understanding the mechanism of cell direction to large aromatic regions on a surface. The results in Figure 53 show that the cells specifically orientate only on the areas containing the aromatic regions, further demonstrating that cells will direct themselves to these areas above the methyl terminated area in direct comparison to previous studies with oligo (ethylene glycol) chains. The need for adding proteins such as

fibronectin, used to aid adhesion in previous studies, is lost as the proteins appear to adhere and spread to the surface without the need for proteins to aid adhesion.

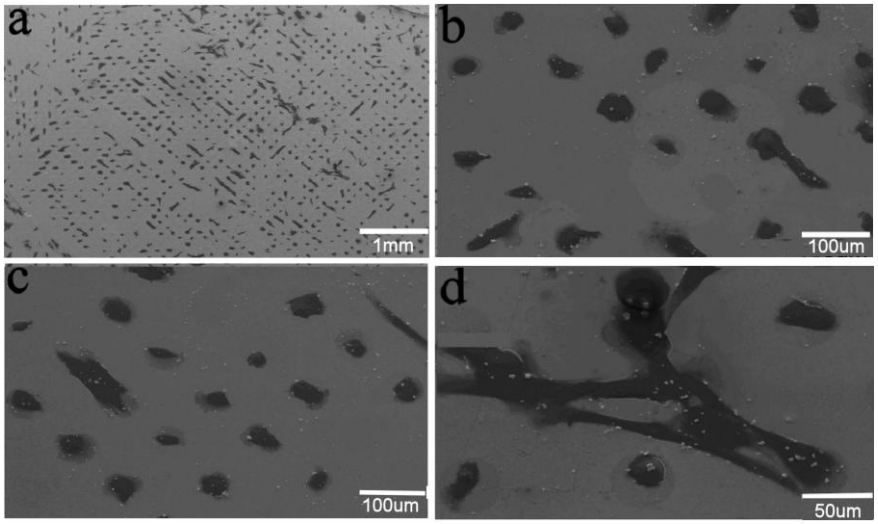

Figure 53 SEM images of the cells on the pyrene Anderson surface (compound 8). Cells can be seen to locate themselves primarily on the patterned areas, sometimes bridging between one patterned area and an adjacent patterned circle containing the pyrene.

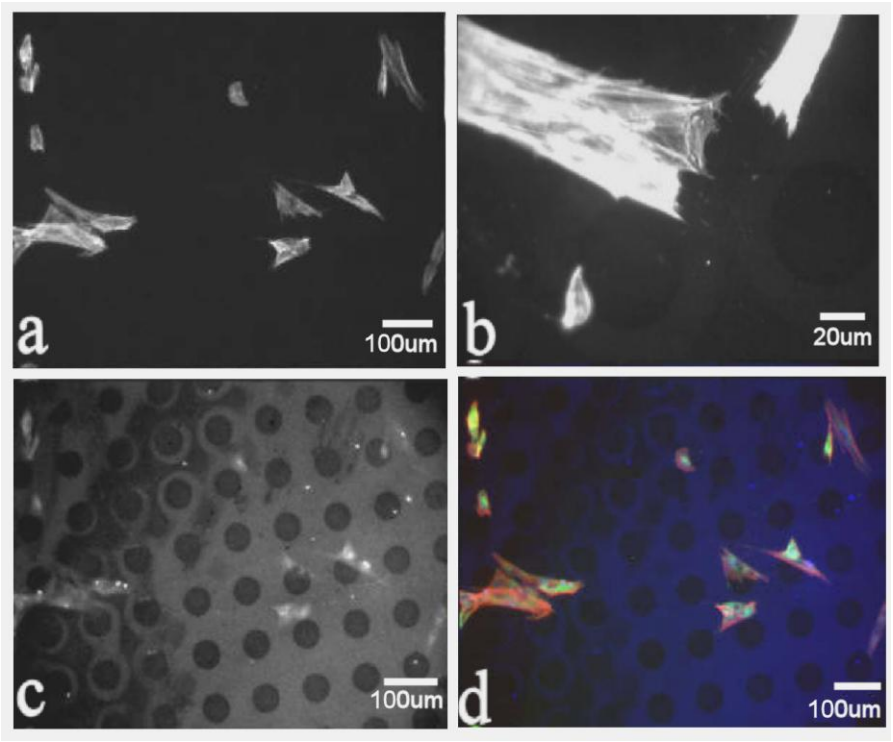

Figure 54 Immuno-staining results of the interactions between hTERT-BJ1 cells fluorescently stained and compound 3 on SAMs. a, c and d are the same images (the same scale bar for these three: 100 μm as shown in d), in which 'a' shows the general view of cell response; 'c' shows the patterning and cell response with black and white image and 'd' shows the patterning and cell response clearly with colour image. b: enlarged image showing cell response (scale bar: 20 μm).

Cells are found to adhere exclusively to the patterned areas of the surface avoiding the alkane regions surrounding the pyrene ring. In some cases the cells spread beyond the patterned area but only to locate themselves on a patterned adjacent area. The cells have a clear preference for the aromatic region offering interesting applications as this is the first time a metal oxide containing molecule has been used to specifically direct a cell to a specific orientation. The ability of a cell to recognise an exclusively aromatic region is an important observation as it gives further insight into the cell affinity for aromatic regions. Further evidence was gathered to determine what was controlling the cell adhesion.

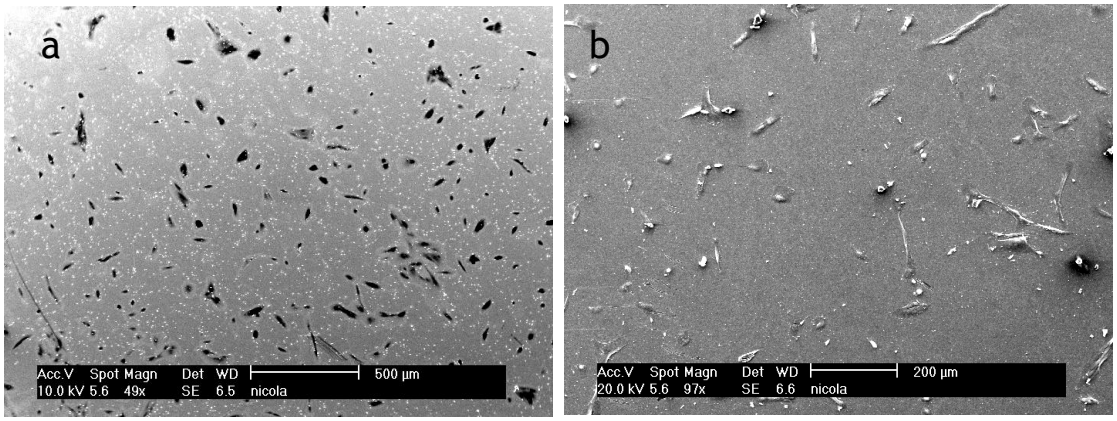

Figure 55 a and b. showing cells on a surface containing terminal amine from the Mn Anderson (compound 1) and carboxylic acid and methyl terminated areas. Cell spreading is random and in no specific pattern compared with the pyrene Anderson.

This cell patterning result demonstrated by the pyrene Anderson is in direct contrast to the SAMs patterned with a terminal carboxy group and the tris terminated Mn-Anderson. This result has been demonstrated in Figure 55 , where no selective cell alignment can be observed. This raises the question as to what directs the cells to the pyrene area, is it specifically the pyrene moiety or does the POM have some influence in patterning the cells?

In order to answer this question a control SAM was prepared. Further studies reveal that SAM-4 (pyrene terminated, no POM, compound 8) showed no obvious cell affinity. This in turn suggests that the presence of the POM plays some role in directing the cells to the pyrene platform and that perhaps the orientation that the pyrene is held in by the POM may be crucial to the SAM creating the perfect platform for cell adhesion. In addition the cell adhesion on the Pyrene Anderson may be due to the negative charge and the nano-scale size of the Mn Anderson cluster, which prevent strong π-π interaction among the neighbouring pyrene

groups on the SAMs**.** As a result, the interaction of ECM proteins with aromatic pyrene groups could display π-π stacking interactions between the pyrene platforms and the aromatic amino acids such as phenylalanine and tyrosine from the ECM proteins.

The cell culture results can be summarised from the schematic in Figure 56 detailing the cells interaction with the terminal region of the various SAMs produce.

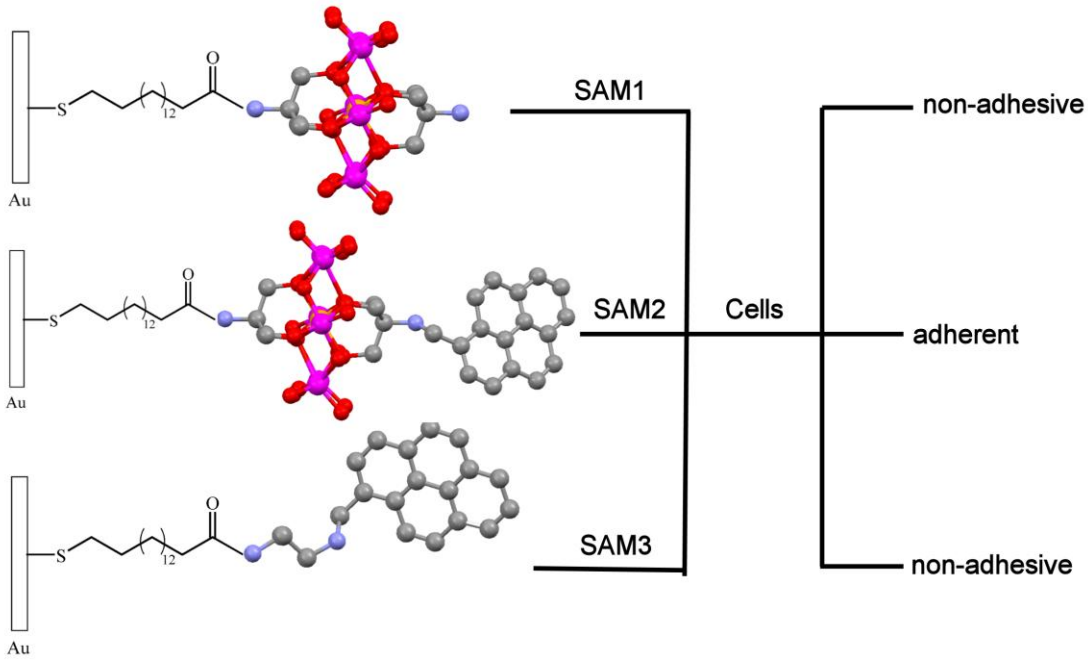

Figure 56 Schematic representation and summary of the 3 substrates created in order to determine cell affinity for the different surfaces.

3.5 **Conclusions**

The ability to modify POM clusters with organic molecules and the evolution of these organic – inorganic Mn Anderson has proven interesting with respect to their surface patterning ability. For the first time the ability to tether alkyl chains to a Mn Anderson has been demonstrated producing POM hybrid assemblies with hydrophilic – hydrophobic nature. Changes in both the organic tether attached to the cluster, the cation surrounding the cluster and the solvent interaction gives interesting surface morphologies and an understanding into the interaction the Mn Anderson has with these external factors.

The presence of the tethered alkane chains on the Mn cluster with TBA as a cation and the generation of the rod like material that are uniform in dimensions across the surface is interesting and could be as a result of the close packing of the molecules when dried from solution onto a surface. In comparison to the C-18 tethers this can be directly compared with the transition in this material through ion – exchange with the $DMDOA^+$ cation. The change is obvious; surrounded by a large mass of hydrophobic regions, the molecules form micelle like morphologies as they have become encapsulated by organic material, thus providing a rare example of surfactant encapsulated materials (SECs).

Therefore, it is clear that the ability to tether molecules onto a POM is a major advance in materials chemistry providing new and interesting surface morphologies with simple changes in the cluster's immediate conditions, whether it is cation or solvent effects, or minor changes in concentration. The great advance of this is the ability to look at the same core cluster with varying tethered molecules and having evidence of change in the surface organisation and the ability to self-pattern these molecules.

In addition these studies can relate to the crystal structure of the cluster and how these effects can be partly explained by looking at the crystal structure in comparison to the formations these clusters create on the surface. With regards to the pyrene functionalised SAM, the crystal structure shows that there is a hexagonal shaped cavity that is determined by the fact here the pyrene moieties lie in two different conformations forming a distinctive alignment with the adjacent pyrene molecule. The fact that this molecule forms micelle like features on the surface may be indicative of this distinctive feature and the pyrene moieties may

be stacking in a particular way to cause this conformation and therefore the pattern.

This provides to evidence that the functionalisation of clusters, and in particular their particular organic tether and counter ion, plays an important role in how these clusters self organise on a surface and give a deeper understanding of the effects these play on the cluster as a whole.

Further to this, the evidence gathered to support the patterning of the clusters onto a gold surface through direct coupling to a self assembled monolayer provides scope for many interesting areas of study. This work describes for the first time the patterning of a symmetric Mn-Anderson cluster onto SAMs via a simple, fast microcontact technique for fabricating chemically patterned surfaces. By changing the terminal functional group, an asymmetric POM-containing framework with pyrene group grafted onto Mn-Anderson cluster has been designed and patterned successfully onto SAMs. The modular approach to the build up of a SAM utilised the presence of the *tris* moiety on the inorganic – organic hybrid cluster to allow the formation of the peptide bond between the terminal carboxylic acid of the SAM and the amine functionality associated with the POM. This in turn created a SAM with a POM being the terminal functional group in a pre determined pattern.

In addition the synthesis of the asymmetric pyrene Anderson often yields a mixture of symmetric and asymmetric structures. This method of patterning the symmetric pyrene Anderson ensures that the two molecules are separated, as only the cluster with the available *tris* moiety can be patterned onto the terminal carboxyl group and as such this technique allows the selective purification of a reaction mixture.

Primarily this investigation has looked at using modified Mn Anderson molecules with pryrene rings in order to further understand the adhesion of cells to surfaces. SAMS have always played a role in understanding more about cellular and molecular biology, but the inorganic aspect of this surface provides a new route to understanding the mechanism of cell adhesion. Previous studies have shown the affinity cells have for aromatic regions[41]. However this has never involved a purely carbon and hydrogen containing area – rhodamine and fluroscein both contain other atoms that could assist in the anchoring of cells to that area. Now there is evidence to suggest that the aromaticity of the region could play some role in

attracting the cells to that specific area without the assistance of other functionalities.

The patterning of both the symmetric Mn Anderson and the pyrene terminated Mn Anderson have been confirmed by a variety of methods. Firstly SEM was used to clarify that that a pattern had indeed been created, and as can be seen from Figure 47 a pattern is visible from SEM and is uniform across the surface. The confirmation of the chemical composition of the surface came from carrying our ToF- SIMs analysis on the patterned surfaces and as is confirmed in Figure 48, it can be seen that the Mn Anderson has indeed been pattered on to the surface and further clarification that the pyrene Anderson has been patterned can be seen from Figure 49. Further characterisation techniques have been carried out and are shown in Figure 50 and Figure 52 respectively.

The studies have shown that interaction of POMs with biological systems is dependent on parameters such as structure, dimension, composition and molecular weight. The difference between the physical and chemical properties of the SAM containing the Mn Anderson functionalised with pyrene and the Mn Anderson could be responsible for the difference in cell adhesion. The non adhesive properties of SAM 3 (pyrene only) show that the Mn Anderson cluster may have some role to play in the cell's behaviour. Although the definite proof for the function of Mn-Anderson cluster core is not yet fully understood, preliminary cell response results to the Anderson cluster**,** which has been designed as a model substrate and patterned onto SAMs, indicates that cells show no preference to the patterned areas, suggesting that Mn-Anderson cluster plays important roles in cell adhesion behaviour of the pyrene Anderson.

4 The Modification and surface decoration of proteins using a DNA intercalator.

4.1 Chapter aims

Previously reported synthetic studies have publicised the formation of di-hydro-imidazo phenanthridinium (DIP) moieties from a simple one-pot, three-step reaction of a primary amine with 2-bromo-ethyl-phenanthridinium bromide salt. The compounds have been shown to bind strongly to DNA and have high cytotoxicity for ovarian cancer cell lines. The following describes the adaptation of this reaction enabling formation of a polyvalent DIP derivative by use of the protein bovine serum albumin, lysozyme and insulin. Such a simple tactic for modification is not only highly unusual but extremely valuable in the field of protein modification. This modification has been analysed by mass spectrometry, circular dichroism and AFM which show distinctive variations in the images seen before and after modification.

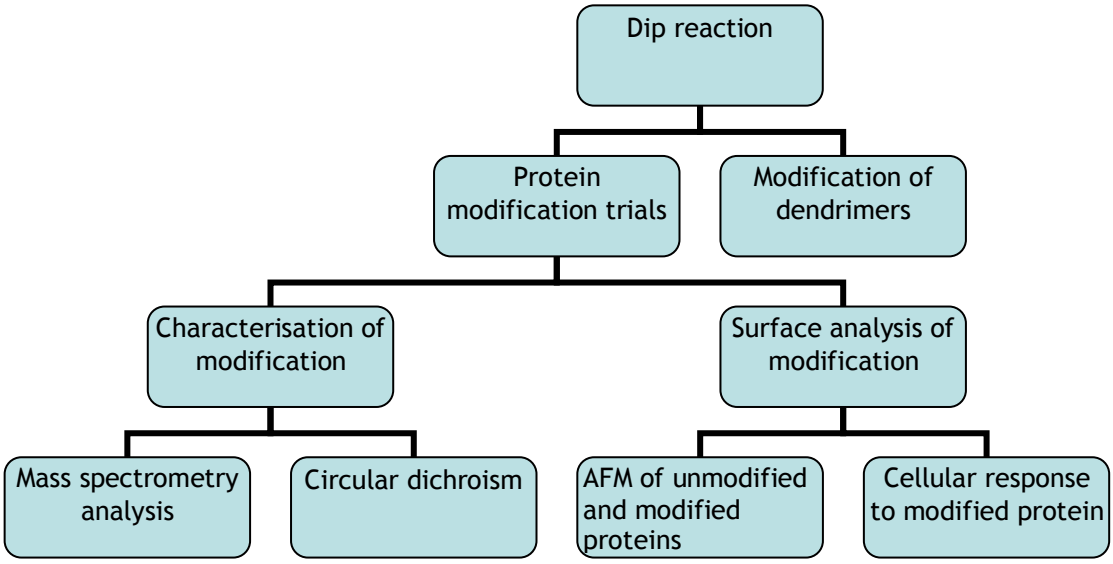

Figure 57 Flow chart of chapter outlook.

In addition to modifying proteins, the effect the DIP modification has on other large molecules e.g. dendrimers and their subsequent surface analysis makes an interesting investigation. This is coupled with the ability to pattern the DIP moiety onto a surface using previously described self assembled monolayer formation and a subsequent modular approach to building on this structure to perhaps further investigate this interesting heterocyclic molecule.[154]

The proposed scope of this investigation is to determine if the reaction between 2 – bromoethyl phenanthridinium bromine and the free primary amine on the lysine residue may be carried out on a biologically active molecule whilst retaining its structure, represented schematically in Figure 58. The effect this modification has on its secondary structure will be evaluated using techniques such as circular dichroism and the effect the modification has on the bulk material will be looked at using Atomic Force Microscopy.

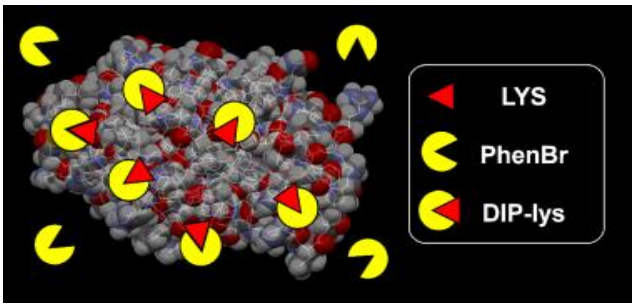

Figure 58 Schematic representation of the process by which the lysine residues are targeted on the surface of the protein.

4.2 Chapter Introduction

4.2.1 Proteins structure and function

Around 100,000 different types of protein exist within the human body.[118] Every molecule that exists is either a protein or has been created by proteins, thus their importance can not be underestimated. Their actions include the ability to catalyse reactions, transport molecules, control gene expression and essentially help us grow in.

Surprisingly of the 100,000 proteins within the body each comprises only 20 essential building blocks. These building blocks or amino acids consist of three parts as can be seen from Figure 59:

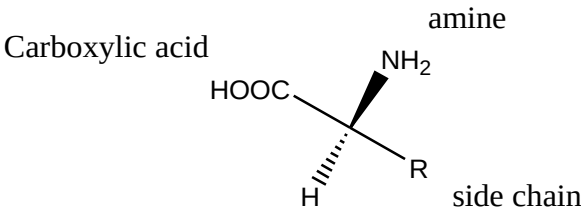

Figure 59 Representation of an amino acid [119]

The side chains represent the important feature of the amino acids[120] and are responsible for the structural and functional diversity between each protein molecule as shown in Figure 60.

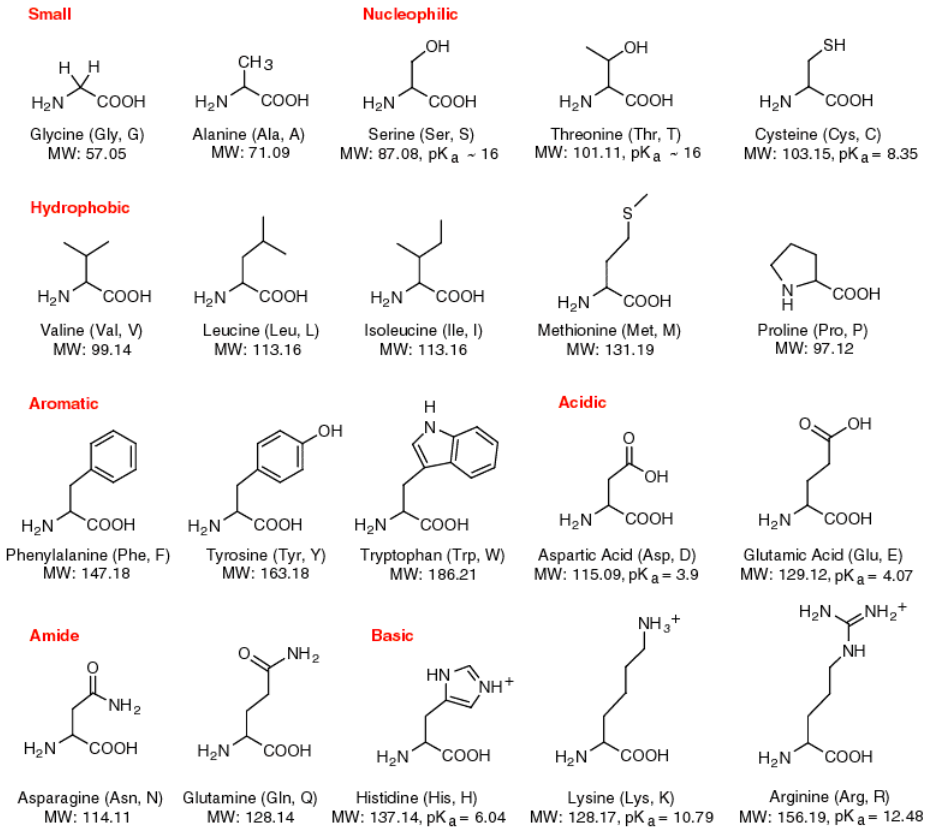

Figure 60 The molecular structure and side chains of the 20 amino acids indicating their diversity the protein structure may have.[121]

The amino acids form the structure of the protein by covalently linking via peptide bonds to create a linear chain, as represented in Figure 61. The structure the protein adopts is based on the protein backbone. The resulting strands fold in such a way as to create a 3 dimensional active biomolecule. The peptide bond

demonstrated in Figure 61 is planar and normally adopts a *trans* confirmation. [122] Between the nitrogen and the α-carbon, rotation is possible and is denoted as φ, in a similar manner the ψ angle is the angle of the bond between the α and β carbon atom. This results in a number if combinations of chain folding, only one of which will represent the native structure of the protein.

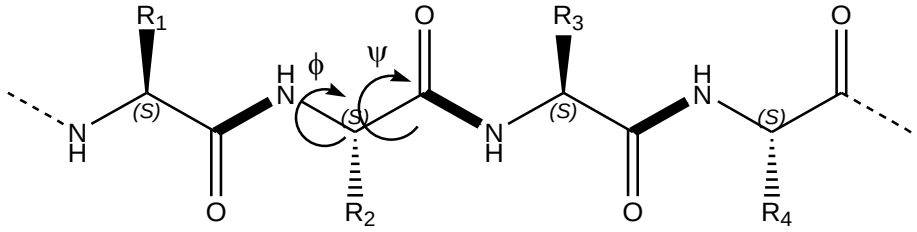

Figure 61 Schematic diagram of the peptide bond[119]

The amino acid chain will develop 3 levels of structural folding. Secondary structure follows three distinct patterns; β-sheets, α-helices and random coils, and the distinct folding will initiate interactions that will form the tertiary structure. When two or more folded chains interact this results in the formation of the quaternary structure.

A protein 3D structure is maintained by covalent and non covalent interactions.[123] A covalent bond e.g. a disulfide bonds are formed through a shared pairing of electrons; whereas non covalent interactions offer a force that allows the stabilisation of the native structure.

Beyond the formation of the amino acid backbone, non covalent interactions are important features that organise the secondary, tertiary and quaternary structure of the proteins. Examples of such interactions include:

- Electrostatic interactions – occur between opposite charged groups within the protein e.g. salt bridges and ionic bonds[124]

- Van der Waals interactions –the fluctuating distribution of charge in an atom forms a momentary dipole that influences induced dipole interactions. These interactions are relatively weak and as such are short range (3-4 Å) [124]

- Hydrogen bonds – involve the sharing of a proton between two atoms, one or which being the H donor and the other being the H acceptor. This is a vital interaction that allows and maintains structural features such as the α helix and the β sheet and cause increased stability (average H bond is between 3-7 kcal mol^{-1}). [125]

- Hydrophobic – these interactions play an important role at the core of the protein. With the key to this interaction being the repulsive force between non polar groups and water; non-polar groups are often found in clusters at the core of the protein so as to minimise their exposure to aqueous substances, as such this interaction plays an important role in protein folding.[126]

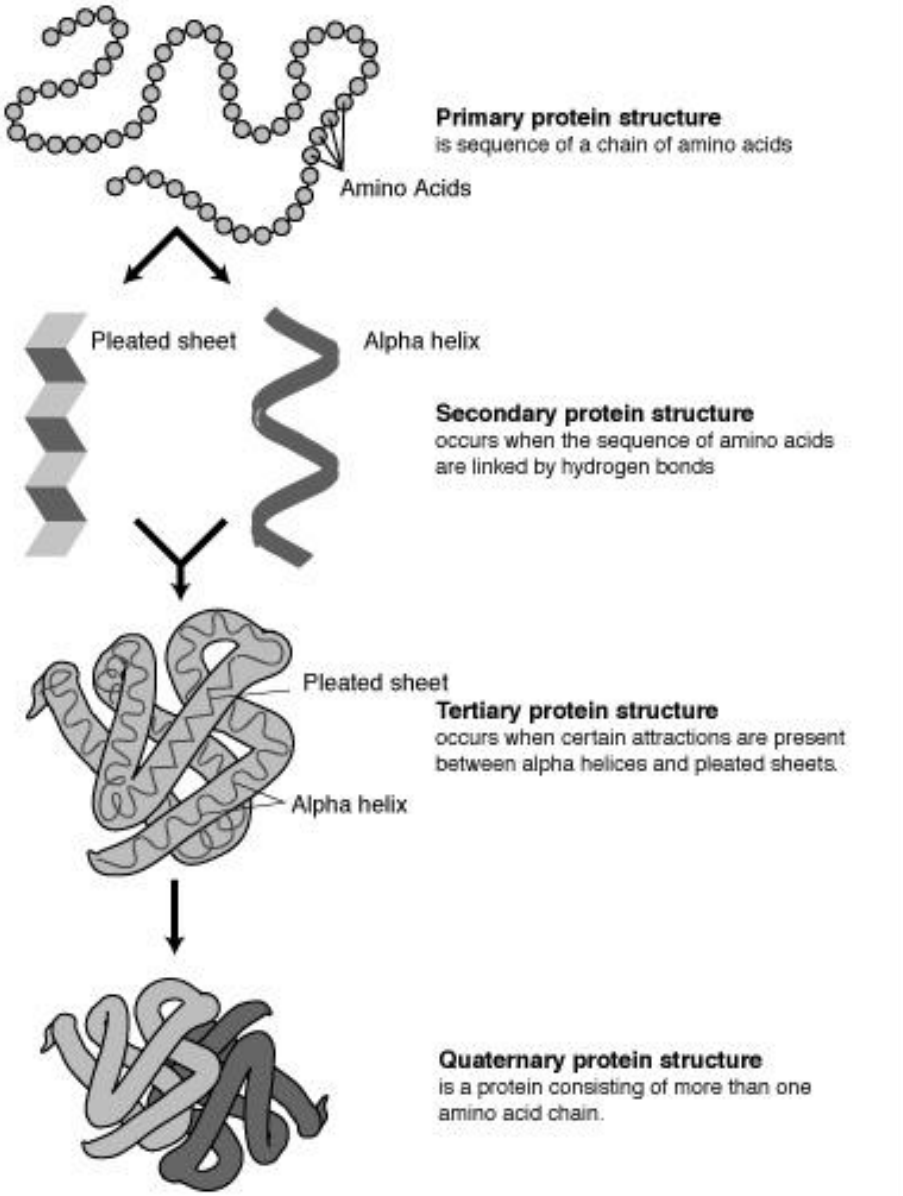

Figure 62 Schematic representation of protein folding hierarchy [127]

With their multitude of interactions and folding possibilities, proteins can be additionally characterised by their structural sub type of which there are four: globular, fibrous, membrane proteins and unfolded. Globular proteins are the most abundant; mainly enzymes, these proteins are soluble in comparison to fibrous, which are insoluble in aqueous media and are often large in size and regular in conformation.[120] Membrane proteins often act as receptors or transporters in the body;[120] however, full characterisation has proven difficult due to their insolubility in aqueous media.[128] Unfolded proteins have a lack of tertiary structure which can be directly related to their function. These molecules bind to a range of ligands

which in turn confers functionality and results in increased order and folding of the protein.

Proteins can therefore be considered versatile but complicated structures that rely on the amino acid backbone and side chains for structure and function. These side chains represent an opportunity for further exploration.

4.2.2 Protein Modification

The ability to chemically modify proteins with relative ease and simplicity has long been a problem to protein scientists who understand that the alteration of protein structures could lead to higher structural diversity and ultimately new protein functions.[129] Protein modification is not new and previous successful modifications have led to developments in biological and biomedical applications. This being the case, protein modification has produced new routes to produce flurophores[129a,b], cofactors for catalysis[129c], biosensors[130] as well as the immobilisation of these molecules onto surfaces. [129d]

Post translational modification (PTM) is the process by which proteins have their amino acid side chains altered chemically and naturally within an organism for functional purposes, and many PTMs exist in nature as part of a molecule's natural life cycle.[131]

In general, modifications carried out in the laboratory have proven difficult with control being lost with respect to which amino acids are to be modified and ultimately separating reaction mixtures into pure components. Although uncommon, modification of proteins has been successful by utilising the following methods;

- modification of proteins by FITC (fluroscein-5'-isothyocynate) used to produce fluorescent proteins[132]
- the Mannich reaction, utilised to reduce tyrosine residues[133]
- diazonium coupling[133]
- Suzuki cross coupling[129c]

Although these examples provide evidence that there is methodology available, these reactions are not easy to complete and it is for this reason that efficient chemical modifications are limited despite the need to drive modifications that have the potential to benefit and be useful not only within an academic setting but have interesting potentials in many biological applications.

4.2.3 DIP Reaction

The recent discovery of a one-pot, three step reaction yielding dihydro-imidazo-phenanthridinium bromide (DIP) molecules from 2-bromo ethyl phenanthridinium bromide and a primary amine as seen in Scheme 4 has sparked a great deal of interest.[79]

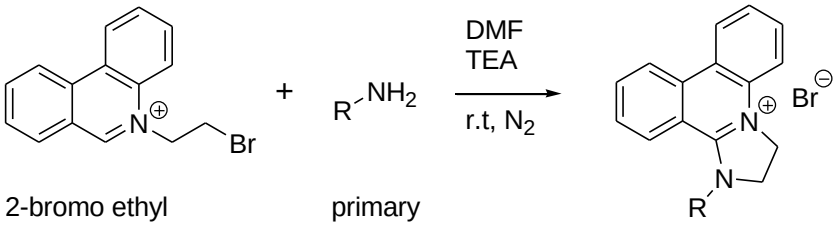

2-bromo ethyl phenanthridinium bromide

primary amine

Di-hydro **I**midazo **P**henanthridinium Bromide

Scheme 4 Reaction of 2-bromo ethyl phenanthridinium and a primary amine to form DIP.

Initially the reaction was carried out with the expectation of functionalizing the side chain of 2-bromo ethyl phenanthridinium bromide with the primary amine. Unexpectedly the aromatic moiety underwent nucleophilic substitution at the α position, followed by 5-*exo*-*tet* cyclization and oxidative hydride loss as shown in Scheme 5. This mechanism was confirmed when intermediates **4** and **5** were isolated and characterized by NMR and mass spectrometry,[79] whilst molecule **3** was isolated by the use of a hindered primary amine, obstructing the 5 membered ring cyclization.[79]

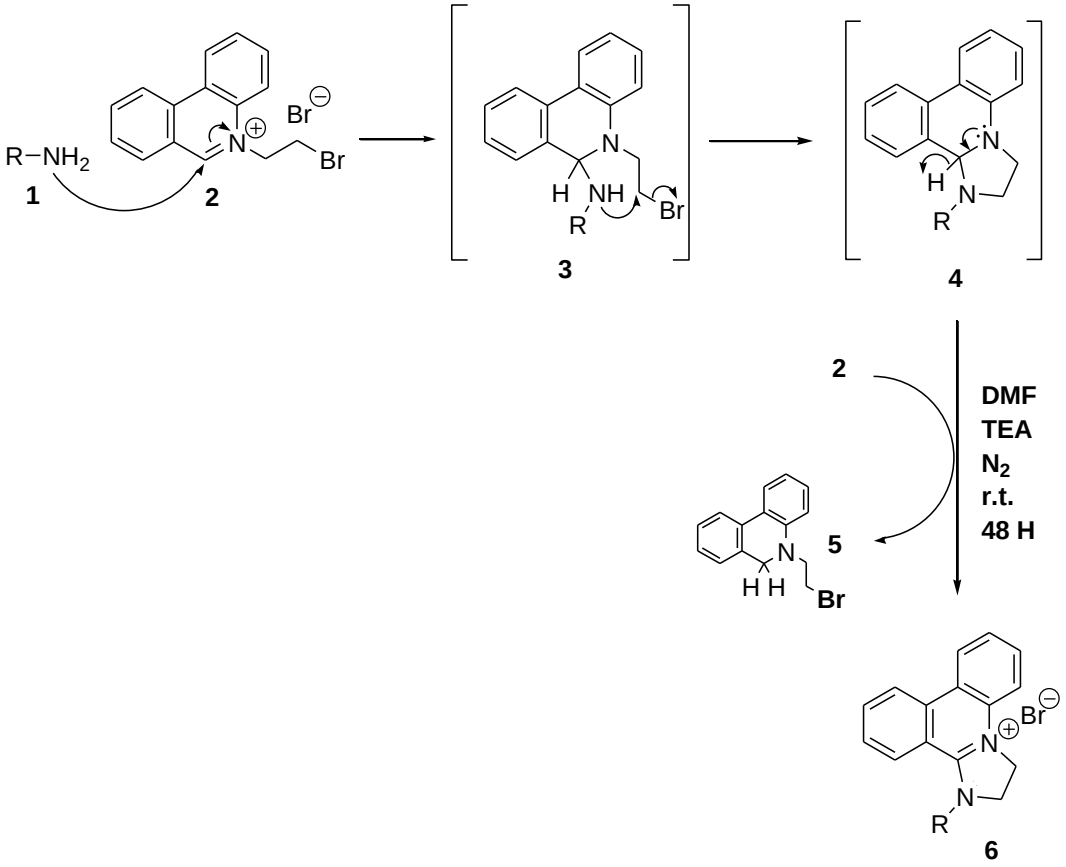

Scheme 5 Mechanism of reaction leading to DIP framework.

The reaction tolerates a wide variety of amines enabling synthesis of a vast library of compounds that show both strong affinity for DNA by Isothermal Titration Calorimetry (ITC),[80c] and cytotoxicity towards ovarian cancer cell lines by MTT assays.[80c,82] In general the DIP molecules synthesized display a binding constant of ~2×10^4 - 7×10^4,[82] comparable to that of ethidium bromide ~12.9×10^4 [82] considered in biology to be a strong DNA intercallator. Cytotoxicity results from MTT assays show varying degrees of toxicity, dependent mainly on the nature of the functional group attached to the DIP,[80c, 82] with the most toxic compound showing a substantially higher toxicity than that of the clinically used cis-platin.[80c,82]

Previous work has focused on the synthesis of monomeric and dimeric DIP products.[79] Viscosity measurements have established the DIP molecules to bind to DNA via intercalation between the DNA base pairs and planar, poly-aromatic core of the DIP.[82] It seems likely that polyvalent systems, with a higher concentration of aromatic regions would show stronger affinity for DNA. Although the exact mode of cell death has not yet been established, any correlation existing between DNA

affinity and cytotoxicity would also benefit through such polyvalent systems. The higher frequency of aromatic regions on such a system should also enable a high cytotoxicity to be achieved from a lower concentration of molecule, reducing any side effects associated with it. Meaning that proteins with their many reaction sites may lead to a multi-DIP system that may be able to exert a toxic effect at low concentrations and a high level of solubility.

Initial synthetic routes led to production of polyvalent systems that were extremely insoluble in aqueous media, a property that ruled the discovery out of being a possible drug candidate. To combat this obstacle, a strategy involving protein molecules as polyvalent starting materials was devised, utilizing the amino residues on the protein surface as starting materials for the DIP reaction. This would not only create a water soluble polyvalent system but would exploit the protein as a "biological carrier", through protein-cell membrane interactions, to direct DIP molecules to specific cell types.

4.2.4 Modification of proteins with DIP

The above reaction offers an interesting starting point to determine if it is possible to use proteins as carriers of DIP, creating biological polyvalent systems. In order for the reaction to be of interest, the protein must retain its secondary structure and the modification must be selective, hence why the reaction involving the formation of the DIP moiety is such an attractive one. [79,80b]This will give a route to modify selected residues within the amino acid sequence that are accessible without disturbing the secondary structure and ultimately develop a route to alter the tertiary structure in such a way that the modifications change the properties of the protein. This in turn may uncover potential uses for the protein which could include using the protein as a biocompatible carrier of drugs and diagnostic probes.

Utilising the primary amine of a lysine residue as the starting material to produce the DIP moiety, is an excellent starting point to determine if modification is possible. The selectivity of the reaction makes it attractive over other potential modifications, as the reaction would only utilise the exposed primary amine residues on the protein, in particular the lysine residues. This in turn would produce proteins decorated with the DIP moiety. This would be a great advantage, as the protein has the potential to act as a biological carrier used to solubilise the

DIP moiety and carry it across the protein cell membrane and expose the DIP directly to various cell types.

Phenanthridinium bromide is used as a reagent and oxidising agent in the reaction with lysine residues and so two equivalents are needed for very primary amine present. In terms of the thiolate modification, phenanthridinium bromide is only the reactant and so only one equivalent is required.

4.2.5 Protein Choice

The choice of protein within this investigation is key to understanding the modification process and the proteins ability to retain its structure if at all. In turn the investigations will look at each protein, post modification, to determine the success of the reaction and look further at the effect this modification has had.

4.2.5.1Lysozyme

Lysozyme is a widely studied protein due to its relatively sturdy structure which seems to have the ability to withstand harsh conditions and yet remain active.[134] Not only this, but the extensive study and characterisation of all aspects of the protein and the wide array of assays available in order to determine its activity, as well as the ease at which a crystal structure can be determined, coupled with the 14.7 kDa molecular weight makes lysozyme, a relatively small protein, an ideal target for study.

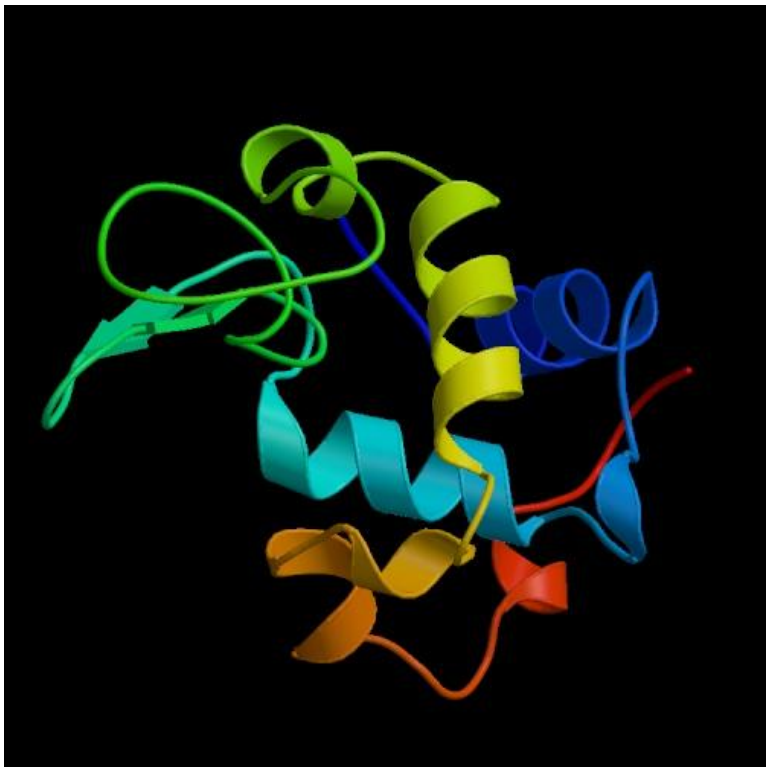

Figure 63 Schematic representation of lysozyme molecule detailing the tertiary structure of the protein. [135]

1963 saw the elucidation of the sequence of lysozyme showing a 129 amino acid residues with 4 disulphide bonds linking a single polypeptide chain.[134a] Its three dimensional structure may be considered to be split into two parts as determined by x-ray analysis. Residues 1-40 form an alpha helix structure with a core of non polar residues, whereas 41-92 form a less stable configuration with a high proportion of polar residues. The remaining residues are what makes up the area in between these two regions. The basic side chains of lysine, arganine and histadine are distributed on the surface of the molecule – therefore exposed for further reaction.

MRSLLILVLC	FLPLAALGKV	FGRCELAAAM	KRHGLDNYRG
YSLGNWVCAA	KFESNFNTQA	TNRNTDGSTD	YGILQINSRW
WCNDGRTPGS	RNLCNIPCSA	LLSSDITASV	NCAKKIVSDG
NGMNAWVAW R	NRCKGTDVQ	AWIRGCRL	

Figure 64 Lysozyme Amino Acid sequence highlighting the presence of lysine residues. [134a]

The structure and function of lysozyme has been studied intensively; so much so that the correlation between its structure and its function has been determined, a rare quality in protein science.

The role of the cysteine residues is important in looking into the modification of the molecule. Lysozyme, from hen egg white, contains 4 disulfide bridges in contrast with lysozyme from other sources containing less or no disulphide links, yet remains active. This discovery determined that these linkages play no role in the activity of the enzyme. It has however been determined that lysozyme containing 4 disulfide bonds is more stable in harsher conditions and able to withstand more acidic conditions than those without; the same can be said for heat stability. This in turn makes lysozyme an ideal model protein to study.

4.2.5.2 BSA

The choice to use Bovine Serum Albumin as a model protein for investigation comes from its natural stability and the fact it is a relatively unreactive molecule often used to stabilise other reactions. This coupled with the molecule being cheap and readily available makes it an ideal candidate for study.

One of the drawbacks of using such a molecule is the size of the protein and the complexity of its structure which makes characterisation difficult. In its entirety The protein is 607 amino acids in length with a molecular weight of 69.4 kDa with an 18 residue signal peptide on the protein that, when removed, makes the protein 66.4 kDa and 583 residues in length.[136] Within the molecule at a Ph of 5-7 there are 17 disulfide bonds present, Figure 65 and Figure 66 which reference structure and sequence of this protein.

BSA is the principal carrier of fatty acids that are otherwise insoluble in circulating plasma. It also performs many other functions such as, sequestering oxygen free radicals and inactivating various toxic lipophilic metabolites such as bilirubin. In general albumins are known for their solubility in water which also adds to their advantage on this project – the initial aim was to solubilise a molecule coated in DIP which could in turn be used to solubilise this in solution - again an ideal characteristic of this protein.

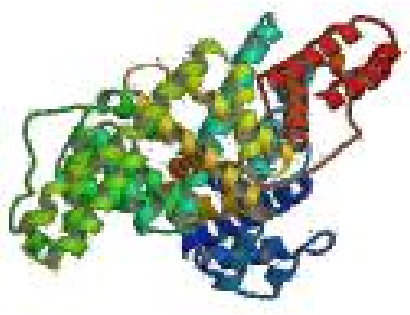

Figure 65 Schematic representation of BSA

mkwvtfisll llfssaysrg vfrrdthkse iahrfkdlge ehfkglvlia
fsqylqqcpf dehvklvnel tefaktcvad eshagceksl htlfgdelck
vaslretygd madccekqep ernecflshk ddspdlpklk pdpntlcdef
kadekkfwgk ylyeiarrhp yfyapellyy ankyngvfqe ccqaedkgac
llpkietmre kvltssarqr lrcasiqkfg eralkawsva rlsqkfpkae
fvevtklvtd ltkvhkecch gdllecaddr adlakyicdn qdtissklke
ccdkplleks hciaevekda ipenlpplta dfaedkdvck nyqeakdafl
gsflyeysrr hpeyavsvll rlakeyeatl eeccakddph acystvfdkl
khlvdepqnl ikqncdqfek lgeygfqnal ivrytrkvpq vstptlvevs
rslgkvgtrc ctkpesermp ctedylslil nrlcvlhekt pvsekvtkcc
teslvnrrpc fsaltpdety vpkafdeklf tfhadictlp dtekqikkqt
alvellkhkp kateeqlktv menfvafvdk ccaaddkeac favegpklvv
stqtala

Figure 66 Amino Acid Sequence of BSA – highlighted regions show the presence of lysine residues.[137]

4.2.5.3 Insulin

Insulin is an interesting protein on which to attempt the DIP modification, because of the presence of the disulfide bonds the reaction should only proceed on the primary amine of the single lysine residue as can be seen from Figure 67. In nature insulin exists as a dimer shown in Figure 68. Insulin exists as a two-chain polypeptide hormone produced by the β-cells of pancreatic islets. Its molecular weight is ~5800 Da. The α and β chains are joined by two interchain disulfide bonds. The α chain contains an intrachain disulfide bond. Insulin regulates the cellular uptake, utilisation and storage of glucose, amino acids and fatty acids and inhibits the breakdown of glycogen, protein and fat.[138]

In addition to its role in regulating glucose metabolism, insulin stimulates lipogenesis, diminishes lipolysis and increases amino acid transport into cells. Insulin also modulates transcription, altering the cell content of numerous mRNAs. It stimulates growth, DNA synthesis and cell replication. [138]

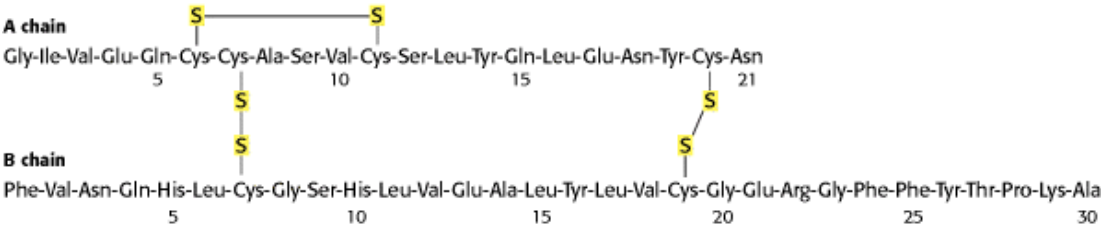

Figure 67 Amino acid sequence of Insulin from bovine pancreas showing the 3 disulphide bridges and the single lys residue.

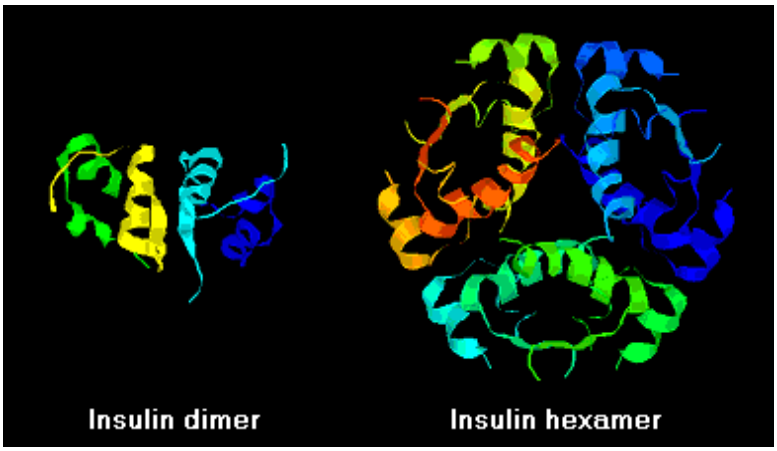

Figure 68 Schematic representation of Insulin dimmer and hexamer[139]

4.2.6 Addition of dendrimers to surfaces.

The DIP moiety offers interesting functionality, other compounds that are eligible for DIP modification are dendrimers. These are a set of molecules that have repeated branches protruding from a central core that are large and spherical in shape. The branches of the dendrimers are all identical and symmetrical around the central core causing a spherical 3D structure. They are molecules, which, from their central core, have repeated branches, whose terminal functionality can be chemically altered and the number of branches coming from the backbone is known as the generation number.[140] The interest surrounding dendrimers is warranted through their potential to be used in chemical and biosensing and as carriers across cell membranes,[141] and as a result have been studied extensively.

Dendrimers are known to have applications as detecting agents, affinity agents and pharmaceutically active compounds, applications all relating to their structure. The nature of the branches means that dendrimers can lead to multivalent systems; one dendrimer molecule potentially has numerous sites for further

reaction. Dendrimers also have the potential to be used as a drug delivery system, in particular anticancer compound delivery. This is due to their physical characteristics including monodispersity, solubility and encapsulation ability.

In recent years dendrimers have become increasingly important in biological science due to their ability to associate with DNA and other biologically important molecules.[142]

It is the poly amido amine (PAMAM) dendrimer that has shown potential to carry material across the cell membrane. The PAMAM dendrimer has been adsorbed onto various surfaces as well as using microcontact printing to add these molecules in a patterned fashion, allowing the molecules to be studied using techniques such as AFM and SEM.

As such this makes dendrimers an attractive addition to this study, as the functional groups on the branches are the same; this makes them an ideal candidate for modification with the DIP moiety

This work was carried out in collaboration with Louise Smith of the Cronin group who prepared all dendrimer – DIP complexes.

4.3 Experimental section

4.3.1 Synthesis of Modified Lysozyme

Proteins containing lysine residues were the obvious target for this reaction due to the presence of primary amines found on the lysine residues – another major factor in the modification process is that the proteins chosen must be able to withstand the reaction conditions and so the reaction was modified to account for this.

Chicken egg white was purchased from Sigma. A 7.5% $NaHCO_3$ solution (3 g in 40 ml H_2O) was prepared and to this Lysozyme (200 mg; 1.4 x 10^{-5} mol) and 2-bromoethyl phenanthridinium bromide (300 mg; 1.7 x 10^{-4} mol) were added. The reaction was stirred at 0˚C, under N_2, for 2 days. Crude product was purified by dialysis and filtration using Sigma cellulose tubing; size 23mm x 15mm, with the

water changed every 3 hrs. After 2 day dialysis was stopped and purified product obtained by freeze drying.

4.3.2 Synthesis of Modified BSA

Bovine Serum Albumin was purchased from Sigma. A 7.5% $NaHCO_3$ solution (3 g in 40 ml H_2O) was prepared and to this BSA (500 mg; 7.58 x 10^{-6} mol) and 2-bromoethyl phenanthridinium bromide (0.028 mg; 7.6 x 10^{-5} mol) were added. The reaction was stirred at 0˚C, under N_2, for 2 days. Crude product was purified by dialysis and filtration using Sigma cellulose tubing; size 23 mm x 15 mm, with the water changed every 3 hrs. After 1 day dialysis was stopped and purified product obtained by freeze drying.

4.3.3 Synthesis of Modified Insulin

Insulin was treated to the same conditions as both lysozyme and BSA, and the reaction proceeded as follows:

A 7.5% $NaHCO_3$ solution (3 g in 40 ml) was prepared and insulin (0.05 g; 8.62 x 10^{-6} mol) added along with phenanthridinium bromide (2.5 mg; 6.96 x 10^{-6}mol). The reaction was stirred at room temperature under nitrogen for 7 days. Most of the solvent was removed *in vacuo* and the rest removed by freeze drying yielding a white solid. The product was purified by dialysis over 2 days with continual water change, yielding a cream powder.

4.4 **Analysis details**

The following techniques and reaction conditions were used to analyse each protein.

4.4.1 Lysozyme Mass Spectrometry

Samples were desalted on a C 18 ZipTip using standard procedures, eluting with 2.0-2.5 µl of 50% acetonitrile/water, 0.5% forming acid. The sample was loaded directly into a single shot nano spray tip (Proxeon) and the tip mounted on a nanospray source (Protana) on a QStar Pulsar I running AnalystQS 1.1 (Applied

Biosystems). Data was collected in the 800-4000 Da range until an acceptable signal noise was obtained (1-5 minutes). The raw data was summed across the whole run and deconvoluted using Analyst BioTools, selecting a mass range of 14-16 Da, a s/n of 5 and a step size of 0.5 Da, running 20 iterations.

4.4.2 BSA Mass Spectrometry

Matrix was prepared by making a saturated solution of alpha-cyano-4-hydroxycinnamic acid (Fluka) in 1:1 acetonitrile water. Small quantities of lyophilised proteins and conjugates were dissolved in deionised water and mixed with matrix in 1:4 ratios. 1uL drops of this solution were applied to a stainless steel MALDI plate (Applied Biosystems) and allowed to dry. Analysis was on a Voyager DE pro MALDI-TOF (Applied Biosystems) operating in linear mode and close to external calibration with the Sequazyme mass standards kit (Applied Biosystems) was performed before analysing each spot. Mass spectra were collected in the positive ion mode at an accelerating voltage of 25 kV and a delay time of 329 ns. All spectra were averaged over 300shots. Instrument control and data analysis was carried out with the DataExplorer software. Spectra were smoothed with a Gaussian window of 101 points and mass determined by centroiding the top 50% of the peak.

4.4.3 Insulin Mass Spectrometry

Samples were desalted on a C18 ZipTip using standard procedures, eluting with 2.0-2.5uL of 50% acetonitrile/water, 0.5% formic acid. The sample was loaded directly in to a single shot nanospray tip (Proxeon), and the tip mounted on a nanospray source (Protana) on a QStar Pulsar i running AnalystQS 1.1 (Applied Biosystems). Data was collected in the 800-4000Da range until an acceptable signal to noise was obtained (1-5 minutes). The raw data was summed across the whole run and deconvoluted using Analyst BioTools, selecting a mass range of 5-7 kDa, a s/n of 5 and a step size of 0.5 Da, running 20 iterations and are shown in Figure 72.

4.4.4 Circular Dichroism studies

Solutions of Lysozyme (modified and native) were prepared in 7.5% sodium hydrogen carbonate and concentrations analysed using the Bradford Assay. Samples were investigated using a Jasco J-810 spectropolarimeter and curves corrected for protein concentration, cell path length, mean residue weight and baseline to remove effects from the buffer and additives[98].

Near UV measurements were made between 320 nm and 250 nm. A data pitch of 0.2 nm (distance between data points) was used with the instrument was in continuous scanning mode. A scanning speed of 10 nm/min, response time of 2 seconds and a bandwidth of 1 nm were also employed. Accumulations of 3 scans were recorded at approximately 1 mg/ml. The cell path length used for carrying out these measurements was 0.5 cm.

Far UV data was collected between 260 and 180 nm. A data pitch of 0.2 nm was used with the instrument in continuous scanning mode. A scan speed of 50 nm/min, response time of 0.5 seconds and a bandwidth of 1 nm were also employed. The CD spectrum of each sample was collected four times and subsequently accumulated to give a smooth spectrum using a cylindrical cell of path length 0.02 cm and a protein concentration of approximately 0.5 mg/ml.

4.5 **Results and Discussion**

The following results were obtained from mass spectrometry, circular dichroism and analysis of the protein on a surface using AFM. These studies will look at the variances between native and modified proteins to ensure that modification has taken place. In order to determine which residues have been modified, mass spectrometry analysis was performed on each giving an indication of the extent of the modification as well as the selectivity of the reaction. The effect on the secondary structure through circular dichroism has been studied, i.e. to determine if the folding of the protein been affected by the modifications. This, in addition to what effect the modification has on the bulk material and how the protein behaves on the surface, essentially determines how DIP moieties change the characteristics of the protein when dried on a surface.

4.5.1 Lysozyme Mass Spectrometry Results

In order to determine if lysozyme had been modified fully with the DIP, the protein was subject to mass spectrometry analysis. This would then determine if the reaction with the primary amine had been successful.

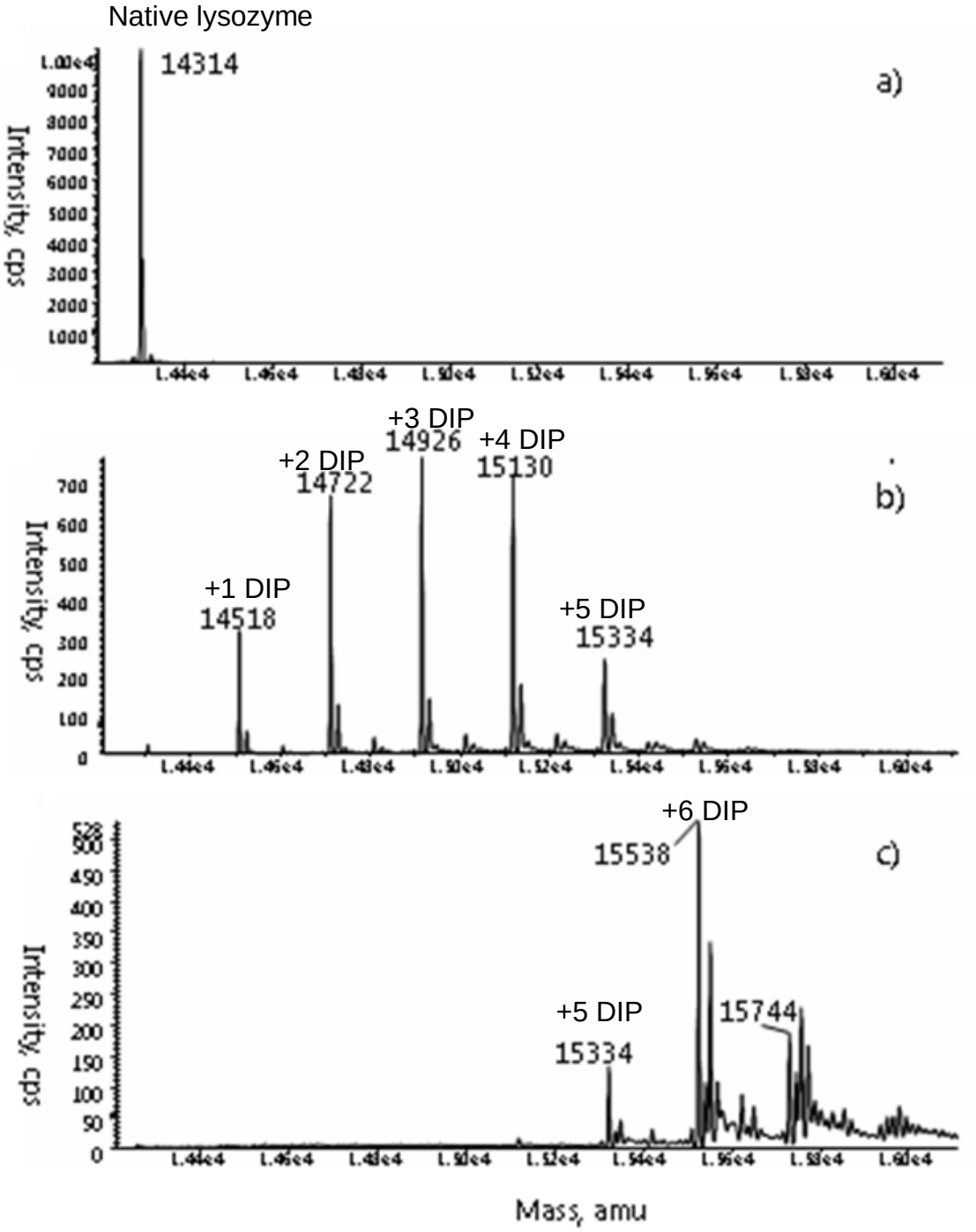

Figure 69 ESI- of lysozyme (a – native) modified with increasing equivalents of reagent (b-c).[143]

The mass spectrometry results shows that in a statistical distribution of 0 to 6 modifications (204 Da increase per cyclised modification), using 7 equivalents of

2-bromoethyl phenanthridinum bromide was observed in (b), whereas (c) shows 6 modifications (15538) resulting from conditions which included a large excess of 68 equivalents of 2-bromoethyl phenanthridinium bromide including a peak at 15744 which probably corresponds to 6 modifications plus reaction with the N-terminus which will not undergo cyclisation for steric reason (206 D difference). Thus this shows that the modification is dose dependent and the preponderance for the modification of 6 residues on treatment with excess reagent correlates well with the protein containing 6 lysines. Minor associated peaks are associated with cation adducts etc. [143]

Matrix assisted laser desorption ionization (MALDI) for lysozyme, showed the mass shift between molecular ion in the modified sample (15,525 Da) and the unmodified sample (14,303 Da) to be 1,222 Da which can be assigned to 6 DIP moieties (204 Da each). This data indicates all 6 lysine residues have been aromatically modified by the cyclisation reaction and this achievement is unprecedented. In particular, lysine K96 is very rarely modified due to its low accessibility caused by H-bonding to the carbonyl group of H-15.

4.5.2 BSA Mass Spectrometry Results

A MALDI study of BSA, shows the triply charged molecular ion of the unmodified protein (66 409 Da) at *m/z* 22,154 and modified protein (67,779 Da) at *m/z* 22,593, differ by 439 Da corresponding to 6 DIP groups. The initial investigation set out to modify on average 6 lysine residues despite the vast number of lysine residues on the chain as highlighted in Figure 70. Attempts to target a higher number caused the protein to precipitate; presumably the most accessible surface residues are modified.

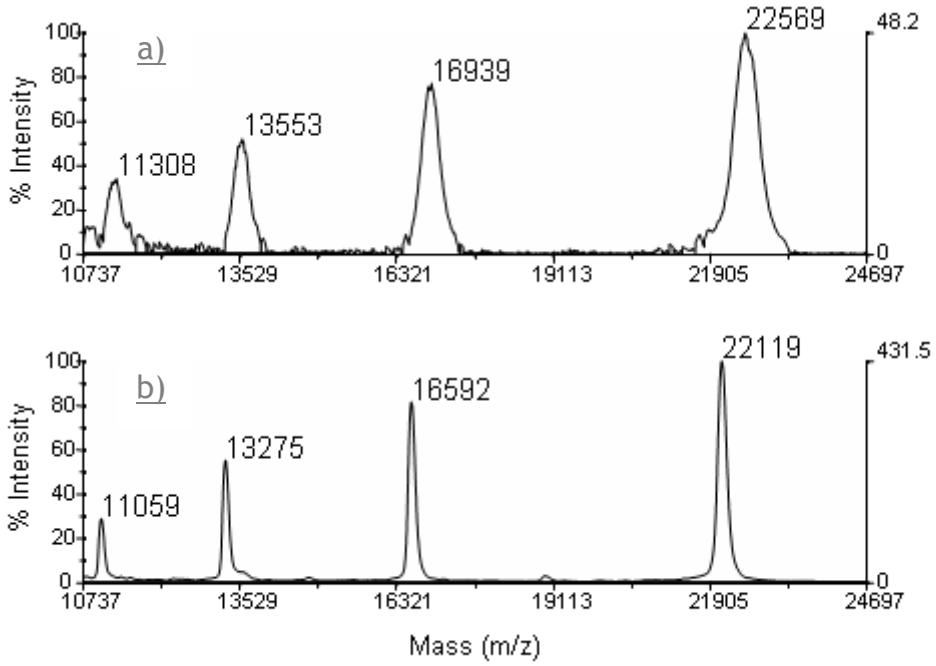

Figure 70 MALDI-ToF analysis of a. DIP modified BSA, and b. native showing 3+ to 6+ ions. Modified protein shows an average shift to higher mass of 1350, equivalent to approximately 7 DIP adducts. The significant broadening of the peaks suggests a statistical distribution of modifications around this average.

4.5.3 Sequence analysis

To identify sites of modification, minimally modified (average 7 modifications by mass spectrometry) and unmodified BSA (35 cysteines and 59 lysines) were analyzed by peptide mass fingerprinting. The samples were treated with dithiothreitol to reduce disulfides and then free cysteines blocked by treatment with iodoacetamide. The samples were digested with tripsin and peptide mass fingerprints obtained by MALDI – ToF MS on a 4700 Proteomic Analyser (Applied Biosystems). The raw data was searched using MASCOT (Matrix Science) with fixed modification: carbamidomethyl; variable modifications: oxidation of methionine and the uncyclised ethylphenanthridinium adduct or DIP modification on lysine, searching the SwissProt mammalian database at 100ppm mass accuracy. Only peaks appearing in the modified, but not in the unmodified sample, were considered significant. Peptides were identified with DIP modifications on lysine 140, 228 and 235 and cystein 58, 147 and either 581, 582 or 590. Other peptides were identified where modifications were present but could not be localised to lysine or cystein residues. These included two modifications on a peptide containing K299, K304, C301 and C302, and one on a peptide containing K88 and C86.

Matched peptides shown in **Bold Red**

```
  1 MKWVTFISLL LLFSSAYSRG VFRRDTHKSE IAHRFKDLGE EHFKGLVLIA
 51 FSQYLQQCPF DEHVKLVNEL TEFAKTCVAD ESHAGCEKSL HTLFGDELCK
101 VASLRETYGD MADCCEKQEP ERNECFLSHK DDSPDLPKLK PDPNTLCDEF
151 KADEKKFWGK YLYEIARRHP YFYAPELLYY ANKYNGVFQE CCQAEDKGAC
201 LLPKIETMRE KVLASSARQR LRCASIQKFG ERALKAWSVA RLSQKFPKAE
251 FVEVTKLVTD LTKVHKECCH GDLLECADDR ADLAKYICDN QDTISSKLKE
301 CCDKPLLEKS HCIAEVEKDA IPENLPPLTA DFAEDKDVCK NYQEAKDAFL
351 GSFLYEYSRR HPEYAVSVLL RLAKEYEATL EECCAKDDPH ACYSTVFDKL
401 KHLVDEPQNL IKQNCDQFEK LGEYGFQNAL IVRYTRKVPQ VSTPTLVEVS
451 RSLGKVGTRC CTKPESERMP CTEDYLSLIL NRLCVLHEKT PVSEKVTKCC
501 TESLVNRRPC FSALTPDETY VPKAFDEKLF TFHADICTLP DTEKQIKKQT
551 ALVELLKHKP KATEEQLKTV MENFVAFVDK CCAADDKEAC FAVEGPKLVV
601 STQTALA
```

a.

b) Start-End Observed Mr (expt) Mr (calc) Delta Miss Sequence

223-232 1369.5181 1368.5108 1368.6648 -0.1540 1 R.CASIQKFGER.A Phenan (K)

233-241 1175.5767 1174.5694 1174.6651 -0.0957 1 R.ALKAWSVAR.L Phenan (K)

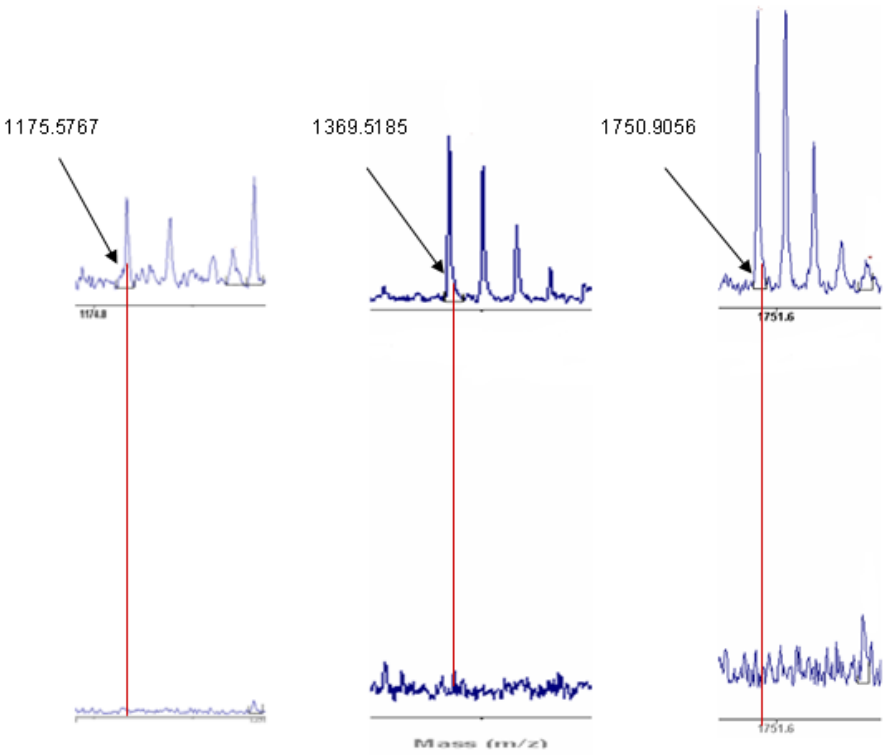

c.

139-151 1750.9056 1749.8983 1749.8463 0.0547 0 K.LKPDPNTLCDEFK.A Phenan (K).

Figure 71 MALDI-ToF analysis of DIP modification. MASCOT analysis of data from BSA. a) Sequence coverage shown in bold red (86%), b) three of the peptides identified as containing DIP modified lysine in MASCOT analysis, c) corresponding regions of MALDI-ToF MS spectrum showing presence in modified (top) and absence in unmodified (bottom) BSA digests respectively[143]

4.5.4 Insulin Mass Spectrometry results

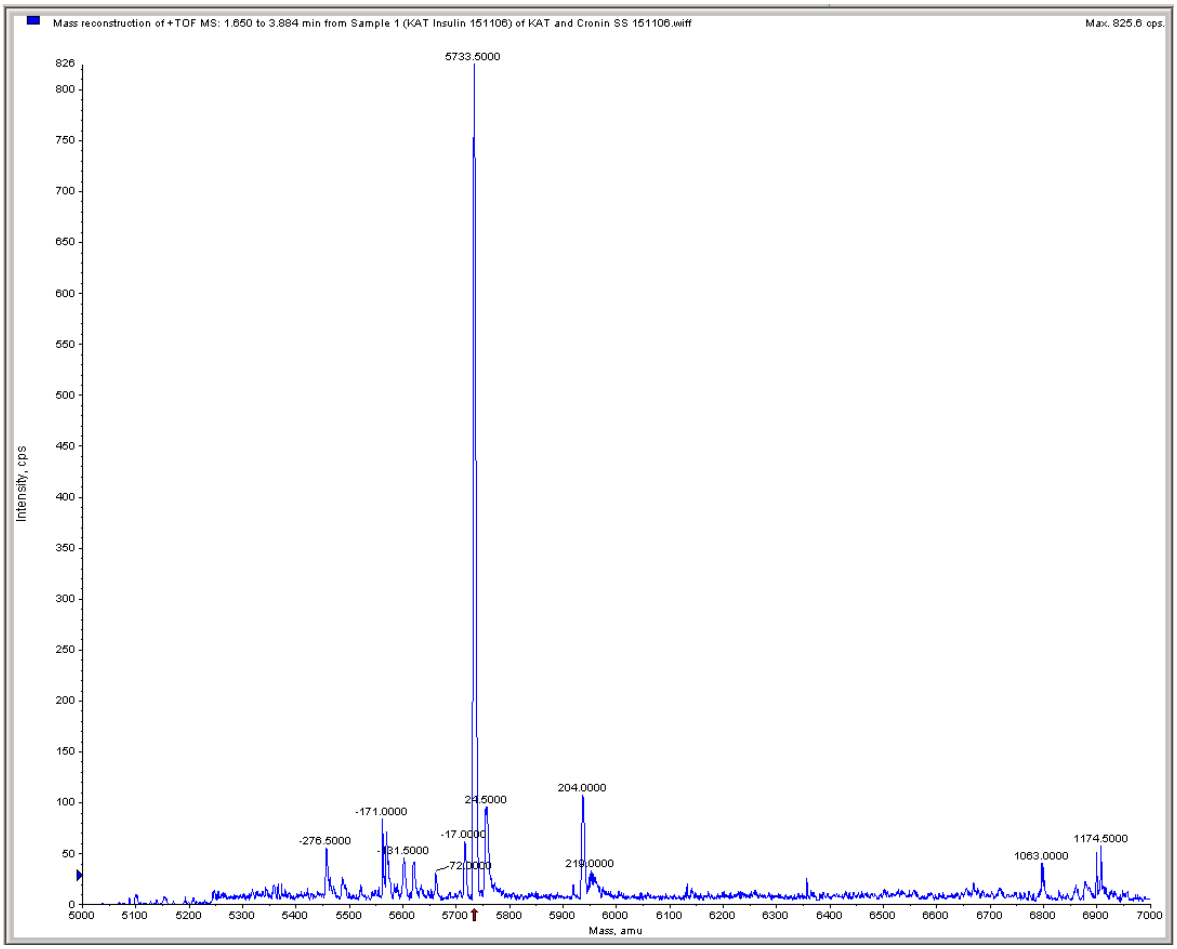

Figure 72 Mass spectrometry analysis shows the mass change from 5733 Da with the addition of 204 Da attributed with a single DIP addition on the single lysine residue.

The mass spectrometry results confirm the addition of the DIP moiety to the single lysine residue of the insulin molecule, the additional 204 Da is evident confirming that the reaction was completed with success and the 5733 Da protein has been successfully modified.

4.5.5 Mass Spectrometry Conclusions

Choosing to study three different proteins gives the opportunity to understand the impact certain aspects of the protein structure etc has on the modification results. Within this study both globular (BSA) and fibrillar (lysozyme) proteins have been looked at, proteins that have their cystein residues “capped” i.e. held in a disulfide bond have also been taken into consideration, this is coupled with the fact proteins have very different molecular weights and distributions of residues that can be targets of this specific reaction. This diversified the study and allowed the understanding of what factors had an impact on successful modification.

Firstly looking at the size of the protein; insulin, the smallest protein, on studying its amino acid sequence had 5 potential sites of modification; 1 lysine residue and 4 cystein residues. Elucidation of its crystal structure showed all cystein residues were “locked” in disulfide bonds between adjacent residues on the amino acid chain. On studying the mass spectrometry results of this protein, the results were conclusive with the fact there was only one site for possible DIP reaction, on the remaining lysine residue, and showed only one modification pertaining to this. The protein’s own amino acid structure, and the bonding between residues are the limiting factor in allowing any further reactions to occur.

The next protein; lysozyme, a mid range protein in terms of molecular weight, was similar to insulin in that although containing cystein residues, the crystal structure of the protein shows that these are again locked in a disulfide bond, leaving only the remaining lysine residues available for modification. The difference however between lysozyme and insulin is the number of lysine residues within the structure. With 6 sites available, the challenge was to modify all 6 residues with DIP. Using mass spectrometry to determine if this had been successful, the results were conclusive and showed all 6 residues had in fact been modified with the DIP moiety. This was in stark contrast to previous modifications using different chemistries reported in the literature; the DIP moiety had managed to react with lysine residues buried deep within the core of the molecule that had before been unavailable to other reactions.

The largest of the three proteins, BSA, proved to be the most difficult to determine if modifications had taken place. Being the largest protein within the group and

having the added difficulty of having “unlocked” cystein residues that were not held in a disulfide bond meant that the determination of which residues had been modified was more difficult and required analysis beyond simple mass spectrometry. In the first instance it was clear on studying the spectra from the mass spectrometry studies that the protein, using the reaction mixture outlined, had been modified with approximately 7 DIP adducts; therefore, not all lysine residues within the protein had been modified. Since BSA has 35 cystein residues and 59 lysine residues within its sequence, the determination of which residues were modified was carried out by sequencing the protein. This technique took each peptide unit and determined the mass of each, thus determining where the additions had taken place. The conclusion of this reaction was that the reactions had taken place on a mixture of cystein and lysine residues. Definitive modification had taken place on several lysine and cystein but no definitive conclusions can be drawn as to where the remaining modifications have taken place. This is due to the fact that many of the available residues are buried deep within this globular proteins core and it is difficult to characterise and distinguish if any modifications have taken place. This protein, in comparison to lysozyme, offers a more complex structure and since the reaction can be selective to some residues full modification has not been possible.

From these results it can be concluded that the type of protein, plus the availability of residues play a role in this reaction. If the protein has sites available for reaction and enough space to proceed then the reaction should go to completion. IN addition the reaction sites can be blocked meaning the residues are in a “locked” formation e.g. a disulfide bond and reaction will not occur. The residues location may also have a pivotal role in determining if a reaction will proceed, if the residue is buried deep within the core of the protein it is unlikely the reaction will proceed to completion due to special constraints. In conclusion it is clear that this method presents a selective and easy route to targeting specific residues on a protein that can be determined by mass spectrometry analysis.

4.5.6 Circular Dichroism results

Circular Dichroism spectroscopy (CD) is a widely used technique that determines the structural characteristics of a protein. The basis for this technique is the

absorption of left and right hand components of circularly polarised light by a chiral chromophore.

The CD spectra is measured over a range of wavelengths. The components of a protein, the amino acid side chains and the peptide backbone are analysed at different wavelengths. The peptide backbone is analysed within the far UV region (240-180 nm) to determine the helical or sheet content of the protein and the aromatic side chains are analysed within the near UV (320-260 nm) region giving information regarding the side chains and the tertiary structure of the protein. This technique is important in determining changes in the protein structure and so is essential for analysing a potentially modified protein.[144]

For determining protein structural changes, CD spectroscopy is used routinely as it can provide details regarding the significance of the structural changes with a greater degree of accuracy over other spectroscopic techniques.

4.5.6.1 Circular Dichroism of Lysozyme, modified and unmodified

CD spectra of the native protein and modified protein in the presence and absence of DIP were obtained. This was to clarify the effect the DIP had upon the structure of the protein and gain an insight into the effect this modification has on the protein at the molecular level.

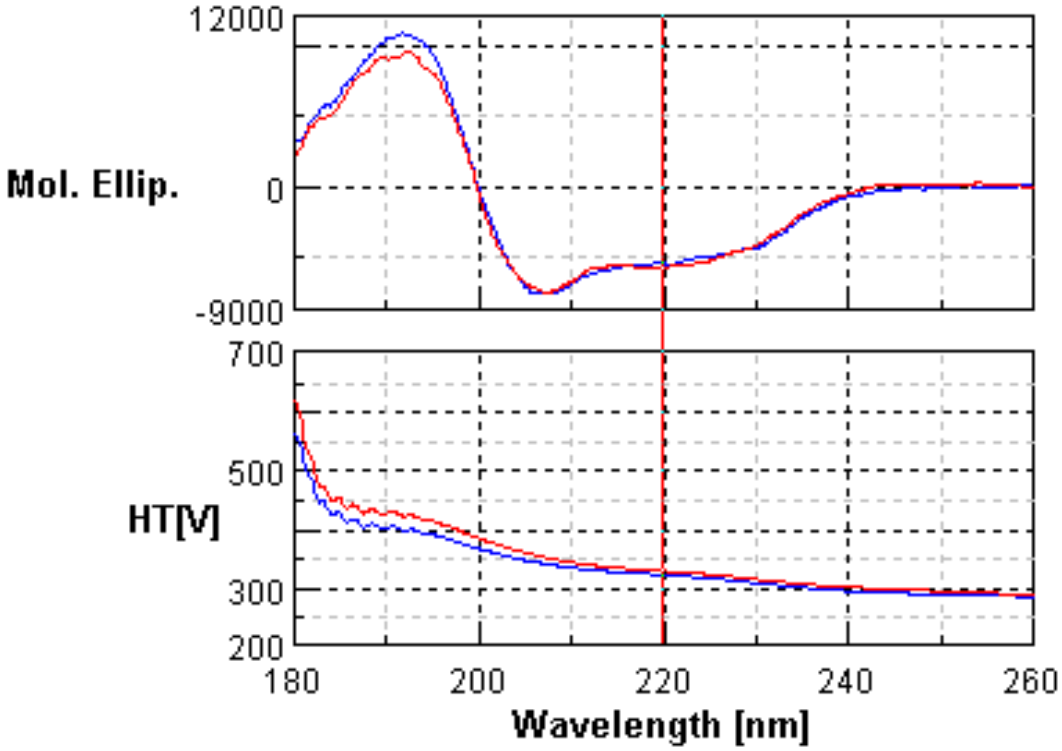

Figure 73 Far UV spectra of native lysozyme (blue) and modified lysozyme (red).

The far UV spectrum Figure 73 of the native and modified lysozyme is shown. As mentioned the secondary structure of the protein can be determined in this region. The peptide backbone acts as the chromophore and it generates a signal when it is located in a folded environment e.g. α helices, β sheets and random coils. [144] The resulting spectrum gives rise to the sum of the fractional multiples for each structural type and reflects the average of the entire protein. [144] CD does not have the power to determine which residues are involved in each of the structural components. Comparisons can be made and after reaction on a protein e.g. CD can be a good source of structural determination and comparison. As can be seen from Figure 73 modification with DIP appears to have little effect upon the secondary structure of the protein as the red trace (modified lysozyme) follows the blue trace (native lysozyme) closely, indicating that the modification with DIP has little effect on the secondary structure elements of the protein. The native protein indicates the protein is composed mainly of α –helices through its distinctive shape which is consistent with the crystal structure of the protein.

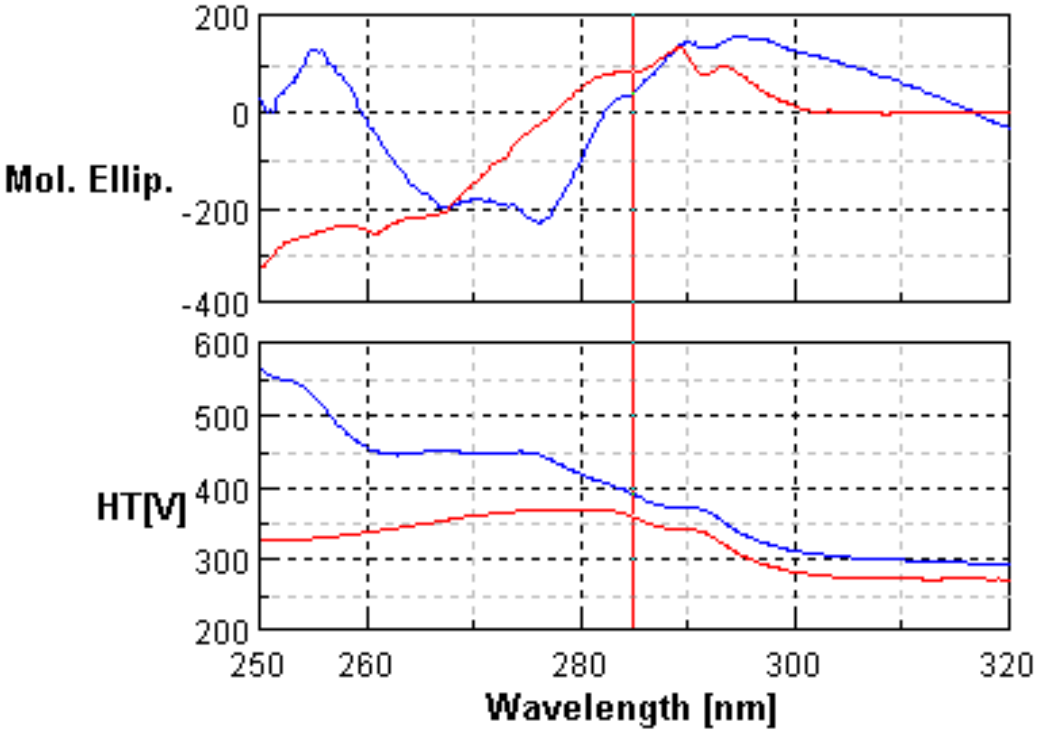

Figure 74 Near UV spectra of naïve lysozyme (blue) and modified lysozyme (red).

The CD spectrum in the near UV region as mentioned is sensitive to aspects of the tertiary structure. Here the involvement of aromatic amino acids and disulfide bonds play a role as well as the overall tertiary structure of the protein. In general if a protein retains its secondary structure and has lost its 3D structure, i.e. it is incorrectly folded, the signal in the near UV region is almost always zero, however when a signal arises it gives the indication that there is a folded structure. [144]

What is interesting for this modification is that the protein now has an additional chromophore associated with the structure and near UV CD is sensitive to this, as well as protein-protein interactions playing an important role. The presence of the DIP moiety on the structure of the modified protein will therefore alter the near UV spectra as can be seen from Figure 74. There are significant differences between the native trace (blue) and the modified trace (red). This is indicative that the DIP chromophore is present on the protein, however as described, the fact that there is a signal in this region for the modified protein means there is a folded structure present.

4.5.7 Circular Dichroism of modified and unmodified BSA

CD spectra of the native protein and modified protein in the presence and absence of DIP were obtained. This was to clarify the effect the DIP had upon the structure of the protein and gain insight into the effect this modification has on the protein at the molecular level.

Solutions of BSA (modified and native) were prepared in 7.5% sodium hydrogen carbonate and concentrations analysed using the Bradford Assay. Samples were investigated using a Jasco J-810 spectropolarimeter and curves corrected for protein concentration, cell path length, mean residue weight and baseline to remove effects from the buffer and additives [98].

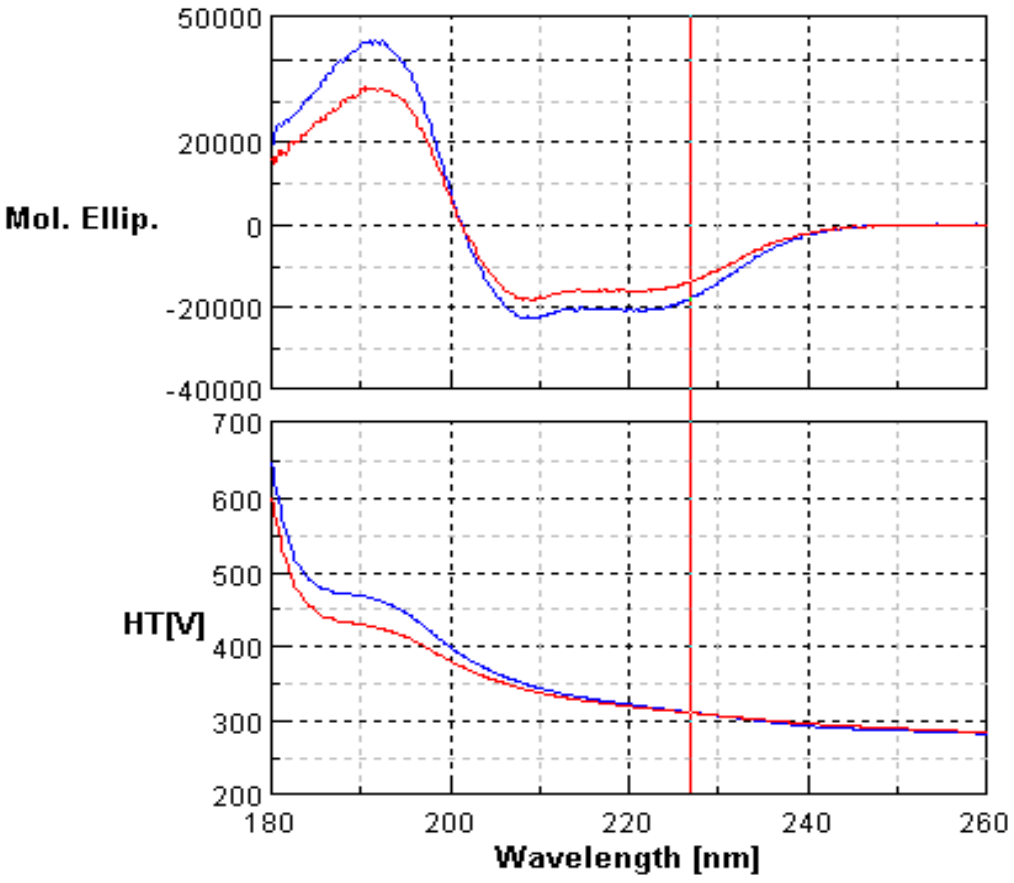

Figure 75 Near UV spectra of native BSA (blue) and modified BSA (red)

As with lysozyme, the CD spectra shown in Figure 75 indicates that the secondary structure of the native protein (blue) consists of α-helices and the red trace of the

modified protein closely follows this same pattern indicating that the secondary structure remains consistent with the native protein despite the modifications.

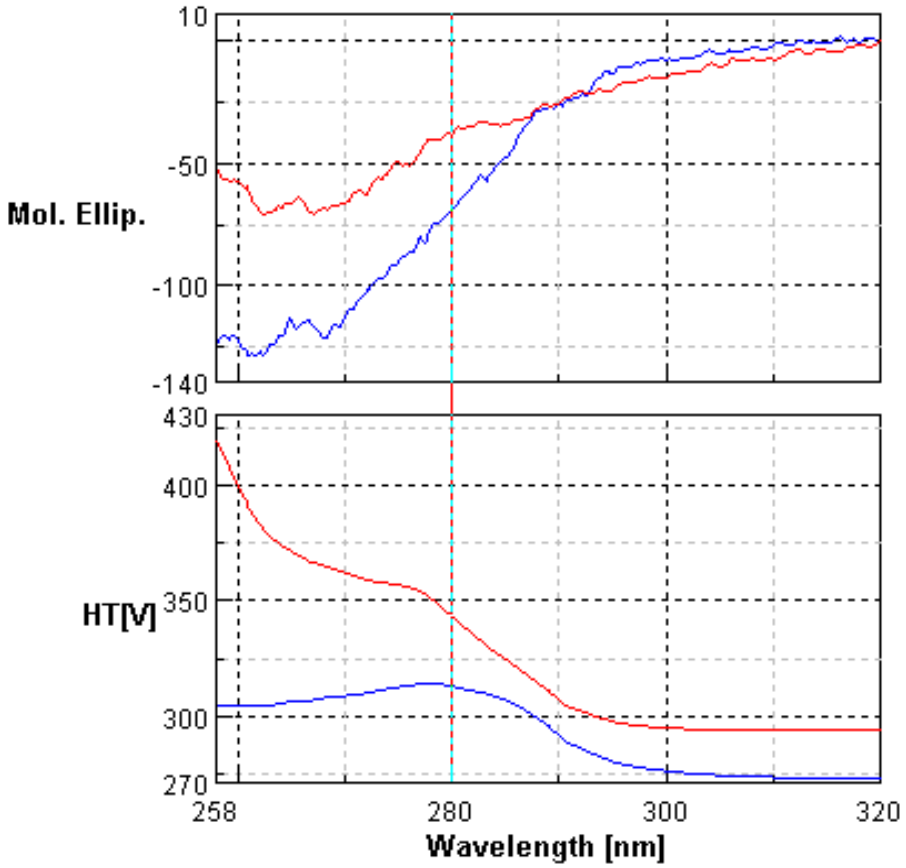

Figure 76 Far UV spectra of native BSA (blue) and modified BSA (red)

Near UV CD spectra of native BSA (blue) and modified BSA (red) shows the trace of the modified BSA is not consistent with the near UV trace of the native protein. This is as a result of the interference of the DIP chromophore at this region of the spectrum; this area highlights the nature of the aromatic regions of the protein, and as such the addition of the aromatic chromophore DIP is having an effect on this area of the spectrum. As mentioned the far UV spectrum also shows the effects of protein-protein interactions and this may be significant since the AFM images demonstrate some interaction between protein molecules. As such this could explain the reason why there is such a large difference in the far UV spectra. In addition as mentioned previously since the spectra is showing a signal in this region, it can be assumed that there are some elements of tertiary structure folding remaining in the modified protein.

4.5.8 Circular Dichroism Conclusions

CD analysis of both compounds confirms that the protein has been modified: the DIP moiety interferes with the near UV-CD spectra whereas the far UV remains consistent with the native protein. This comparison allows us to suggest that the secondary remains largely unaltered and this is an important discovery. Successful protein modification should not interfere with the secondary structure as the proteins activity relies on this. This is particularly exciting in the case of BSA, which is a “soft” globular protein and can easily change its internal structure. In addition the changes in the near UV spectra are consistent with the addition of an aromatic moiety as this part of the spectrum gives an indication of the aromatic residues of the protein. The fact that there is a change gives further indication that both proteins have been modified with the aromatic moiety.

4.5.9 Atomic Force Microscopy Results

Atomic force microscopy (AFM) was used to determine the effect the modification had on the protein as a bulk material, solutions of each protein were dried onto a substrate and investigated.

4.5.9.1Lysozyme Atomic Force Microscopy

Solutions of the unmodified and modified protein were dissolved to 1 mg/ml in water and added drop wise to a silicon substrate of 1 cm^2 in dimension that had previously been sonicated in ethanol for 10 minutes. The substrates were left to dry in air until the solvent had evaporated and tapping mode AFM was carried out presenting the results shown in Figure 77 and Figure 78.

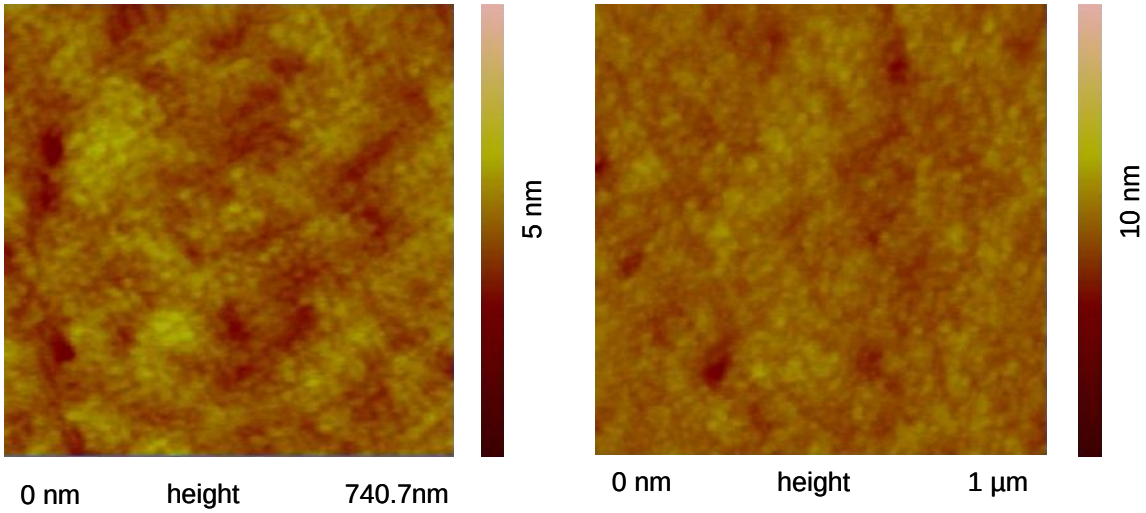

Figure 77 Tapping mode AFM images of unmodified lysozyme – showing no distinct features on the surface.

In the same manner, solutions of unmodified lysozyme were dried onto a surface and AFM showed no distinct features, Figure 77.

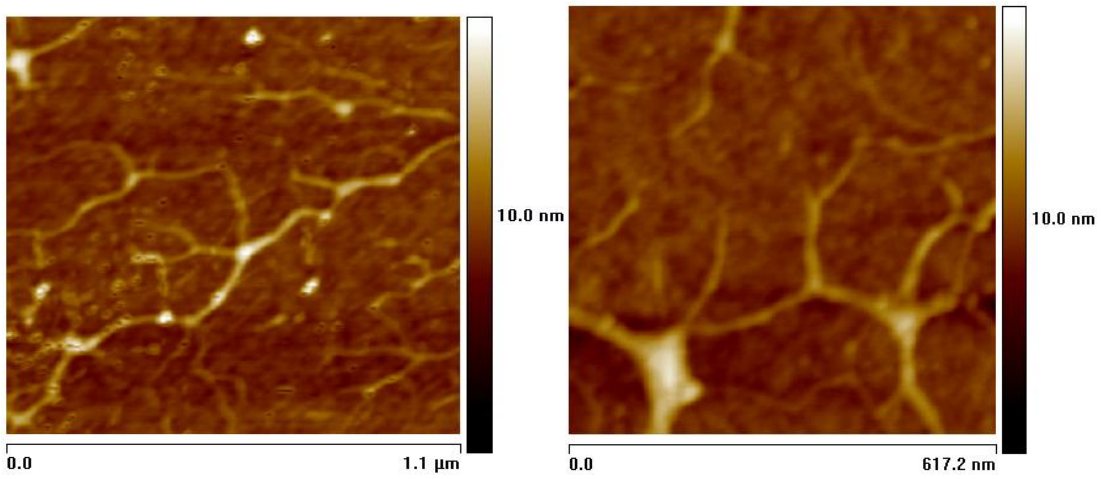

Figure 78. Tapping mode height images of 1mg/ml lysozyme-DIP complex on silicon. Long vein like networks can be seen after modification.

Tapping mode AFM images of both modified and unmodified lysozyme show distinct differences. Images of unmodified lysozyme, after drying onto the substrate, form a generally flat uniform layer with no distinct features present. This is contrast to the fibrillar features formed when modified lysozyme is dried in a similar way. Long fibres like networks cover the surface with no uniform size or shape associated with them. It is obvious the modification with DIP has some

effect on the protein. Long fibrils similar to those reported in Figure 78 are not an unusual feature for lysozyme.

Further section analysis of the modified protein shows the maximum height of the fibrillar features to be in the region of 5 nm at the “junction” sections and the long fibre like features within the region of 2.5 nm. Quantitative analysis has been carried out using the Rq value which is the root mean square average of the height taken from the mean data plane, expressed as:

$$Rq = \sqrt{\sum (Z_i)^2 / n}$$

Where Z_i is the current Z value and n is the number of points considered, representing the surface roughness.

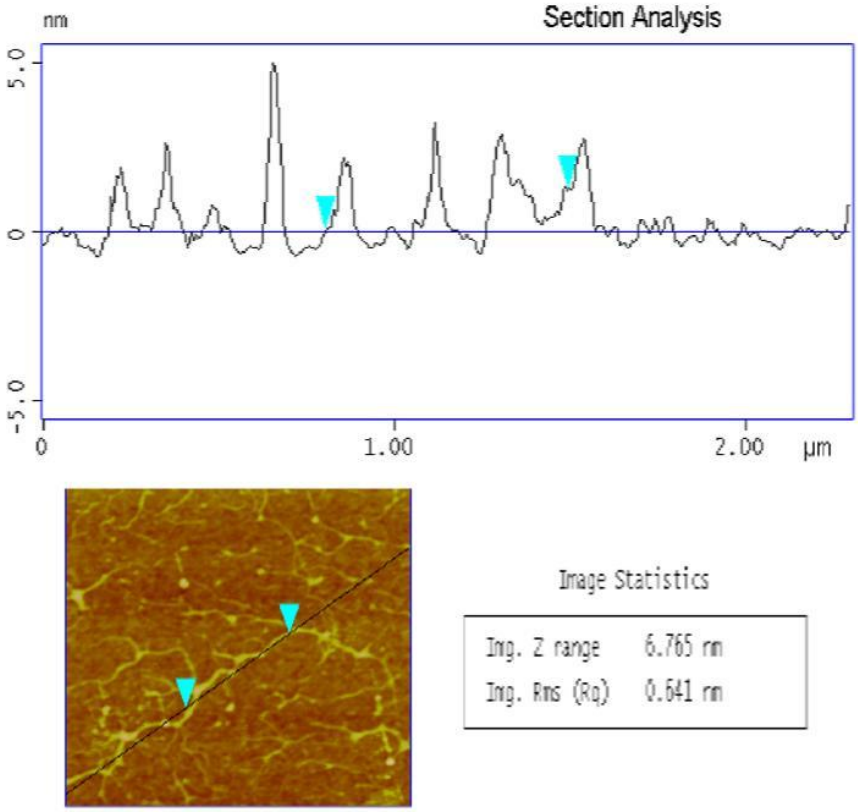

Figure 79 Section analysis of modified lysozyme showing a cross section of the surface and the Rq value of 0.541 nm.

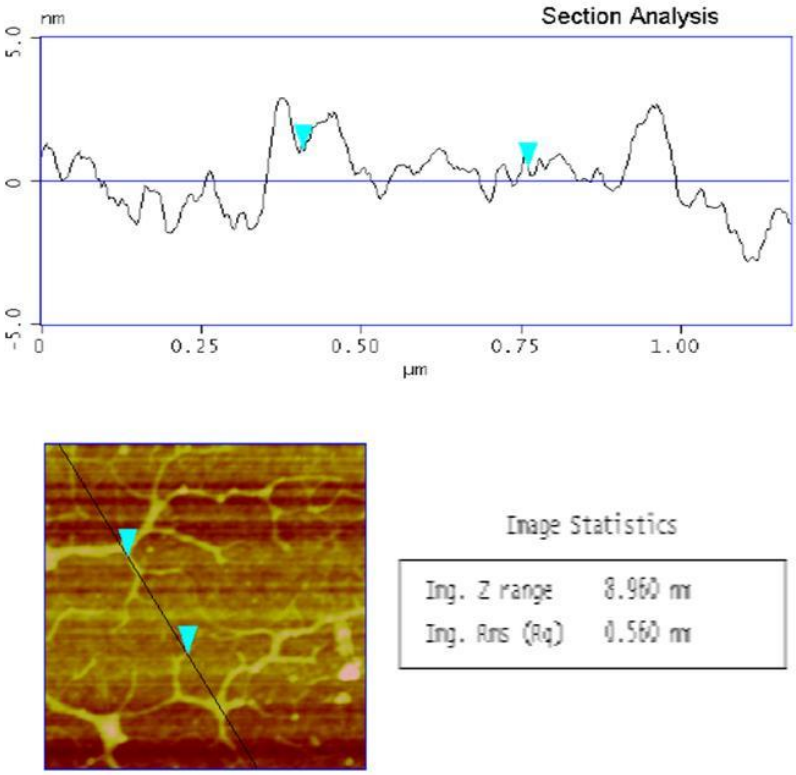

Figure 80 Section analysis of modified lysozyme showing a cross section of the surface and the Rq value of 0.560 nm.

As stated fibrillar features is not uncommon for proteins. Proteins creating amyloid like features are common in disease such as Alzheimer's where a fibrillar like structures have been reported.[145] As mentioned the process by which a linear amino acid sequence folds into a 3D structure is unknown. When a protein fails to fold properly this leads to a functional issue that sometimes has serious consequence, and the images are reminiscent of such a process. Other examples of fibrilar networks being imaged are shown in Figure 81 .

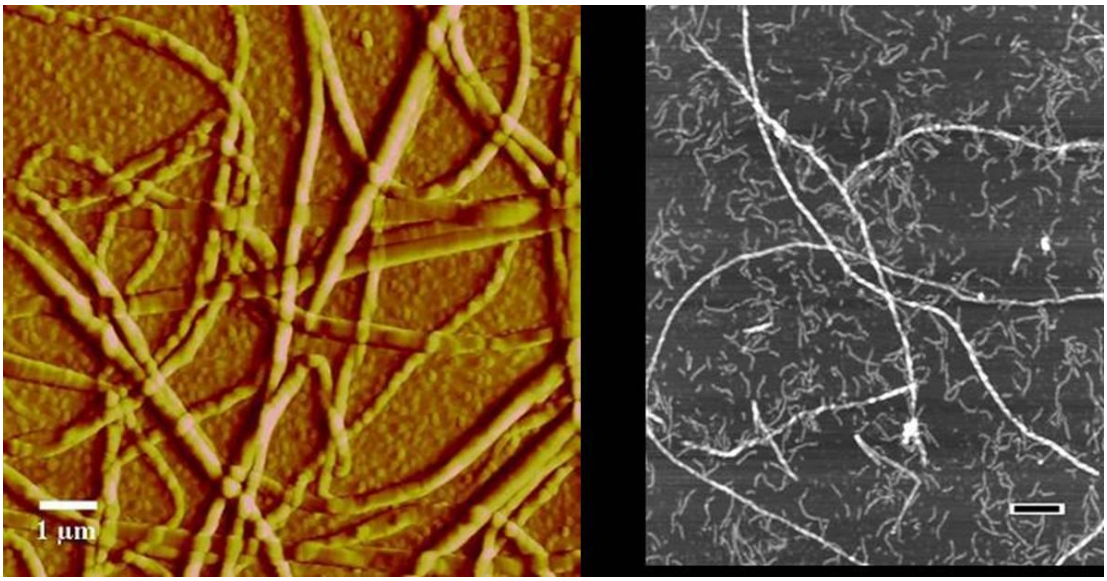

Figure 81 a. AFM Image of Collagen Fibrils[146] b. Atomic-force microscopy of Aβ1–40 demonstrating assembly of amyloid fibrils from protofibrils[147]

The lysozyme fibrils are also reminiscent of the features formed when lysozyme is in acidic conditions or as a result of mutations.[148]

These differences may be attributed to changes in the tertiary structure of the proteins, since circular dichroism indicates no secondary structure changes on the protein. Another reason could lie in the interaction of adjacent DIP molecules on the protein surface interacting and associating due to π-π stacking. The DIP moieties could arrange themselves in such a way that the molecules pack themselves in a complimentary manner forming such features on the surface.

4.5.9.2 BSA Atomic Force Microscopy results

Solutions of the modified and unmodified protein were dissolved to 1 mg/ml in water and added drop wise to a silicon substrate of 1 cm^2 in dimension that had previously been sonicated in ethanol for 10 minutes. The substrates were left to dry in air until the solvent had evaporated and tapping mode AFM was carried out presenting the results shown in Figure 82 and Figure 83. AFM studies of the proteins adsorbed onto a silicon substrate showed distinct variations before and after chemical modification of the proteins.

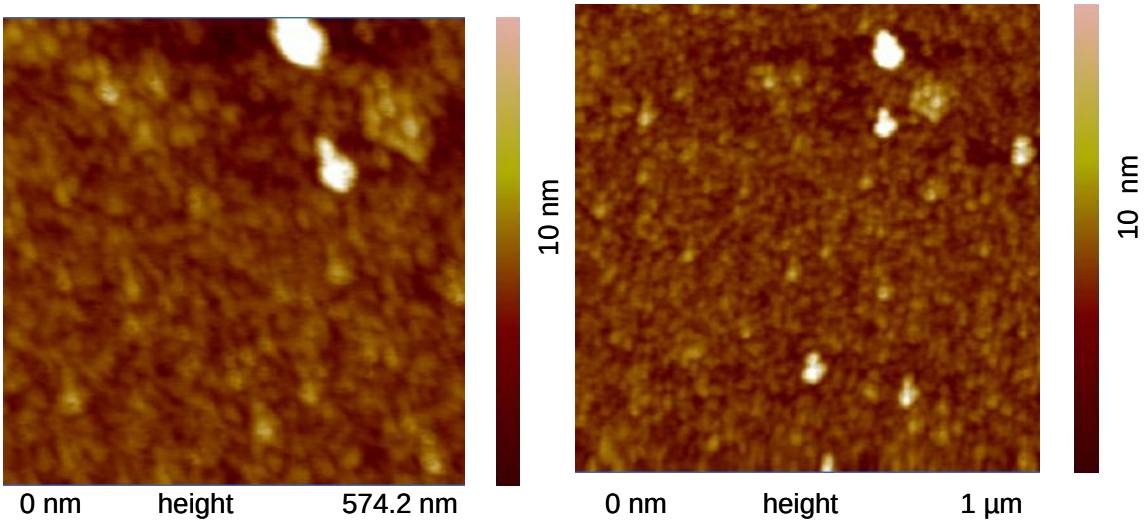

Figure 82 Tapping mode AFM images of native BSA on silicon.

As can be seen from the control experiment, there the AFM shows single and in some instances multiple globular proteins on the surface in contrast to the modified protein drawing the conclusion that the DIP has significant effects on the BSA. The profile of these structures are shown in Figure 84 and Figure 85.

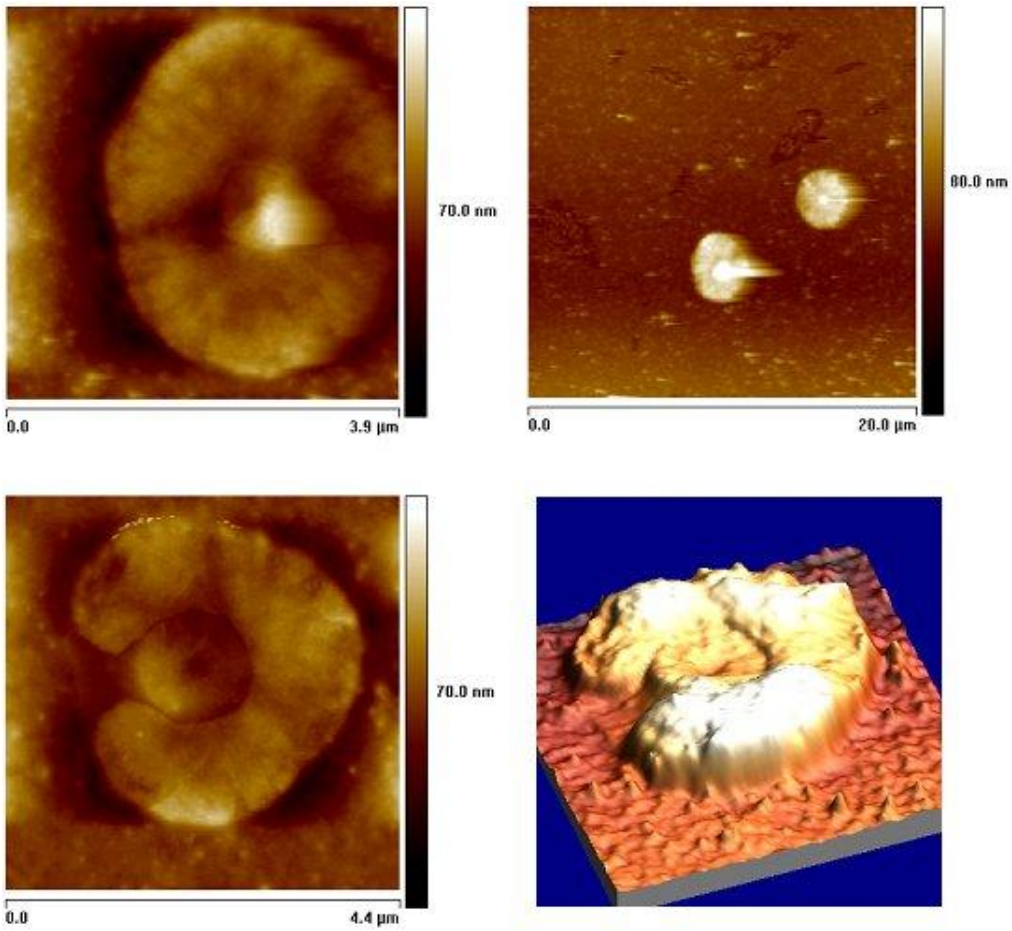

Figure 83 Tapping mode AFM images of 1mg/ml BSA – DIP complex on a silicon surface, again the large circular moiety with the central compartment can be seen, in stark contrast to the undecorated surface of the unmodified protein.

Tapping mode AFM images show that the contrast between modified and native BSA is striking, Figure 83, with only small globular features around 100-120 nm in size visible for native BSA, Figure 82. The difference between the unmodified and modified BSA samples is interesting since the samples containing modified BSA show large circular objects uniformly covering the silicon surface. These objects possess similar dimensions with an inner region seen to protrude from an outer shell, giving the structure a “mushroom” like appearance. It would appear that the architectures are formed due to inter protein interactions due to structural changes induced by modification or even between surface modified lysine residues.

Figure 84 a) shows the 3 dimensional image of the “mushroom” structure and the cross section of the structure. From (a) the feature measures 72.6 nm in height at the central point. The distance from one side to the other is 3.3 µm as seen from image (b) Image (c) shows 36.2 nm; height in the surrounding area and (d) shows the internal feature has a diameter of 1.1 nm.

This can be directly compared to analysis of another feature on the same sample shown in Figure 85; instead of a protruding internal feature of height 72.6 nm, the internal feature forms a cavity. This could be due to the arrangement of BSA molecules and association of DIP molecules.

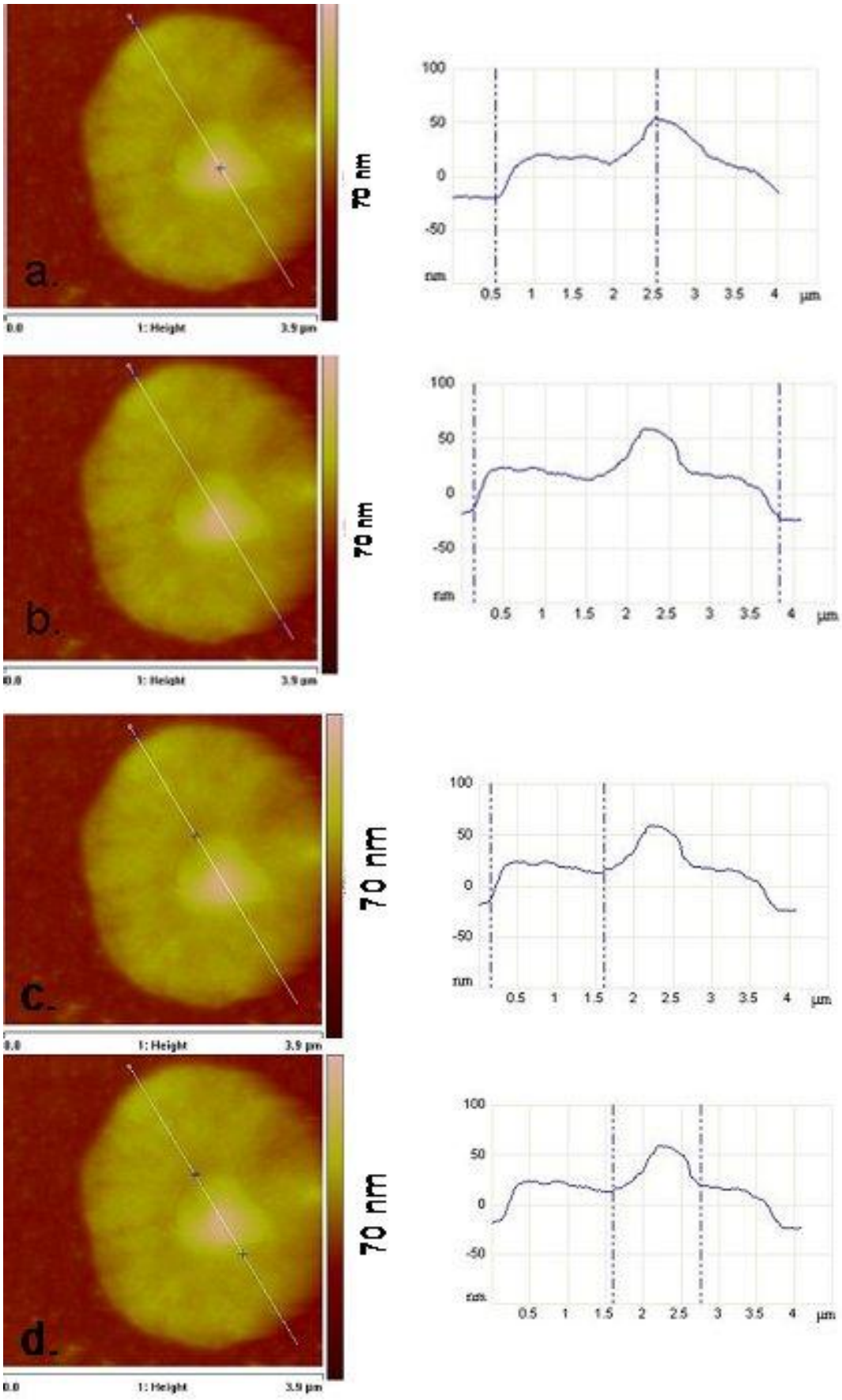

Figure 84 AFM analysis of the "mushroom" feature.

In addition to Figure 84, other areas of the substrate were analysed. The profiles are as follows: -

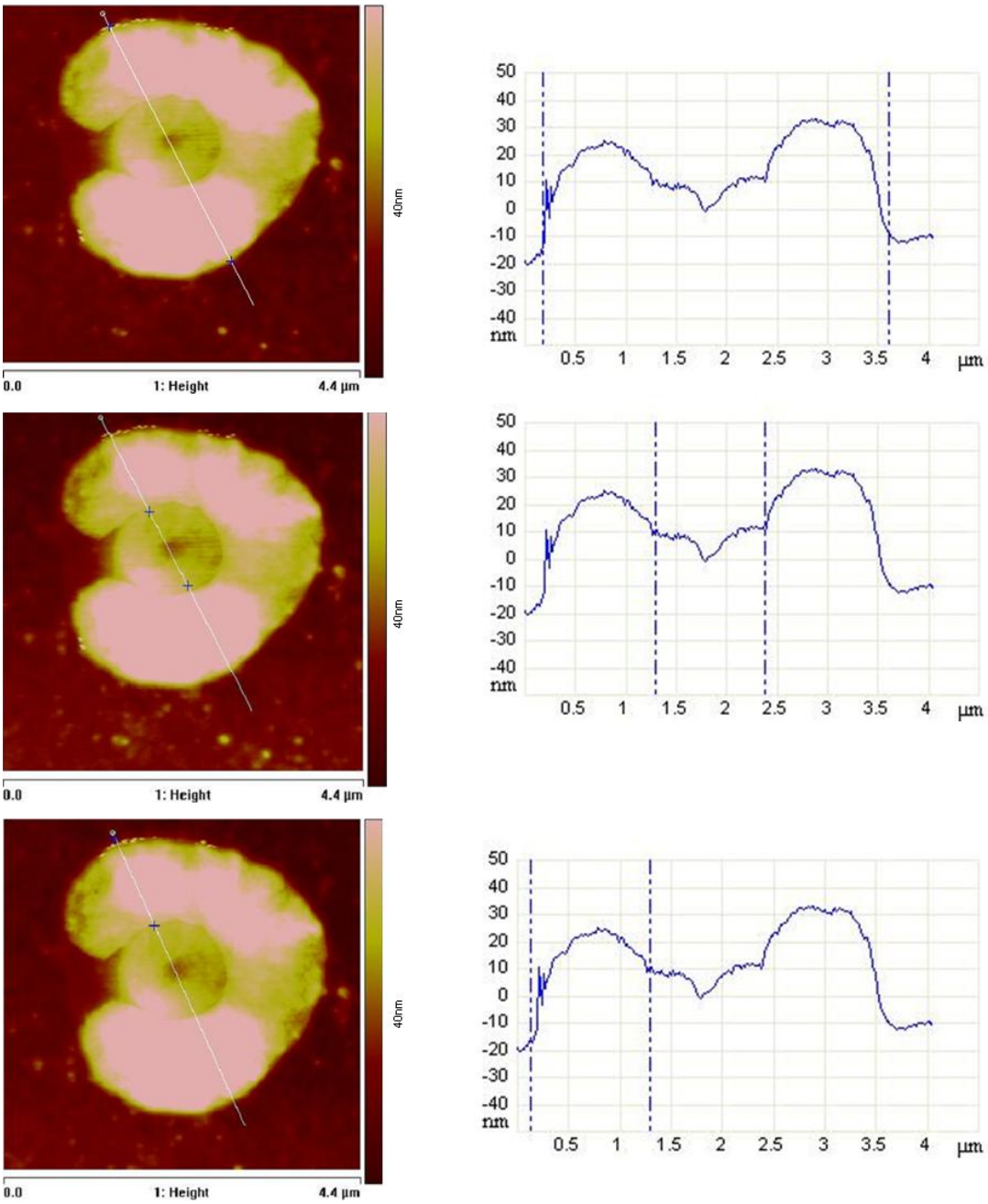

Figure 85 Further analysis and profiles of the BSA –DIP modified complex.

From the cross sections it can be seen from (a) that the horizontal distance from one side to the other is 3.4 µm, the distance at the point measured from the outer portion to the circular central region is 1.1 µm. The inner circular region had a horizontal distance of about 1.1 µm. The height of various portions has also been determined, the outer region has a height of 30.1 nm and the circular region dips below the surrounding area by 11.3 nm.

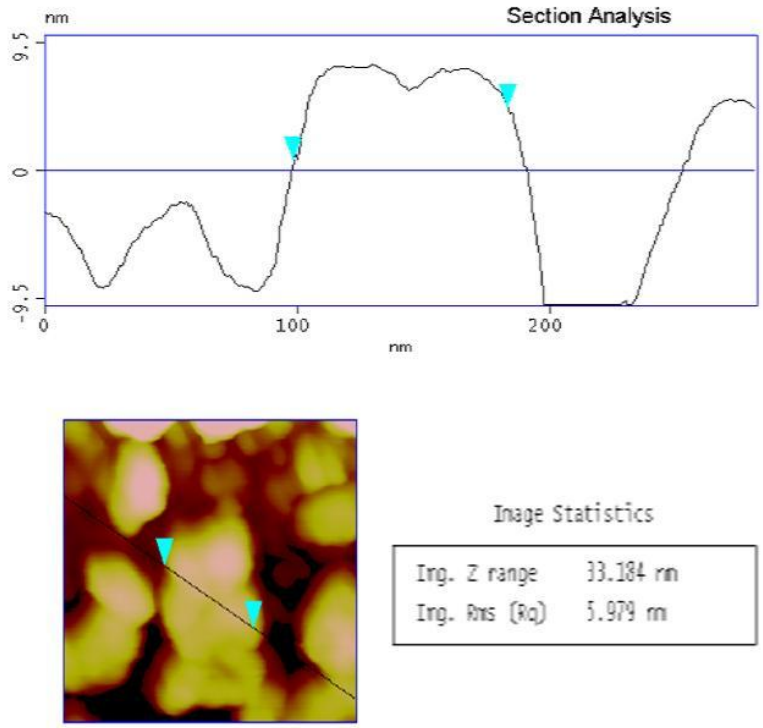

Figure 86 Section analysis of native BSA showing a cross section of the surface and the Rq value of 5.979 nm.

The section analysis of the native protein, Figure 86 shows the height of the feature as around 8 nm and the width approximately 100 nm. This would be indicative of a cluster of protein molecules of approximately 7 BSA molecules wide and 2 BSA molecules high, since the dimensions of a BSA molecule is 14 nm x 4nm. The roughness analysis of the image shows the Rq value as being 5.979 nm.

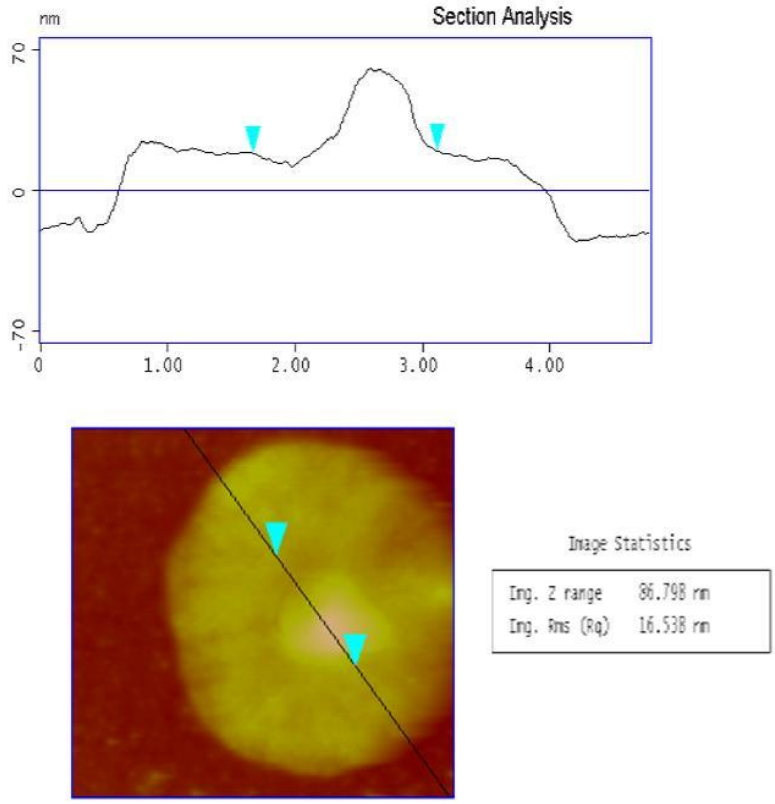

Figure 87 Section analysis of modified BSA showing a cross section of the surface and the Rq value of 16.538 nm.

The Section analysis of the modified BSA shows a maximum surface height in the region of 60 nm, and a feature width of around 3 µm consistent with data in previous sections. The interesting point to not from Figure 87 is the large increase in the surface roughness value, from native to modified the Rq value has increased from 5.979 nm to 16.538 nm, indicating the vast change in the surface.

Therefore the formation of the “mushroom” like features is distinctive in comparison to the native proteins’ AFM results. Again this formation could be attributed to the fact that there is now a large planar aromatic moiety on the protein that causes an attraction between adjacent BSA molecules. The protein is a large globular protein in itself and as such the interaction of several molecules could be the cause of the features formed on the surface of the substrate.

4.5.9.3 Insulin AFM results

As carried out on the two previous proteins AFM studies were carried out on modified and unmodified insulin. Samples were prepared as follows:

1 mg/ml of modified/native protein was dissolved in water and added drop wise to a silicon substrate previously sonicated in ethanol and dried under a stream of nitrogen. The solvent was allowed to evaporate and the samples were subject to AFM and the results are as follows:

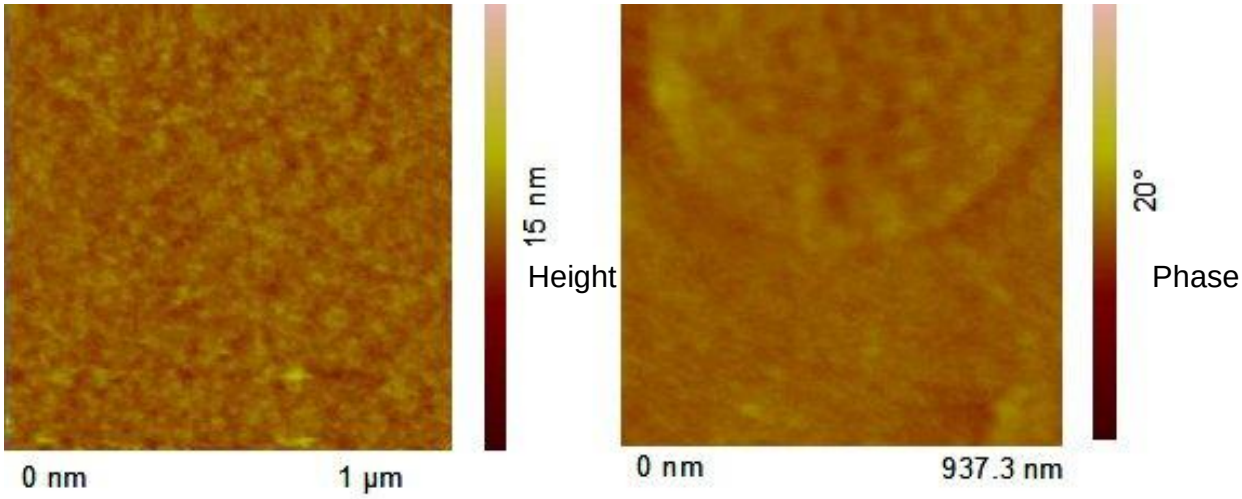

Figure 88 Control experiment showing unmodified insulin on a silicon substrate.

The control AFM shows no distinct features on the surface instead, the grainy surface, as observed by the height image in Figure 88, is indicative of the individual protein molecules on the surface. Insulin can exist as a hexamer, although this is the inactive form, and as such although a small protein, can be observed on the surface.

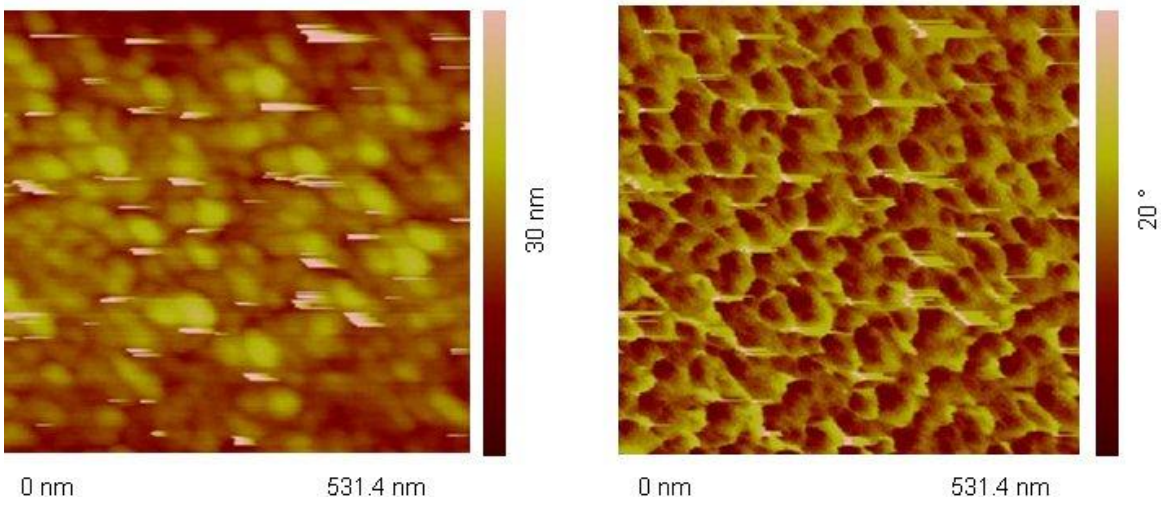

Figure 89 AFM images on modified insulin show distinct structure on the surface.

From Figure 89 it can be seen that there are globular features on the surface that have a maximum dimension of 33 nm in width, and around 30 nm in height when the modified protein was subject to AFM, this is in direct contrast to the control experiment carried out on the unmodified insulin as shown in Figure 88. The AFM images show no distinct features on the surface of the silicon substrate. This suggests that the DIP molecule plays some role in the alteration of the bulk material on the surface, perhaps indicating that DIP - DIP interactions have some role to play in the formation of such distinct features.

4.5.10 Cell behaviour towards modified BSA

In order to determine the effect the DIP adduct has on the behaviour of cells ,studies were carried out where a cell line was exposed to a surface coated in the modified protein. To compare the effect of the DIP addition, the experiment was repeated with a series of controls including unmodified BSA and a substrate without protein.

The substrates, glass slides, were immersed in solutions of:

1. water – no protein
2. 1 mg/ml unmodified BSA
3. 1 mg/ml DIP modified BSA

The slides were immersed in the solutions for 24 hours and allowed to air dry. The slides were then immersed in a solution of BHK cells, prepared to 20,000 cells per

vial and cultured overnight then fixed and stained. Each sample was examined with microscopy and the following results were obtained.

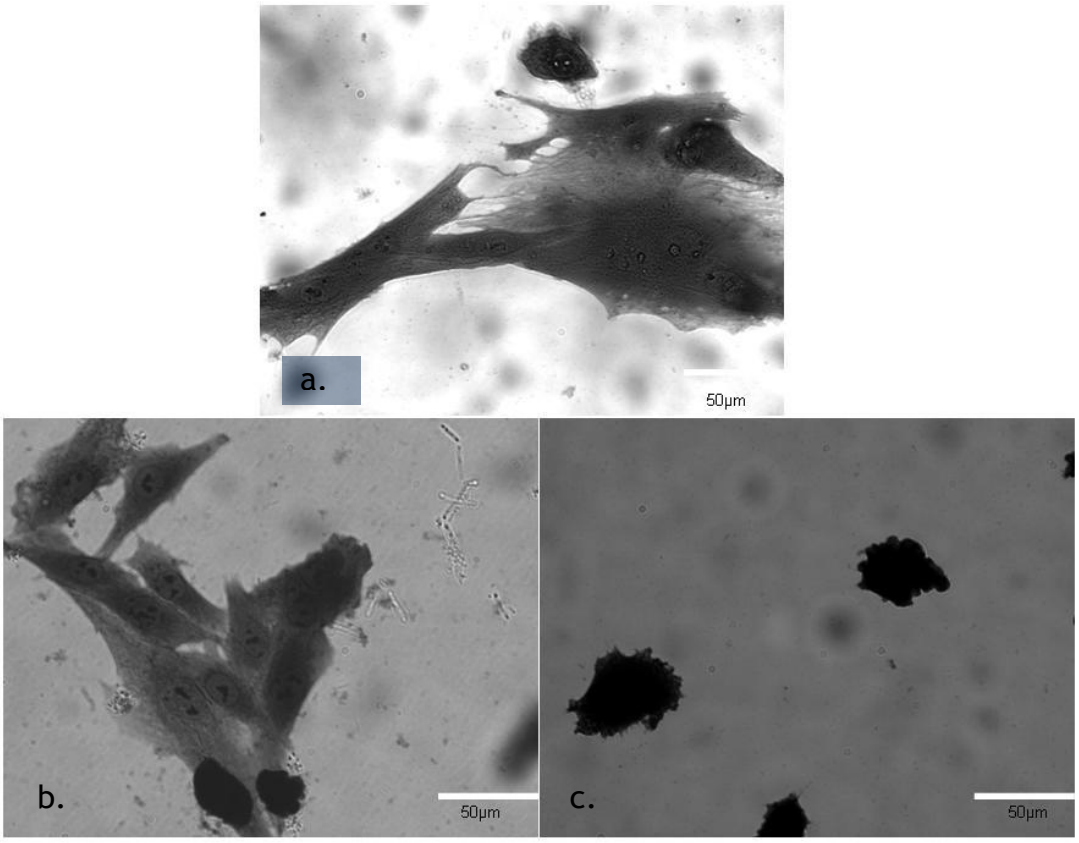

Figure 90 a. shows BHK cells on glass, b. shows cells with BSA on glass, and c. chows cells on the surface when exposed to BSA-DIP complex on glass.

It can be seen from the striking difference in the cell response to the surface that there is some reaction from the cells towards the presence of both the BSA and the BSA – DIP complex. From Figure 90 the response the cells have to the untreated glass is as expected – the cells elongate themselves and spread over the surface of the substrate. This is in contrast to b, where the cells appear to stretch themselves over the surface with elongated features and finally (c) shows the response the cells have in the presence of the BSA DIP complex. It can be concluded that the DIP on the surface of the BSA molecules is toxic to the cells and causes cell death.

This is an interesting starting point in determining if the DIP has the potential to be used as a drug target.

4.5.11 Dendrimer – DIP reaction

DIP modified dendrimers were chosen for their interesting structural characteristics and in particular PAMAM Gt 1, 1,4 diaminobutane dendrimer was studied.

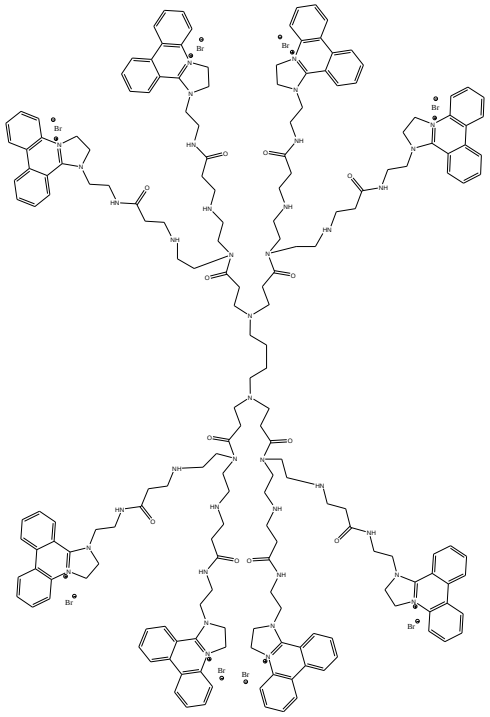

Figure 91 Structural representation of PAMAM Gt 1, 1,4 diaminobutane dendrimer.

1 mM solutions of each were prepared by dissolution in methanol and added drop wise to a silicon substrate and left to dry overnight to remove any solvent present. The silicon substrates had previously been sonicated in ethanol and dried in air. The dendrimer – DIP complex monolayers were then analysed using AFM.

4.5.12 PAMAM Gt1 1,4 diamino butane dendrimer + DIP results

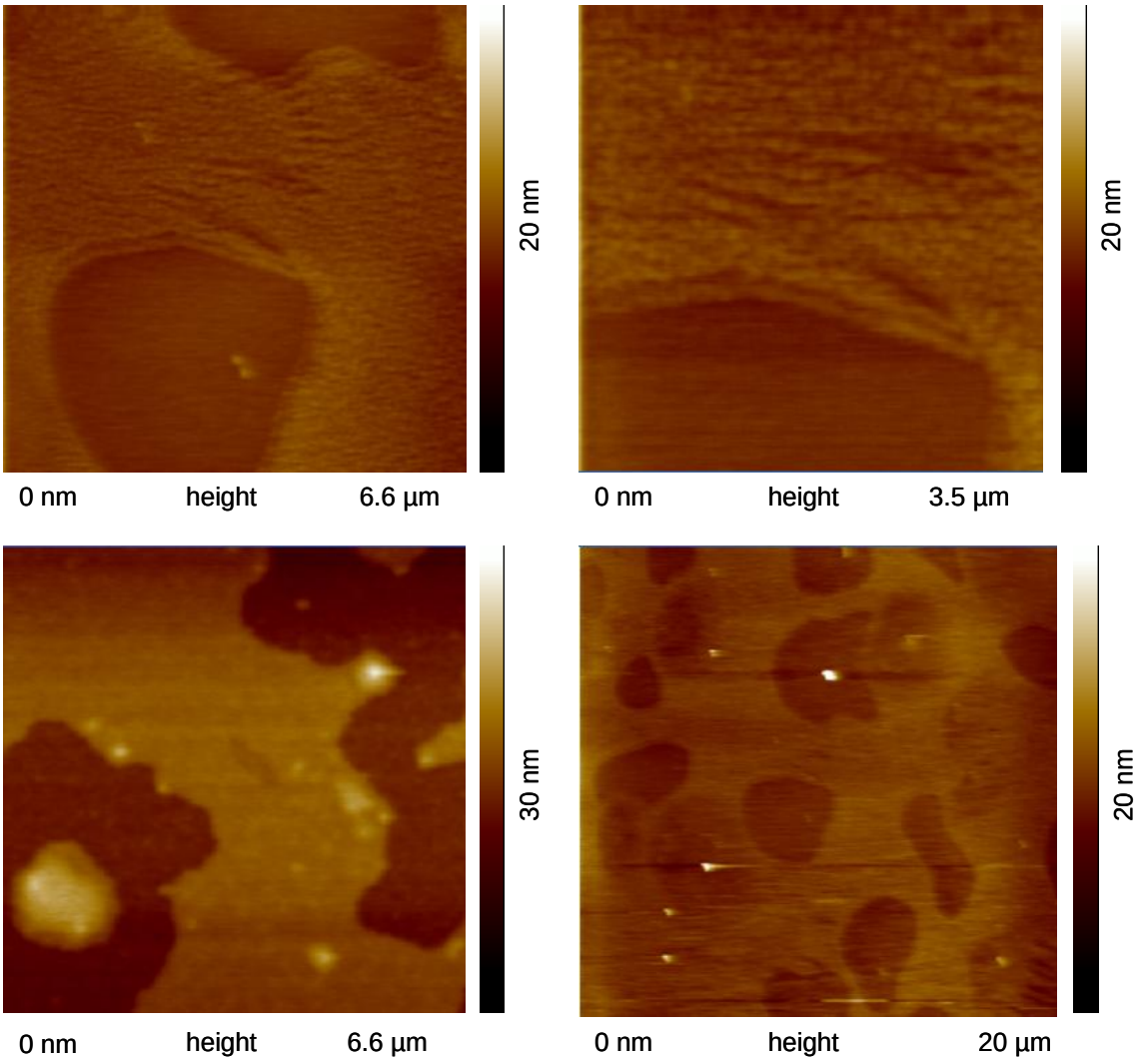

Figure 92 Tapping mode AFM was used to provide height profiles of the dendrimer DIP complex on the surface.

Depth profiles of the resulting layers were analysed and shown in Figure 93 and Figure 94.

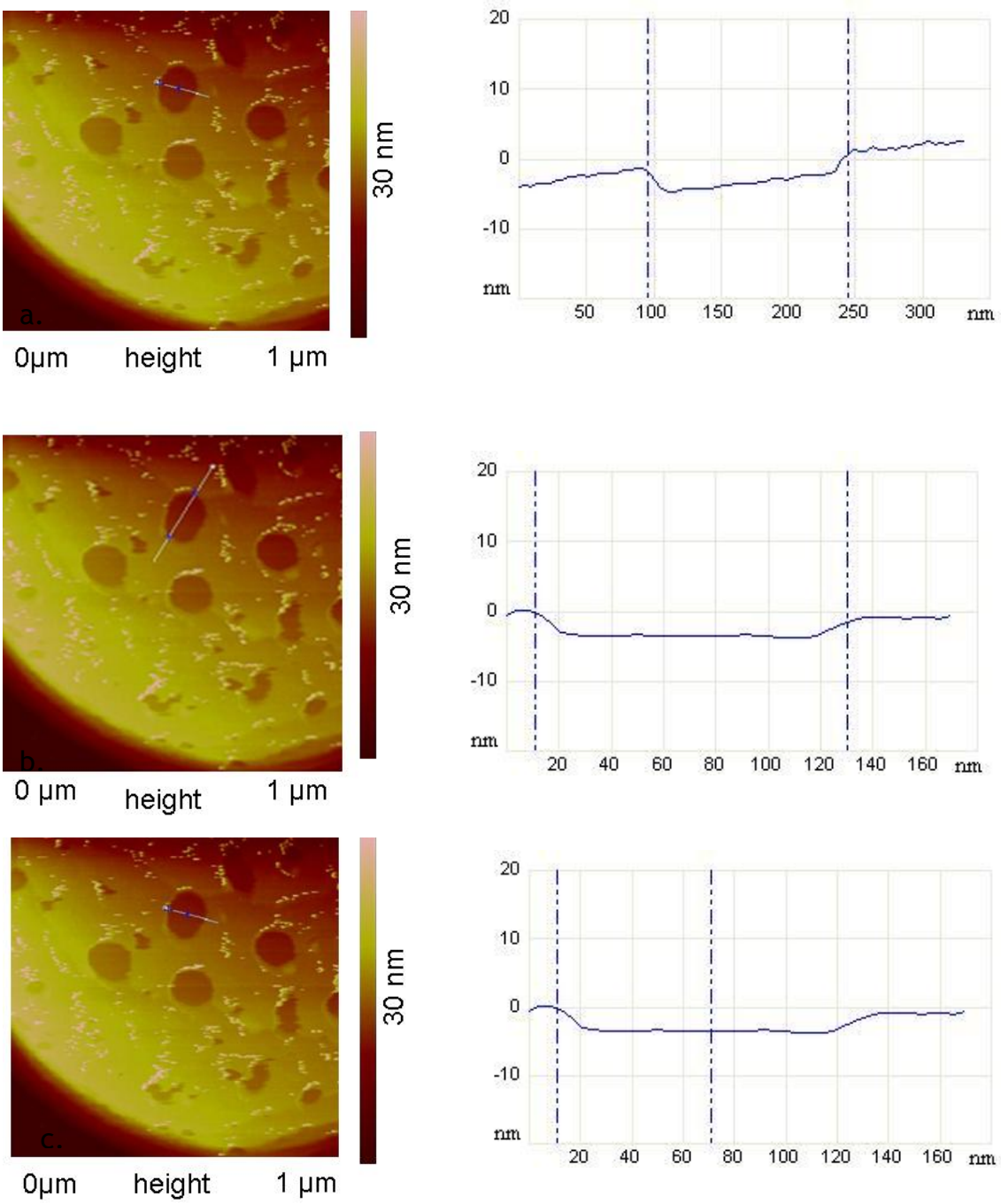

Figure 93 The cross sections indicate the distance from each side of the DIP dendrimer complex. From top to bottom the distance is 0.15µm and the distance from one side to the other is 0.11µm. The height of the step can be seen from image c and measures 3nm from bottom to top.

The dendrimers appear to layer themselves on the surface in order to minimise contact, there are areas of the surface without any Dendrimer – DIP complex, as shown from the profiles in Figure 93. In addition to this, the complex appears to layer on top of one another as shown in Figure 94;

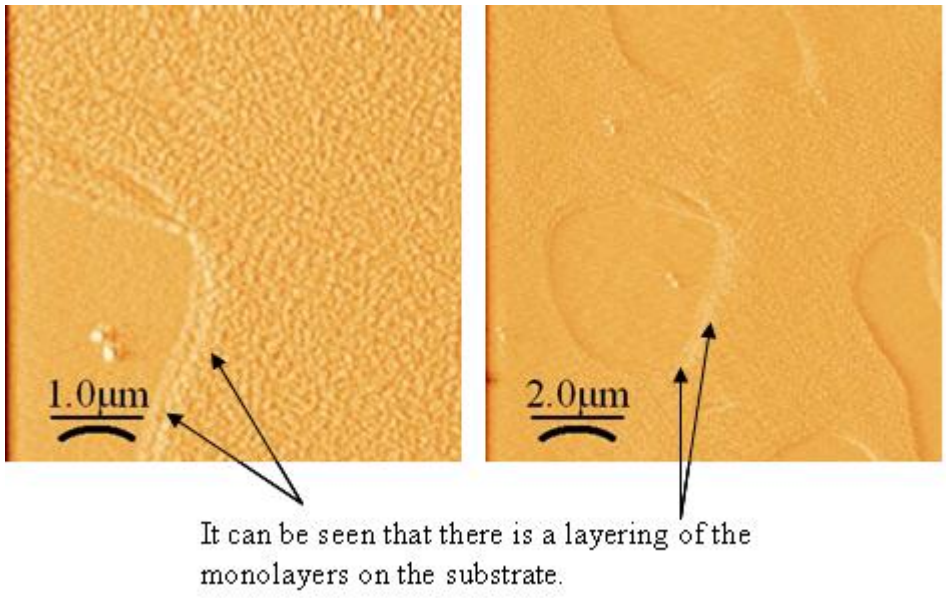

Figure 94 AFM images showing the layering of the dendrimer Dip complex.

A profile examining the roughness and the layering of the surface is seen from

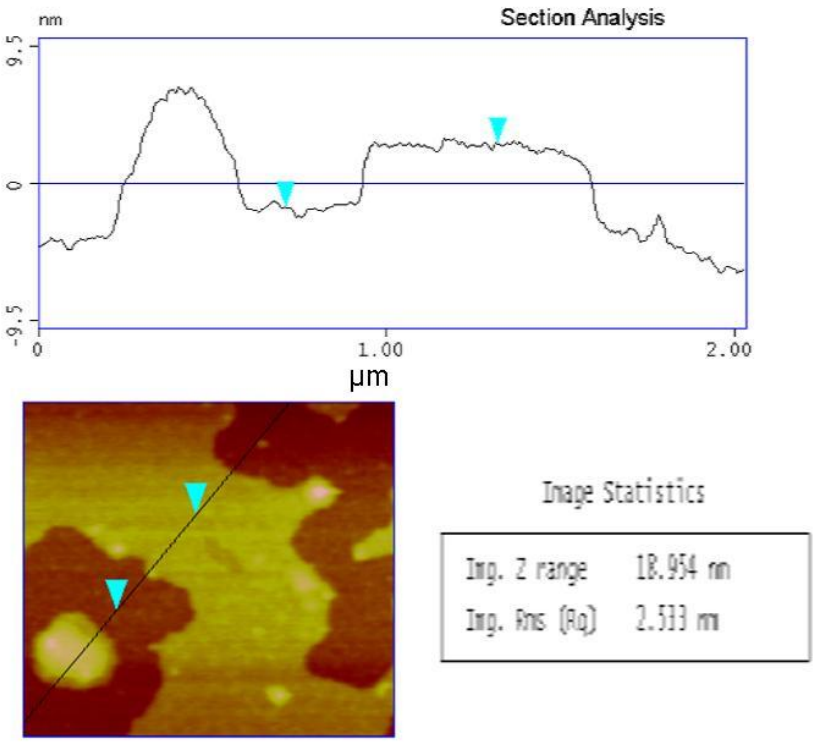

Figure 95 Section analysis shows the height change indication that there is a surface effect with the dendrimer not orientating on the surface uniformly. Surface roughness (RMS) has an Rq value of 2.533 nm.

The section analysis shows further confirmation that the dendrimer molecules align themselves in such a way as to minimise contact with the surface. The step height for the areas that include dendrimers vary as can be seen from the analysis and the Rq value of the surface is 2.533 nm.

This offers interesting conclusions, the dendrimers, which are planer molecules are derivitised with large poly aromatic groups meaning the monolayers formed could be orientated so they stack on top of one another, allowing interaction between the adjacent molecules DIP features.

4.6 **Conclusions**

The aims of this chapter were to determine if there was an efficient method to modify and purify proteins by selectively targeting certain residues with a high degree of control. In addition, if modifications are successful then what effect did this have on the structure of the protein and the properties of the bulk material? Through identifying what residues were targeted for modification, how many modifications were possible, and looking at the structure of the potentially modified protein, an assumption could be made on the success and ease of the reaction as well as the effects of this.

The modification of lysozyme in particular is not unknown, there have been reported examples in the literature that utilise various chemistries e.g. modification by acetylation using acetic anhydride[149]. The limiting factor however in many of these reactions is that only 4 of the 6 available lysine residues on lysozyme have previously been modified. This is a result of the accessibility of the remaining two residues which exist buried deep within the core of the folded protein.[149]

The results of this investigation show however that the DIP reaction has modified all 6 residues without significantly altering the secondary structure of the protein as can be seen from mass spectrometry and circular dichroism studies carried out in this investigation. This method of modification is also advantageous as it is a relatively simple “one pot” procedure requiring only one purification step which is in contrast to the complicated methodologies used in the past. Other methodologies often require extensive purification, whereas this method offers a biocompatible

medium and a relatively simple purification procedure offering a distinct advantage over other procedures.

For lysozyme, mass spectrometry results clearly show that all 6 lysine residues have been modified. In looking at the circular dichroism results these are key in, determining the effect of the modification. In order to achieve a successful modification little disruption to the proteins' fundamental structure would be an ideal situation, as the structure of the protein is fundamental to its activity and any loss of activity would render the protein useless. Confirmation by circular dichroism suggests that despite the DIP moiety interfering with the near UV spectras, the far UV spectra is consistent with the native protein. This infers that the secondary structure remains largely unaltered. AFM studies have also highlighted the modifications. The non uniform, long fibrillar networks are in contrast to the featureless surfaces of the unmodified lysozyme. This modification offers potentially important results, fibrillar features are often found to be toxic *in vivo* and perhaps this result suggests that these modifications may have potential interesting applications on further study.

The studies carried out on BSA also show interesting results. Distinctively different from lysozyme in many of its properties, this protein proved a challenge to clarify which residues, if any, had been modified. In stark contrast to the lysozyme with only 6 lysine residues, the vast number of residues that exist on BSA made this reaction more difficult to quantify.

The results for BSA, although similar, offer some interesting observations. Whereas the modifications of lysine residues in lysozyme was straightforward, sequence analysis of modified BSA suggests that the reaction targeted cysteine residues as well as lysine. This is due to the fact that within both lysozyme and insulin, all cysteine residues are held in disulfide bonds and so are unavailable for reaction. MALDI mass spectrometry show a triply charged molecular ion of the unmodified protein (66, 354 Da) at *m/z* 22, 119 and modified protein (67, 704 Da) at *m/z* 22, 569. This corresponds to a mass difference of 1, 350 Da corresponding to around 7 modifications. Sequence analysis by tripsin digest and mass fingerprinting show the sites of modification are lysine 581, 582, 590 and cysteine 58, 147 and either 581, 582 or 590. Presumably these modifications are the most accessible out of the 59 lysine and 35 cysteine residues available.

AFM studies for BSA show interesting results: the large “mushroom” like structure of the modified BSA on a substrate are in stark contrast to native BSA. This result is attributed to either protein interactions due to the modifications or interactions between modified residues. This will form the basis of the future work carried out on these modifications. Circular Dichrosim studies are similar to that of lysozyme indicating the secondary structure remains largely unaltered.

An interesting addition to the studies carried out on BSA was the effect this modification had on cell behaviour. When cells were analysed in contact with the DIP-BSA on glass slides the cells can be seen to undergo necrosis, in comparison with native BSA, this toxicity again shows an interesting result and the reasons for this will be investigated further in future work.

Studies for Insulin were consistent with results form lysozyme and BSA, mass spectrometry analysis shows the single lysine residue available is modified and AFM results show a honeycomb structure not seen from the native insulin.

Through the following sequence, Scheme 4, of events it was possible to determined that proteins containing lysine, and in some instances cystein, could be selectively targeted for modification by DIP.

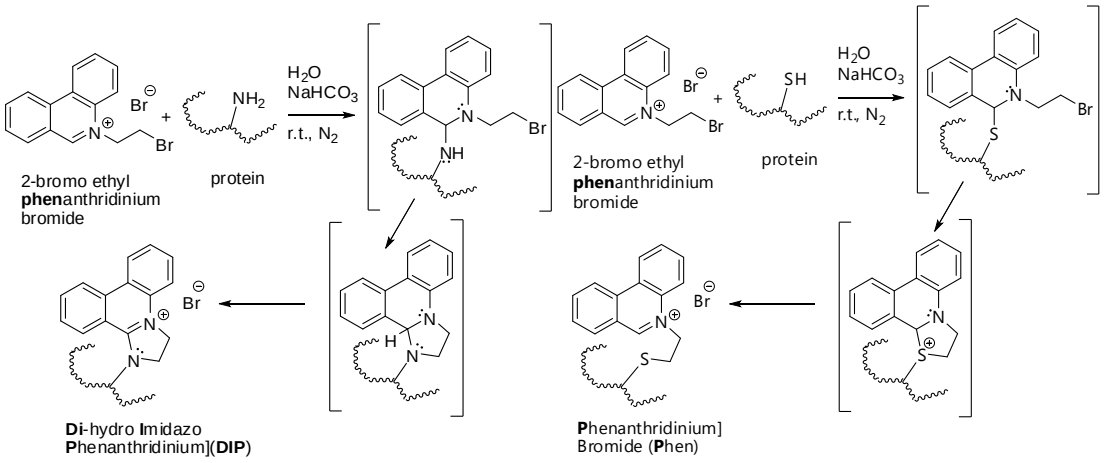

Scheme 6 Description of the reaction and basic mechanism of reaction yielding a DIP protein adduct by reaction with primary amines (a) and Phen protein adducts by reaction with thiolates [79,80b].

In conclusion, the ability to modify proteins with a one pot, three step methodology targets lysine residues via a cyclisation reaction and potentially cysteine residues via an addition reaction to give DIP and Phen based heterocyclic cations is unprecedented.

This method is in direct comparison to conventional methods of modification which are often difficult to carry out with any great selectivity and often require extensive purification. This method offers a biocompatible medium and a relatively simple purification procedure that offers an advantage over other methodologies.

This chapter has demonstrated the unprecedented modification of proteins using a one pot, three step methodology that targets exclusively lysine residues and in some cases cystein where the residues are not held within a cystein-cystein bond. This represents the first instance where a protein has been modified in such a manner and has been demonstrated through a variety of analytical methods.

5 Surface Mediated Reactions

5.1 Chapter aims

Previous work has been carried out on the $[\{Mo^{VI}O_3\}_{18}(S^{IV}O_3)_2]^{4-}$ cluster and it has been proven to display thermochromatic behaviour and extensive redox chemistry. The main issue however is that the cluster does not undergo a reversible intramolecular redox reaction in either solution or solid state. The aim of this chapter is to determine if cluster 1, β-$[Mo_{18}O_{54}(SO_3)_2]^{4-}$ can be "pushed" into a complete intramolecular redox reaction by using the surface it is on to drive the reaction. The method utilised to achieve this will be to isolate the cluster as a monolayer on various surfaces, i.e. remove the cluster from the crystal lattice and adsorbing it onto a surface. Three surfaces will be examined: gold, highly ordered polycrystalline graphite and cystein modified gold. The basic chapter outlook is shown in Figure 96.

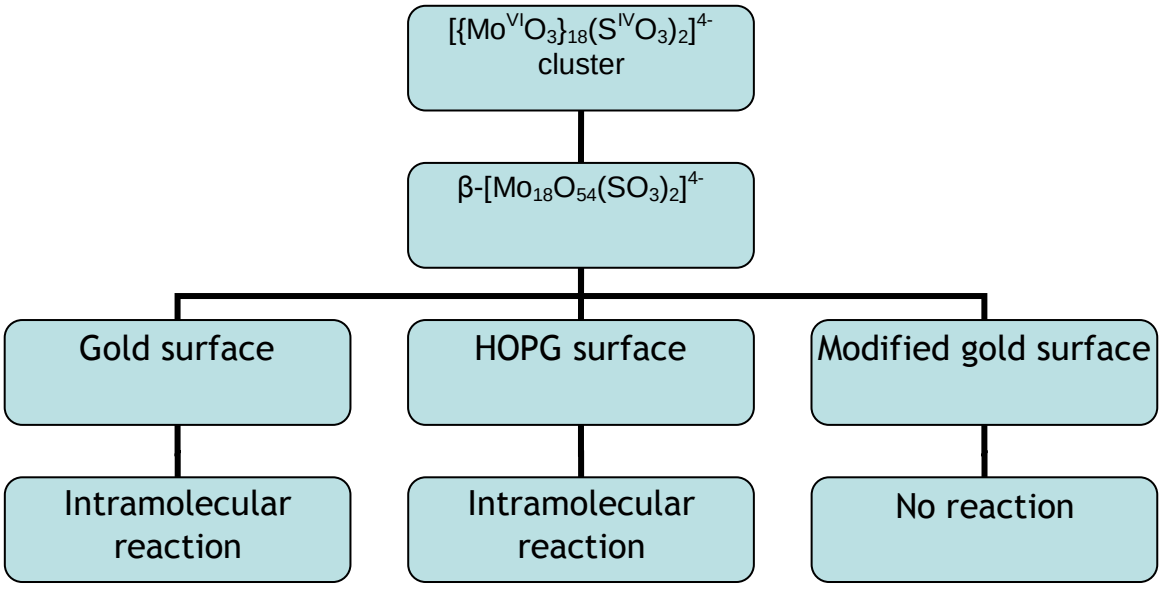

Figure 96 Schematic of the proposed investigation.

5.2 *Chapter introduction*

Single molecule devices are a topic currently receiving by great interest. Transition metal oxides (TMOs) with their already well established properties such as their catalytic ability[150], ultra high density magnetic data storage and their impact on materials science[55,108,116,151], have the potential to be used for such single molecule electronic devices and the eventual development of single molecule switches. The main criteria for such a device is that its effects must be reversible and, since this is generally not the case for TMOs where the electronic properties are altered by the irreversible addition of a dopant, the route to such devices has been limited. Until now it is the reversibility of the electron transfer which has proven difficult. However the exploration of POM chemistry has developed molecules that can potentially be involved in such reactions and be considered a single molecule molecular switch, dependent on the environment in which the molecules find themselves placed.[152]

The development of the molybdenum (VI) oxide cluster $[Mo_{18}O_{54}(SO_3)_2]^{4-}$ (compound 1) as seen in Figure 97 has the potential to be developed into a switchable molecular device. [153]

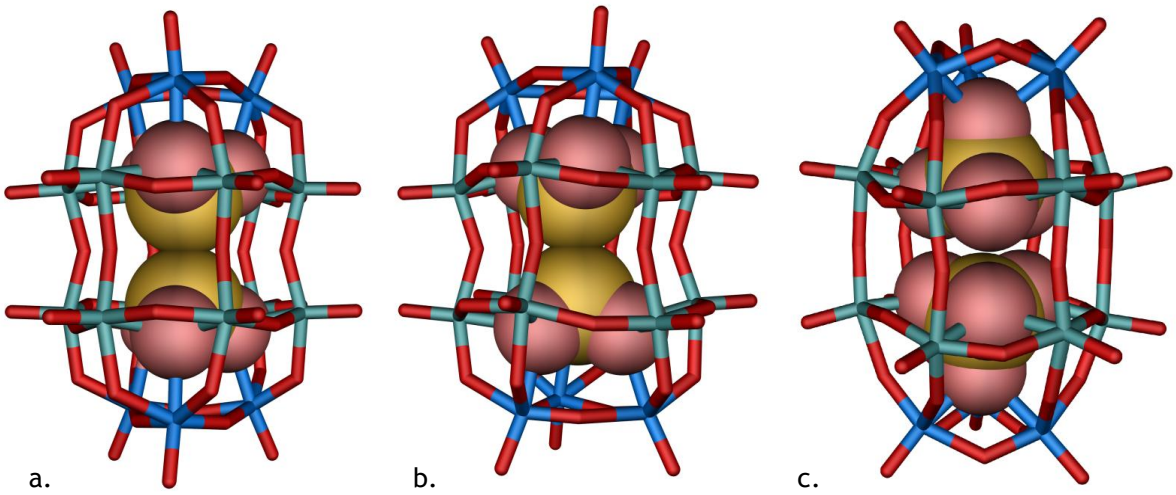

Figure 97 A representation of the structures of the sulfite-based Dawson clusters: (a) α-$[M_{18}O_{54}(SO_3)_2]^{4-}$, (b) β-$[M_{18}O_{54}(SO_3)_2]^{4-}$(Compound 1) , and (c) a comparison with the conventional α-type sulphate-based Dawson anion $[Mo_{18}O_{54}(SO_4)_2]^{4-}$, (Compound 2) whereby the central anion templates are shown in a space-filling mode (S: yellow; O: red; Capping Mo: blue; "belt" Mo: green).

The interior cavities associated with the molecular cluster $\{Mo_{18}{}^{VI}O_{54}\}$ have the capacity to hold two pyramidal sulfite anions $(S^{IV}O_3)^{2-}$, in a non bonding regime

with the cluster. What is interesting about this molecule are the S centres within. The bond distance between the two S centres lies at 3.29 Å which is in contrast to the S-S bond associated with a dithionate anion ($O_3S\text{-}SO_3^{2-}$) of 2.15 Å. The possibility of binding the 2 sulfur molecules to release two electrons into the system is an interesting advance.[60]

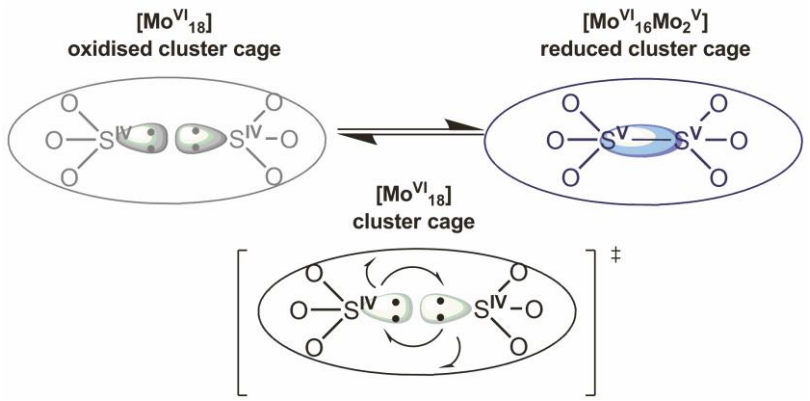

Figure 98 Schematic showing the transformation of the fully oxidised cluster cage of $[\{Mo_{18}{}^{VI}O_{54}\}(S^{IV}O_3)_2]^{4-}$ on the left to the reduced cluster cage on the right, $[\{Mo^{V}{}_2Mo^{VI}{}_{16}O_{54}\}(S^{V}{}_2O_6)]^{4-}$. The oval graphs represent the $\{Mo_{18}O_{54}\}$ shells.

There have been extensive studies carried out on the cluster[154] and it has been proven that it holds extensive redox properties in addition to rich thermochromic behaviour[155]. However the ability to reverse the reaction in the solid or solution phase has yet to be achieved, as has been described in earlier work by the Cronin group[154]. It is this process that is of interest. Can the cluster be forced into a state where a complete intramolecular redox reaction takes place? In order to attempt such a reaction, investigations into the cluster's environment were carried out. In particular the forming of monolayers of the cluster on a highly polarisable metallic substrate was performed in order to determine if this would activate the formation of a bond between the two internal sulphite groups. The following study will determine if this process is possible.

5.3 **Experimental**

5.3.1 Preparation of Monolayers of the Clusters

In order to determine if the cluster will undergo a redox reaction when it is isolated on a highly polarised metallic substrate, monolayers of the cluster were prepared on gold using the following method.

Silicon wafers were used as the substrate for the reaction. The wafer was prepared using e-beam evaporation of 10nm titanium to aid gold adhesion to the silicon followed by 25nm of gold. Samples were prepared by dipping polycrystalline Au films in 1mM of the cluster solutions in acetonitrile. After immersion the samples were dried in a stream of nitrogen gas. This method has been applied by Barteau and co-workers on other POM systems and has been found to produce single monolayers for analysis.[156]

As a control, monolayers of the sulfate-based Dawson anion $[\{Mo^{VI}_{18}O_{54}\}(S^{VI}O_4)_2]^{4-}$ (compound 2) were also produced using the same techniques. This compound is a good control as the SO_4^{2-} template is chemically inert in comparison to the $(S^{IV}O_3)^{2-}$ anion which is chemically active. This is due to the sulfur atoms being in an intermediate oxidation state and the fact that there is a vacant coordination site with a lone pair of electrons associated with it. As mentioned previously it is the location of the sulfur atoms within the clusters cavity that makes compound 1 such an interesting molecule in comparison to compound 2 with its inert core.

Both clusters 1 and 2 were subject to valence level photoemmision spectroscopy and x-ray photoelectron spectroscopy (XPS) to determine the temperature dependence at two temperatures 298 K and 77 K of the cluster layers valence level electronic structure and the oxidation state of the Mo centres respectively. Both procedures were carried out at ultra high vacuum condition. This work was carried out in conjunction with the Kadodwala group, who carried out the analysis techniques on the prepared surfaces, to give a full understanding of the method of electron transfer.

5.3.2 Methods for Photoemission

All experiments were performed at the Central Laboratories of the Research Councils (CLRC) laboratory at Daresbury, at station 4.1 of the Synchrotron Radiation Source (SRS). This station comprises of an UHV beamline with a spherical grating monochromator which provided photons in the 14-170 eV range. [153]The UHV end station was equipped with a CLAM 2 (VG ltd) concentric hemispherical analyser and a X-ray source (Al Kα) for XPS analysis. Electron bombardment heating was used on the samples and temperature was monitored

either with an optical pyrometer (elevated temperatures) or a chromel alumel thermocouple (cyrogenic temperature ca. 140 K). The valence region photoemission measurements were collected using photon energies of 140 eV, all binding energies are referenced to the E_F. Valence region spectra were collected in normal emission geometry with the photon beam incident at 55° (with respect to the surface normal). Core level spectra (C(1s), O(1s) and Mo (3d)) were collected at normal emission using a Al Kα source, the x-rays from which were incident at 73° with respect to the surface normal.

5.3.3 Effect of the substrate on the redox reaction

In order to fully understand the effect the surface has on the thermally driven reaction, compounds 1 and 2 were tested on a variety of different substrates:

1. Gold surface modified with a monolayer of cysteine

2. Highly ordered pyrolytic graphite (HOPG)

5.3.4 Formation of Cysteine monolayers

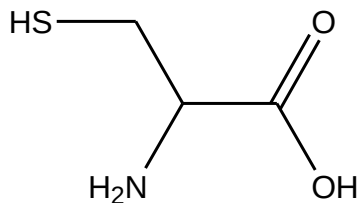

Figure 99 Cysteine molecule with exposed primary thiol group essential for formation of a self assembled monolayer.

1 mM solution of cysteine as shown in Figure 99 was prepared in ethanol and a gold substrate was submersed in the solution for 30 minutes. The substrate was removed from solution and the gold surface dried under a stream of N_2 resulting in self assembled monolayers of cysteine as shown in Figure 100.

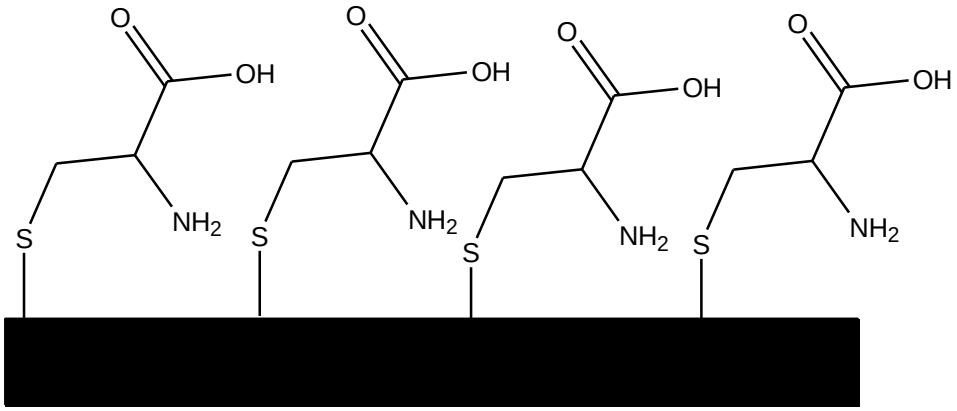

Figure 100 Monolayers of cysteine on gold surface attached through a thiol – gold bond.

Both compounds 1 and 2 were prepared to 1 mM in acetonitrile and the modified surfaces immersed in the solution. The substrates were dried under a stream of nitrogen.

5.4 **Results**

The spectra obtained as shown in figure 101.

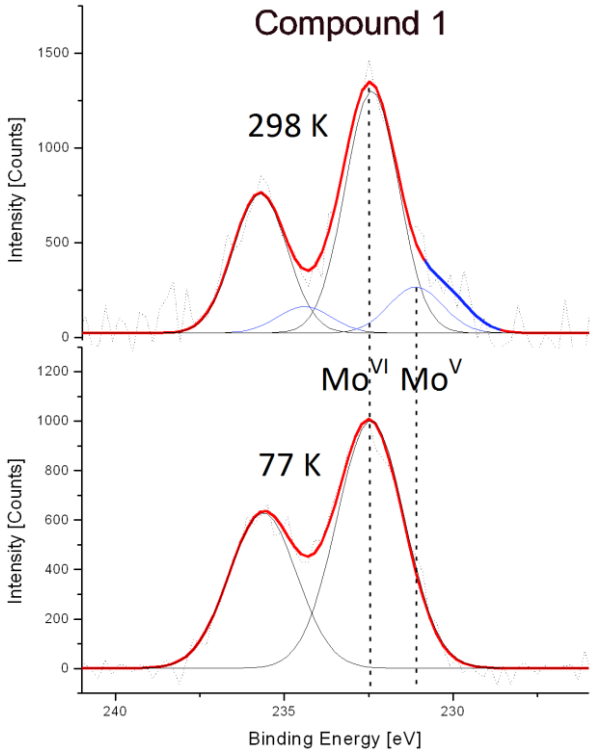

Figure 101. Mo 3d core level spectra for the sulfite cluster at 298 K (TOP) and 77 K (BOTTOM) showing the appearance of bands associated with Mo^{V} at 298 K. The dotted lines refer to the expected positions for Mo(VI) and Mo(V).[13] The fitted curves are shown in blue and the shoulder that develops at 298 K is highlighted in blue.

From Figure 101 it can be seen that compound 1 does in fact show electronic changes when there is a temperature shift. These changes can be attributed to the intramolecular redox reaction that has been postulated to occur as shown in Figure 98. The spectrum at 77 K and the spectrum at 298 K can be compared. At 77 K a single pair of 3d peaks corresponding to the binding energies of 232.5 and 235.6 eV indicate that the cluster contains fully oxidised Mo (VI) ions. This is in direct comparison to the spectrum at 298 K which shows the major component (86±4%) is the oxidised Mo (VI), but also characteristic binding energies at 230.5 and 233.6 eV corresponding to $d^{5/2}$ and $d^{3/2}$ respectively indicating reduced Mo (V). The heating up of the cluster from 77 K to 298 K shows the reduction of the cluster by almost 2 electrons. The results for compound 2 show no difference when heated indicating, as expected, no intramolecular redox reaction.

This result is further expanded in the photoemission spectra taken from the valence region as shown in Figure 102. Carried out at both cryogenic temperature and room temperature the oxidation states of the Mo centres as a function of the temperature are as described previously. Four different examples were used:

1. The α sulphite at room temperature (see also Figure 97)

2. The β sulphite at room temperature (see also Figure 97)

3. The β sulphite at cryogenic temperature

4. The sulphate (see also Figure 97)

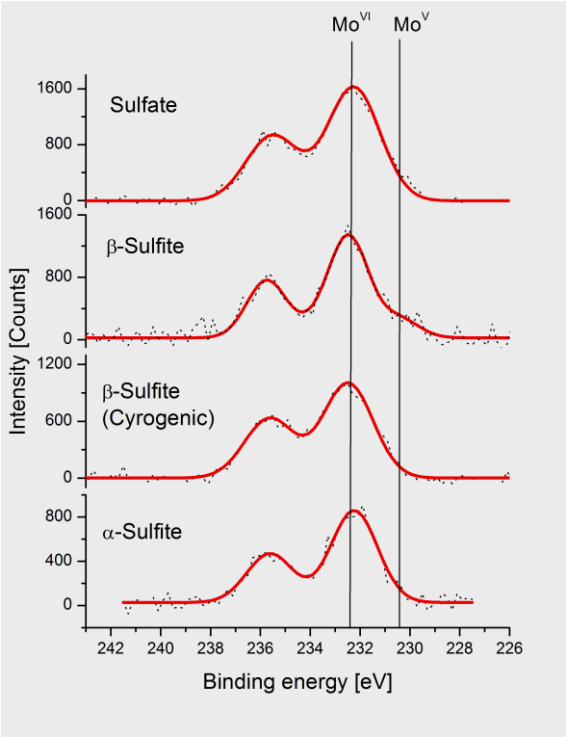

Figure 102 Mo 3d core level spectra showing the formation of 2-3 reduced Mo centres per cluster of compound 1 at room temperature.

This offers a comparison between the sulfite and sulfate cluster (Compound 1 and 2), and confirms the temperature dependence of the reaction. There is a common feature at room temperature between both clusters shown at 31.1 eV which is not seen in the cryogenic cluster spectrum shown in Figure 103

The difference spectra of compound 1 is shown in Figure 103. The bands shown at 3.5 and 6.3 eV are similar to the results obtained from previous work determining that the components at 3.7 and 6.6 eV are associated with the electronic states of the bridging and terminal oxygen of the Mo cage. This is in addition to the peak at 2.6 eV which can be associated with a Mo $4d^1$ electron. This is consistent with the Mo(V) component.

5.4.1 Photoemission results

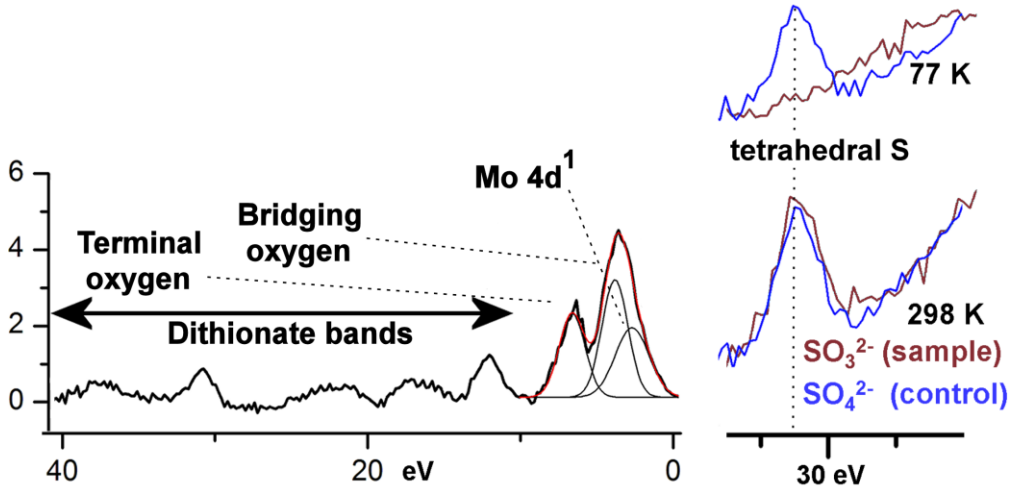

Figure 103 LEFT: Photoemission spectra: Difference spectra (298 K – 77 K) for the compound 1 in the valence region. Bands associated with the reduced Mo ions and the formation of $[O_3S\text{-}SO_3]^{2-}$ (dithionate) are observed at 12.1, 16.7, 22.3 and 31.1 eV. The three peaks at 2.7, 3.5, and 6.3 eV can be fitted with three Gaussians (smooth black curves) at 2.6 (assigned to the Mo $4d^1$), 3.7 and 6.6 eV to give an overall envelope shown in red. RIGHT: The region centred around 30 eV in the photoemission spectra for the control (2) and sample (1) covering the region characteristic for tetrahedral sulfur. A common peak at 31.1 eV is seen in both the control compound, 2, at 298 and 77 K (blue line) and then appears in the spectra of 1 (brown line) at 298 K showing the reversible development of a tetrahedral sulfur centre in cluster 1.

These results are indicative of compound 1 cage being partially reduced at room temperature and the presence of the bands at 3.5 and 6.3 eV show a change in the distribution of electrons due to the reduction of the Mo centres.

The peaks at 12.1, 16.7, 22.3 and 31.1 eV are indicative of an oxidised, tetrahedral sulfur based species, adding further confirmation that the sulfite groups have formed dithionate through oxidation and now occupy a tetrahedral geometry. This in turn confirms that the electrons for the reduction of the Mo centres have not come from the gold surface.

Therefore the effect of absorbing the compound on to the gold surface induces a local electric field associated with the image charge that activates the thermally controlled electron rearrangement. This change is not a structural one attributed to the bulk material, instead the change occurs within the molecular cage through the formation of the S-S bond. This results in the generation of a new populated electronic state in the band gap of the oxide cluster molecule.

This cluster can then therefore be thought of as a new type of molecular transport switch that is activated via the surface through the local electric field.

5.4.2 XPS results

XPS studies were carried out on the cluster on all surfaces to determine what effect, if any, this change of surface has on the ability for the reversible reaction to occur. The results are summarised in Figure 104.

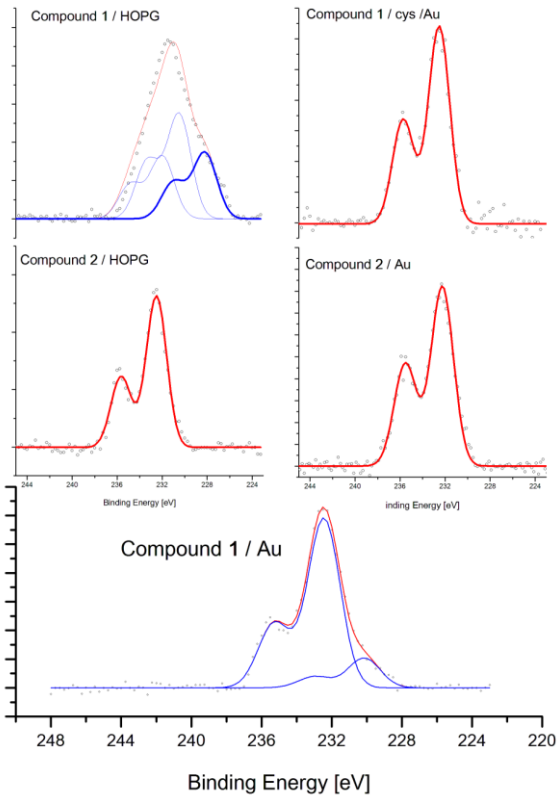

Figure 104 XPS of the clusters on various surfaces at 298 K. Bottom shows Compound 1 on Au showing the appearance of the Mo(V) band at around 230. The middle Right and middle Left show the sulphate control, 2, on gold and HOPG respectively showing no change. The top Left shows the dramatic effect of depositing the cluster on HOPG; the envelope is fitted to three sets of $Mo^{d3/2}$ / $Mo^{d5/2}$ corresponding to Mo6 (235, 232), Mo5 (234, 231) and Mo0 (231, 228) eV. N.B. The same pattern is seen in the spectrum of 1 and 2 on Au after thermal decomposition > 500 K. The top Right shows Compound 1 on the cysteine monolayer on gold showing no change with respect to the control samples.

The results show that neither compound 1 or 2 shows any reaction when on the cysteine coated gold. However this is not true for the clusters on HOPG; compound 1 gives an interesting result, the cluster does undergo reduction;

however the reaction is rapid and irreversible in direct comparison with the same cluster on gold, where there is a thermally induced reversible reaction. Compound 2 on HOPG shows no change.

The reaction on HOPG can be attributed to the localised charge within the surface graphene sheet. This means that in comparison to the gold substrate, where the cluster and the image charge are equidistant from the surface, the separation between the cluster and the induced charge is shorter on HOPG as can be seen from Figure 105.

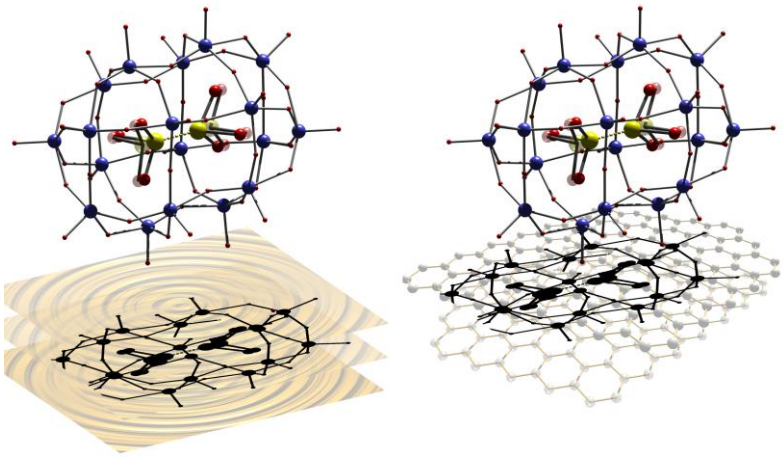

Figure 105 Scheme depicting the development of the image charge (black image) that develops when the cluster is adsorbed on the surface Au (LEFT) and HOPG (RIGHT). On Au the image charge will develop within the surface at a distance that mirrors the distance between the cluster and the surface. However on HOPG the image charge will be confined to the top graphene layer hence the field will be larger for HOPG than Au.

This in turn creates a higher local field than gold which the S atoms are then subjected to. This means that, even at room temperature, there is activation of the cluster. From XPS in Figure 104 the formation of Mo (V) and Mo(0) can be seen demonstrating the irreversible change.

This result is an interesting result. On the basis that in the control experiment using the sulfate cluster, it is not reduced, this means that it can be postulated that the HOPG induces the internal rearranging of the sulfite cluster without directly transferring charge, otherwise the control itself would be reduced.

The effect of the mirror charge on HOPG can be shown in Figure 106.

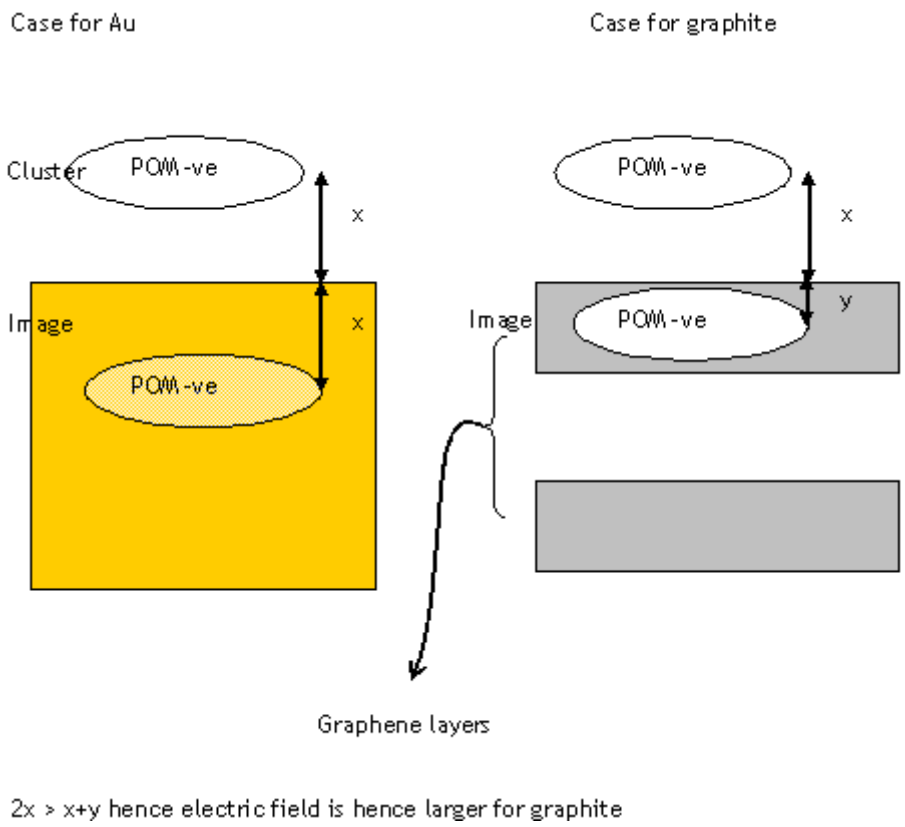

Figure 106 Schematic of the clusters on Au (LEFT) and HOPG (RIGHT) respectively. The development of a higher electric field at the cluster on HOPG can be rationalised due to the fact that the mirror charge of the cluster will be confined to graphene layers.

5.5 **Conclusion**

The development of POM clusters which incorporate molecules within the structure has led the way in not only development within the polyoxometalate community but also within the nanoscale device sector.

This TMO molecule, in particular containing the sulfite anion and prepared as a monolayer on a gold substrate, facilitates the development of a reversible redox reaction. This reaction promotes the formation of an S-S bond within the cavity of the metal cluster and allows the movement of electrons within the metal Mo (VI) oxide cage. This movement of electrons within the confined space, creating a Mo (V) dopant in the system changes the clusters overall electronic structure. Not only this, but the electrons are localised within the cage and the reaction is considered reversible. It is postulated that the presence of the gold surface is the mediator of the electron movement since the electric field that it generates promotes the formation of the S-S bond within the cage and the subsequent expulsion of electrons within the surrounding area. The system will therefore introduce a new

concept to the industry and aid the development of the nanoscale switchable devices.

6 Thesis conclusions

At the commencement of this project the initial aims were to:

1. Demonstrate the surface patterning of Polyoxometalate's; both the self organisation mediated by external factors such as cation and solvent exchange, to patterning of POMs in a specific orientation.
2. Modify a protein with Dihydro-Imidazo Phenanthridinium bromide and surface analysis of the effect of this modification.
3. To demonstrate the effect of the surface on transition metal oxide clusters and the surface mediated intramolecular redox reaction.

The purpose of these aims was to demonstrate the self assembly of hybrid nanostructures encompassing inorganic, organic and biological applications.

The surface patterning of polyoxometalate clusters using two approaches was carried out. The investigation focussed on both the self organisation of clusters mediated by external factors such as cation, solvent and concentration, to the specific surface patterning of POMs and for the first time the demonstration of the ability to specifically tether a POM to a surface in a pre-determined pattern.

The extension of POM chemistry to help identify possible new applications was the main aim in chapter 3. The investigation utilised new POM clusters chemically linked to different organic tethers, these being:

- C-16 and C-18 alkane chains
- Pyrene

A detailed review of their ability to self pattern and the external factors that affect this ensued. On investigating the organic tethers of the POM clusters, the C-16 and C-18 chains were studied using SEM and TEM. This demonstrated that the length of the alkane plays an important role in how the cluster self organises on the surface. The C-16 chain did not create the uniform rod like structures observed for the C-18 chain. Although some organisation is observed, the C-18 cluster showed "rod" or "needle" like structures with uniform dimensions indicating that the

alignment of each cluster may stack in a lamellar fashion that causes the rods/needles to occur.

In addition, the effect of the cation on the surface patterning was investigated. Cation exchange from TBA to DMDOA had a significant effect on the organisation of the cluster. SEM and TEM images illustrated that unlike the long needle like formations observed for the C-18 modified cluster, spherulite like features were observed. These features highlight the major change within the cluster on cation exchange from TBA^+ to $DMDOA^+$. The $DMDOA^+$ with its 4 long alkyl chains, extends the number of alkyl chains associated with the cluster and has an obvious effect on the surface morphology. In essence the $DMDOA^+$ has imparted qualities such as hydrophobicity into the molecule. Each $DMDOA^+$ counterion adds a total of 2 long alkyl chain and in conjunction with the 2 alkyl chains chemically linked to the cluster, resulting in 8 chains in total. This essentially has created surfactant effects and when dissolved in a solvent e.g. chloroform a core-shell hydrophilic hydrophobic surfactant encapsulated cluster, in conjunction with the surface grafted cluster is created.

The role of the solvent has also proven to be significant. An interesting feature of the DMDOA salts lies in the fact that they are soluble in chloroform whereas the TBA salts are not. When dissolved in chloroform and dried on a surface the DMDOA salts of both chain lengths create spherical shaped features on the surface as observed by SEM. On changing the solvent ratio to include acetonitrile in a 1:4 ratio with chloroform, this also alters the morphology significantly. The grafting of specific molecules; be it alkane chains or aromatic moieties has effect on the crystals organisation and this van be further explained by the clusters crystal structure. Crystallographic data for the symmetric pyrene Anderson work has uncovered the specific conformation the cluster adopt and this shape has been emulate don the surface. From the SEM circular micelle like morphology is observed that is consistent with the crystal structure.

Therefore the effects of the tether, the cation, solvent and concentration have been demonstrated. Each aspect has a significant effect on the surface organisation of the cluster and this has been observed through surface analysis techniques SEM and TEM. These surface studies have given further insight into the generation of needle like features and creating surfactant encapsulated (SECs) and surface grafted molecules. It is clear that these variables have an

effect on the self patterning of the POM clusters and this used in conjunction with the crystallographic information already obtained for each cluster has demonstrated that the POM materials can exhibit SEC like qualities and self organise and pattern in conjunction with external factors on a surface.

Secondly the surface patterning of POMs, for the first time has been demonstrated. The chemical tethering of a POM cluster to a self assembled monolayer through the development of an inorganic – organic hybrid molecule, and the ability to surface pattern a POM was realised. In using the organic tether of the hybrid molecule to chemically link the cluster to the surface represents the 1st time POMs being patterned and utilised in such a way. Moreover, this process of adding the asymmetric pyrene to the surface acts as a chromatographic medium, as the mixture contained both the asymmetric and symmetric Mn Anderson molecule. Since the symmetric molecule has no reactive sites only the asymmetric was chemically tethered to the surface. Using Tof Sims, the pattern and the composition of the surface was confirmed demonstrating the successful chemical linkage of the cluster.

An additional examination into the potential applications of the chemical linkage of the POMs to a surface was carried out. The initial aim of this was to determine more information regarding POMs role in potential biological applications. Cell studies with the POM surfaces confirmed that the cells were attracted to the areas that contained the pyrene Anderson cluster, giving new insight into a new potential application. This aim has therefore been achieved, the self patterning and the specific patterning of POMs showing new and interesting features regarding the behaviour of these clusters and for the first time the ability to specifically organise a cluster on the surface.

Continuing the theme of investigating the surface behaviour and pattering of a material, organically modified proteins were investigated. This section of the project had two main aims: to generate a reaction protocol to successfully modify proteins with a heterocyclic molecule, and secondly to determine the effect this modification has on not only the protein itself but how the protein organises itself onto a surface.

A successful methodology has been described. Utilising the one pot, three step procedure detailed previously resulting in proteins being decorated to varying

degrees with the DIP moiety. This represents a new method of post translationally modifying a protein with relative ease over other procedures reported in the literature. This specific reaction was chosen to attempt in the first instance to create multivalent systems containing many DIP moieties n the hope that successful intercalation with DNA would ensue. The modification was confirmed by mass spectrometry and sequencing and the effect this reaction has had on the secondary structure of the protein was investigated using circular dichroism, and the success of the reaction was confirmed. Secondly the effect this modification has on the bulk material was observed using AFM. Preparing surface that contain the native and modified protein gave the opportunity to observe the differences between them which were obvious. Whereas the native proteins showed no distinct features on the surface the effect of the modification was significant. With regards to lysozyme the identification of fibrillar like features was unexpected. These fibrillar like networks are indicative of features described in the literature that are common in amyloidosis highlighting the effect this modification has on the protein.

This effect can also be seen for BSA, whereas the AFM of the native protein identified features in the region of around 50 nm, equivalent to a cluster of around 3 individual protein molecules, each with dimensions ~14 nm. The modified protein was significantly different, showing large globular “mushroom” like features.

The scope for further work within this project is vast. From the three distinct chapters reported the results may act as the starting point for further investigation. The demonstration that it is possible to tailor inorganic materials, and in particular POMs, and chemically link these materials in a predetermined pattern to a surface is only the starting point. The applications of such a discovery may hold interesting opportunities to extend POM use in areas they are already prevalent e.g. for localised catalysis or anti viral use as described previously.

With regards to the protein modification, this work represents the start of what could be a new method to easily post translationally modify a protein without substantially affecting the structural components or the activity of the protein. Determining the modification is only scratching the surface of what information could be elucidated from this. Further investigation into the following would be beneficial:

- The secondary structure of the modified proteins could be further investigated using methods such as FTIP. This would give in depth indication into any changes in the secondary structure of the protein as a direct consequence of the modification

- NMR – to further detect with grater precision the alterations in the protein confirmation

- X-Ray Diffraction and crystallisation – carrying this out on the modified protein would enable a full understanding of the site of the modification.

- Activity assays – would be an invaluable source of information, to determine if the modifications had a negative effect on the function of the protein.

Finally the successful adsorption of transition metal oxides (TMOs) onto gold surfaces has been demonstrated. The TMO contains sulfite anions encapsulated within the cluster cage and through the mediation with the gold surface the promotion of a reversible intramolecular redox reaction occurs. Through the surface, electrons are effectively injected into the nanoscale Mo (VI) oxide shell resulting in the introduction of Mo (V) dopants through a reduction reaction. This thermally activated reaction is reversible as a result of the electron movement occurring within the cluster shell.

The fact that the surface facilitates the process is an interesting observation and as demonstrated the use of HOPG to rapidly induce the process, gives scope for using this surface to generate POM containing electronic devices. The mechanism for the reaction through the generation of an image charge to generate an electrostatic field to penetrate the cluster and allow the bonding between the sulphate groups and the transfer of two electrons to the outer metal oxide shell has strong implications that reaction may be advanced further. This starting point gives scope for further work to be carried out to fully understand the process and offer the potential to fabricate molecular devices.

In conclusion the objectives of this thesis have been demonstrated, the bringing together of inorganic, organic and biological material and a number of analysis techniques has resulted in many interesting observations and novel reaction pathways. The work has opened up avenues that may lead to the

development of functional devices, the use of inorganic materials in biological applications and the preparation of nanoscale molecular devices may be possible.

7 Appendices

Sample Parameter		Spectrum Parameter	
Sample:	**Anderson cluster**	Polarity:	negative
Origin:	**Nicola**	Area / µm²:	500x500
		Time / s:	100
File:	AC1_1N.dat	PI dose:	4.56E+007
Comments: on 100 um square thiol (?) patterns; ;			

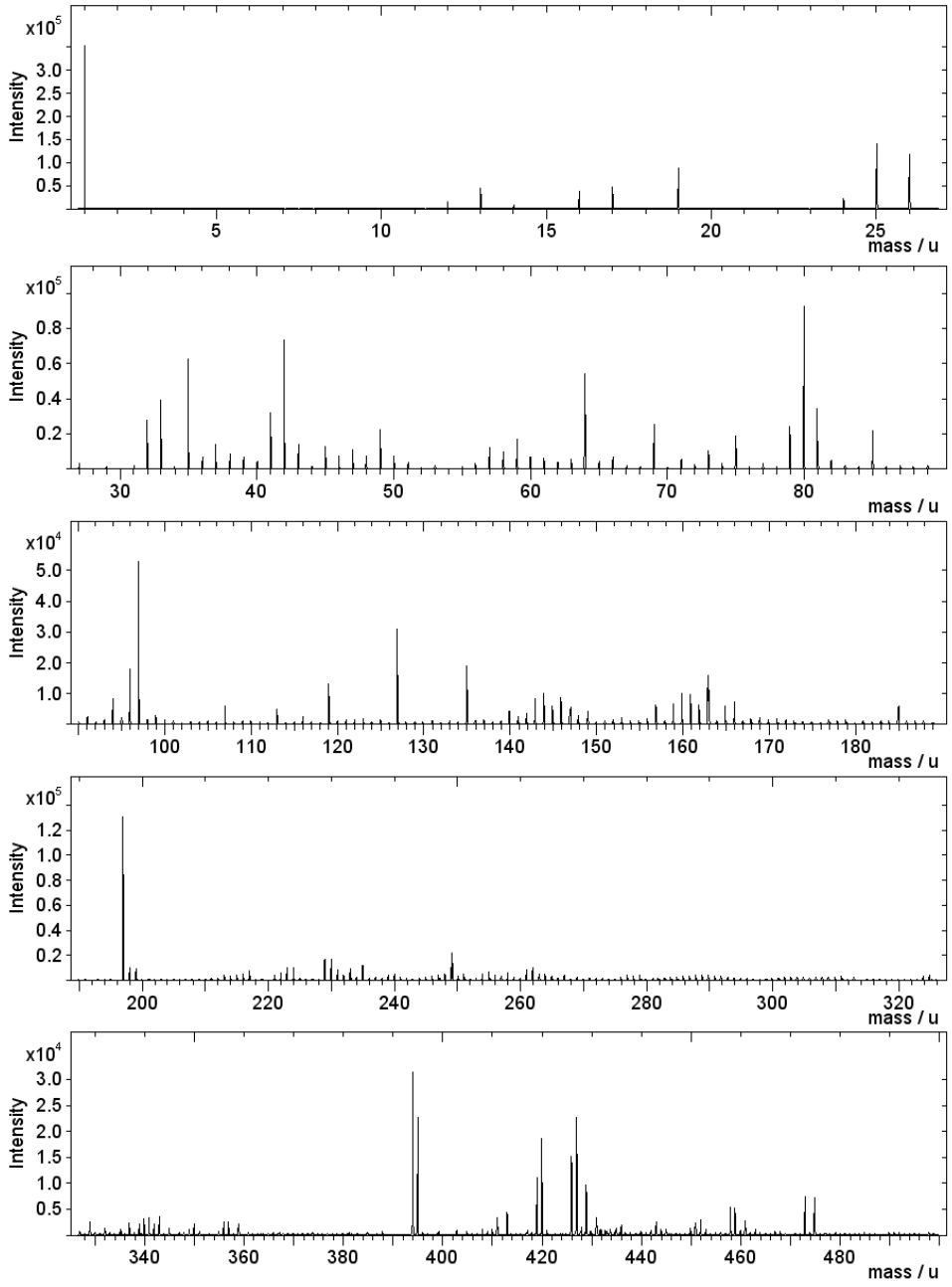

Sample Parameter		Spectrum Parameter	
Sample:	**Anderson cluster**	Polarity:	positive
Origin:	**Nicola**	Area / µm²:	500x500
		Time / s:	122
File:	AC2_2P.dat	PI dose:	4.72E+007

Comments: on 100 um square thiols; ;

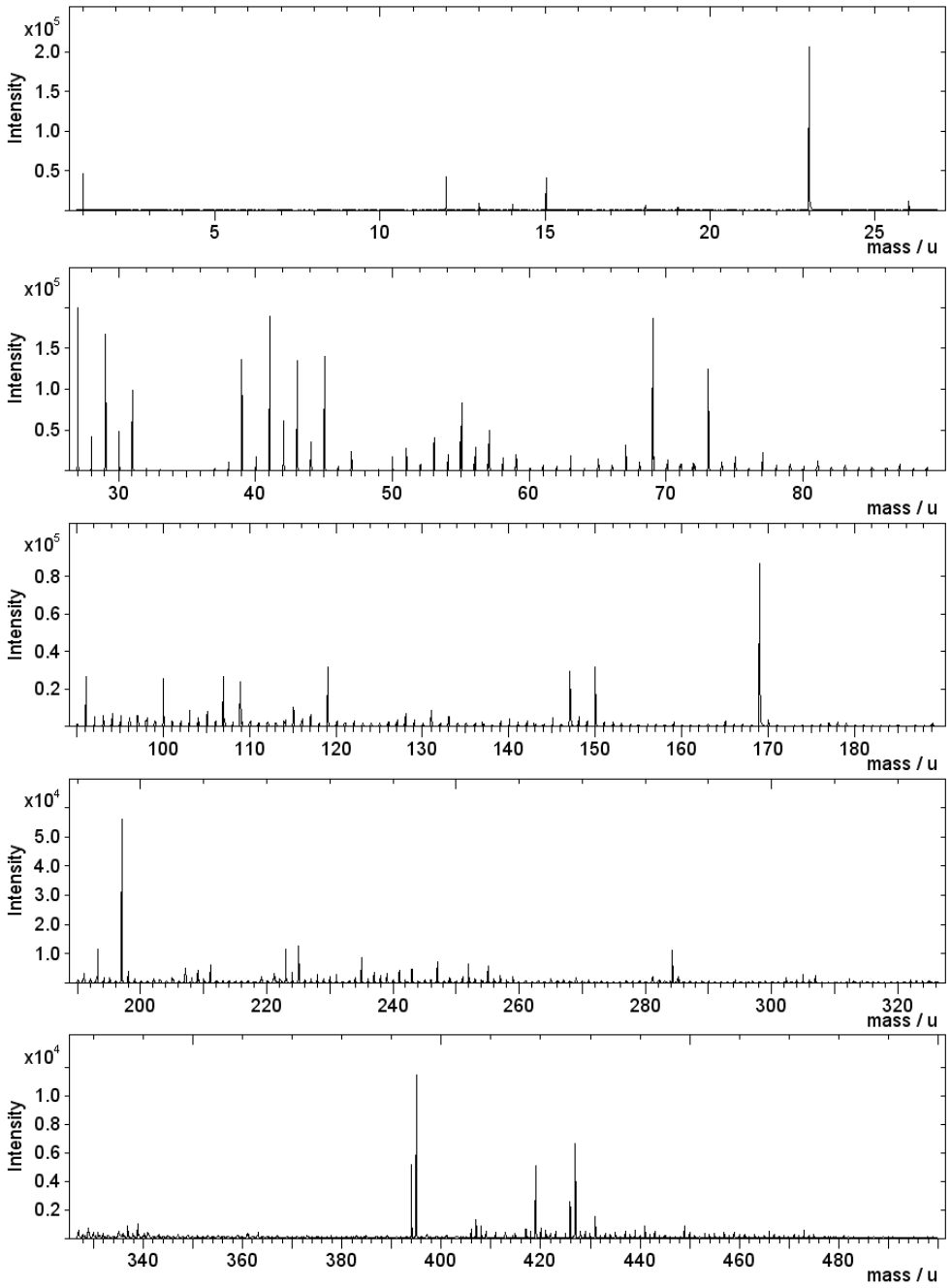

8 Reference section

(1) (a) Whitesides, G. M. *Abstracts Of Papers Of The American Chemical Society* **1996**, *212*, 31(b) Whitesides, G. M.; Ostuni, E.; Takayama, S.; Jiang, X. Y.; Ingber, D. E. *Annual Review of Biomedical Engineering* **2001**, *3*, 335.

(2) A. W. Adamson, A. P. G. *Physical Chemistry of Surfaces* 6th edition ed.: New York, 1966.

(3) (a) Nuzzo, R. G.; Allara, D. L. *Journal Of The American Chemical Society* **1983**, *105*, 4481(b) Porter, M. D.; Bright, T. B.; Allara, D. L.; Chidsey, C. E. D. *Journal Of The American Chemical Society* **1987**, *109*, 3559(c) Fenter, P.; Eisenberger, P.; Li, J.; Camillone, N.; Bernasek, S.; Scoles, G.; Ramanarayanan, T. A.; Liang, K. S. *Langmuir* **1991**, *7*, 2013(d) Troughton, E. B.; Bain, C. D.; Whitesides, G. M.; Nuzzo, R. G.; Allara, D. L.; Porter, M. D. *Langmuir* **1988**, *4*, 365(e) Bain, C. D.; Biebuyck, H. A.; Whitesides, G. M. *Langmuir* **1989**, *5*, 723(f) Bain, C. D.; Evall, J.; Whitesides, G. M. *Journal Of The American Chemical Society* **1989**, *111*, 7155(g) Rubinstein, I.; Steinberg, S.; Tor, Y.; Shanzer, A.; Sagiv, J. *Nature* **1988**, *332*, 426(h) Chidsey, C. E. D.; Loiacono, D. N. *Langmuir* **1990**, *6*, 682(i) Bryant, M. A.; Pemberton, J. E. *Journal Of The American Chemical Society* **1991**, *113*, 8284(j) Finklea, H. O.; Ravenscroft, M. S.; Snider, D. A. *Langmuir* **1993**, *9*, 223.

(4) Love, J. C.; Estroff, L. A.; Kriebel, J. K.; Nuzzo, R. G.; Whitesides, G. M. *Chemical Reviews* **2005**, *105*, 1103.

(5) Roy, D.; Fendler, J. *Advanced Materials* **2004**, *16*, 479.

(6) Bain, C. D.; Whitesides, G. M. *Journal of Physical Chemistry* **1989**, *93*, 1670.

(7) Duwez, A. S. *Journal of Electron Spectroscopy and Related Phenomena* **2004**, *134*, 97.

(8) Rieley, H.; Kendall, G. K.; Zemicael, F. W.; Smith, T. L.; Yang, S. H. *Langmuir* **1998**, *14*, 5147.

(9) Samant, M. G.; Brown, C. A.; Gordon, J. G. *Langmuir* **1991**, *7*, 437.

(10) (a) Tarlov, M. J.; Newman, J. G. *Langmuir* **1992**, *8*, 1398(b) Frisbie, C. D.; Martin, J. R.; Duff, R. R.; Wrighton, M. S. *Journal Of The American Chemical Society* **1992**, *114*, 7142(c) Hagenhoff, B.; Benninghoven, A.; Spinke, J.; Liley, M.; Knoll, W. *Langmuir* **1993**, *9*, 1622.

(11) (a) Vettiger, P.; Despont, M.; Drechsler, U.; Durig, U.; Haberle, W.; Lutwyche, M. I.; Rothuizen, H. E.; Stutz, R.; Widmer, R.; Binnig, G. K. *Ibm Journal*

Of Research And Development **2000**, *44*, 323(b) Stranick, S. J.; Weiss, P. S.; Parikh, A. N.; Allara, D. L. 39th National Symp of the American Vacuum Soc, Chicago, Il, 1992; p 739.

(12) Hostetler, M. J.; Wingate, J. E.; Zhong, C. J.; Harris, J. E.; Vachet, R. W.; Clark, M. R.; Londono, J. D.; Green, S. J.; Stokes, J. J.; Wignall, G. D.; Glish, G. L.; Porter, M. D.; Evans, N. D.; Murray, R. W. *Langmuir* **1998**, *14*, 17.

(13) (a) Benfield, R. E.; Grandjean, D.; Kroll, M.; Pugin, R.; Sawitowski, T.; Schmid, G. *Journal Of Physical Chemistry B* **2001**, *105*, 1961(b) Modrow, H. *Appl. Spectrosc. Rev.* **2004**, *39*, 183(c) Murayama, H.; Ichikuni, N.; Negishi, Y.; Nagata, T.; Tsukuda, T. *Chemical Physics Letters* **2003**, *376*, 26(d) Zhang, P.; Sham, T. K. *Applied Physics Letters* **2002**, *81*, 736.

(14) (a) Badia, A.; Demers, L.; Dickinson, L.; Morin, F. G.; Lennox, R. B.; Reven, L. *Journal Of The American Chemical Society* **1997**, *119*, 11104(b) Hostetler, M. J.; Stokes, J. J.; Murray, R. W. *Langmuir* **1996**, *12*, 3604.

(15) Alvarez, M. M.; Khoury, J. T.; Schaaff, T. G.; Shafigullin, M. N.; Vezmar, I.; Whetten, R. L. *Journal Of Physical Chemistry B* **1997**, *101*, 3706.

(16) Hostetler, M. J.; Murray, R. W. *Current Opinion in Colloid & Interface Science* **1997**, *2*, 42.

(17) Wuelfing, W. P.; Templeton, A. C.; Hicks, J. F.; Murray, R. W. *Analytical Chemistry* **1999**, *71*, 4069.

(18) Venables, J. A. *Introduction to Surface and Thin FilmProcesses*; Cambridge University Press: Cambridge, 2000.

(19) (a) Dubois, L. H.; Nuzzo, R. G. *Annual Review of Physical Chemistry* **1992**, *43*, 437(b) Laibinis, P. E.; Whitesides, G. M.; Allara, D. L.; Tao, Y. T.; Parikh, A. N.; Nuzzo, R. G. *Journal Of The American Chemical Society* **1991**, *113*, 7152(c) Love, J. C.; Wolfe, D. B.; Haasch, R.; Chabinyc, M. L.; Paul, K. E.; Whitesides, G. M.; Nuzzo, R. G. *Journal Of The American Chemical Society* **2003**, *125*, 2597.

(20) Bareman, J. P.; Klein, M. L. *Journal of Physical Chemistry* **1990**, *94*, 5202.

(21) (a) Ferguson, M. K.; Low, E. R.; Morris, J. R. *Langmuir* **2004**, *20*, 3319(b) Lewis, P. A.; Smith, R. K.; Kelly, K. F.; Bumm, L. A.; Reed, S. M.; Clegg, R. S.; Gunderson, J. D.; Hutchison, J. E.; Weiss, P. S. *Journal Of Physical Chemistry B* **2001**, *105*, 10630(c) Barrena, E.; Palacios-Lidon, E.; Munuera, C.; Torrelles, X.; Ferrer, S.; Jonas, U.; Salmeron, M.; Ocal, C. *Journal Of The American Chemical Society* **2004**, *126*, 385(d) Gurau, M. C.; Kim, G.; Lim, S. M.; Albertorio, F.; Fleisher, H. C.; Cremer, P. S. *Chemphyschem* **2003**, *4*, 1231(e) Valiokas, R.;

Ostblom, M.; Svedhem, S.; Svensson, S. C. T.; Liedberg, B. *Journal Of Physical Chemistry B* **2002**, *106*, 10401.

(22) Bain, C. D.; Troughton, E. B.; Tao, Y. T.; Evall, J.; Whitesides, G. M.; Nuzzo, R. G. *Journal Of The American Chemical Society* **1989**, *111*, 321.

(23) Yamada, R.; Sakai, H.; Uosaki, K. *Chemistry Letters* **1999**, 667.

(24) Yamada, R.; Wano, H.; Uosaki, K. *Langmuir* **2000**, *16*, 5523.

(25) Kawasaki, M.; Sato, T.; Tanaka, T.; Takao, K. *Langmuir* **2000**, *16*, 1719.

(26) Bensebaa, F.; Voicu, R.; Huron, L.; Ellis, T. H.; Kruus, E. *Langmuir* **1997**, *13*, 5335.

(27) Love, J. C.; Urbach, A. R.; Prentiss, M. G.; Whitesides, G. M. *Journal Of The American Chemical Society* **2003**, *125*, 12696.

(28) (a) Whitesides, G. M.; Laibinis, P. E. *Langmuir* **1990**, *6*, 87(b) Colorado, R.; Lee, T. R. *Langmuir* **2003**, *19*, 3288.

(29) Houston, J. E.; Kim, H. I. *Accounts of Chemical Research* **2002**, *35*, 547.

(30) (a) Lahiri, J.; Isaacs, L.; Tien, J.; Whitesides, G. M. *Analytical Chemistry* **1999**, *71*, 777(b) Herrwerth, S.; Rosendahl, T.; Feng, C.; Fick, J.; Eck, W.; Himmelhaus, M.; Dahint, R.; Grunze, M. *Langmuir* **2003**, *19*, 1880.

(31) (a) Dillmore, W. S.; Yousaf, M. N.; Mrksich, M. *Langmuir* **2004**, *20*, 7223(b) Yousaf, M. N.; Mrksich, M. *Journal of the American Chemical Society* **1999**, *121*, 4286.

(32) www.dowcorning.com. accessed 10/9/2008

(33) (a) Clarson, S. J. S., J. A. *Siloxane polymers*; Prentice Hall, 1993(b) Choi, K. M.; Rogers, J. A. *Journal Of The American Chemical Society* **2003**, *125*, 4060.

(34) Gates, B. D.; Xu, Q. B.; Love, J. C.; Wolfe, D. B.; Whitesides, G. M. *Annual Review of Materials Research* **2004**, *34*, 339.

(35) (a) Love, J. C.; Wolfe, D. B.; Chabinyc, M. L.; Paul, K. E.; Whitesides, G. M. *Journal Of The American Chemical Society* **2002**, *124*, 1576(b) Fischer, D.; Marti, A.; Hahner, G. *J. Vac. Sci. Technol. A-Vac. Surf. Films* **1997**, *15*, 2173(c) Losic, D.; Shapter, J. G.; Gooding, J. J. *Electrochemistry Communications* **2001**, *3*, 722(d) Fujihira, M.; Furugori, M.; Akiba, U.; Tani, Y. *Ultramicroscopy* **2001**, *86*, 75(e) Bass, R. B.; Lichtenberger, A. W. *Applied Surface Science* **2004**, *226*, 335.

(36) Lee, J. N.; Park, C.; Whitesides, G. M. *Analytical Chemistry* **2003**, *75*, 6544.

(37) (a) Trimbach, D.; Feldman, K.; Spencer, N. D.; Broer, D. J.; Bastiaansen, C. W. M. *Langmuir* **2003**, *19*, 10957(b) Delamarche, E.; Schmid, H.; Bietsch, A.; Larsen, N. B.; Rothuizen, H.; Michel, B.; Biebuyck, H. *Journal Of Physical Chemistry B* **1998**, *102*, 3324.

(38) Veiseh, M.; Zareie, M. H.; Zhang, M. Q. *Langmuir* **2002**, *18*, 6671.

(39) Csucs, G.; Michel, R.; Lussi, J. W.; Textor, M.; Danuser, G. *Biomaterials* **2003**, *24*, 1713.

(40) Chen, C. S.; Mrksich, M.; Huang, S.; Whitesides, G. M.; Ingber, D. E. *Science* **1997**, *276*, 1425.

(41) De La Fuente, J. M.; Andar, A.; Gadegaard, N.; Berry, C. C.; Kingshott, P.; Riehle, M. O. *Langmuir* **2006**, *22*, 5528.

(42) Ostuni, E.; Yan, L.; Whitesides, G. M. *Colloids and Surfaces B-Biointerfaces* **1999**, *15*, 3.

(43) Kane, R. S.; Takayama, S.; Ostuni, E.; Ingber, D. E.; Whitesides, G. M. *Biomaterials* **1999**, *20*, 2363.

(44) (a) Mrksich, M. *Abstracts of Papers of the American Chemical Society* **2005**, *229*, U652(b) Mrksich, M. *Cellular and Molecular Life Sciences* **1998**, *54*, 653(c) Mrksich, M. *Mrs Bulletin* **2005**, *30*, 180(d) Mrksich, M.; Chen, C. S.; Xia, Y.; Dike, L. E.; Ingber, D. E.; Whitesides, G. M. *Proceedings of the National Academy of Sciences of the United States of America* **1996**, *93*, 10775(e) Mrksich, M.; Whitesides, G. M. *Annual Review of Biophysics and Biomolecular Structure* **1996**, *25*, 55.

(45) (a) Prime, K. L.; Whitesides, G. M. *Journal Of The American Chemical Society* **1993**, *115*, 10714(b) Prime, K. L.; Whitesides, G. M. Symp on Interface Dynamics and Growth, at the 1991 Fall Meeting of the Materials Research Soc, Boston, Ma, 1991; p 311.

(46) Patel, N.; Davies, M. C.; Hartshorne, M.; Heaton, R. J.; Roberts, C. J.; Tendler, S. J. B.; Williams, P. M. *Langmuir* **1997**, *13*, 6485.

(47) Lopez, G. P.; Albers, M. W.; Schreiber, S. L.; Carroll, R.; Peralta, E.; Whitesides, G. M. *Journal Of The American Chemical Society* **1993**, *115*, 5877.

(48) Zhang, G.; Yan, X.; Hou, X. L.; Lu, G.; Yang, B.; Wu, L. X.; Shen, J. C. *Langmuir* **2003**, *19*, 9850.

(49) Lange, S. A.; Benes, V.; Kern, D. P.; Horber, J. K. H.; Bernard, A. *Analytical Chemistry* **2004**, *76*, 1641.

(50) (a) Pope, M. T. *Heteropoly and Isopolyoxometalates*; Springer: Berlin, 1983(b) Long, D. L.; Burkholder, E.; Cronin, L. *Chemical Society Reviews* **2007**, *36*, 105(c) Pope M.T., M. A. *Polyoxometalates: From platonic solids to anti-retroviral activity*; Springer: Berlin, 1994.

(51) (a) Yamase, T. *Chemical Reviews* **1998**, *98*, 307(b) Gatteschi, D.; Pardi, L.; Barra, A. L.; Muller, A.; Doring, J. *Nature* **1991**, *354*, 463.

(52) Liu, S. Q.; Volkmer, D.; Kurth, D. G. *Journal of Cluster Science* **2003**, *14*, 405.

(53) Ma, H. Y.; Peng, J.; Han, Z. G.; Yu, X.; Dong, B. X. *Journal of Solid State Chemistry* **2005**, *178*, 3735.

(54) (a) Coronado. E., C. S., Gimenez-Saiz. C., Gomez-Garcia. C. J., and Roth. J., , , , *Synthetic Metals* **2005**, *154*, 241(b) Coronado. E., G.-S. C., and Gomez-Garcia. C. J. *Coord. Chem. Rev.,* **2005**, 1776(c) Liu, S. Q.; Volkmer, D.; Kurth, D. G. *Analytical Chemistry* **2004**, *76*, 4579(d) Liu, S. Q.; Kurth, D. G.; Volkmer, D. *Chemical Communications* **2002**, 976.

(55) Long, D. L.; Cronin, L. *Chemistry-a European Journal* **2006**, *12*, 3699.

(56) Yamase, T. *Journal Of Materials Chemistry* **2005**, *15*, 4773.

(57) Nomiya, K.; Torii, H.; Hasegawa, T.; Nemoto, Y.; Nomura, K.; Hashino, K.; Uchida, M.; Kato, Y.; Shimizu, K.; Oda, M. *Journal of Inorganic Biochemistry* **2001**, *86*, 657.

(58) Scheele, W. *ed. D. S. F. Hermbstädt, M. Sändig oHG* **1971**.

(59) (a) Muller, A.; Serain, C. *Accounts of Chemical Research* **2000**, *33*, 2(b) Muller, A.; Roy, S. *Coordination Chemistry Reviews* **2003**, *245*, 153.

(60) Long, D. L.; Abbas, H.; Kogerler, P.; Cronin, L. *Angewandte Chemie-International Edition* **2005**, *44*, 3415.

(61) (a) Hill, C. L.; Gall, R. D. *Journal of Molecular Catalysis a-Chemical* **1996**, *114*, 103(b) Kholdeeva, O. A.; Vanina, M. P.; Timofeeva, M. N.; Maksimovskaya, R. I.; Trubitsina, T. A.; Melgunov, M. S.; Burgina, E. B.; Mrowiec-Bialon, J.; Jarzebski, A. B.; Hill, C. L. *Journal of Catalysis* **2004**, *226*, 363.

(62) (a) Yin, C. X.; Sasaki, Y.; Finke, R. G. *Inorganic Chemistry* **2005**, *44*, 8521(b) Weiner, H.; Trovarelli, A.; Finke, R. G. *Journal of Molecular Catalysis a-Chemical* **2003**, *191*, 253(c) Weiner, H.; Finke, R. G. *Journal Of The American Chemical Society* **1999**, *121*, 9831.

(63) (a) Neumann, R.; Dahan, M. *Nature* **1997**, *388*, 353(b) Neumann, R.; Dahan, M. *Polyhedron* **1998**, *17*, 3557.

(64) (a) Kozhevnikov, I. V. *Chemical Reviews* **1998**, *98*, 171(b) Kozhevnikov, I. V. *Catalysis Reviews-Science and Engineering* **1995**, *37*, 311(c) Kozhevnikov, I. V.; Mulder, G. P.; Steverink-de Zoete, M. C.; Oostwal, M. G. International Symposium on Organic Chemistry and Catalysis, Delft, Netherlands, 1997; p 223.

(65) (a) Misono, M. *Catalysis Today* **2005**, *100*, 95(b) Misono, M. *Chemical Communications* **2001**, 1141.

(66) (a) Mizuno, N.; Misono, M. *Current Opinion in Solid State & Materials Science* **1997**, *2*, 84(b) Kamata, K.; Yonehara, K.; Sumida, Y.; Yamaguchi, K.; Hikichi, S.; Mizuno, N. *Science* **2003**, *300*, 964.

(67) Renneke, R. F.; Hill, C. L. *Angewandte Chemie-International Edition in English* **1988**, *27*, 1526.

(68) Kaur, J.; Kozhevnikov, I. V. *Chemical Communications* **2002**, 2508.

(69) Lehmann, J.; Gaita-Arino, A.; Coronado, E.; Loss, D. *Nature Nanotechnology* **2007**, *2*, 312.

(70) Chen, Q.; Hill, C. L. *Inorganic Chemistry* **1996**, *35*, 2403.

(71) Judd, D. A.; Nettles, J. H.; Nevins, N.; Snyder, J. P.; Liotta, D. C.; Tang, J.; Ermolieff, J.; Schinazi, R. F.; Hill, C. L. *Journal of the American Chemical Society* **2001**, *123*, 886.

(72) Swiegers, G. F.; Malefetse, T. J. *Chemical Reviews* **2000**, *100*, 3483.

(73) Kagan, C. R.; Mitzi, D. B.; Dimitrakopoulos, C. D. *Science* **1999**, *286*, 945.

(74) (a) Hasenknopf, B.; Delmont, R.; Herson, P.; Gouzerh, P. *European Journal of Inorganic Chemistry* **2002**, 1081(b) Marcoux, P. R.; Hasenknopf, B.; Vaissermann, J.; Gouzerh, P. *European Journal of Inorganic Chemistry* **2003**, 2406.

(75) (a) Hou, Y. Q.; Hill, C. L. *Journal of the American Chemical Society* **1993**, *115*, 11823(b) Zeng, H. D.; Newkome, G. R.; Hill, C. L. *Angewandte Chemie-International Edition* **2000**, *39*, 1772.

(76) (a) Strong, J. B.; Yap, G. P. A.; Ostrander, R.; Liable-Sands, L. M.; Rheingold, A. L.; Thouvenot, R.; Gouzerh, P.; Maatta, E. A. *Journal Of The American Chemical Society* **2000**, *122*, 639(b) Clegg, W.; Errington, R. J.; Fraser, K. A.; Holmes, S. A.; Schafer, A. *Journal of the Chemical Society-Chemical Communications* **1995**, 455.

(77) Kang, J.; Xu, B. B.; Peng, Z. H.; Zhu, X. D.; Wei, Y. G.; Powell, D. R. *Angewandte Chemie-International Edition* **2005**, *44*, 6902.

(78) Bar-Nahum, I.; Narasimhulu, K. V.; Weiner, L.; Neumann, R. *Inorganic Chemistry* **2005**, *44*, 4900.

(79) Parenty, A. D. C.; Smith, L. V.; Pickering, A. L.; Long, D. L.; Cronin, L. *Journal of Organic Chemistry* **2004**, *69*, 5934.

(80) (a) Parenty, A. D. C.; Cronin, L. *Synthesis-Stuttgart* **2008**, 155(b) Parenty, A. D. C.; Smith, L. V.; Cronin, L. *Tetrahedron* **2005**, *61*, 8410(c) Parenty, A. D. C.; Smith, L. V.; Guthrie, K. M.; Long, D. L.; Plumb, J.; Brown, R.; Cronin, L. *Journal of Medicinal Chemistry* **2005**, *48*, 4504.

(81) Guthrie, K. M.; Parenty, A. D. C.; Smith, L. V.; Cronin, L.; Cooper, A. *Biophysical Chemistry* **2007**, *126*, 117.

(82) Smith, L. V.; Parenty, A. D. C.; Guthrie, K. M.; Plumb, J.; Brown, R.; Cronin, L. *Chembiochem* **2006**, *7*, 1757.

(83) Binnig, G.; Quate, C. F.; Gerber, C. *Physical Review Letters* **1986**, *56*, 930.

(84) Binnig G. Roher H, G. C., Weible E *Pysical review letter* **1982**, *49*, 57

(85) (a) Hansma, P. K.; Cleveland, J. P.; Radmacher, M.; Walters, D. A.; Hillner, P. E.; Bezanilla, M.; Fritz, M.; Vie, D.; Hansma, H. G.; Prater, C. B.; Massie, J.; Fukunaga, L.; Gurley, J.; Elings, V. *Applied Physics Letters* **1994**, *64*, 1738(b) Putman, C. A. J.; Vanderwerf, K. O.; Degrooth, B. G.; Vanhulst, N. F.; Greve, J. *Applied Physics Letters* **1994**, *64*, 2454.

(86) http://www.purdue.edu/REM/rs/graphics/sem2.gif. accessed 28/9/2010

(87) Knoll, M. *Zeitschrift für technische Physik* **1935**, *16*, 467.

(88) Ardenne, M. v. *Zeitschrift für Physik* **1938**, *108*, 553.

(89) Castejon, O. J. *Scanning Microsc.* **1991**, *5*, 461.

(90) (a) Belu, A. M.; Graham, D. J.; Castner, D. G. *Biomaterials* **2003**, *24*, 3635(b) Sanni, O. D.; Wagner, M. S.; Briggs, D.; Castner, D. G.; Vickerman, J. C. *Surface and Interface Analysis* **2002**, *33*, 715.

(91) http://www.fkf.mpg.de/ga/machines/sims/How_does_work_1.jpg. accessed 28/9/2010

(92) http://www.cascade.co.uk/tofsims.pdf. accessed 28/9/2010

(93) "http://en.wikipedia.org/wiki/File:Scheme_TEM_en.svg."; wikipedia, 2010.

(94) http://www.dia.unisa.it/~ads/BIOINFORMATICA/Proteomica/index.html; Professore A. De Santis, 28/9/2010

(95) Kelly, S. M., Price, N.C *Current Protein and Peptide Science* **2000**, 349.

(96) Kelly, S. M. P., N. C. *Biochimica Et Biophysica Acta-Protein Structure and Molecular Enzymology* **1997**, *1338*, 161.

(97) Norde, A. W. P. V. a. W. *Journal of Colloid and Interface Science* **2000**, *225*, 394.

(98) Kelly, S. M. J., T. J.; Price, N. C. *Biochimica Et Biophysica Acta-Proteins and Proteomics* **2005**, *1751*.

(99) http://www.biochem.arizona.edu/classes/bioc462/462a/NOTES/Protein_Properties/protein_purification.htm; The University of Arizona.

(100) Hasenknopf, B. *Frontiers in Bioscience* **2005**, *10*, 275.

(101) (a) Wang, L.; Li, J.; Wang, E. B.; Xu, L.; Peng, J.; Li, Z. *Materials Letters* **2004**, *58*, 2027(b) Cheng, L.; Niu, L.; Gong, J.; Dong, S. *Chemistry of Materials* **1999**, *11*, 1465(c) Ruben, M.; Lehn, J. M.; Muller, P. *Chemical Society Reviews* **2006**, *35*, 1056(d) Cannizzo, C.; Mayer, C. R.; Secheresse, F.; Larpent, C. *Advanced Materials* **2005**, *17*, 2888.

(102) Keggin, J. F. *Nature* **1933**, *132*, 351.

(103) Li, H. L.; Sun, H.; Qi, W.; Xu, M.; Wu, L. X. *Angewandte Chemie-International Edition* **2007**, *46*, 1300.

(104) Whitesides, G. M. 225th National Meeting of the American-Chemical-Society, New Orleans, La, 2003; p 422.

(105) Mrksich, M.; Whitesides, G. M. *Trends in Biotechnology* **1995**, *13*, 228.

(106) Errington, R. J.; Petkar, S. S.; Horrocks, B. R.; Houlton, A.; Lie, L. H.; Patole, S. N. *Angewandte Chemie-International Edition* **2005**, *44*, 1254.

(107) Song, Y.-F.; McMillan, N.; Long, D.-L.; Kane, S.; Malm, J.; Riehle, M. O.; Pradeep, C. P.; Gadegaard, N.; Cronin, L. *Journal of the American Chemical Society* **2009**, *131*, 1340.

(108) Song, Y. F.; Long, D. L.; Cronin, L. *Angewandte Chemie-International Edition* **2007**, *46*, 3900.

(109) (a) Houseman, B. T.; Mrksich, M. *Angewandte Chemie-International Edition* **1999**, *38*, 782(b) Martins, M. C. L.; Ratner, B. D.; Barbosa, M. A. *Journal of Biomedical Materials Research Part A* **2003**, *67A*, 158(c) Chen, X. X.; Ferrigno, R.; Yang, J.; Whitesides, G. A. *Langmuir* **2002**, *18*, 7009(d) Ostuni, E.; Grzybowski, B. A.; Mrksich, M.; Roberts, C. S.; Whitesides, G. M. *Langmuir* **2003**, *19*, 1861(e) Mrksich, M.; Sigal, G. B.; Whitesides, G. M. *Langmuir* **1995**, *11*, 4383.

(110) Massia, S. P.; Hubbell, J. A. *J. Cell Biol.* **1991**, *114*, 1089.

(111) (a) Lee, Y. S.; Mrksich, M. *Trends in Biotechnology* **2002**, *20*, S14(b) Wegner, G. J.; Lee, N. J.; Marriott, G.; Corn, R. M. *Analytical Chemistry* **2003**, *75*, 4740.

(112) Prime, K. L.; Whitesides, G. M. *Science* **1991**, *252*, 1164.

(113) Svedhem, S.; Hollander, C. A.; Shi, J.; Konradsson, P.; Liedberg, B.; Svensson, S. C. T. *Journal of Organic Chemistry* **2001**, *66*, 4494.

(114) (a) Mrksich, M.; Chen, C. S.; Xia, Y. N.; Dike, L. E.; Ingber, D. E.; Whitesides, G. M. *Proceedings Of The National Academy Of Sciences Of The United States Of America* **1996**, *93*, 10775(b) Mrksich, M.; Dike, L. E.; Tien, J.; Ingber, D. E.; Whitesides, G. M. *Experimental Cell Research* **1997**, *235*, 305.

(115) Chen, C. S.; Mrksich, M.; Huang, S.; Whitesides, G. M.; Ingber, D. E. *Biotechnology Progress* **1998**, *14*, 356.

(116) Song, Y. F.; McMillan, N.; Long, D. L.; Thiel, J.; Ding, Y. L.; Chen, H. S.; Gadegaard, N.; Cronin, L. *Chemistry-a European Journal* **2008**, *14*, 2349.

(117) Yu-Fei Song, N. M., De-Liang Long, Struan Kane, Jakob Malm, Mathis O Riehle, Chullikkattil P. Pradeep, Nikolaj Gadegaard, and Leroy Cronin *J. Am. Chem. Soc.* **2009**, *131*, 1340.

(118) Dobson, C. M. *Protein Misfolding, Evolution and Disease.*; TiBS, 1999.

(119) Clayden, J., Greeves, N., Warren, S., Wothers, P. *Organic Chemistry*; University Press: Oxford, 2001.

(120) Creighton, T. E. *Proteins; Structures and Molecular Properties.*; 2nd ed ed.; W.H. Freeman and Company, New York, 1993.

(121) Biolabs, N. E., 2010.

(122) Cooper, A. *Biophysical Chemistry.*; The Royal Society of Chemistry: Cambridge, 2004.

(123) Van Holde, K. E., Johnson, W.C., and Shing Ho, P. *Principles of Physical Biochemistry.*; Prentice-Hall International: London, 1998.

(124) Berg, J. M., Tymoczko, J. L., Stryer, L. *Biochemistry.*; Fifth ed. ed.; Freeman Press: New York, 2002.

(125) Karshikoff, A. *Non-Covalent Interactions in Proteins*; 2006 ed.; Imperial College Press.

(126) Cooper, A. *Thermodynamics of Protein Folding and Stability. In Protein: A Comprehensive Treatise*; JAI Press Inc, 1999.

(127) Institute., N. H. G. R.; .

(128) Fink, A. L. *Current Opinion in Biotechnology* **2005**.

(129) (a) Kaiser, E. T. *Angewandte Chemie-International Edition in English* **1988**, *27*, 913(b) Tann, C. M.; Qi, D. F.; Distefano, M. D. *Current Opinion in Chemical Biology* **2001**, *5*, 696(c) Benson, D. E.; Conrad, D. W.; de Lorimer, R. M.; Trammell, S. A.; Hellinga, H. W. *Science* **2001**, *293*, 1641(d) Smith, J. J.; Conrad, D. W.; Cuneo, M. J.; Hellinga, H. W. *Protein Science* **2005**, *14*, 64.

(130) Domen, P. L.; Nevens, J. R.; Mallia, A. K.; Hermanson, G. T.; Klenk, D. C. 8th International Symp on Affinity Chromatography and Biological Recognition, Jerusalem, Israel, 1989; p 293.

(131) Ojida, A.; Tsutsumi, H.; Kasagi, N.; Hamachi, I. *Tetrahedron Lett.* **2005**, *46*, 3301.

(132) Schnaible, V.; Przybylski, M. *Bioconjugate Chem.* **1999**, *10*, 861.

(133) Schweppe, R. E.; Haydon, C. E.; Lewis, T. S.; Resing, K. A.; Ahn, N. G. *Accounts of Chemical Research* **2003**, *36*, 453.

(134) (a) Canfield, R. E. *Journal of Biological Chemistry* **1963**, *238*, 2698(b) Canfield, R. E.; Anfinsen, C. B. *Journal of Biological Chemistry* **1963**, *238*, 2684(c) Canfield, R. E.; Anfinsen, C. B. *Biochemistry* **1963**, *2*, 1073(d) Canfield, R. E.; Liu, A. K. *Journal of Biological Chemistry* **1965**, *240*, 1997.

(135) www.pdb.co.uk accessed 10/4/2009

(136) Brown, J. R.; Low, T.; Beherns, P.; Sepulved.P; Parker, K.; Blakeney, E. *Federation Proceedings* **1971**, *30*, 1241.

(137) http://www.expasy.ch/uniprot/P02769, 2009.

(138) Zhang, Y. S. *Biochemical Society Transactions* **1983**, *11*, 417.

(139) http://www.vivo.colostate.edu/hbooks/pathphys/endocrine/pancreas/insulin_struct.html. accessed 10/4/2009

(140) Arrington, D.; Curry, M.; Street, S. C. *Langmuir* **2002**, *18*, 7788.

(141) Muller, T.; Yablon, D. G.; Karchner, R.; Knapp, D.; Kleinman, M. H.; Fang, H. B.; Durning, C. J.; Tomalia, D. A.; Turro, N. J.; Flynn, G. W. *Langmuir* **2002**, *18*, 7452.

(142) Betley, T. A.; Banaszak Holl, M. M.; Orr, B. G.; Swanson, D. R.; Tomalia, D. A.; Baker, J. R. *Langmuir* **2001**, *17*, 2768.

(143) N. McMillan, L. V. S., J. M. de la Fuente, A. D. C. Parenty, N. Gadegaard, A. R. Pitt, K. Thomson, C. MacKenzie, S. M. Kelly, and L. Cronin *Chem. Commun* **2007**, 2581.

(144) Purdie, N. *Circular Dichroism and the Conformational Analysis of Biomolecules*; Plenum Press: New York., 1996.

(145) Gharibyan, A. L.; Zamotin, V.; Yanamandra, K.; Moskaleva, O. S.; Margulis, B. A.; Kostanyan, I. A.; Morozova-Roche, L. A. *Journal of Molecular Biology* **2007**, *365*, 1337.

(146) http://www.nist.gov/cstl/biochemical/cell_systems/collagen_fibril.cfm; National Institute of Standards and Technology; Vol. 2010.

(147) Koo, E. H. *PNAS* **1999**, 9989.

(148) Kim, D. T.; Blanch, H. W.; Radke, C. J. *Langmuir* **2002**, *18*, 5841.

(149) Yeboah, F. K.; Alli, I.; Yaylayan, V. A.; Yasuo, K.; Chowdhury, S. F.; Purisima, E. O. *Bioconjugate Chem.* **2004**, *15*, 27.

(150) Rhule, J. T.; Neiwert, W. A.; Hardcastle, K. I.; Do, B. T.; Hill, C. L. *Journal Of The American Chemical Society* **2001**, *123*, 12101.

(151) Song, Y. F.; Abbas, H.; Ritchie, C.; McMillian, N.; Long, D. L.; Gadegaard, N.; Cronin, L. *Journal Of Materials Chemistry* **2007**, *17*, 1903.

(152) Lewis, P. A.; Inman, C. E.; Maya, F.; Tour, J. M.; Hutchison, J. E.; Weiss, P. S. *Journal Of The American Chemical Society* **2005**, *127*, 17421.

(153) C. Fleming, D.-L. L., N. McMillan, J. Johnson, N. Bovet, V. Dhanak, N. Gadegaard, P. Kögerler, L. Cronin, M. Kadodwala *Nature Nanotechnology* **2008**, *3*, 229.

(154) Long, D. L.; Kogerler, P.; Cronin, L. *Angewandte Chemie-International Edition* **2004**, *43*, 1817.

(155) Baffert, C.; Boas, J. F.; Bond, A. M.; Kogerler, P.; Long, D. L.; Pilbrow, J. R.; Cronin, L. *Chemistry-a European Journal* **2006**, *12*, 8472.

(156) Song, I. K.; Kaba, M. S.; Barteau, M. A. *Langmuir* **2002**, *18*, 2358.